

**University of Alberta**

**Branchial Cellular Mechanisms for Acid/Base Regulation in Aquatic Animals**

by

Martin Tresguerres



A thesis submitted to the Faculty of Graduate Studies and Research

in partial fulfillment of the requirements for the degree of

Doctor of Philosophy

in

Physiology and Cell Biology

Department of Biological Sciences

Edmonton, Alberta

Fall 2007

**University of Alberta**



Library and  
Archives Canada

Bibliothèque et  
Archives Canada

Published Heritage  
Branch

Direction du  
Patrimoine de l'édition

395 Wellington Street  
Ottawa ON K1A 0N4  
Canada

395, rue Wellington  
Ottawa ON K1A 0N4  
Canada

*Your file    Votre référence*

*ISBN: 978-0-494-33081-4*

*Our file    Notre référence*

*ISBN: 978-0-494-33081-4*

#### NOTICE:

The author has granted a non-exclusive license allowing Library and Archives Canada to reproduce, publish, archive, preserve, conserve, communicate to the public by telecommunication or on the Internet, loan, distribute and sell theses worldwide, for commercial or non-commercial purposes, in microform, paper, electronic and/or any other formats.

The author retains copyright ownership and moral rights in this thesis. Neither the thesis nor substantial extracts from it may be printed or otherwise reproduced without the author's permission.

#### AVIS:

L'auteur a accordé une licence non exclusive permettant à la Bibliothèque et Archives Canada de reproduire, publier, archiver, sauvegarder, conserver, transmettre au public par télécommunication ou par l'Internet, prêter, distribuer et vendre des thèses partout dans le monde, à des fins commerciales ou autres, sur support microforme, papier, électronique et/ou autres formats.

L'auteur conserve la propriété du droit d'auteur et des droits moraux qui protège cette thèse. Ni la thèse ni des extraits substantiels de celle-ci ne doivent être imprimés ou autrement reproduits sans son autorisation.

---

In compliance with the Canadian Privacy Act some supporting forms may have been removed from this thesis.

Conformément à la loi canadienne sur la protection de la vie privée, quelques formulaires secondaires ont été enlevés de cette thèse.

While these forms may be included in the document page count, their removal does not represent any loss of content from the thesis.

Bien que ces formulaires aient inclus dans la pagination, il n'y aura aucun contenu manquant.

  
**Canada**

***“Number of good ideas x number of test tubes = constant”***

Federico Leloir, Nobel prize in chemistry, 1970)

*I dedicate this thesis to **Moi**, I couldn't have done it without you.*

## Abstract

I have investigated the cellular branchial mechanisms for acid/base (A/B) regulation in gills of the dogfish *Squalus acanthias*, the hagfish *Eptatretus stoutii*, the rainbow trout *Oncorhynchus mykiss* -a teleost- and the crab *Chasmagnathus granulatus*. Acid secretion in dogfish takes place in distinct cells and it involves  $\text{Na}^+/\text{K}^+$ -ATPase, apical  $\text{Na}^+/\text{H}^+$  exchangers (NHE) and cytosolic carbonic anhydrase (CA). Bicarbonate secretion in dogfish gills take place in  $\text{V-H}^+$ -ATPase-rich cells. Normally,  $\text{V-H}^+$ -ATPase is stored in cytoplasmic vesicles. However, during blood alkalosis  $\text{V-H}^+$ -ATPase translocates into the basolateral membrane in a cytoskeleton-dependent manner. The basolateral  $\text{V-H}^+$ -ATPase presumably reabsorbs  $\text{H}^+$  into the blood and energizes bicarbonate secretion to seawater. CA inhibition prevents  $\text{V-H}^+$ -ATPase translocation during blood alkalosis, suggesting that intracellular bicarbonate is important for the mechanism. Supporting this hypothesis, cAMP production in gill homogenates is significantly increased by bicarbonate. This points to a soluble adenylyl cyclase (sAC) downstream of CA that may act as the sensor that signals the  $\text{V-H}^+$ -ATPase translocation *via* cAMP. The  $\text{V-H}^+$ -ATPase translocation can also take place in isolated gill pieces subjected to alkaline stress, indicating that the mechanism can occur independently of any extrinsic input. Lastly,  $\text{V-H}^+$ -ATPase translocation also takes place in gills of dogfish experiencing a post-feeding blood alkaline tide. This puts the  $\text{V-H}^+$ -ATPase translocation into the context of the normal physiology of dogfish.

In hagfish  $\text{Na}^+/\text{K}^+$ -ATPase,  $\text{V-H}^+$ -ATPase and NHE are present in the same cells. The hagfish branchial response to metabolic alkalosis also involves  $\text{V-H}^+$ -ATPase translocation into the basolateral membrane. Additionally,  $\text{Na}^+/\text{K}^+$ -ATPase is removed from the membrane. Therefore, differential insertion of ion-transporting proteins is an important A/B regulatory mechanism in hagfish gills.

In freshwater trout, I propose that a basolateral  $\text{V-H}^+$ -ATPase is involved in bicarbonate secretion and  $\text{H}^+$  reabsorption, just like in the marine dogfish and hagfish. However, in trout  $\text{V-H}^+$ -ATPase might also be involved in energizing chloride uptake from freshwater, as a part of a metabolon.

Bicarbonate stimulates ion transport in isolated gills of *C. granulatus*, in agreement with the results from dogfish. The bicarbonate secretory mechanism in this crab differs from fish in that the basolateral route of  $\text{H}^+$  exit to the blood is an NHE.

## **Preface**

Most of the chapters and appendices in this thesis have been already published in (or have been submitted to) the following specialized research journals: The Journal of Experimental Biology, Comparative Biochemistry and Physiology A, Physiological and Biochemical Zoology, American Journal of Physiology and The Canadian Journal of Zoology. I have been the main contributor to the research described, and I am the first author of all the articles. However, modern and prolific science can only be done as a collaborative effort, and it is thus only natural that all of those manuscripts count with several co-authors who I must thank. They are Dr. Fumi Katoh, Ms. Heather Fenton, Ms. Edyta Jasinska, Mr. Scott K. Parks, Prof. Chris Wood, Mr. Sebastian E. Sabatini, Dr. Carlos M. Luquet, Ms. Elizabeth Orr, Tyson MacCormack and my supervisor Dr. Greg G. Goss.

## **Acknowledgements**

I would like to start by thanking my supervisor Greg Goss. You have helped my career in several ways, starting by accepting me into your lab after I contacted you from Argentina. Over these 4 ½ years you have always supported me, initially with close-up guidance, and then by giving me the freedom to explore my ideas and hypotheses. I also greatly appreciate the opportunities you gave me to meet other scientists, all the reference letters you wrote for me and all the trips to conferences and research locations.

Many fellow lab members have helped me during my thesis, but I would like to thank especially Scott Parks and Fumi Katoh. Fumi taught me how to do immunohistochemistry, a technique that I have used in almost every chapter of this thesis. I couldn't start to explain how grateful I am to Scott. You are the ideal lab partner, hard working and yet easy going and fun to be around. It will be extremely difficult to find another lab partner like you, who is also such a good friend. Shake and bake.

Other fellow students and friends I want to thank are Pat, Kee-Chan, Chris, Kessen, Tyson, Liz, Walter and James, for their technical help and discussions over beer. Special thanks to Sampson Law and Shawn Parries, my beer buddies for the first two years. I will also miss The Pacific Fish, my basketball team for three seasons. To Rod Schmaltz, Trevor Hamilton and Sampson, thanks for all the great moments. Thanks to my adoptive parents in Canada, Sandy and Steve, for giving Moira and I unbelievable support in every aspect.



The support staff in BioSci has been extremely helpful in general, but the following people really made a huge difference for me: Jack Scott, Rakesh Bhatnagar, Randy Mandryk, Tad Plesowicz, Clarence Gerla, Chesceri Mason, Michelle Green, Maggie Haag, Cristina Muñoz and Louise McBain. The staff at the Bamfield Marine Sciences Centre was also very helpful during my research campaigns. I really appreciate the company and also the scientific advice from professors Declan Ali, John Chang, Mike Belosevic and Marek Duszyk. The fish physiology scientific community in Canada (a.k.a. the Canadian fish mafia) has been extremely welcoming. I am especially grateful to Katie Gilmour, Chris Wood, Dan Baker, Bruce Cameron and Colin Brauner. To my scientific Argentinean connection -Carlos Luquet, Iara Rochetta, Seba Sabatini-, I am glad I was able to visit you along with Greg and Scott. Thanks to Prof. Jochen Buck and Lonny Levin, and also to Mr. Ken Hess, for the reagents and discussions related to soluble adenylyl cyclase.

Funding during my PhD included the Donald Ross scholarship, the SEB Company of Biologists and the FGSR Travel Grants, and a Teaching Assistance and Differential fee waiver scholarships from BioSci. I especially want to thank the Izaak Walton Killam memorial scholarship for paying for my salary and tuition fees during the last two years of my program.

To my family -Papá, Mamá, Seb and Jimena- who is always with me.

Thanks to Moi, for everything.

## Table of Contents

<b>Chapter I: General Introduction</b> .....	1
<i>-Intracellular pH (pH<sub>i</sub>) regulation</i> .....	3
<i>-Extracellular pH (pH<sub>i</sub>) regulation</i> .....	3
<i>-pH<sub>e</sub> regulation in marine elasmobranches</i> .....	7
<i>- Structure and cell composition of the gills of the Pacific</i>	
<i>dogfish Squalus acanthias</i> .....	9
<i>-pH<sub>e</sub> regulation in hagfish</i> .....	11
<i>-pH<sub>e</sub> regulation in aquatic crustaceans</i> .....	12
<i>-Experimental animals</i> .....	13
<i>-Objectives of this thesis</i> .....	15
Figures.....	18
References.....	22
<b><u>Section on the Pacific spiny dogfish <i>Squalus acanthias</i></u></b>	30
<b>Chapter II: Regulation of branchial V-H<sup>+</sup>-ATPase, Na<sup>+</sup>/K<sup>+</sup>-ATPase</b>	
<b>and NHE2 in response to acid and base infusions in the Pacific spiny</b>	
<b>dogfish (<i>Squalus acanthias</i>)</b> .....	31
Introduction.....	32
Materials and methods.....	34
<i>-Animals</i> .....	34
<i>-Antibodies and reagents</i> .....	34
<i>-Surgery and acid-base infusions</i> .....	35
<i>-Blood samples</i> .....	36
<i>-Analytical procedures on plasma samples</i> .....	36
<i>-Terminal sampling</i> .....	37
<i>-Immunohistochemistry</i> .....	37
<i>-Transmission electron microscopy (TEM)</i> .....	39
<i>-Western blot analysis</i> .....	39
<i>-ATPase assays</i> .....	41
<i>-Statistics</i> .....	41
Results.....	43

<i>i- Blood parameters</i> .....	43
<i>ii- Na<sup>+</sup>/K<sup>+</sup>-ATPase</i> .....	43
<i>iii- V-H<sup>+</sup>-ATPase</i> .....	44
<i>iv- Colocalization of Na<sup>+</sup>/K<sup>+</sup>-ATPase and V-H<sup>+</sup>-ATPase</i> .....	45
<i>v- NHE2</i> .....	45
<i>vi- Transmission Electron Microscopy (TEM)</i> .....	46
Discussion.....	47
<i>-Blood acid-base status during infusions</i> .....	47
<i>-Ion transporting cell subtypes</i> .....	49
<i>-Acid sécrétion</i> .....	49
<i>-Base secretion</i> .....	51
Tables and figures.....	53
References.....	65
<b>Chapter III: Microtubule-dependent relocation of branchial V-H<sup>+</sup>-ATPase to the basolateral membrane in the Pacific spiny dogfish (<i>Squalus acanthias</i>): a role in base secretion</b> .....	70
Introduction.....	71
Materials and methods.....	73
<i>-Animals</i> .....	73
<i>-Antibodies and reagents</i> .....	73
<i>-Surgery and acid-base infusions</i> .....	73
<i>-Blood samples and analytical procedures on plasma samples</i> .....	73
<i>-Colchicine treatment</i> .....	74
<i>-Terminal sampling</i> .....	75
<i>-Immunohistochemistry</i> .....	75
<i>-Western blot analysis</i> .....	76
<i>-Statistics</i> .....	77
Results.....	78
<i>i- 6h-infusions. Blood pH and plasma total CO<sub>2</sub></i> .....	78
<i>ii- 6h-infusions. V-H<sup>+</sup>-ATPase abundance</i> .....	79

iii- 6h-infusions. Number of V-H <sup>+</sup> -ATPase-rich cells and cellular distribution.....	79
iv- 24h-infusions. Blood pH and plasma total CO <sub>2</sub> .....	80
v- 24h-infusions. V-H <sup>+</sup> -ATPase abundance.....	81
vi- 24h-infusions. Number of V-H <sup>+</sup> -ATPase-rich cells and cellular distribution.....	82
Discussion.....	83
Tables and Figures.....	88
References.....	100
<b>Chapter IV: V-H<sup>+</sup>-ATPase translocation during blood alkalosis in dogfish gills: interaction with carbonic anhydrase and involvement in the post-feeding alkaline tide.....</b>	<b>105</b>
Introduction.....	106
Materials and Methods.....	109
- Animals.....	109
- Surgery, NaHCO <sub>3</sub> infusion and acetazolamide injection.....	109
-Blood sampling, analytical procedures on plasma samples.....	109
-Terminal sampling.....	109
-Feeding experiments.....	111
-Immunohistochemistry.....	112
-Western blotting.....	113
-Statistics.....	113
Results.....	114
i- Carbonic anhydrase immunolabeling.....	114
ii- Effect of carbonic anhydrase inhibition on blood and plasma variables during NaHCO <sub>3</sub> infusion.....	114
iii- Effect of carbonic anhydrase inhibition on V-H <sup>+</sup> -ATPase translocation and abundance.....	115
iv- Base efflux and V-H <sup>+</sup> -ATPase translocation and abundance during post-feeding alkalosis.....	116
Discussion.....	117

- Role of carbonic anhydrase (CA) .....	117
- Physiological role of the V-H <sup>+</sup> -ATPase translocation.....	120
Figures.....	123
References.....	130
<b>Chapter V: V-H<sup>+</sup>-ATPase translocation and HCO<sub>3</sub><sup>-</sup>-activated cAMP production in isolated gill pieces of the Pacific spiny dogfish (<i>Squalus acanthias</i>) .....</b>	<b>136</b>
Introduction.....	137
Materials and Methods.....	140
-Animals.....	140
-Antibodies and reagents.....	141
-Gill perfusion and isolation.....	140
-Gill incubation.....	141
-Incubation solutions.....	141
-Immunohistochemistry.....	142
-cAMP assay in gill homogenates.....	142
Results.....	143
i- V-H <sup>+</sup> -ATPase translocation in isolated gill pieces.....	143
ii- cAMP in gill homogenates.....	143
Discussion.....	145
- V-H <sup>+</sup> -ATPase translocation in isolated gill fragments.....	145
- cAMP in gill homogenates.....	148
- Integration.....	151
Tables and figures.....	153
References.....	160
<b>Section on the Pacific hagfish <i>Eptatretus stoutii</i></b> .....	<b>163</b>
<b>Chapter VI: V-H<sup>+</sup>-ATPase, Na<sup>+</sup>/K<sup>+</sup>-ATPase and NHE2 immunoreactivity in the gill epithelium of the Pacific hagfish (<i>Eptatretus stoutii</i>).....</b>	<b>164</b>
Introduction.....	165

Materials and methods.....	166
-Animals.....	168
-Antibodies and reagents.....	168
-Western blotting.....	169
-Immunohistochemistry.....	169
Results.....	171
i- Antibody specificity.....	171
ii- Immunohistochemistry in gill pouches.....	171
iii- $\text{Na}^+/\text{K}^+$ -ATPase, V- $\text{H}^+$ -ATPase and NHE2 subcellular localization.....	172
iv- Co-localization study.....	172
Discussion.....	174
-Cellular localization of the transporters.....	175
-Comparison to MR cells from lampreys, elasmobranchs and teleosts.....	178
Figures.....	180
References.....	188
<b>Chapter VII: Recovery from blood alkalosis in the Pacific hagfish (<i>Eptatretus stoutii</i>): involvement of gill V-<math>\text{H}^+</math>-ATPase and <math>\text{Na}^+/\text{K}^+</math>- ATPase.....</b>	<b>194</b>
Introduction.....	195
Materials and methods.....	197
-Animals.....	197
-Antibodies and reagents.....	197
- $\text{NaHCO}_3$ infusions.....	197
-Blood samples and analytical procedures on plasma samples.....	198
-Terminal sampling.....	198
-Immunohistochemistry.....	199
-Western blot analysis.....	199
-Statistics.....	200

Results.....	201
<i>i- 6 h. Blood and plasma variables.....</i>	201
<i>ii- 6 h. Na<sup>+</sup>/K<sup>+</sup>-ATPase and V-H<sup>+</sup>-ATPase gill</i>	
<i>immunohistochemistry.....</i>	201
<i>iii- 6 h. Na<sup>+</sup>/K<sup>+</sup>-ATPase and V-H<sup>+</sup>-ATPase gill abundance....</i>	202
<i>iv- 24 h. Blood and plasma variables.....</i>	202
<i>v- 24 h. Na<sup>+</sup>/K<sup>+</sup>-ATPase and V-H<sup>+</sup>-ATPase gill</i>	
<i>immunohistochemistry.....</i>	203
<i>vi- 24 h. Na<sup>+</sup>/K<sup>+</sup>-ATPase and V-H<sup>+</sup>-ATPase gill abundance...</i>	204
<i>vii- 24 h. NHE2-like protein (lp) abundance and cellular</i>	
<i>localization.....</i>	204
Discussion.....	205
Tables and figures.....	211
References.....	219
<b>Section on the rainbow trout <u>Oncorhynchus mykiss</u></b>	224
<b>Chapter VIII: Chloride uptake and base secretion in freshwater fish: a</b>	
<b>transepithelial ion-transport metabolon? .....</b>	225
Introduction.....	226
- <i>Historical background.....</i>	226
- <i>Evidence for linkage between Cl<sup>-</sup> uptake and HCO<sub>3</sub><sup>-</sup></i>	
<i>secretion.....</i>	228
Apical electroneutral anion exchange: thermodynamic	
considerations.....	230
- <i>What is the mechanism for elevating [HCO<sub>3</sub><sup>-</sup>]<sub>i</sub> to high</i>	
<i>enough levels to allow for transport? .....</i>	232
Cellular and molecular components involved in branchial Cl <sup>-</sup>	
/HCO <sub>3</sub> <sup>-</sup> exchange.....	235
- <i>Nomenclature of ion transporting cells in the gill.....</i>	235
- <i>MR cell subtypes.....</i>	236
- <i>MR cell and Cl<sup>-</sup>/HCO<sub>3</sub><sup>-</sup> exchange.....</i>	238
- <i>Structure-function relationships: importance of MR cell</i>	

<i>ultrastructure</i> .....	239
-Molecular identity of the apical $\text{Cl}^-/\text{HCO}_3^-$ exchanger.....	240
-Carbonic anhydrase (CA) in trout gill cells.....	243
-Basolateral $\text{V-H}^+$ -ATPases moving $\text{H}^+$ from the MR cells into the blood.....	245
Perspectives.....	250
Materials and Methods.....	253
Tables and figures.....	254
References.....	263
<b>Section on the South American rainbow crab <i>Chasmagnathus</i></b>	
<b><i>granulatus</i></b> .....	279
<b>Chapter IX: High <math>[\text{HCO}_3^-]</math> stimulates ion transport across isolated gills of the crab <i>Chasmagnathus granulatus</i>: involvement of apical anion exchangers, carbonic anhydrase and basolateral <math>\text{Na}^+/\text{H}^+</math> exchangers..</b>	280
Introduction.....	281
Materials and methods.....	283
-Animals.....	283
- Transepithelial Potential Difference ( $V_{te}$ ) across isolated gills.....	283
-Solutions and reagents.....	284
-Statistics.....	285
Results.....	286
Discussion.....	287
-Carbonic anhydrase.....	289
-High $[\text{HCO}_3^-]$ -stimulating mechanism.....	289
- Final remarks.....	291
Figures.....	292
References.....	297
<b>Chapter X: General discussion.....</b>	301
Dogfish.....	302



-Synopsis.....	302
-Branchial cellular ion-transporting mechanisms for blood	
A/B regulation.....	304
i- Acid secretion.....	304
ii- Base secretion and $H^+$ reabsorption.....	305
iii- Integration of branchial $H^+$ and $HCO_3^-$ secretion at the cellular level.....	306
iv- V- $H^+$ -ATPase translocation: physiological role.....	311
Hagfish.....	315
Freshwater rainbow trout.....	316
Crab <i>C. granulatus</i> .....	317
Future directions.....	318
i- V- $H^+$ -ATPase translocation in dogfish gill cells.....	319
ii- Acid/base regulation in hagfish.....	320
iii- Acid/base regulation in teleost fish.....	322
iv- Acid/base regulation in aquatic crabs.....	323
Corollary.....	324
Figures.....	327
References.....	331
<b>Appendix I: Blood and gill responses to HCl infusions in the Pacific hagfish (<i>Eptatretus stoutii</i>)</b> .....	339
Introduction.....	340
Materials and methods.....	342
-Animals.....	342
-Antibodies and reagents.....	342
-HCl infusions.....	342
-Blood sample analysis and terminal sampling.....	342
-Immunohistochemistry.....	342
-Western blotting.....	343
-Statistics.....	343
Results.....	345

-i) 24 HCl Infusions: Blood and plasma variables.....	345
-ii) Na <sup>+</sup> /K <sup>+</sup> -ATPase, V-H <sup>+</sup> -ATPase, and Na <sup>+</sup> /H <sup>+</sup> -exchanger 2 (NHE2) gill abundance.....	346
-iii) Na <sup>+</sup> /K <sup>+</sup> -ATPase, V-H <sup>+</sup> -ATPase, and NHE2 gill immunohistochemistry.....	347
-iv) Quantification of cytoplasmic, intermediate, and apical NHE2 L-IR localization.....	347
Discussion.....	349
Tables and figures.....	354
References.....	361
<b>Appendix II: Low pH stimulates ion transport across isolated gills of the crab <i>Chasmagnathus granulatus</i>: involvement of apical anion V- H<sup>+</sup>-ATPase and carbonic anhydrase.....</b>	<b>368</b>
Introduction and Materials and Methods.....	369
Results.....	370
Discussion.....	372
-Low pH-stimulating mechanism.....	372
Figures.....	374
References.....	379

## List of Tables

### Chapter I

No tables

### Chapter II

<b>Table 2.1.</b> Acid, base and NaCl infusion rates in each of the infusion treatments.....	53
--	----

<b>Table 2.2.</b> Blood parameters in blood or plasma of the experimental fish at the sampling times.....	54
---	----

### Chapter III

<b>Table 3.1.</b> Base and NaCl infusion rates in each of the infusion treatments.....	88
--	----

<b>Table 3.2.</b> 6h-infusions. V-H <sup>+</sup> -ATPase staining patterns in gills from colchicine-treated, NaCl infused, base-infused and colchicine-treated, base-infused fish.....	89
--	----

<b>Table 3.3.</b> 24h-infusions. V-H <sup>+</sup> -ATPase staining patterns in gills from colchicine-treated, NaCl infused, base-infused and colchicine-treated, base-infused fish.....	90
---	----

### Chapter IV

No Tables

### Chapter V

<b>Table 5.1.</b> pH, PCO <sub>2</sub> and [HCO <sub>3</sub> <sup>-</sup> ] of the incubation solutions....	153
---	-----

<b>Table 5.2.</b> Incubation solutions in the [cAMP] determination experiments.....	154
---	-----

### Chapter VI

No tables

### Chapter VII

<b>Table 7.1.</b> Plasma [Na <sup>+</sup> ] and [Cl <sup>-</sup> ] of the experimental hagfish at the sampling times.....	211
---	-----

### Chapter VIII

<b>Table 8.1.</b> Theoretical requirements for electroneutral Cl <sup>-</sup>	
---	--

/HCO <sub>3</sub> <sup>-</sup> exchange in typical freshwater systems.....	254
--	-----

<b>Table 8.2.</b> Theoretical occupancy for arbitrary volumes inside the mitochondria-rich cells.....	255
--	-----

## Chapter IX

No tables

## Chapter X

No tables

## Appendix I

<b>Table 11.1.</b> Plasma [Na <sup>+</sup> ] (mmol l <sup>-1</sup> ) of the experimental hagfish at the sampling times.....	354
--	-----

<b>Table 11.2.</b> NHE2 staining patterns from control infused (NaCl) and acid-infused (HCl) fish following 24 hour experiments.....	355
---	-----

## Appendix II

No tables

## List of Figures

### Chapter I

<b>Figure 1.1.</b> Most common mechanisms for intracellular pH ( $\text{pH}_i$ ) regulation.....	18
<b>Figure 1.2.</b> Cellular mechanisms for extracellular pH ( $\text{pH}_e$ ) regulation in the mammalian kidney.....	19
<b>Figure 1.3.</b> Morphology of dogfish gills and gill filaments.....	20
<b>Figure 1.4.</b> Phylogenetic relationship between the experimental organisms used in this thesis.....	21

### Chapter II

<b>Figure 2.1.</b> Blood parameters of fish infused intravenously with HCl, $\text{NaHCO}_3$ or NaCl .....	55
<b>Figure 2.2.</b> $\text{Na}^+/\text{K}^+$ -ATPase in the membrane fraction of gills sham-operated, NaCl-, acid- and base-infused fish.....	56
<b>Figure 2.3.</b> Representative images of $\text{Na}^+/\text{K}^+$ -ATPase immunostaining in gills from sham-operated, acid-infused, base-infused, and NaCl-infused fish.....	57
<b>Figure 2.4.</b> High magnification LM micrographs showing the $\text{Na}^+/\text{K}^+$ -ATPase subcellular localization in control, acid-, and base-infused fish.....	58
<b>Figure 2.5.</b> V- $\text{H}^+$ -ATPase in the membrane fraction of gills of sham-operated, NaCl-, acid- and base-infused fish.....	59
<b>Figure 2.6.</b> Representative images of V- $\text{H}^+$ -ATPase immunostaining in gills from sham-operated, acid-infused, base-infused, and NaCl-infused fish.....	60
<b>Figure 2.7.</b> High magnification light microscopy micrographs showing the V- $\text{H}^+$ -ATPase subcellular localization in control, acid-, and base-infused fish.....	61
<b>Figure 2.8.</b> Immunohistochemistry of consecutive sections from the trailing edge region of gills from sham operated fish, acid-	

infused fish, and base-infused fish.....	62
<b>Figure 2.9.</b> Quantitative immunoblotting of the membrane fraction of gills of sham-operated, NaCl-, acid- and base-infused fish...	63
<b>Figure 2.10.</b> Transmission electron microscopy picture of a mitochondria-rich cell located on the lamella of a base infused fish.....	64
<b>Chapter III</b>	
<b>Figure 3.1.</b> 6h-infusions. Blood parameters of colchicine-treated NaCl-infused fish, HCO <sub>3</sub> <sup>-</sup> infused fish, and colchicine-treated HCO <sub>3</sub> <sup>-</sup> infused fish.....	91
<b>Figure 3.2.</b> 6h-infusions. Quantitative analysis of V-H <sup>+</sup> -ATPase in gills from colchicine-treated, NaCl infused, base-infused and colchicine-treated, base-infused fish.....	92
<b>Figure 3.3.</b> 6h-infusions. Representative images of V-H <sup>+</sup> -ATPase immunostaining in gills from colchicine-treated, NaCl infused, base-infused and colchicine-treated, base-infused fish.....	93
<b>Figure 3.4.</b> 6h-infusions. High magnification (2000X) light micrographs showing V-H <sup>+</sup> -ATPase staining in gills from colchicine-treated, NaCl-infused, base-infused and colchicine-treated, base-infused fish.....	94
<b>Figure 3.5.</b> 24h-infusions. Blood parameters of colchicine-treated NaCl-infused fish, NaHCO <sub>3</sub> -infused fish, and colchicine-treated NaHCO <sub>3</sub> -infused fish.....	95
<b>Figure 3.6.</b> 24h-infusions. Quantitative analysis of V-H <sup>+</sup> -ATPase in gills from colchicine-treated, NaCl infused, base-infused and colchicine-treated, base-infused fish.....	96
<b>Figure 3.7.</b> 24h-infusions. Representative images of V-H <sup>+</sup> -ATPase immunostaining in gills from colchicine-treated, NaCl infused, base-infused and colchicine-treated, base-infused fish.....	97
<b>Figure 3.8.</b> 24h-infusions. High magnification (2000X) light micrographs showing V-H <sup>+</sup> -ATPase staining in gills from colchicine-treated, NaCl-infused, base-infused and colchicine-treated, base-	

infused fish.....	98
<b>Figure 3.9.</b> V-H <sup>+</sup> -ATPase-dependent base secretion in V-H <sup>+</sup> -ATPase-rich cells.....	99
<b>Chapter IV</b>	
<b>Figure 4.1.</b> Western blotting of dogfish gills with the $\alpha$ -CA antibody.....	123
<b>Figure 4.2.</b> Representative micrographs of 4 $\mu$ m consecutive sections of dogfish gills immuno-labeled for Na <sup>+</sup> /K <sup>+</sup> -ATPase, carbonic anhydrase, and V-H <sup>+</sup> -ATPase.....	124
<b>Figure 4.3.</b> Blood parameters of fish infused intravenously with NaHCO <sub>3</sub> and injected with either DMSO or acetazolamide.....	125
<b>Figure 4.4.</b> Representative micrographs of V-H <sup>+</sup> -ATPase immunolabeling in gills from fish infused with NaHCO <sub>3</sub> for 12h.....	126
<b>Figure 4.5.</b> Fluorometric analysis of V-H <sup>+</sup> -ATPase abundance in gills from fish infused with NaHCO <sub>3</sub> for 12h.....	127
<b>Figure 4.6.</b> Representative micrographs of V-H <sup>+</sup> -ATPase immunolabeling in gills from fasted and fed fish.....	128
<b>Figure 4.7.</b> Fluorometric analysis of V-H <sup>+</sup> -ATPase abundance in gills from fasted and fed fish (24-26 h after feeding).....	129
<b>Chapter V</b>	
<b>Figure 5.1.</b> V-H <sup>+</sup> -ATPase immunolabeling in isolated gills perfused with normal dogfish saline and incubated in media with different [HCO <sub>3</sub> <sup>-</sup> ], P <sub>CO</sub> <sub>2</sub> and pH.....	155
<b>Figure 5.2.</b> V-H <sup>+</sup> -ATPase immunolabeling in isolated gills perfused and incubated with 50 mmol l <sup>-1</sup> NaHCO <sub>3</sub> .....	157
<b>Figure 5.3.</b> [cAMP] in gill homogenates.....	158
<b>Chapter VI</b>	
<b>Figure 6.1.</b> Western blotting in hagfish gill homogenates using antibodies against Na <sup>+</sup> /K <sup>+</sup> -ATPase, V-H <sup>+</sup> -ATPase and Na <sup>+</sup> /H <sup>+</sup> exchanger 2.....	180

<b>Figure 6.2.</b> Schematic of the hagfish gill pouch gross anatomy and fine structure.....	181
<b>Figure 6.3.</b> $\text{Na}^+/\text{K}^+$ -ATPase, $\text{V-H}^+$ -ATPase and NHE2 like-immunoreactivity in sections from hagfish gill filaments and lamella.....	183
<b>Figure 6.4.</b> High magnification micrographs of sections immunostained for $\text{Na}^+/\text{K}^+$ -ATPase, $\text{V-H}^+$ -ATPase and NHE2.....	185
<b>Figure 6.5.</b> Co-localization $\text{Na}^+/\text{K}^+$ -ATPase (NKA) and $\text{V-H}^+$ -ATPase (VHA), NKA and NHE2 and VHA and NHE2.....	186
<b>Figure 6.6.</b> Working model of an ion-transporting cell in hagfish gills.....	187

## Chapter VII

<b>Figure 7.1.</b> 6 h experiments. Blood parameters of hagfish injected with either $250 \text{ mmol l}^{-1} \text{ NaHCO}_3^-$ ( $6000 \mu\text{equiv. kg}^{-1}$ ) or an equivalent volume of $500 \text{ mmol l}^{-1} \text{ NaCl}$ .....	212
<b>Figure 7.2.</b> 6 h experiments. $\text{Na}^+/\text{K}^+$ -ATPase and $\text{V-H}^+$ -ATPase immunoreactivity in gill consecutive sections from $\text{NaCl}$ -injected and $\text{NaHCO}_3$ -injected hagfish.....	213
<b>Figure 7.3.</b> 6 h experiments. $\text{Na}^+/\text{K}^+$ -ATPase and $\text{V-H}^+$ -ATPase abundance in gills from sham (not-infused), $\text{NaCl}$ - and $\text{NaHCO}_3$ -infused hagfish.....	214
<b>Figure 7.4.</b> 24 h experiments. Blood parameters of hagfish injected with either $250 \text{ mmol l}^{-1} \text{ NaHCO}_3^-$ or $500 \text{ mmol l}^{-1} \text{ NaCl}$ .....	215
<b>Figure 7.5.</b> 24 h experiments. $\text{Na}^+/\text{K}^+$ -ATPase and $\text{V-H}^+$ -ATPase immunoreactivity in gill consecutive sections from $\text{NaCl}$ -injected and $\text{NaHCO}_3$ -injected hagfish.....	216
<b>Figure 7.6.</b> 24 h experiments. $\text{Na}^+/\text{K}^+$ -ATPase and $\text{V-H}^+$ -ATPase abundance in whole gill homogenates from $\text{NaCl}$ - and $\text{NaHCO}_3$ -infused hagfish.....	217
<b>Figure 7.7.</b> 24 h experiments. $\text{Na}^+/\text{K}^+$ -ATPase and $\text{V-H}^+$ -ATPase abundance in gill cell membranes from $\text{NaCl}$ - and $\text{NaHCO}_3$ -infused hagfish.....	218



## Chapter VIII

<b>Figure 8.1.</b> Schematic diagram of the freshwater $\text{Cl}^-$ uptake metabolon model in mitochondria-rich cells.....	256
<b>Figure 8.2.</b> The freshwater $\text{Cl}^-$ uptake metabolon.....	257
<b>Figure 8.3.</b> Overlay image of the trailing edge of a gill filament from a rainbow trout acclimated to freshwater showing the localization of $\text{PNA}^+$ cells.....	258
<b>Figure 8.4.</b> The tubular system of mitochondria-rich (MR) cells.	259
<b>Figure 8.5.</b> $\text{V-H}^+$ -ATPase and $\text{Na}^+/\text{K}^+$ -ATPase immunoreactivity in the gills of freshwater trout.....	260
<b>Figure 8.6.</b> Transmission electron microscopy immuno-gold against $\text{V-H}^+$ -ATPase.....	261

## Chapter IX

<b>Figure 9.1.</b> $\text{HCO}_3^-$ -induced $\text{V}_{\text{te}}$ stimulation, inhibition by basolateral acetazolamide and lack of inhibition by basolateral bafilomycin.....	292
<b>Figure 9.2.</b> Inhibition of $\text{HCO}_3^-$ -induced $\text{V}_{\text{te}}$ stimulation by basolateral amiloride.....	294
<b>Figure 9.3.</b> Lack of $\text{HCO}_3^-$ -induced $\text{V}_{\text{te}}$ stimulation in $\text{Cl}^-$ -free conditions.....	295
<b>Figure 9.4.</b> Model for acid/base regulation in the gill epithelium of <i>Chasmagnathus granulatus</i> .....	296

## Chapter X

<b>Figure 10.1.</b> Cellular mechanism for $\text{H}^+$ secretion and $\text{HCO}_3^-$ reabsorption in dogfish gills.....	327
<b>Figure 10.2.</b> Cellular mechanism for $\text{HCO}_3^-$ secretion and $\text{H}^+$ reabsorption in dogfish gills.....	328
<b>Figure 10.3.</b> Integration of feeding, A/B at the gills and $\text{NaCl}$ secretion at the rectal gland.....	329
<b>Figure 10.4.</b> Insertion/removal of ion-transporting proteins involved in $\text{HCO}_3^-$ and $\text{H}^+$ secretion and reabsorption in hagfish gills...	330

## Appendix I

<b>Figure 11.1.</b> Blood parameters of hagfish injected with either 250 mmol l <sup>-1</sup> HCl (6000 µequiv. kg <sup>-1</sup> ) or an equivalent volume of 500 mmol l <sup>-1</sup> NaCl.....	356
<b>Figure 11.2.</b> Na <sup>+</sup> /H <sup>+</sup> exchanger 2 (NHE2)-like abundance and representative western blots of whole gill and membrane fractions from NaCl and HCl infused hagfish.....	357
<b>Figure 11.3.</b> Na <sup>+</sup> /K <sup>+</sup> -ATPase, V-H <sup>+</sup> -ATPase, and NHE2 like-immunoreactivity in consecutive sections from NaCl and HCl infused hagfish.....	359
<b>Figure 11.4.</b> High magnification (1600 x) pictures showing the stereotypical NHE2 like-immunoreactivity pattern for cytoplasmic, intermediate, and apical localization as quantified in table 2.....	360

## Appendix II

<b>Figure 12.1.</b> Repeatability of the acid-induced V <sub>te</sub> stimulation...	374
<b>Figure 12.2.</b> Inhibition of the acid-induced V <sub>te</sub> stimulation by basolateral acetazolamide.....	375
<b>Figure 12.3.</b> Inhibition of the acid-induced V <sub>te</sub> stimulation by basolateral bafilomycin.....	376
<b>Figure 12.4.</b> Acid-induced V <sub>te</sub> stimulation in Cl <sup>-</sup> -free conditions..	377
<b>Figure 12.5.</b> Inhibition of the Acid-induced V <sub>te</sub> stimulation by basolateral DIDS.....	378

## **List of symbols, nomenclature and abbreviations**

$\alpha$  (Greek letter alpha)

$\beta$  (Greek letter beta)

a.f.u. (arbitrary fluorometric units)

A/B (acid-base)

AIF (acid-infused fish)

AIH (acid-infused hagfish)

BIF (base-infused fish)

BIH (base-infused hagfish)

CA (carbonic anhydrase)

cAMP (adenosine 3':5'-cyclic monophosphate; cyclic AMP)

CD (kidney collecting duct)

CBE (chloride-bicarbonate exchanger)

Col-BIF (colchicine-treated base-infused fish)

col-NaCl IF (colchicine-treated NaCl infused fish)

DT (kidney distal tubule)

$g$  (g-force)

$H^+$  (hydrogen ion or proton)

$HCO_3^-$  (bicarbonate ion)

Lp (like-protein)

mmHg (millimeters of mercury)

mmol (millimol)

mmol  $l^{-1}$  (millimolar)

mol  $l^{-1}$  (molar)

MR (mitochondria-rich)

$Na^+$  (sodium)

$NaHCO_3$  (sodium bicarbonate)

NaCl (sodium chloride)

$\text{Na}^+/\text{K}^+$ -ATPase (sodium-potassium ATPase)

NBC (sodium-bicarbonate cotransporter)

NHE (sodium-proton exchanger)

NKCC (sodium-potassium-chloride-chloride cotransporter)

$P$  (partial pressure)

$\text{pH}_i$  (intracellular pH)

$\text{pH}_e$  (extracellular pH)

ppt (parts per thousand)

PT (kidney proximal tubule)

sAC (soluble adenylyl cyclase)

s.e.m. (standard error of the mean)

TS (tubular system)

$\text{V-H}^+$ -ATPase (vacuolar proton ATPase)

## **Chapter I**

### **General introduction**

Organisms must maintain a stable internal environment, which is essential for the proper function of cells, organs and ultimately organism survival and reproduction. The maintenance of a stable internal medium despite a changing environment is called homeostasis (Bernard, 1878; Cannon, 1929), and it is achieved by the coordinated action of various physiological systems.

One of these functions is acid/base (A/B) regulation. Although the specifics of this function largely depend on the environment and life history, the basics are the same for every organism. The most important molecule for A/B regulation is the hydrogen ion ( $H^+$ ). The concentration of  $H^+$  in a solution is measured in terms of pH, and it is given by the following equation:

$$(1) \text{ pH} = -\log [H^+]$$

This equation implies that the lower the pH, the greater the  $[H^+]$  (and the greater the acidity of the solution being considered) (Karp, 1996). Due to electrostatic interactions, the concentration of protons ( $H^+$ ) affects the ionic state of biological molecules. For example,  $H^+$  can change the structure, function and even the solubility of proteins. Even slight variations in the  $H^+$  concentration (in either direction) can have a detrimental effect, and thus they must be readily corrected. Small pH fluctuations are compensated by buffer systems in the blood and cells ( $H_2CO_3/HCO_3^-$  and phosphate buffer systems, proteins) (Karp, 1996). However, the buffer systems cannot cope with larger

H<sup>+</sup> variations. Under these circumstances, H<sup>+</sup> and HCO<sub>3</sub><sup>-</sup> importing and exporting mechanisms are activated both at the cellular and systemic levels.

#### *Intracellular pH (pH<sub>i</sub>) regulation*

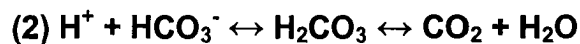
The vast majority of intracellular pH (pH<sub>i</sub>) regulatory mechanisms involve H<sup>+</sup> extrusion or HCO<sub>3</sub><sup>-</sup> import, which are equivalent in A/B terms. At the molecular level, the most common proteins involved are Na<sup>+</sup>/H<sup>+</sup> exchangers (NHEs) and Cl<sup>-</sup>/HCO<sub>3</sub><sup>-</sup> exchangers (CBEs) secondarily energized by the enzyme Na<sup>+</sup>/K<sup>+</sup>-ATPase; V-H<sup>+</sup>-ATPases are also involved in certain systems and conditions (Hoffmann and Simonsen, 1989) (Fig. 1.1). In addition, there is some evidence supporting a HCO<sub>3</sub><sup>-</sup>-exporting mechanism via CBEs working in reverse mode (Roos and Boron, 1981) (Fig. 1.1). In the following sections it will become evident that some of these transporters can also be involved in transepithelial transport of H<sup>+</sup> and HCO<sub>3</sub><sup>-</sup>, for the aim of extracellular pH regulation.

#### *Extracellular pH (pH<sub>e</sub>) regulation*

For multicellular organisms, it is advantageous to depend upon specialized physiological systems to maintain the pH of the internal fluids at a relatively constant level. In this way, large pH variations due to metabolism or environmental changes can be corrected, and cells can use pH<sub>i</sub> regulatory mechanisms to take care of smaller pH variations ("fine tuning").

Regulation of pH<sub>e</sub> largely depends on the environment where the organism lives. Among vertebrates, great differences exist between air-breathers and aquatic-breathers. Air-breathing vertebrates have developed

two main strategies to cope with changes in  $pH_e$ . The first strategy relies on the chemistry of  $CO_2$ , it involves the control of the ventilation rate (Henderson, 1925), and it is often referred to as the respiratory regulation of A/B balance (or “respiratory defense”, Koeppen and Stanton, 1996). Although most of this model comes from work on mammals, it has been hypothesized that most air-breathing vertebrates have similar characteristics (Randall *et al.*, 2002). Very briefly, when blood is acidotic, ventilation rate increases, thus blowing off more  $CO_2$ . This drives the reaction



ultimately eliminating  $H^+$  from the blood. Eventually, blood can return to control pH conditions. Conversely, a reduction in the blood partial pressure of  $CO_2$  ( $PCO_2$ ) will slow down breathing, or even make it cease (Randall *et al.*, 2002). These responses are mediated by central and peripheral chemoreceptors, and take advantage of internal gas exchange organs that can maintain an elevated  $PCO_2$  in the blood (~40 mmHg) compared to the atmosphere (0.2 - 0.4 mmHg) (Truchot, 1987). These mechanisms have been extensively studied, in particular in regards to adaptation to high altitude, and the specifics can be found elsewhere (e.g. Randall *et al.*, 2002).

In addition to the respiratory control of A/B balance, air-breathing vertebrates can regulate their A/B status using specialized cells of the kidney. These responses, which again have been better characterized in mammals,



are often referred as renal control of A/B balance (or “renal defense”, Koeppen and Stanton, 1996). The cells responsible for A/B balance in the kidney reside in the proximal tubule (PT), the distal tubule (DT) and the collecting duct (CD) of the kidney (Randall *et al.*, 2003). These cells have similar ion-transporting proteins to those involved in  $\text{pH}_i$  regulatory mechanisms, but their polarized localization in either the apical or basolateral membrane allow them to mediate transepithelial transport of ions (Fig. 1.2). Some of these cells are involved in acid secretion, and depend upon basolateral  $\text{Na}^+/\text{K}^+$ -ATPases to energize the transepithelial movement of  $\text{Na}^+$ . At the apical membrane,  $\text{Na}^+$  influx drives the secretion of  $\text{H}^+$  into the lumen of the kidney tubules. A major difference between the acid secreting cells of the PT and those from the DT and CD is the apical mechanism of  $\text{H}^+$  secretion. While in the PT it takes place *via* NHEs, in the DT and CD it is through  $\text{Na}^+$  channels energized by V- $\text{H}^+$ -ATPases. The existence of these different mechanisms is due to differences in  $[\text{Na}^+]$  in the lumen, which is much higher in the PT. This topic will resurface when I discuss A/B regulation in gills from marine and freshwater fish. A different cell sub-type in the DT and the CD is responsible for base secretion. In these cells, basolateral V- $\text{H}^+$ -ATPases energize the apical exchange of  $\text{HCO}_3^-$  for  $\text{Cl}^-$ . A common component in both acid- and base-secreting cells is the enzyme carbonic anhydrase (CA), which catalyzes the reaction described in equation 2 (Meldrum and Roughton, 1933). Both  $\text{H}^+$  and  $\text{HCO}_3^-$  are produced by CA inside both the acid- and base-secreting cells. However,  $\text{H}^+$  leaves the acid-

secreting cells across the apical membrane and  $\text{HCO}_3^-$  across the basolateral membrane, a situation that is reversed in the base-secreting cells (Fig. 1.2). Thus, acid-secreting cells reabsorb  $\text{HCO}_3^-$ , and base-secreting cells reabsorb  $\text{H}^+$ .

The ability of aquatic organisms to use ventilation to regulate blood pH is limited (Perry and Gilmour, 2006). The reason is the lower relative solubility of  $\text{O}_2$  in water than in air. As a consequence of the low  $\text{O}_2$  content in water, aquatic organisms must maintain an elevated ventilation volume relative to air breathers resulting in a low blood  $\text{PCO}_2$  (for fish, typically  $\sim 1$  mmHg) (Truchot, 1987). Thus, differences in ventilation have only minor effects on  $\text{PCO}_2$  and thus on pH in water breathers. Because of the low  $\text{PCO}_2$ , blood  $[\text{HCO}_3^-]$  is also much lower compared to mammals, and so is the blood buffering capacity (Evans *et al.*, 2005).

Living surrounded by water also has important implications for the metabolic control of A/B balance in fish. For example the gills, and not the kidneys, are the main organs involved in the secretion of metabolic  $\text{H}^+$  and  $\text{HCO}_3^-$  (Perry and Gilmour, 2006). As pointed out in Evans *et al.* (2005), the surrounding water can act as an infinite source and sink of A/B relevant solutes. This represents a major advantage over the kidney, “which could build-up opposing gradients because of the limited volume of the urine” (Evans *et al.*, 2005).

A great amount of work has dealt with A/B regulation at the whole fish level (reviewed in Evans *et al.*, 2005 and Goss *et al.*, 1998). One common

conclusion from those studies is that the secretion of  $\text{H}^+$  and  $\text{HCO}_3^-$  are linked to the uptake of  $\text{Na}^+$  and  $\text{Cl}^-$ , respectively. An important point is that  $\text{Na}^+$  and  $\text{Cl}^-$  are taken in from the surrounding water. Therefore, their concentration in the water will have tremendous effects on the mechanics of the A/B ion-transporting involved. For example,  $[\text{NaCl}]$  in seawater is around  $500 \text{ mmol l}^{-1}$ , but it can be as low as  $0.01 \text{ mmol l}^{-1}$  in certain freshwater systems (Tresguerres *et al.*, 2006). Seawater fish can take advantage of the inward directed NaCl gradient in order to drive  $\text{H}^+$  and  $\text{HCO}_3^-$  across the apical membrane of the A/B ion-transporting cells (Claiborne *et al.*, 2002). In contrast, freshwater fish need high affinity transporters and additional energizing components in order for  $\text{Na}^+/\text{H}^+$  and  $\text{Cl}^-/\text{HCO}_3^-$  exchanges to work (Perry, 1997). Chapter VIII deals in detail with the characteristics and implications of A/B in freshwater fish, so the rest of this general introduction will focus on marine elasmobranchs and hagfish.

#### *pH<sub>e</sub> regulation in marine elasmobranchs*

The involvement of the elasmobranch gill on A/B regulation was first demonstrated by Hodler *et al.* (1955), from the pioneer research group of Homer W. Smith. These authors used a 'divided box' that contained the head and the tail of dogfish in separate chambers and measured changes in  $[\text{HCO}_3^-]$  in each chamber after intravenous infusions of  $\text{NaHCO}_3$ . Since only the head chamber presented increases in  $[\text{HCO}_3^-]$ , Hodler and colleagues concluded that the gills were responsible for  $\text{HCO}_3^-$  secretion. Moreover, administration of Diamox, an inhibitor of CA, greatly reduced  $\text{HCO}_3^-$  excretion.

Complementary experiments demonstrated that the kidneys and the gut play a minor role -if any- in  $\text{HCO}_3^-$  secretion (Hodler *et al.*, 1955). Subsequent studies on elasmobranch A/B physiology (almost exclusively in dogfish) confirmed these findings (reviewed in Murdaugh and Robin, 1967). However, it was Norbert Heisler who clearly established that the gills accounted for the majority ( $\geq 97\%$ ) of A/B regulation in elasmobranchs under diverse A/B disturbances such as hypercapnia, temperature changes and HCl and  $\text{NaHCO}_3$  infusions (reviewed in Heisler, 1988).

More recent studies confirmed a role of gill CA in  $\text{HCO}_3^-$  excretion (Swenson and Maren, 1987; Wilson *et al.*, 2000), and also the presence of V- $\text{H}^+$ -ATPase (Wilson *et al.*, 1997) and  $\text{Na}^+/\text{K}^+$ -ATPase (Wilson *et al.*, 2002) in the dogfish gill epithelium. The papers by Peter Piermarini, Dave Evans and colleagues were significant steps towards elucidating the cellular mechanisms for A/B regulation in the gills of elasmobranchs. Their finding of separate  $\text{Na}^+/\text{K}^+$ -ATPase- and V- $\text{H}^+$ -ATPase-rich cells in the gills of the Atlantic stingray *Dasyatis sabina* (Piermarini and Evans, 2001) was indicative of the existence of acid-secreting and base-secreting cells. Soon after, Piermarini *et al.* (2002) were the first to find solid evidence for an apical anion exchanger (a CBE related to the mammalian SLC26a4, Pendrin) in the apical membrane of specific gill cells of any fish. It was also confirmed that the anion exchanger and V- $\text{H}^+$ -ATPase localized to the same gill cells in the Atlantic stingray and also in dogfish (Piermarini *et al.*, 2002; Evans, 2004). These authors were quick to find an analogy to the A/B regulatory cells of the mammalian kidney

illustrated in figure 1.2. However, immunolabeled gill sections from marine stingray and dogfish indicated that V-H<sup>+</sup>-ATPase was primarily located in the cytoplasm (Evans *et al.*, 2004; Piermarini and Evans, 2001; Piermarini *et al.*, 2002; Wilson *et al.*, 1997). Thus, it was unclear how V-H<sup>+</sup>-ATPase could reabsorb H<sup>+</sup> back into the blood when the enzyme itself was not in contact with the blood compartment. This contradiction weakened the argument that the V-H<sup>+</sup>-ATPase-rich cells were indeed base-secreting cells.

With regards to H<sup>+</sup> secretion across elasmobranch gills, the stereotypical model included acid-secreting cells with basolateral Na<sup>+</sup>/K<sup>+</sup>-ATPases and apical NHEs 2 and/or 3. This model is based on the immunoreactivity of antibodies against mammalian NHE isoforms in the gill epithelia of several elasmobranchs (Choe *et al.*, 2002, Edwards *et al.*, 2002), including dogfish (Weakly *et al.*, 2003).

At the beginning of this thesis the accepted cellular models for acid and base secretion in the gills of marine elasmobranchs mimicked those from the mammalian kidney. However, no empirical evidence supporting the involvement of V-H<sup>+</sup>-ATPase in HCO<sub>3</sub><sup>-</sup> secretion and H<sup>+</sup> reabsorption was available, neither was there any supporting the roles of Na<sup>+</sup>/K<sup>+</sup>-ATPases or any NHE isoform in H<sup>+</sup> secretion.

#### *Structure and cell composition of the gills of the Pacific dogfish Squalus acanthias*

The Pacific dogfish has four pairs of gills, plus a hemi-gill (hemibranch). Each gill contains a cartilaginous gill arch and several gill rays

that radiate laterally from the arch (Evans *et al.*, 2005). Adjacent rays are connected by connective tissue called the interbranchial septum, where several rows of gill filaments are located (Evans *et al.*, 2005). Each filament includes the filament itself, and finger-like projections called lamellae that increase the surface area of the gill epithelium. The outer layer of the epithelium is primarily comprised by pavement (PV) cells and mitochondria-rich (MR) cells. A schematic of the gill gross morphology and a cross section view of a filament and lamella are shown in figure 1.4. The latter is representative of the gill immunolabeled sections shown in chapters II-V.

The most common cell type in the gills of fish, including those from elasmobranchs, is the PV cell. PV cells represent around 90% of the total cells in gill epithelia, and are typically very thin (Laurent, 1984). Therefore, their role has traditionally been assumed to be in gas exchange between the blood and seawater.

MR cells account for most of the remaining 10% of epithelial cells (Laurent, 1984). A detailed description of the ultrastructure of dogfish MR cells can be found in Wilson *et al.* (2002). The predominant organ for salt extrusion in marine elasmobranchs is the rectal gland (Burger and Hess, 1960). Although it has been proposed that dogfish gill MR cells could also be involved in salt extrusion (Shuttleworth, 1988), no changes in their number, size or relevant biochemical variables were detected after removal of the rectal gland (Wilson *et al.*, 2002). Therefore, and by elimination, the MR cells in elasmobranch gills have been assumed to play a role in acid and base

secretion (Evans *et al.*, 2005). However, this hypothesis has never been empirically tested.

For more information about fish gill anatomy, the flows of seawater and blood, and a detailed description of the PV and MR cells, the reader can consult the exhaustive reviews by Laurent (1984) and Evans *et al.* (2005). This thesis contains details about the morphology and cell composition of the gills of hagfish (chapter VI) and teleost fish (chapter VIII). Crustacean gill morphology can be found in the review by Onken and Riestenpatt (1998).

#### *pH<sub>e</sub> regulation in hagfish*

Hagfish appear in the fossil record around 450 million years ago, and based on their external morphology they have remained relatively unchanged (Holland and Chen, 2001). Assuming this is also true of their physiology, hagfish provide an excellent opportunity to study the most basal characteristics of A/B regulatory mechanisms in vertebrates.

Hagfish internal fluids are almost identical in composition to seawater (Morris, 1965). The capacity to acclimate to different salinities is very limited in hagfish, and consequently they are described as osmoconformers. In these aspects, hagfish resemble some invertebrates. Their blood ionic composition and osmconforming physiological strategy are unique among modern fish and vertebrates in general. Although the hagfish is a textbook osmoconformer, they possess abundant MR cells in the gills (Bartels, 1992; Elger and Hentschel, 1983; Mallat and Paulsen, 1986). Based on other A/B regulatory systems, this has been interpreted as an indication that the gills play a major

role in blood A/B regulation (Mallat *et al.*, 1987). However, the knowledge about A/B regulation in hagfish is much scarcer than for elasmobranch and teleost fish. What little data that do exist suggest they can rapidly recover from HCl infusions by secreting  $H^+$  in exchange for  $Na^+$  (Evans, 1984) *via* NHEs (Edwards *et al.*, 2001; McDonald *et al.*, 1991) energized by  $Na^+/K^+$ -ATPases (Choe *et al.*, 1999). Information about  $HCO_3^-$  is limited to a single study (Evans, 1984), which indicates that  $HCO_3^-$  is secreted in exchange for  $Cl^-$  from seawater.

#### *pH regulation in aquatic crustaceans*

The mechanisms of  $pH_i$  regulation in crustaceans are virtually the same as in vertebrates: buffering by proteins, phosphates and  $HCO_3^-$ , and transmembrane exchange of A/B equivalents (reviewed by Walsh and Milligan, 1989). In fact, most of our current knowledge on  $pH_i$  regulation comes from original results from invertebrates, which were later shown to also apply to vertebrates (Roos and Boron, 1981).

With regards to  $pH_e$  regulation, the gills are the main organ involved in A/B exchange with the environment, and thus they are probably the main A/B regulatory organ (Wheatly and Henry, 1992). Other possible sources of  $pH_e$  regulation are the exoskeleton (Cameron, 1985), the antennal gland and the gut (Wheatly and Henry, 1992), but they are clearly less important compared to the gills and will not be discussed further.

The overall branchial mechanism for A/B regulation appears to be similar to fish: apical  $Na^+/H^+$  and  $Cl^-/HCO_3^-$  exchanges (Dejours *et al.*, 1982;



Henry and Cameron, 1982, 1983). At the cellular level, the only A/B regulation relevant proteins identified so far are carbonic anhydrase (Henry, 1984) and  $\text{Na}^+/\text{K}^+$ -ATPase (Siebers *et al.*, 1994). Several other ion-transporting proteins have been molecularly or pharmacologically identified in crab gills (Luquet *et al.*, 2005; Onken *et al.*, 2003; Towle *et al.*, 1997; Tsai and Lin, 2007, Weihrauch *et al.*, 2001), but to my knowledge their role in A/B regulation has not been tested directly.

#### *Experimental animals*

I have used a variety of aquatic animals, viz. an elasmobranch (the dogfish *Squalus acanthias*), a myxinoidean (the hagfish *Eptatretus stoutii*), a teleost (the rainbow trout *Oncorhynchus mykiss*) and a crustacean (the South American rainbow crab *Chasmagnathus granulatus*). As seen in figure 1.4, the experimental organisms belong to different phylogenetic groups. The four experimental animals can be divided into two major groups. *C. granulatus* is an invertebrate that belongs to the phylum Crustacea, which are protostomes. Hagfish, dogfish and trout are in the other group. These three organisms are chordates and also vertebrates, although there is some controversy on whether or not hagfish are vertebrates or just craniates (Holland and Chen, 2001). All chordates are deuterostomes, as opposed to protostomes. Protostomes and deuterostomes are believed to have separated from each other around 600 million years ago, and they differ in certain important characteristics of their embryonic development (Campbell and Reece, 2005). The specific differences between protostomes and deuterostomes are the

fate of the blastopore (anus vs. mouth) and the type of cleavage (spiral and determinate vs. radial and indeterminate). By using such diverse organisms I expect to be able to draw conclusions about the evolution of branchial A/B regulatory mechanisms at the cellular level based on their similarities, their differences, and the phylogenic position of each organism. However, it is also important to keep in mind the limitations related to working with only a few representative organisms from each phylogenic group (and with just one crustacean).

The experimental organisms also differ in their osmoregulatory strategies. The hagfish is a marine stenohaline fish, and the only vertebrate with a blood ionic composition similar to seawater (Morris, 1965). Dogfish are also marine stenohaline fish, but they hypo-regulate their blood [NaCl] to  $\sim 260 \text{ mmol l}^{-1}$  by secreting the excess NaCl *via* the rectal gland (Burger and Hess, 1960). Trout are hyper-hypo regulators (they can live in environments ranging from freshwater to seawater), but I have only worked with freshwater trout. In this condition, trout are strong NaCl hyper-regulators, maintaining blood [NaCl] at around  $145 \text{ mmol l}^{-1}$  despite the much lower [NaCl] in the external water (see chapter VIII for a detailed explanation). The crab *C. granulatus* is also a strong hyper-hypo regulator (Charmantier *et al.*, 2002), and, like for trout, I have only experimented with freshwater crabs. However, blood [NaCl] in this crab in freshwater is roughly double ( $\sim 320 \text{ mmol l}^{-1}$ ) that of trout. The different osmoregulatory strategies will be useful for comparisons related to branchial A/B regulatory mechanisms in different environments.

### *Objectives of this thesis*

*A posteriori*, the general objective of this thesis seems to be the characterization of some of the cellular A/B regulatory mechanisms in the gills of several aquatic animals. However, the original focus of this thesis was on the A/B regulatory mechanisms in dogfish gills. My original hypothesis was that specific gill cells were involved in A/B regulation, and that  $\text{Na}^+/\text{K}^+$ -ATPase and  $\text{V-H}^+$ -ATPase were involved in  $\text{H}^+$  and  $\text{HCO}_3^-$  secretion, respectively. Accordingly, my specific objectives regarding this topic were:

- 1) to investigate the existence of different acid- and base-secreting cells.
- 2) to test the involvement of  $\text{Na}^+/\text{K}^+$ -ATPase, CA and NHEs in acid secretion.
- 3) to test the involvement of  $\text{V-H}^+$ -ATPase and CA in base secretion.

Based on my earliest results, I decided to focus on the role of  $\text{V-H}^+$ -ATPase on  $\text{HCO}_3^-$  secretion and  $\text{H}^+$  reabsorption. Here, my specific objectives were:

- 4) to characterize the cellular mechanism that allows the movement of  $\text{V-H}^+$ -ATPase from cytoplasmic vesicles to the basolateral membrane under blood alkalosis. This includes identifying the sensor, auxiliary enzymes, and investigating the putative involvement of the cytoskeleton.
- 5) to confirm that  $\text{V-H}^+$ -ATPase translocation from the cytoplasm to the basolateral membrane is necessary for proper  $\text{HCO}_3^-$  elimination from the blood.
- 6) to investigate the role of  $\text{V-H}^+$ -ATPase translocation during an event of naturally occurring blood alkalosis such as the post-feeding alkaline tide.

The experiments on hagfish also branched from the earliest results on dogfish. However, the study on hagfish was more limited, and was focused on V-H<sup>+</sup>-ATPase and base secretion. The aims for this part of the thesis were to determine

(7) the presence of different Na<sup>+</sup>/K<sup>+</sup>-ATPase- and V-H<sup>+</sup>-ATPase-rich cells

(8) if hagfish could recover from a large induced alkaline stress, and

(9) if branchial V-H<sup>+</sup>-ATPase was involved in the recovery.

The chapter on freshwater trout is more theoretical, and its intention is (10) to review the literature about Cl<sup>-</sup> uptake and HCO<sub>3</sub><sup>-</sup> secretion in freshwater fish.

(11) to relate the HCO<sub>3</sub><sup>-</sup>-secretory mechanisms described for dogfish with a possible mechanism for Cl<sup>-</sup>-uptake in freshwater fish, and

(12) to investigate if a basolateral V-H<sup>+</sup>-ATPase is involved in energizing Cl<sup>-</sup> uptake from freshwater

Finally, the study on the crab *C. granulatus* was designed in order to test the model for HCO<sub>3</sub><sup>-</sup> secretion and H<sup>+</sup> reabsorption described for dogfish in a well characterized crustacean ion-transporting gill model. In addition, the gills of *C. granulatus* can be isolated from the animal and perfused. This isolated gill preparation has several advantages: the epithelial polarity is maintained, haemolymph circulation is artificially restored *via* cannula and a peristaltic pump, and the ion transporting physiology of the gill can be monitored in real time using transepithelial potential difference (V<sub>te</sub>) electrodes. This technique is very difficult to execute with fish gills due to

problems related to achieving proper blood-like and water flow (Perry *et al.*, 1984). Therefore, my objectives for the *C. granulatus* experiments were:

13) to investigate  $\text{HCO}_3^-$  secretion and  $\text{H}^+$  reabsorption in the gills of a crustacean, and

14) to take advantage of an isolated gill preparation to test the effect of specific ion-transporting inhibitory drugs on  $\text{HCO}_3^-$  secretion and  $\text{H}^+$  reabsorption.

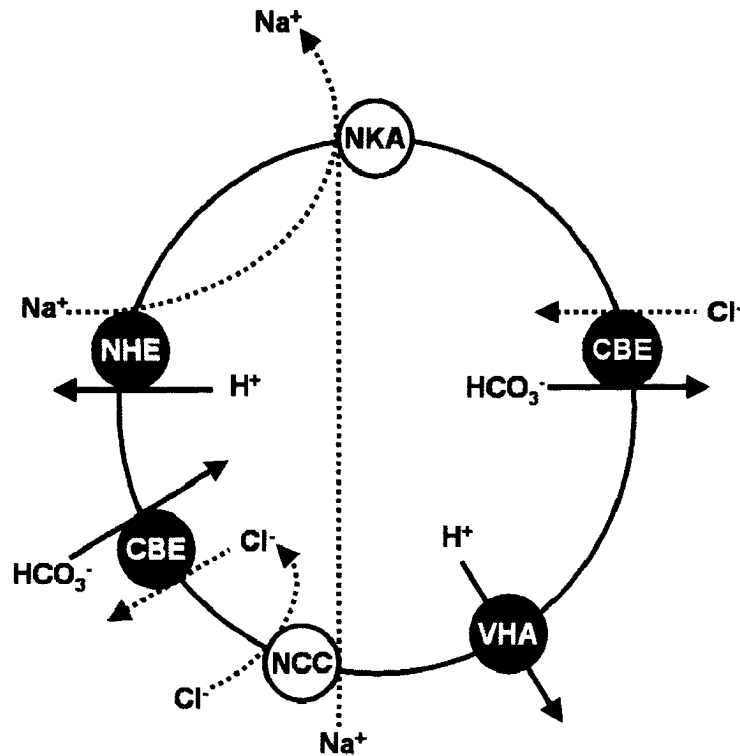


**Figure 1.1.** Most common mechanisms for intracellular pH ( $\text{pH}_i$ ) regulation. Transporters that facilitate  $\text{H}^+$  extrusion or  $\text{HCO}_3^-$  uptake are in grey (recovery from low  $\text{pH}_i$ ). Transporters that mediate  $\text{HCO}_3^-$  extrusion are in black (recovery from high pH).  $\text{Na}^+/\text{K}^+$ -ATPase (NKA) and  $\text{Na}^+/\text{Cl}^-$  cotransporter (NCC) are in white, and do not directly transport  $\text{H}^+$  or  $\text{HCO}_3^-$ . However, they are involved in secondarily energizing the carrier-mediated low  $\text{pH}_i$  recovery mechanisms. NHE:  $\text{Na}^+/\text{H}^+$  exchanger; CBE:  $\text{Cl}^-/\text{HCO}_3^-$  cotransporter; VHA: V- $\text{H}^+$ -ATPase. The movement of A/B relevant solutes ( $\text{H}^+$  and  $\text{HCO}_3^-$ ) is represented by solid line arrows, and the complementary movement of other ions is represented with dotted line arrows. Adapted from Hoffmann and Simonsen (1989).

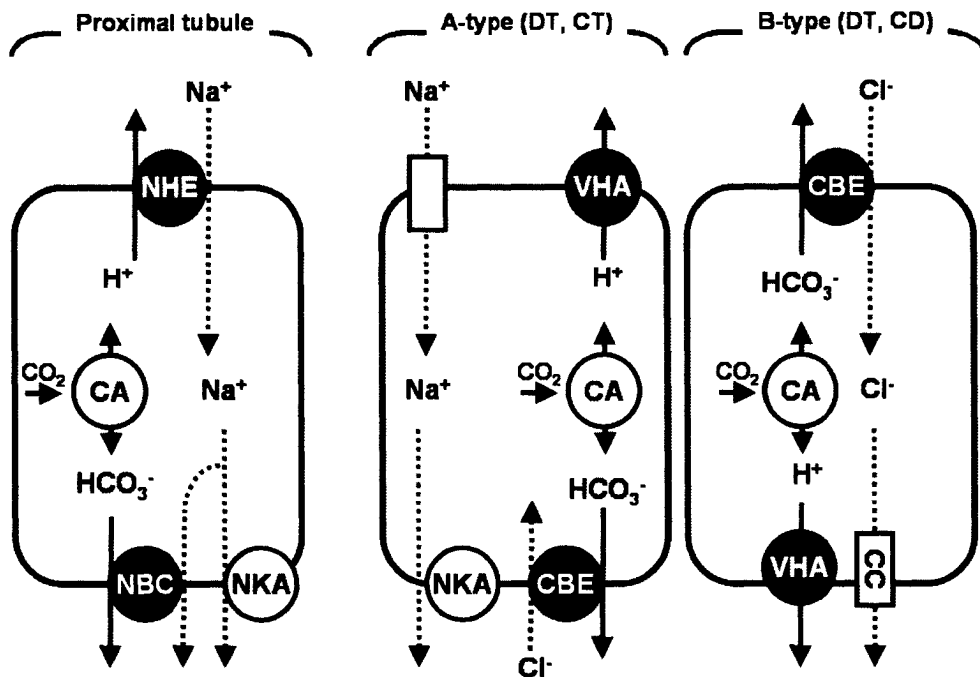


**Figure 1.2.** Cellular mechanisms for extracellular pH ( $pH_e$ ) regulation in the mammalian kidney. Transporters that facilitate  $H^+$  extrusion are in grey. Transporters that mediate  $HCO_3^-$  extrusion are in black.  $Na^+/K^+$ -ATPase (NKA) and carbonic anhydrase (CA) are in white. NKA energizes  $Na^+$  uptake and  $H^+$  secretion. CA hydrates  $CO_2$  into  $H^+$  and  $HCO_3^-$ , which are ultimately secreted or re-absorbed. CC: chloride channel; NHE:  $Na^+/H^+$  exchanger; CBE:  $Cl^-/HCO_3^-$  exchanger; NBC:  $Na^+/HCO_3^-$  cotransporter, VHA: V- $H^+$ -ATPase. DT: distal tubule. CD: collecting duct. The movement of A/B relevant solutes ( $H^+$  and  $HCO_3^-$ ) is represented by solid line arrows, and the complementary movement of other ions is represented with dotted line arrows. Adapted from Koeppen and Stanton, 1996.

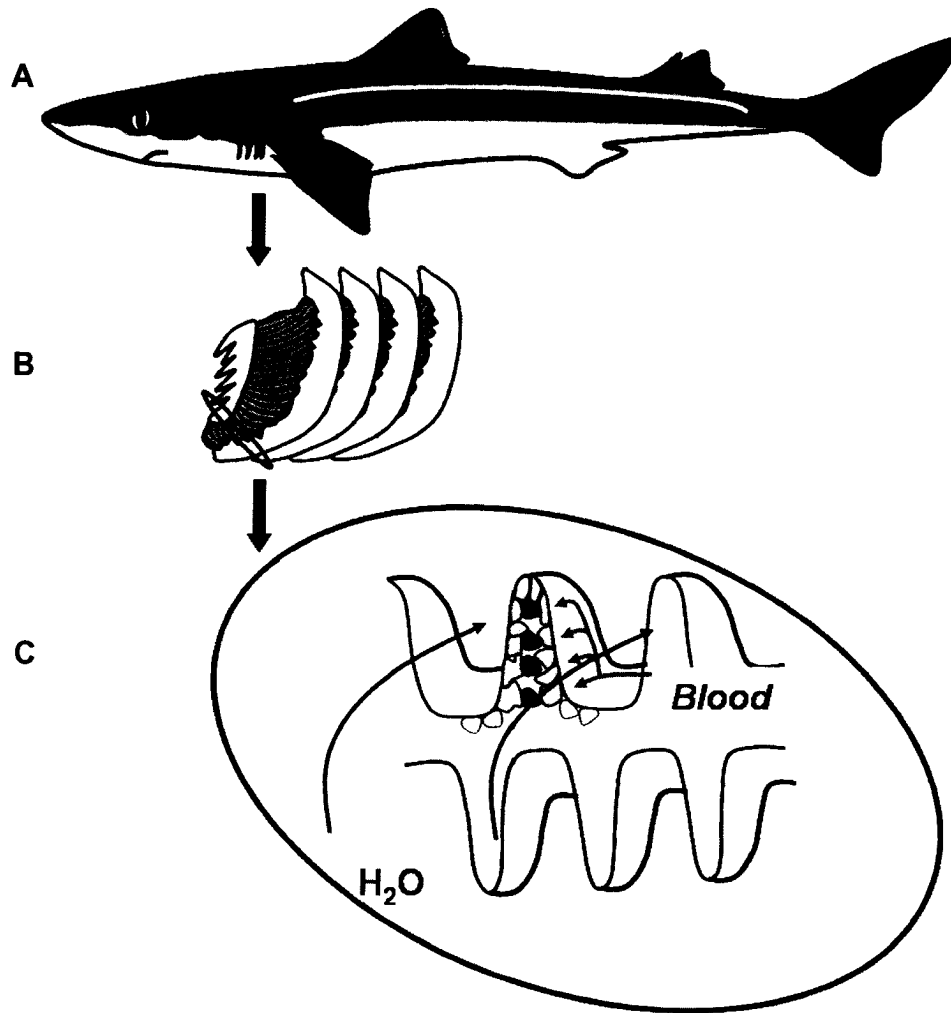


**Figure 1.3.** Morphology of dogfish gills and gill filaments. Dogfish (A) have four pairs of gills (B) and one pair of hemi-gill (not shown). The functional unit of the gill is the gill filament (C). The finger-like projections in C are called lamellae. The grey cells are cells in the outer layer of the gill epithelium. The majority of these cells are pavement (respiratory), and most of the rest are mitochondria-rich cells (probably involved in acid-base regulation). Red cells represent blood vessels. Notice how blood and water flow in a counter-current manner.



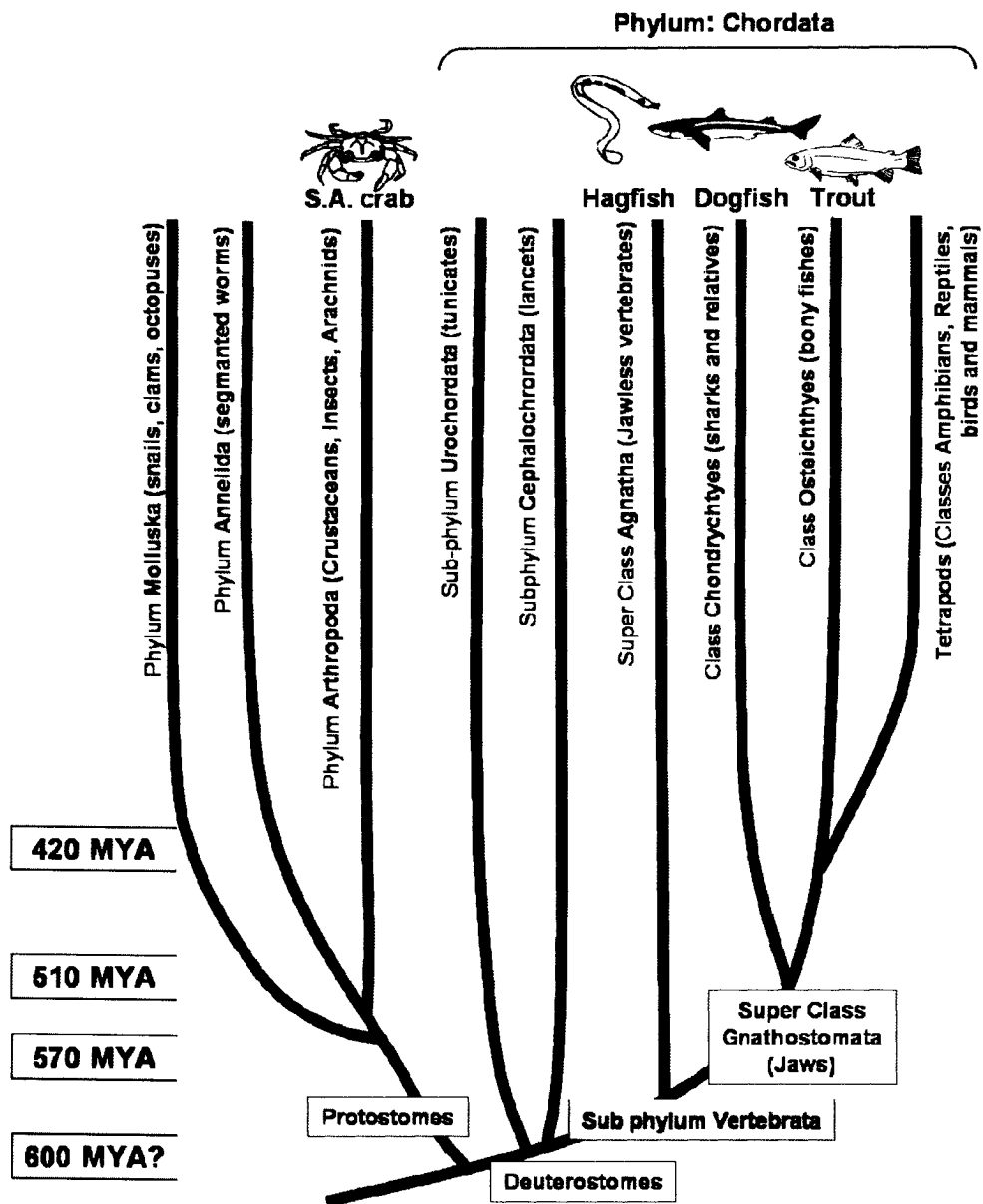


**Figure 1.4.** Phylogenetic relationship between the experimental organisms used in this thesis. S.A. crab: South American crab *Chasmagnathus granulatus*. Hagfish: *Eptatretus stoutii*. Dogfish: *Squalus acanthias*. Trout: Rainbow trout *Oncorhynchus mykiss*. MYA: million years ago. Adapted from Campbell and Reece (2005).

## References

- Bartels, H.** (1992). The gills of hagfishes. In: *The Biology of Hagfishes* (eds. J. Jorgensen, J. Lomholt, R. Weber and R. Malte). Chapman and Hall, London, pp 205-222.
- Bernard, C.** (1878). *Leçons sur les phénomènes de la vie communs aux animaux et aux vegetaux.* (eds. J. B. Ballièr et fills), Paris, France.
- Burger, J.W. and Hess, W.N.** (1960). Function of the rectal gland in the spiny dogfish. *Science* **131**, 670-671.
- Campbell, N.A. and Reece, J.B.** (2005). *Biology.* Palo Alto, CA, USA: Benjamin/Cummings.
- Cameron, J.N.** (1985). Compensation of hypercapnic acidosis in the aquatic blue crab, *Callinectes sapidus*: the predominance of external seawater over carapace carbonate as the proton sink. *J. Exp. Biol.* **114**, 197-206.
- Cannon, W.B.** (1929). Organization for physiological homeostasis. *Physiol. Rev.* **9**, 399-433.
- Charmantier, G., Gimenez, L., Charmantier-Daures, M. and Anger, K.** (2002). Ontogeny of osmoregulation, physiological plasticity and larval export strategy in the grapsid crab *Chasmagnathus granulatus* (Crustacea, Decapoda). *Mar. Ecol. Prog. Ser.* **229**, 185-194.
- Choe, K. P., Edwards, S., Morrison-Shetlar, A. I., Toop, T. and Claiborne, J. B.** (1999). Immunolocalization of Na<sup>+</sup>/K<sup>+</sup>-ATPase in mitochondrion-rich cells of the Atlantic hagfish (*Myxine glutinosa*) gill. *Comp. Biochem. Physiol. A* **124**, 161-168.

**Choe, K. P., Morrison-Shetlar, A. I., Wall, B. P. and Claiborne, J. B.** (2002). Immunological detection of  $\text{Na}^+/\text{H}^+$  exchangers in the gills of a hagfish, *Myxine glutinosa*, an elasmobranch, *Raja erinacea*, and a teleost, *Fundulus heteroclitus*. *Comp. Biochem. Physiol. A*. 131, 375-385.

**Claiborne, J. B., Edwards, S. L. and Morrison-Shetlar, A. I.** (2002). Acid-base regulation in fishes: cellular and molecular mechanisms. *J. Exp. Zool.* **293**, 302-319.

**Dejours, P., Armand, J. and Beekenkamp, H.** (1982). The effect of ambient chloride concentration changes on branchial chloride-bicarbonate exchanges and haemolymph acid-base balance of crayfish. *Resp. Physiol.* **48**, 375-386.

**Edwards, S.L., Claiborne, J.B., Morrison-Shetlar A. I. and Toop, T.** (2001). Expression of  $\text{Na}^+/\text{H}^+$  exchanger mRNA in the gills of the Atlantic hagfish (*Myxine glutinosa*) in response to metabolic acidosis. *Comp. Biochem. Physiol. A* 130, 81-91.

**Edwards, S. L., Donald, J. A., Toop, T., Donowitz, M. and Tse, C. M.** (2002). Immunolocalisation of sodium/proton exchanger-like proteins in the gills of elasmobranchs. *Comp. Biochem. Physiol. A*. 131, 257-265.

**Elger, M. and Hentschel, H.** (1983). Morphological evidence for ionocytes in the gill epithelium of the hagfish *Myxine glutinosa* L. *Bull. Mt. Desert Isl. Biol. Lab.* 23: 4-8.

**Evans, D. H.** (1984). Gill  $\text{Na}^+/\text{H}^+$  and  $\text{Cl}^-/\text{HCO}_3^-$  exchange systems evolved before the vertebrates entered freshwater. *J. Exp. Biol.* **113**, 465-469.

**Evans, D. H., Piermarini, P. M. and Choe, K. P. (2004).** Homeostasis: osmoregulation, pH regulation, and nitrogen excretion. In *Biology of Sharks and their relatives*, (eds. J.C. Carrier, J.A. Musick and M.R. Heithaus), pp. 247-268. Boca Raton, FL, USA: CRC Press LLC.

**Evans, D.H., Piermarini, P.M. and Choe, K.P. (2005).** The multifunctional fish gill: dominant site of gas exchange, osmoregulation, acid-base regulation, and excretion of nitrogenous waste. *Physiol. Rev.* 85, 97-177.

**Goss, G. G., Perry, S. F., Fryer, J. N. and Laurent, P. (1998).** Gill morphology and acid-base regulation in freshwater fishes. *Comp. Biochem. Physiol., A.* **119**, 107-115.

**Heisler, N. (1988).** Acid-base regulation. In *Physiology of Elasmobranch Fishes.*, (ed. T. J. Shuttleworth), pp. 215-252. Berlin: Springer-Verlag.

**Henry, R.P. (1984).** The role of carbonic anhydrase in blood ion and acid-base regulation. *Am. Zool.* **24**, 241-251.

**Henry, R.P. and Cameron, J.N. (1982).** Acid-base balance in *Callinectes sapidus* during acclimation from high to low salinity. *J. Exp. Biol.* **101**, 255-264.

**Henry, R.P. and Cameron, J.N. (1983).** The role of carbonic anhydrase in respiration, ion regulation and acid-base balance in the aquatic crab *Callinectes sapidus* and the terrestrial crab *Gecarcinus lateralis*. *J. Exp. Biol.* **103**, 205-223.

**Hodler, J., Heinemann, H. O., Fishman, A. P. and Smith, H. W.** (1955). Urine pH and carbonic anhydrase activity in the marine dogfish. *Am. J. Physiol.* **183**, 155-162.

**Hoffmann, E. K. and Simonsen, L. O.** (1989). Membrane mechanisms in volume and pH regulation in vertebrate cells. *Physiol. Rev.* **69**, 315-382.

**Holland, N.H. and Chen, J.** (2001). Origin and early evolution of the vertebrates: new insights from advances in molecular biology, anatomy, and palaeontology. *BioEssays* **23**, 142-151.

**Koeppen, B.M. and Stanton, B.A.B** (1996). Renal physiology. St. Louis, MO, USA: Mosby-Year Book, Inc.

**Laurent, P.** (1984). Gill internal morphology. In: Fish Physiology, vol. 10A (ed. H. S. Hoar and D. W. Randall), pp. 73-183. New York, NY, USA: Academic Press.

**Luquet, C. M., Weihrauch, D., Senek, M. and Towle, D. W.** (2005). Induction of branchial ion transporter mRNA expression during acclimation to salinity change in the euryhaline crab *Chasmagnathus granulatus*. *J. Exp. Biol.* **208**, 3627-3636.

**Mallat, J., Conley, D.M. and Ridgway, R.L.** (1987). Why do hagfish have gill “chloride cells” when they need not regulate plasma NaCl concentration? *Can. J. Zool.* **65**, 1956-1965.

**Mallat, J. and Paulsen, C.** (1986). Gill ultrastructure of the Pacific hagfish *Eptatretus stouti*. *Am. J. Anat.* **177**, 243-269.

**McDonald, D.G., Cavdek, V., Calvert, L. and Milligan, C.L.** (1991). Acid-base regulation in the Atlantic hagfish *Myxine glutinosa*. *J. Exp. Biol.* **161**, 201-215.

**Meldrum, N.U. and Roughton, F.J.** (1933). Carbonic anhydrase. Its preparation and properties. *J. Physiol. (London)* **80**, 113-142.

**Morris, R.** (1965). Studies on salt and water balance in *Myxine glutinosa* (L.). *J. Exp. Biol.* **42**, 359-371.

**Murdaugh, H. V. and Robin, E. D.** (1967). Acid-base metabolism in the dogfish shark. In *Sharks, skates and rays*, (eds. W. Gilbert R. F. Mathewson and D. P. Rall), pp. 249-264. Baltimore, MD, USA.: Hopkins.

**Onken, H. and Riestenpatt, S.** (1998). NaCl absorption across split gill lamellae of hyperregulating crabs: transport mechanisms and their regulation. *Comp. Biochem. Physiol. A* **119**, 883-893.

**Onken, H., Tresguerres, M. and Luquet, C. M.** (2003). Active NaCl absorption across posterior gills of hyperosmoregulating *Chasmagnathus granulatus*. *J. Exp. Biol.* **206**, 1017-1023.

**Perry, S. F.** (1997). The chloride cell: structure and function in the gills of freshwater fishes. *Ann. Rev. Physiol.* **59**, 325-347.

**Perry, S.F., Davie, P.S., Daxboeck, C., Ellis, A.G. and Smith, D.G.** (1984). Perfusion methods for the study of gill physiology. In: *Fish Physiology*, vol. 10A. (ed. H. S. Hoar and D. W. Randall). Pp. 325-388. New York, NY, USA: Academic Press.

**Perry, S. F. and Gilmour, K. M.** (2006). Acid-base balance and CO<sub>2</sub> excretion in fish: unanswered questions and emerging models. *Resp. Physiol. Neurobiol.* **154**, 199-215.

**Piermarini, P. M. and Evans, D. H.** (2001). Immunochemical analysis of the vacuolar proton-ATPase B-subunit in the gills of a euryhaline stingray (*Dasyatis sabina*): effects of salinity and relation to Na<sup>+</sup>/K<sup>+</sup>-ATPase. *J. Exp. Biol.* **204**, 3251-3259.

**Piermarini, P. M., Verlander, J. W., Royaux, I. E. and Evans, D. H.** (2002). Pendrin immunoreactivity in the gill epithelium of a euryhaline elasmobranch. *Am. J. Physiol. Reg. Int. Comp. Physiol.* **283**, R983-992.

**Randall, D.J., Burggren, W. and French, K.** (2002). Eckert animal physiology: mechanisms and adaptations. New York, NY, USA: W.H. Freeman and company.

**Roos, A. and Boron, W. F.** (1981). Intracellular pH. *Physiol. Rev.* **61**, 296-434.

**Shuttleworth, T. J.** (1988). Salt and water balance. Extrarenal mechanisms. In *Physiology of elasmobranch fishes*, (ed. T. J. Shuttleworth), pp. 171-199. Berlin: Springer-Verlag.

**Siebers, D., Lucu, C., Bottcher, K. and Jurss, K.** (1994). Regulation of pH in the isolated-perfused gills of the shore crab *Carcinus maenas*. *J. Comp. Physiol. B* **164**, 16-22.

**Swenson, E. R. and Maren, T. H.** (1987). Roles of gill and red cell carbonic anhydrase in elasmobranch  $\text{HCO}_3^-$  and  $\text{CO}_2$  excretion. *Am. J. Physiol. Reg. Int. Comp. Physiol.* **253**, R450-458.

**Towle, D., Rushton, M., Heidysch, D., Magnani, J., Rose, M., Amstutz, A., Jordan, M., Shearer, D. and Wu, W.** (1997). Sodium/proton antiporter in the euryhaline crab *Carcinus maenas*: molecular cloning, expression and tissue distribution. *J. Exp. Biol.* **200**, 1003-1014.

**Truchot, J.P.** (1987). Comparative Aspects of Extracellular Acid-Base Balance. Berlin: Springer.

**Tsai, J.-R. and Lin, H.-C.** (2007). V-type  $\text{H}^+$ -ATPase and  $\text{Na}^+, \text{K}^+$ -ATPase in the gills of 13 euryhaline crabs during salinity acclimation. *J. Exp. Biol.* **210**, 620-627.

**Walsh, P.J. and Milligan, C.L.** (1989). Coordination of metabolism and intracellular acid-base status: ionic regulation and metabolic consequences. *Can. J. Zool.* **67**, 2994-3004.

**Weakley, J., Choe, K. P. and Claiborne, J.B.** (2003). Immunological detection of gill NHE2 in the dogfish (*Squalus acanthias*). *Bull. Mt. Desert Isl. Biol. Lab.* **42**, 81-82.

**Weihrauch, D., Ziegler, A., Siebers, D. and Towle, D.** (2001). Molecular characterization of V-type  $\text{H}^+$ -ATPase (B-subunit) in gills of euryhaline crabs and its physiological role in osmoregulatory ion uptake. *J. Exp. Biol.* **204**, 25-37.

**Wheatly, M.G. and Henry, R.P.** (1992). Extracellular and intracellular



pH regulation in crustaceans. *J. Exp. Zool.* **263**, 127-142.

**Wilson, J. M., Morgan, J. D., Vogl, A. W. and Randall, D. J.** (2002). Branchial mitochondria-rich cells in the dogfish *Squalus acanthias*. *Comp. Biochem. Physiol. A* **132**, 365-374.

**Wilson, J.M., Randall, D.J., Vogl, A.W., Harris, J., Sly, W.S. and Iwama, G.K.** (2000). Branchial carbonic anhydrase is present in the dogfish, *Squalus acanthias*. *Fish Physiol. Biochem.* **22**, 329-336.

**Wilson, J. M., Randall, D. J., Vogl, A. W. and Iwama, G. K.** (1997). Immunolocalization of proton-ATPase in the gills of the elasmobranch, *Squalus acanthias*. *J. Exp. Zool.* **278**, 78-86.

**Pacific spiny dogfish *Squalus acanthias***

## Chapter II

### **Regulation of branchial V-H<sup>+</sup>-ATPase, Na<sup>+</sup>/K<sup>+</sup>-ATPase and NHE2 in response to acid and base infusions in the Pacific spiny dogfish (*Squalus acanthias*)<sup>1</sup>**

<sup>1</sup>A version of this chapter has been published. **Tresguerres, M.**, Katoh, F., Fenton, H., Jasinska, E., and Goss, G.G. (2005). *The Journal of Experimental Biology* 208, 345-354. Reproduced with permission of the Company of Biologists and the co-authors of the manuscript.

## Introduction

The gills of marine elasmobranchs are an excellent model for studying the acid-base regulatory mechanism of fishes. While they are the principal acid-base regulatory organs (Heisler, 1988), they also have a substantial advantage relative to the gills of teleosts in that ion secretion principally takes place in the rectal gland (Burger and Hess, 1960; Shuttleworth, 1988). This eliminates ion secretion as one potentially confounding factor when studying branchial ionic transfers for acid-base regulation. Despite these advantages, the underlying cellular mechanisms for acid-base regulation are far from being fully understood.

For branchial acid secretion in marine elasmobranchs two mechanisms have been proposed. The first mechanism involves extrusion of protons in electroneutral exchange for environmental sodium (i.e. *via*  $\text{Na}^+/\text{H}^+$  exchangers, NHEs), and the second *via* secretion of protons by a Vacuolar-type proton ATPase ( $\text{V-H}^+\text{-ATPase}$ ). At first sight, the former has the advantage of being energetically less expensive, because it would take advantage of the inward directed sodium gradient to drive proton secretion. The proposed apical transporters are members of the NHE family, homologous to the mammalian NHE2 and NHE3. These transporters would be localized in the same cells as the enzyme sodium-potassium ATPase ( $\text{Na}^+/\text{K}^+\text{-ATPase}$ ) (see Claiborne *et al.*, 2002). The second hypothesis is based on the description of  $\text{H}^+\text{-ATPase}$  in the gills of *Squalus acanthias* by Wilson *et al.* (1997). However, the relationship between this transporter and

acid secretion are based only on the subapical localization, and an analogy to the  $\alpha$ -secreting cells of the mammalian collecting duct, the frog skin, and the turtle urinary bladder (Brown and Breton, 1996; Kirschner, 2004). Recently, the V-H<sup>+</sup>-ATPase has also been proposed to be involved in base secretion in a euryhaline elasmobranch, the Atlantic stingray *Dasyatis sabina* (Piermarini and Evans, 2001). These authors found strong cytoplasmic H<sup>+</sup>-ATPase staining in cells that were not labeled for Na<sup>+</sup>/K<sup>+</sup>-ATPase. They proposed that V-H<sup>+</sup>-ATPase stored in vesicles could be recruited to the basolateral membrane under alkalotic stress, but this hypothesis was not investigated further. Demonstration of cellular remodeling and basolateral localization following alkalotic stress would support their hypothesis that these cells are involved in base secretion, in an analogous way to the  $\beta$ -type intercalated cells in the mammalian collecting duct and turtle urinary bladder. However, it is worth noticing that the Atlantic stingray is a euryhaline rajiform, and this model might differ from the one present in exclusively marine elasmobranchs.

The objective of this study was to examine the involvement of V-H<sup>+</sup>-ATPase, Na<sup>+</sup>/K<sup>+</sup>-ATPase, and NHE2 in the branchial acid-base regulatory mechanism of the dogfish, *Squalus acanthias*. In order to magnify the signals, I infused the fish with acid and base solutions for 24 hours. My results support the role of NHE2 in acid secretion, and indicate that increases in V-H<sup>+</sup>-ATPase abundance and activity, as well as a change in its subcellular localization, are required for upregulation of base secretion.

## Materials and methods

### *Animals*

Pacific spiny dogfish (*Squalus acanthias* L) were obtained from commercial fishermen, and held in a 288 m<sup>3</sup> tank provided with flowing seawater (11°C, 31 ppt salinity) at the Bamfield Marine Research Centre (British Columbia). Fish were fed twice per week with pieces of dead flounder and squid while being housed in this tank. They were not fed following removal from the tank.

### *Antibodies and reagents*

Rabbit anti-NHE2 antibody was kindly provided by Dr. Mark Donowitz (National Institutes of Health, Bethesda, Maryland, MD, USA). This antibody was designed against 87 amino acids of the C-terminal region of mammalian NHE2, so the protein we detect should be regarded as a NHE-2 like protein (NHE2-lp) throughout the text. This antibody has been successfully used to detect NHE2-lp in elasmobranchs (Edwards et al, 2002). Rabbit anti-Na<sup>+</sup>/K<sup>+</sup>-ATPase antibody was raised against a synthetic peptide corresponding to a part of a highly conserved region of the  $\alpha$ -subunit (Katoh *et al.*, 2000; Katoh and Kaneko, 2003). Rabbit anti-V-H<sup>+</sup>-ATPase was raised against a synthetic peptide based on the highly conserved and hydrophilic region in the A-subunit (Katoh *et al.*, 2003). A donkey anti-rabbit fluorescent secondary antibody (Li-Cor Inc., Lincoln, NE, USA) was used for Western analysis. Due to unavailability of the correspondent proteins, I was unable to run pre-absorption controls. However, in the western analyses I always found very

distinct bands of about the expected molecular weights for all the antibodies tested. Together with the absence of signal in nitrocellulose membranes incubated with blocking buffer without the primary antibody, it suggests that the antibodies used have an acceptable specificity.

Unless otherwise mentioned, the reagents used in this study were purchased from Sigma (St. Louis, MO, USA).

#### *Surgery and acid-base infusions*

A total of 16 animals ( $2.28 \pm 0.31$  kg) were removed from the housing tank and cannulated for this study. I used fish of equivalent sizes to standardize infusion rates. Fish were caught by hand, anesthetized with MS-222 (1:10000), and transferred to an operating table, where the gills were irrigated with aerated seawater containing MS-222. Two cannulae (PE-50, Clay-Adams) were fitted into the caudal vein and artery. The incision was sutured with stitches and a small volume of a heparanized ( $50 \text{ i.u. ml}^{-1} \text{ Na}^+$ -heparin)  $500 \text{ mmol l}^{-1} \text{ NaCl}$  solution was injected before blocking the end of the tubing with a pin. The animals were transferred to experimental boxes (36 L) with aerated flowing seawater. After a 24 hour recovery period, the venous cannula was connected to a Gilson miniplus peristaltic pump (Middleton, WI, USA), and the experimental solution was infused at a rate of  $4.04 \pm 0.83 \text{ ml h}^{-1} \text{ kg}^{-1}$ . The arterial cannula allowed me to obtain blood samples during the course of the experiment.

In order to induce acidosis or alkalosis in the blood, fish were infused with either  $125 \text{ mmol l}^{-1} \text{ HCl}$  or  $250 \text{ mmol l}^{-1} \text{ NaHCO}_3$  to achieve nominal  $\text{H}^+$

and  $\text{HCO}_3$  infusion rates of 500 and 1000  $\mu\text{mol kg}^{-1} \text{h}^{-1}$ . Actual acid and base loads were  $495 \pm 79$  and  $981 \pm 235 \mu\text{mol kg}^{-1} \text{h}^{-1}$ , respectively. These concentrations were selected after previous trial experiments and references from the literature (Gilmour *et al.*, 2001; Wood *et al.*, 1995). Infusion of acid at a nominal rate of 1000  $\mu\text{mol kg}^{-1} \text{h}^{-1}$  in early experiments proved to be fatal after ~6 h, possibly due to haemolysis.

To minimize osmotic disturbances, the osmolarity of the infusion solutions was adjusted to 1000 mOsm with the addition of NaCl. Animals infused with 500 mmol  $\text{l}^{-1}$  NaCl served as control. Table 2.1 shows the base, acid, and NaCl load in each of the treatments. In addition, four other animals were subjected to surgery, but no cannula was inserted into the caudal vein or artery. These fish represented the sham-operated group, and they were otherwise treated exactly the same as the experimental fish.

#### *Blood samples*

Arterial blood samples (300  $\mu\text{l}$ ) were taken at times = 0, 1, 3, 6, 12 and 24 h. After the blood extraction, an equal volume of heparanized 500 mmol  $\text{l}^{-1}$  NaCl saline was injected into the fish to minimize changes in blood volume and prevent clotting. Aliquots of blood sample were used for haematocrit analysis (~50  $\mu\text{l}$ ), and pH determination (~80  $\mu\text{l}$ ). The rest of the sample was centrifuged at 12000  $\times g$  and plasma osmolarity and total  $\text{CO}_2$  ( $\text{TCO}_2$ ) were measured immediately. The remaining plasma was preserved at  $-80^\circ \text{C}$  for later sodium and chloride concentrations assays.

#### *Analytical procedures on plasma samples*



Osmolarity was measured with a micro osmometer (Precision Systems Inc.). A pH sensitive electrode (Radiometer, Copenhagen) was used to measure blood pH. The total content of CO<sub>2</sub> (TCO<sub>2</sub>) was determined in a Cameron chamber equipped with a CO<sub>2</sub> electrode (Radiometer, Copenhagen). Na<sup>+</sup> concentration was read by flame spectrometry (Perkin-Elmer model 3300, Norwalk, CT, USA). Cl<sup>-</sup> concentration was measured by the mercuric thiocyanate method (Zall *et al.*, 1956).

#### *Terminal sampling*

After 0 (sham) or 24 h of infusion, fish were anaesthetized and terminated by injection of 3 ml of a saturated KCl solution. Samples of gill were excised and snap frozen in liquid nitrogen for later western blot and ATPase analyses. Other gill samples were immersed in fixative for immunohistochemistry and electron microscopy (see below).

#### *Immunohistochemistry*

Gill samples for immunohistochemistry were fixed in 3% paraformaldehyde, 0.1 mmol l<sup>-1</sup> cacodylate buffer (pH 7.40) for 6 h at 4°C and dehydrated in a graded ethanol series. After embedding in paraffin, 4 µm sections were cut from gill filaments. Sections from the trailing and leading edges, as well as from the middle portion of the filament, were placed in glycerol-albumin (Mayer's fixative) coated slides (1 section per slide). Sections were deparaffinized in toluene, hydrated in a decreasing ethanol series, washed in double distilled water (ddH<sub>2</sub>O), and then exposed to 0.6% H<sub>2</sub>O<sub>2</sub> for 30 min to devitalize endogenous peroxidase activity. After blocking

with 2% normal goat serum (NGS) for 30 min, the sections were incubated overnight at 4°C with the respective antibody, which was diluted in 2% NGS, 0.1% bovine serum albumin, 0.02% limpet haemocyanin, 0.01% NaN<sub>3</sub> in 10 mmol l<sup>-1</sup> PBS, pH 7.40. The anti-Na<sup>+</sup>/K<sup>+</sup>-ATPase antibody was diluted 1:4000, and the antibody against the A-subunit of the V-H<sup>+</sup>-ATPase was diluted 1:1000. In order to look for colocalization of the transporters, consecutive sections were incubated with different antibodies. The next steps were performed at room temperature, using the Vectastain ABC kit (Vector laboratories, CA, USA) as follows. Sections were incubated with a biotinylated goat anti-rabbit secondary antibody for 30 min, and then incubated with a horseradish peroxidase-labeled streptavidin solution for 1 h. Sections were rinsed in ddH<sub>2</sub>O for 6 min and then in PBS for 2 min in between steps. Binding of the antibodies was visualized by soaking the sections in a solution containing 20% w/v 3,3'-diaminobenzidine tetrahydrochloride (DAB) and 0.005% H<sub>2</sub>O<sub>2</sub> in 50 mmol l<sup>-1</sup> Tris-buffered saline, pH 7.60. DAB reacts with the horseradish peroxidase, producing a brown coloration. As controls, gill sections from every fish were incubated without any primary antibody. These sections never showed specific staining, regardless of the treatment and location in the gill (trailing or leading edge of the filament). The qualitative description of the amount of positive labeled cells is based on three pairs of sections from the leading edge, three pairs of sections from the approximate middle of the filament, and three pair of sections from the leading edge. Each pair of sections containing one section labeled for Na<sup>+</sup>/K<sup>+</sup>-ATPase and the

other for V-H<sup>+</sup>-ATPase. A minimum of 2 filaments per fish, and 3 fish per treatment were analyzed.

#### *Transmission electron microscopy (TEM)*

Gill samples for TEM were fixed in 1.5% glutaraldehyde, 3% paraformaldehyde, 0.1 mmol l<sup>-1</sup> cacodylate buffer (pH 7.40) for 6 h at 4°C, immersed in 50% ethanol for 2 h and stored in 70% ethanol at 4°C. Samples were re-hydrated after arrival to Edmonton, post-fixed in 2% OsO<sub>4</sub> for 2 h, dehydrated in an ethanol graded series, transferred to propylene oxide and embedded into Epon. Ultrathin sections (~90 nm) were cut with an automatic microtome (Reichert Ultracut E), mounted in copper grids, counter stained with 1% uranyl acetate (1 h) and 0.02 % lead citrate (1 min), and observed using a TEM (Philips model 201).

#### *Western blot analysis*

Frozen gill samples were weighed, immersed in liquid nitrogen and pulverized in a porcelain grinder. The resultant powder was resuspended in 1:10 w/v of ice-cold homogenization buffer (250 mmol l<sup>-1</sup> sucrose, 1 mmol l<sup>-1</sup> EDTA, 30 mmol l<sup>-1</sup> Tris, 100 mg ml<sup>-1</sup> PMSF and 2 mg ml<sup>-1</sup> pepstatin, pH 7.40), and sonicated on ice for 20 seconds. Debris was removed by two low speed centrifugations (3000 g for 5 min, 4°C), and gill membranes were pelleted by a final high speed centrifugation (20800 g for 30 min, 4°C). The resulting pellets were resuspended in homogenization buffer and an aliquot was saved for protein determination analysis (Pierce, IL, USA), which was performed in triplicate. The remaining sample was combined with 2X Laemmli

buffer (Laemmli, 1970) for Western analysis. 30  $\mu\text{g}$  (for NHE2) or 50  $\mu\text{g}$  (for V-H<sup>+</sup>-ATPase) of total protein were separated in a 7.5 % polyacrylamide mini-gel (45 min at 180 V) and transferred to a nitrocellulose (NC) membrane using a semi-dry transfer cell (Bio-Rad Laboratories, Inc., USA). Following blocking (5% chicken ovalbumin in 0.5 mol l<sup>-1</sup> Tris-buffered saline (TBS) with 0.1% Triton-X, pH 8.00, overnight at 4°C), the NC membranes were incubated with primary antibodies against either the A-subunit of the V-H<sup>+</sup>-ATPase or NHE2 (1:2500 in blocking buffer) with gentle rocking at 4°C overnight. After four washes with TBS-Triton X (0.2%), the NC membrane was blocked briefly for 15 min, and incubated with the fluorescent secondary antibody (4°C overnight). Bands were visualized and quantified using the Odyssey infra-red imaging system and software (Li-Cor Inc., Lincoln, NE, USA), which allows direct linear quantification of Western blots. After quantification, NC membranes probed against V-H<sup>+</sup>-ATPase were soaked in stripping buffer (50 mmol l<sup>-1</sup> Tris (pH 8.00), 1% SDS, 0.7%  $\beta$ -mercaptoethanol) for 30 min at 60°C to remove the previously used antibodies. After stripping, NC membranes were washed three times with TBS-Triton X (0.2%) (20 min each), blocked for 15 min, and incubated with the primary antibody against Na<sup>+</sup>/K<sup>+</sup>-ATPase following the protocol described above. To correct for differences in loading, protein concentration in each lane was quantified after staining with Coomassie Brilliant Blue. Hence, the amount of V-H<sup>+</sup>-ATPase, Na<sup>+</sup>/K<sup>+</sup>-ATPase and NHE2 in each sample was given by:  $\text{fluorescence}_{\text{antibody}} / \text{fluorescence}_{\text{Coomassie Blue}}$ . Values are presented

relative to the samples from sham-operated fish in each gel. Membranes incubated with blocking buffer without the primary antibody served as controls. These membranes did not show any labeling.

#### *ATPase assays*

Gill membranes were obtained as described above, with the difference that homogenization was performed in ice-cold SEID buffer (200 mmol l<sup>-1</sup> sucrose, 20 mmol l<sup>-1</sup> Na<sub>2</sub>EDTA, 40 mmol l<sup>-1</sup> imidazole, 0.5% Na<sup>+</sup>-deoxycholic acid) (McCormick, 1993). Homogenate (10 µl) from each sample was added to nine wells in a 96-well plate. This provided three treatments for each sample: control, ouabain (500 µmol l<sup>-1</sup>) and ouabain (500 µmol l<sup>-1</sup>) + bafilomycin (50 nmol l<sup>-1</sup>), with triplicate measurements of each treatment. Na<sup>+</sup>/K<sup>+</sup>-ATPase activity was obtained by subtracting the ouabain-treated ATPase activity from control ATPase activity (see McCormick, 1993). V-H<sup>+</sup>-ATPase activity was assessed by calculating the difference in ATPase activity between the ouabain- and the ouabain + bafilomycin-treated, as described in Hawkins *et al.*, 2004. Protein concentration in each well was determined (Pierce, IL, USA) after evaporation of the assay solution (60°C overnight).

#### *Statistics*

All data are given as means ± s.e.m. Differences between groups were tested using one way analysis of variance (1-way ANOVA) or repeated-measures analysis of variance (RM-ANOVA) when appropriate. When RM-ANOVA was used, differences at each sampling time were tested using 1-way ANOVA followed by Dunnet's post test, using the sham-operated or the

NaCl-infused fish as the control treatment. In all cases, the fiducial level of significance was set at  $P < 0.05$ .

## Results

### *i- Blood parameters*

The infusions induced alkalotic and acidotic states in the blood of the experimental fish. The blood pH of base-infused fish (BIF) increased from  $7.80 \pm 0.65$  to  $8.21 \pm 0.26$  pH units after 1 h of infusion, and remained elevated for the rest of the experiment. The blood pH of acid-infused fish (AIF) dropped significantly after 6 h of infusion ( $7.34 \pm 0.14$  pH units), but it recovered to control values by time = 12 h. The blood pH of control fish (NaCl-infused) did not show significant differences throughout the experiment. These results are summarized in figure 2.1A. Total CO<sub>2</sub> (TCO<sub>2</sub>) only changed significantly in the BIF (Fig. 2.1B). It increased from  $3.55 \pm 0.92$  to  $7.43 \pm 0.25$  mmol l<sup>-1</sup> after 1 h, and remained at a significant elevated value for the rest of the experimentation period. The values for TCO<sub>2</sub> in the AIF were almost identical to the control, except for a transient increase at t=12 h ( $4.38 \pm 0.95$  vs.  $3.03 \pm 0.21$  mmol l<sup>-1</sup>). However, the differences between AIF and control fish were not significant at any experimental time. Blood haematocrit, and plasma [Na<sup>+</sup>], [Cl<sup>-</sup>] and osmolarity did not show any significant difference between the treatments or sampling times (Table 2.2).

### *ii- Na<sup>+</sup>/K<sup>+</sup>-ATPase*

Na<sup>+</sup>/K<sup>+</sup>-ATPase abundance in gill cell membranes was significantly increased after acid infusion to  $315 \pm 88$  % of the sham-operated fish (Fig. 2.2A, B). However, Na<sup>+</sup>/K<sup>+</sup>-ATPase activity did not vary significantly among the treatments (Fig. 2.2C), a discrepancy that might be explained by the low

number of samples analyzed (N=4) or by the potential lost of cofactors during sample processing. In all the treatments the number of immunolabeled cells decreased from the trailing to the leading edge region of the gill filaments, with no detectable signal in the latter. In the gill filaments from sham-operated fish and NaCl-infused fish, Na<sup>+</sup>/K<sup>+</sup>-ATPase immunolabeling was mostly found in cells at the interlamellar region, but some sections also showed extensive labeling on the lamella. In AIF and BIF, comparatively more Na<sup>+</sup>/K<sup>+</sup>-ATPase positive cells appear higher on the lamella (Fig. 2.3), but I cannot tell if the differences are real due to high variability in the control fish. The Na<sup>+</sup>/K<sup>+</sup>-ATPase immunostaining was restricted to the basolateral region of the cells in all the treatments, as shown in the higher magnification micrographs in figure 2.4.

### *iii- V-H<sup>+</sup>-ATPase*

V-H<sup>+</sup>-ATPase abundance in the membrane fraction of gills from BIF was 3-fold higher than in gills from the rest of the treatments, as estimated from Western blots (Fig. 2.5A, B). The V-H<sup>+</sup>-ATPase specific activity was also significantly higher in the BIF (Fig. 2.5C). Similarly to Na<sup>+</sup>/K<sup>+</sup>-ATPase, the V-H<sup>+</sup>-ATPase immunoreactive signal decreased from the trailing to the leading edge region, being absent in the latter. This was the case for all the treatments. In sham-operated and NaCl-infused fish, V-H<sup>+</sup>-ATPase immunostaining was concentrated in the interlamellar region of the gills and at the base of the lamella. Qualitatively, there appear to be more V-H<sup>+</sup>-ATPase positive cells in gill sections from AIF and BIF, especially on the lamella (Fig.



2.6). In control and AIF, V-H<sup>+</sup>-ATPase-positive cells showed a diffuse signal throughout the cytoplasm, slightly stronger in the apical region (Fig. 2.7A, B). This sub-cellular localization is similar to that previously described by Wilson *et al.* (1997). Remarkably, the V-H<sup>+</sup>-ATPase immunoreactivity in gills from BIF was distinctly confined to the basolateral region of the cells (Fig. 2.7C).

#### *iv- Colocalization of Na<sup>+</sup>/K<sup>+</sup>-ATPase and V-H<sup>+</sup>-ATPase*

In Atlantic stingray gills, Piermarini and Evans (2001) reported that the cells rich in Na<sup>+</sup>/K<sup>+</sup>-ATPase did not show positive labeling for V-H<sup>+</sup>-ATPase, and *vice-versa*. To address this possibility in the dogfish, I incubated consecutive 4 µm sections with antibodies against either Na<sup>+</sup>/K<sup>+</sup>-ATPase or V-H<sup>+</sup>-ATPase. I then identified cells in both sections, and looked at the localization of the two transporters. I found that most of the Na<sup>+</sup>/K<sup>+</sup>-ATPase-positive cells were different than those that were V-H<sup>+</sup>-ATPase-positive, but I also found a minority of cells where the two transporters were colocalized (Fig. 2.8). No obvious differences could be seen among the treatments.

#### *v- NHE2*

To determine the involvement of a NHE2-like protein in the branchial acid-base regulatory mechanism of the dogfish, I performed quantitative immunoblottings on gill membrane samples from the fish from the various treatments. I found specific ~80 kDA bands in all the treatments, but the relative intensity of the acid-infused was the only significantly different (213 ± 5 % of the sham-operated fish) treatment (Fig. 2.9). I attempted to perform colocalization studies for Na<sup>+</sup>/K<sup>+</sup>-ATPase, V-H<sup>+</sup>-ATPase and NHE2, but,

unfortunately, the anti NHE2-antibody did not work for immunohistochemistry, despite trying some antigen retrievals techniques (pre treatment with 1% SDS, 10 mmol l<sup>-1</sup> citric acid buffer at 97°C).

*vi- Transmission Electron Microscopy (TEM)*

The likely place where V-H<sup>+</sup>-ATPase is located is in mitochondria-rich (MR) cells. Using TEM, I found MR cells in the filament and lamella of fish gills from all the treatments. The MR cell fine structure was similar to the previously reported by Laurent (1984), and Wilson *et al.* (2002), among others. MR cells had an ovoid appearance, with large numbers of mitochondria, long microvilli, abundant subapical vesicles, and numerous basolateral membrane infoldings (Fig. 2.10). Importantly, these infoldings match the basolateral localization of V-H<sup>+</sup>-ATPase in BIF. No qualitative differences in the ultrastructure of MR cells were found in either AIF or BIF.

## Discussion

Infusions of acid and base solutions have been extensively used to study the branchial acid-base regulation in elasmobranchs. These earlier works investigated where the relevant ion fluxes take place, and their magnitude (reviewed by Heisler, 1988). Recent studies have focused on gill  $\text{NH}_4^+$  excretion (Wood *et al.*, 1995), the role of gill carbonic anhydrase (CA) in  $\text{HCO}_3^-$  excretion (Swenson and Maren, 1987), or the involvement of extra cellular CA in  $\text{CO}_2$  excretion (Gilmour *et al.*, 2001). To my knowledge, my study is the first to combine acid and base infusions with immunological techniques to try to elucidate the gill cellular responses to acid-base disturbances. My conclusions are based on the assumption that the extra NaCl that is loaded into the fish blood together with the acidic and base equivalents do not have a major effect on the gill epithelium. This assumption is based on previous research that the gills of dogfish play a minor role (if any) in net salt secretion, being clearly secondary to the rectal gland (Shuttleworth, 1988), and that removal of rectal gland did not induce appreciable change in gill ultrastructure (Wilson *et al.*, 2002). In the current experiment, fish infused with  $500 \text{ mmol l}^{-1}$  NaCl (NaCl-infused fish) did not show any significant differences compared to the sham-operated fish for the variables analyzed. Since plasma osmolarity,  $[\text{Na}^+]$  and  $[\text{Cl}^-]$  remained similar to initial values throughout the infusion periods, I postulate that the extra salt load must have been handled by the rectal gland.

### *Blood acid-base status during infusions*

The rate of acid infusion was of  $495 \pm 79 \mu\text{mol kg}^{-1} \text{h}^{-1}$ . As expected, blood pH showed a tendency to drop, reaching statistical significance after 6 h of infusion,  $\sim 0.45$  pH units lower than at the beginning of the experiment. However, by  $t=12$  h blood pH had recovered to control values, where it remained until the end of the infusions. Moreover, I also found a transient, although not statistically significant, increase in blood  $\text{TCO}_2$  at  $t=12$  h. Put together, this suggests an augmentation in the capacity for acid excretion and  $\text{HCO}_3^-$  reabsorption after 6 h of continuous acid-loading due to increased expression of proteins involved in these mechanisms. Nevertheless, I cannot rule out a contribution of intracellular buffering and net  $\text{H}^+$  transfer into this compartment as a potential mechanism for regulation of extra cellular pH independently of branchial ionic transfers. This is a question that will form the basis for further experimentation.

$\text{HCO}_3^-$  was infused at an even higher rate, roughly twice as much as  $\text{H}^+$  ( $981 \pm 235 \mu\text{mol kg}^{-1} \text{h}^{-1}$ , the rationale for the mismatch is explained in Materials and Methods) producing immediate increases in blood pH and in plasma total  $\text{CO}_2$ . By times 6 and 24 h these parameters equilibrated at  $\sim 8.00$  pH units and  $10 \text{ mmol l}^{-1} \text{CO}_2$ , suggesting that a new steady state status was reached by increased  $\text{HCO}_3^-$  secretion and/or  $\text{H}^+$  reabsorption.

The magnitude of the acid-base disturbances induced by my infusions is severe. However, even greater drops in the blood pH of dogfish have been reported to occur in situations like exhaustive exercise (Richards *et al.*, 2003) and environmental hypercapnia (Claiborne and Evans, 1992). Similarly, Wood

*et al.* (2005) have shown that arterial blood pH increases significantly between 3 and 9 h after feeding. In their study, arterial pH peaked at 8.10 compared to control conditions of 7.90 pH units, values very similar to those obtained in our study.

#### *Ion transporting cell subtypes*

The immunostained sections suggest that there are at least two potential subpopulations of ion-transporting cells in the gills of the dogfish: V-H<sup>+</sup>-ATPase-rich cells and Na<sup>+</sup>/K<sup>+</sup>-ATPase-rich cells, whose roles in acid-base regulation are discussed below. These findings are in agreement with previous research in the Atlantic stingray by Piermarini and Evans (2001), who similarly found independent V-H<sup>+</sup>-ATPase- and Na<sup>+</sup>/K<sup>+</sup>-ATPase-rich cells in the gills. In contrast, I also found a small proportion of cells that labeled positive for both transporters. However, this result must be treated with caution, since these cells may either represent a true subpopulation of cells carrying the two transporters or may represent an artifact of using two antibodies on consecutive sections. Regardless, the relatively small proportion of double-labeled cells likely indicates that, if they represent a true subtype, their role in the branchial acid-base regulation in the dogfish would be of minor importance compared to either the V-H<sup>+</sup>-ATPase- or Na<sup>+</sup>/K<sup>+</sup>-ATPase-rich cells.

#### *Acid secretion*

It is generally accepted that the primary gill acid-secretory mechanism in marine fish involves apical Na<sup>+</sup>/H<sup>+</sup> exchange through specialized gill cells.

This hypothesis is based on the inward directed  $\text{Na}^+$  gradient that fish face in seawater, which could drive acid secretion, and supported by several studies that show the presence of either NHE2- and/or NHE3-like proteins in the gills of hagfish (Choe *et al.*, 2002), squaliform, myliobatiform and rajiform elasmobranchs (Choe *et al.*, 2002; Edwards *et al.*, 2002) and a variety of teleosts (Claiborne *et al.*, 1999; Choe *et al.*, 2002; Wilson *et al.*, 2000a). The increase in NHE2 abundance in my acid-infused fish is evidence for the involvement of this protein in branchial acid secretion in the dogfish. Unfortunately, I was unable to detect its cellular localization as immunohistochemical analysis was not possible. Still, based on numerous studies in both mammalian tissue (see Féraillé and Doucet, 2001) and in other marine fishes (Claiborne *et al.*, 2002; Edwards *et al.*, 2002; Wilson *et al.*, 2000a), I propose that NHE2 in dogfish is also localized on the apical membrane of polarized epithelial cells rich in  $\text{Na}^+/\text{K}^+$ -ATPase. Supporting this theory, I found an increase in abundance of the  $\alpha$ -subunit of the  $\text{Na}^+/\text{K}^+$ -ATPase that after acid infusion, suggesting that  $\text{Na}^+/\text{K}^+$ -ATPase is involved in powering electroneutral apical  $\text{Na}^+/\text{H}^+$  by secondary active transport. In order for this hypothesis to be tested, the generation of specific antibodies for dogfish NHE2 is imperative.

Another mechanism to increase net branchial  $\text{H}^+$  secretion could be to use a V-type  $\text{H}^+$ -ATPase located on the apical membrane. While I found an increased number of V- $\text{H}^+$ -ATPase-rich cells on the lamella of AIF, V- $\text{H}^+$ -ATPase abundance and activity in gill membrane fractions remained

unchanged compared to the control fish. This apparent contradiction could be due to the fact that the V-H<sup>+</sup>-ATPase subcellular localization in AIF and control fish is mainly on cytoplasmic vesicles. My assays for activity and quantity involved differential centrifugation which loses the cytoplasmic fraction, which may explain the discrepancy in our current findings. At this point that it is worth noticing that using V-H<sup>+</sup>-ATPases to extrude protons to seawater, a hypernatric and typically alkaline milieu, seems to be an energetically less convenient alternative than electroneutral Na<sup>+</sup>/H<sup>+</sup> exchange. Regardless, I do see an apparent increase in the number of V-H<sup>+</sup>-ATPase-positive cells after acid infusion, the reasons for this increase remain obscure. It is thus possible that both mechanisms (NHE2 and V-H<sup>+</sup>-ATPase) contribute to acid secretion, like in the proximal tubule and thick ascending limb of the mammalian kidney (reviewed by Gluck and Nelson, 1992).

#### *Base secretion*

The samples from the base-infused fish (BIF) showed an increase in all three variables related to V-H<sup>+</sup>-ATPase tested. Although no statistical analysis was performed, it was apparent that more V-H<sup>+</sup>-ATPase-rich cells were located on the lamella and on the gill filament of BIF compared to control fish, together with a significantly higher V-H<sup>+</sup>-ATPase abundance and activity in gill membranes. The immunostained sections provided further information regarding the involvement of V-H<sup>+</sup>-ATPase in base secretion. In contrast with the rest of the treatments, V-H<sup>+</sup>-ATPase was distinctly confined to the basolateral region of gill cells in the BIF, where extensive basolateral

infoldings are visualized using TEM. To compensate for an alkalosis, excess  $\text{HCO}_3^-$  would need to be secreted by the gills and/or  $\text{H}^+$  retained within the body. I believe that V- $\text{H}^+$ -ATPases insert in the basolateral membrane under alkalotic stress and function to rid the cell of excess  $\text{H}^+$  generated by hydration of  $\text{CO}_2$  by intracellular CA, which is present in dogfish gills (Swenson and Maren, 1987; Wilson *et al.*, 2000b). Furthermore, when gill intracellular CA was selectively blocked in fish made alkalotic by  $\text{NaHCO}_3$  infusion, there was a significant reduction of  $\text{HCO}_3^-$  secretion (Swenson and Maren, 1987), suggesting an involvement in acid-base regulation via an apical anion exchange. Current research in our lab is focused on elucidating the identity of the apical anion exchanger. By analogy to the Atlantic stingray (Piermarini *et al.*, 2002), the most promising lead points to a Pendrin like protein.

In summary, I have established the presence of at least two types of ion-transporting cells,  $\text{Na}^+/\text{K}^+$ -ATPase- and V- $\text{H}^+$ -ATPase-rich cells in the gills of a marine stenohaline elasmobranch. Based on responses to acid and base infusions, I propose that a NHE2-like protein participates in acid secretion, and that basolateral V- $\text{H}^+$ -ATPases are involved in net base secretion.



**Table 2.1.** Acid, base and NaCl infusion rates in each of the infusion treatments. The values are expressed as  $\mu\text{mol kg}^{-1} \text{h}^{-1}$ . N=4.

Infusion	$\text{H}^+$	$\text{HCO}_3^-$	$\text{Na}^+$	$\text{Cl}^-$
250 $\text{mmol l}^{-1} \text{HCO}_3^-$	-	981 $\pm$ 235	1962 $\pm$ 470	981 $\pm$ 235
125 $\text{mmol l}^{-1} \text{HCl}$	495 $\pm$ 79	-	1484 $\pm$ 237	1978 $\pm$ 317
500 $\text{mmol l}^{-1} \text{NaCl}$	-	-	1832 $\pm$ 128	1832 $\pm$ 128

**Table 2.2.** Blood parameters in blood or plasma of the experimental fish at the sampling times. Data are mean  $\pm$  s.e.m. from the combination of NaCl-, acid- and base-infused fish at each time. There were no significant differences between sampling times or treatments. N=12.

<b>Time (h)</b>	<b>Haematocrit (%)</b>	<b>[Na<sup>+</sup>] (mmol l<sup>-1</sup>)</b>	<b>[Cl] (mmol l<sup>-1</sup>)</b>	<b>Osmolarity (mosm l<sup>-1</sup>)</b>
0	15.2 $\pm$ 2.5	246.5 $\pm$ 2.6	273.7 $\pm$ 8.4	968.8 $\pm$ 0.9
1	15.1 $\pm$ 2.1	256.8 $\pm$ 5.6	275.9 $\pm$ 4.3	973.0 $\pm$ 4.0
3	14.7 $\pm$ 2.4	247.0 $\pm$ 7.5	282.0 $\pm$ 2.1	979.1 $\pm$ 8.1
6	13.9 $\pm$ 2.2	259.3 $\pm$ 4.5	279.7 $\pm$ 4.8	958.8 $\pm$ 7.8
12	13.3 $\pm$ 2.5	247.2 $\pm$ 7.2	260.5 $\pm$ 2.4	956.9 $\pm$ 3.4
24	12.6 $\pm$ 2.3	239.2 $\pm$ 11.1	266.8 $\pm$ 11.1	960.2 $\pm$ 8.1

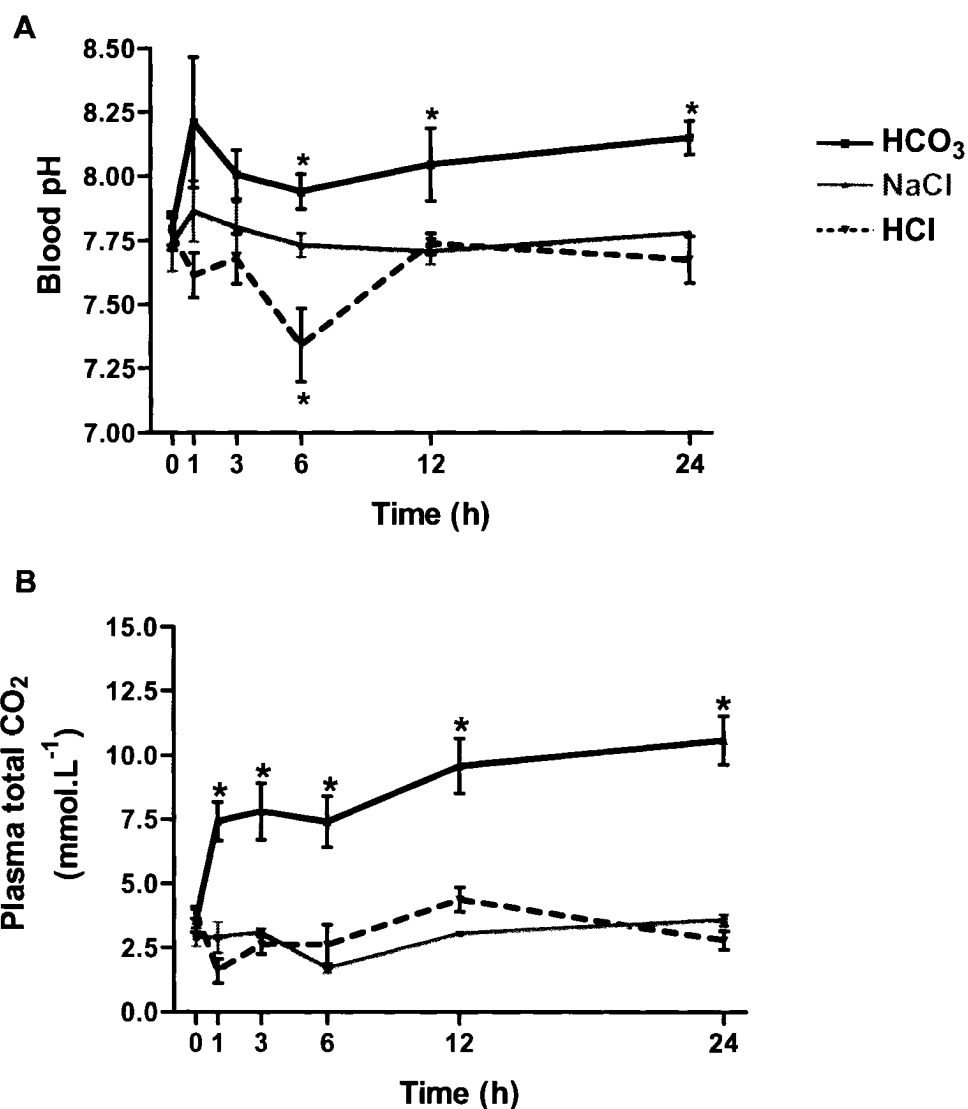


**Figure 2.1.** Blood parameters of fish infused intravenously with either 125 mmol l<sup>-1</sup> HCl (495 ± 79 μmol kg<sup>-1</sup> h<sup>-1</sup>), 250 mmol l<sup>-1</sup> NaHCO<sub>3</sub> (981 ± 235 μmol kg<sup>-1</sup> h<sup>-1</sup>) or 500 mmol l<sup>-1</sup> NaCl (1832 ± 128 μmol kg<sup>-1</sup> h<sup>-1</sup>) (mean ± s.e.m.). A: Arterial blood pH. B: Total CO<sub>2</sub> in plasma from arterial blood samples. \**P*<0.05 compared to the control value (NaCl) of the respective time (RM-ANOVA, 1-way ANOVA, Dunnet's post test). (N=4).

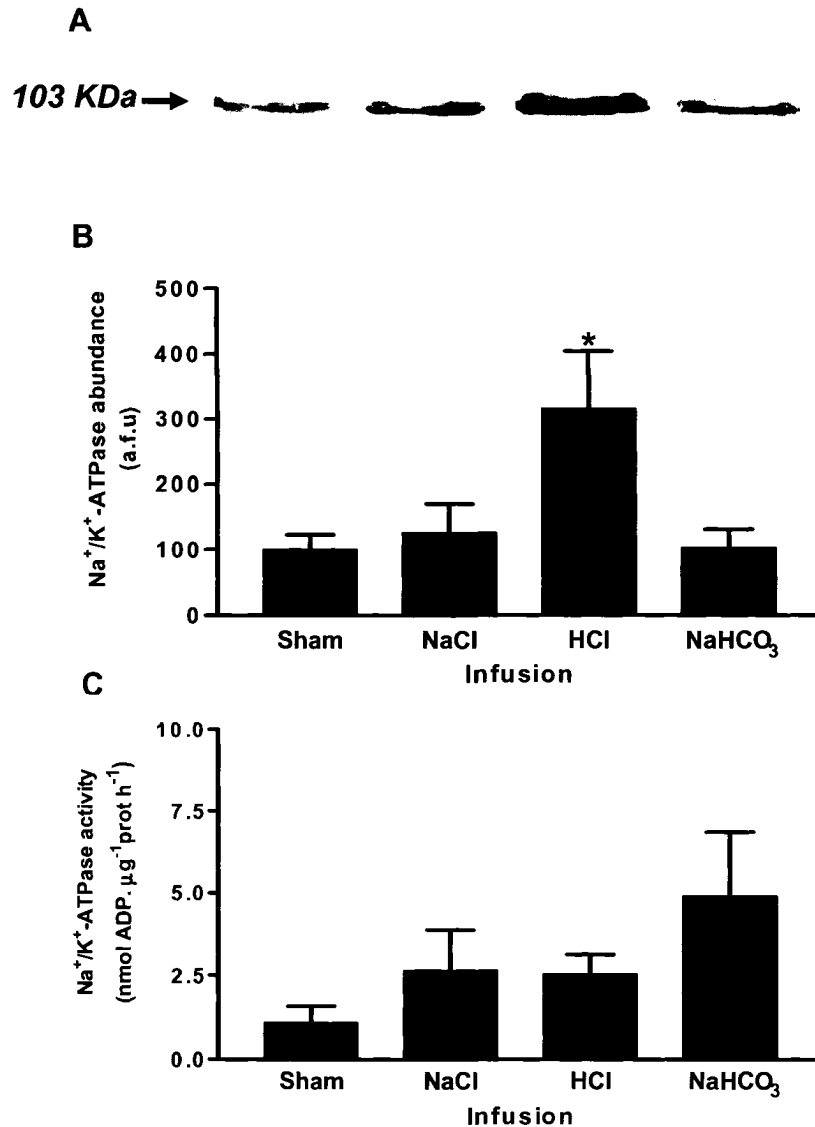


**Figure 2.2.** Na<sup>+</sup>/K<sup>+</sup>-ATPase in the membrane fraction of gills sham-operated, NaCl-, acid- and base-infused fish. *A*: Representative quantitative immunoblotting against the α-subunit of the Na<sup>+</sup>/K<sup>+</sup>-ATPase: a distinct band of ~102.8 kDa was obtained. *B*: Fluorometric analysis revealed that Na<sup>+</sup>/K<sup>+</sup>-ATPase abundance in acid-infused fish increased to 315 ± 88 % of sham-operated fish (100 ± 22 %) (N=4). *C*: Na<sup>+</sup>/K<sup>+</sup>-ATPase activity. No significant differences were found among treatments (N=4). \**P*<0.05 (1-way ANOVA, Dunnet's post test). Results are mean ± s.e.m. a.f.u.: arbitrary fluorometric units.

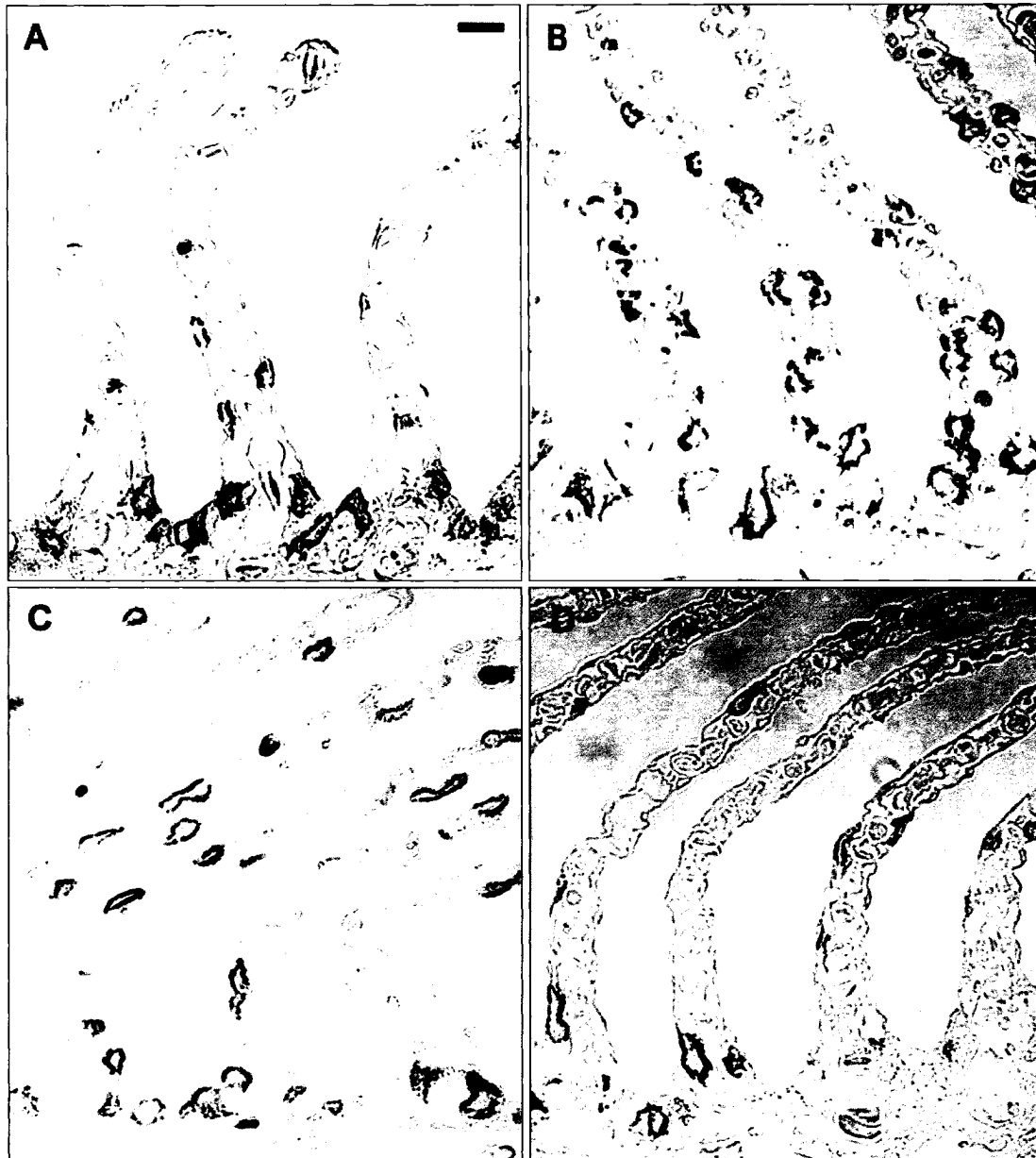


**Figure 2.3.** Representative images of  $\text{Na}^+/\text{K}^+$ -ATPase immunostaining in gills from sham-operated (A), acid-infused (B), base-infused (C), and NaCl-infused (D) fish. The sections were from equivalent regions in the gill filament, near the trailing edge. Note the greater number of labeled cells in the lamella in B and C. Scale bar: 10  $\mu\text{m}$ .

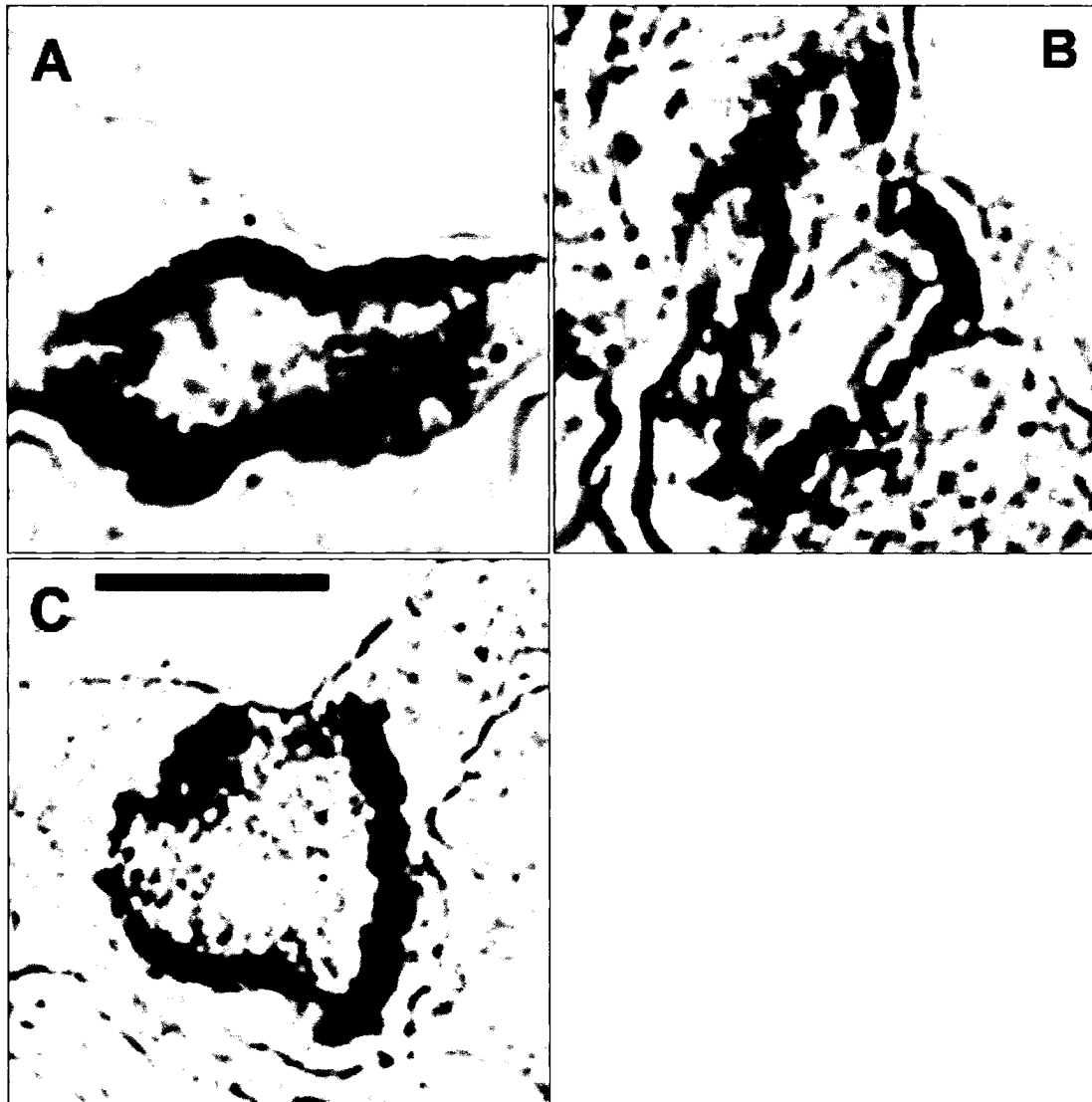


**Figure 2.4.** High magnification LM micrographs showing the Na<sup>+</sup>/K<sup>+</sup>-ATPase subcellular localization in control (A), acid- (B), and base-infused (C) fish. Note that the immunostaining is basolateral in all cases Scale bar: 10  $\mu$ m.

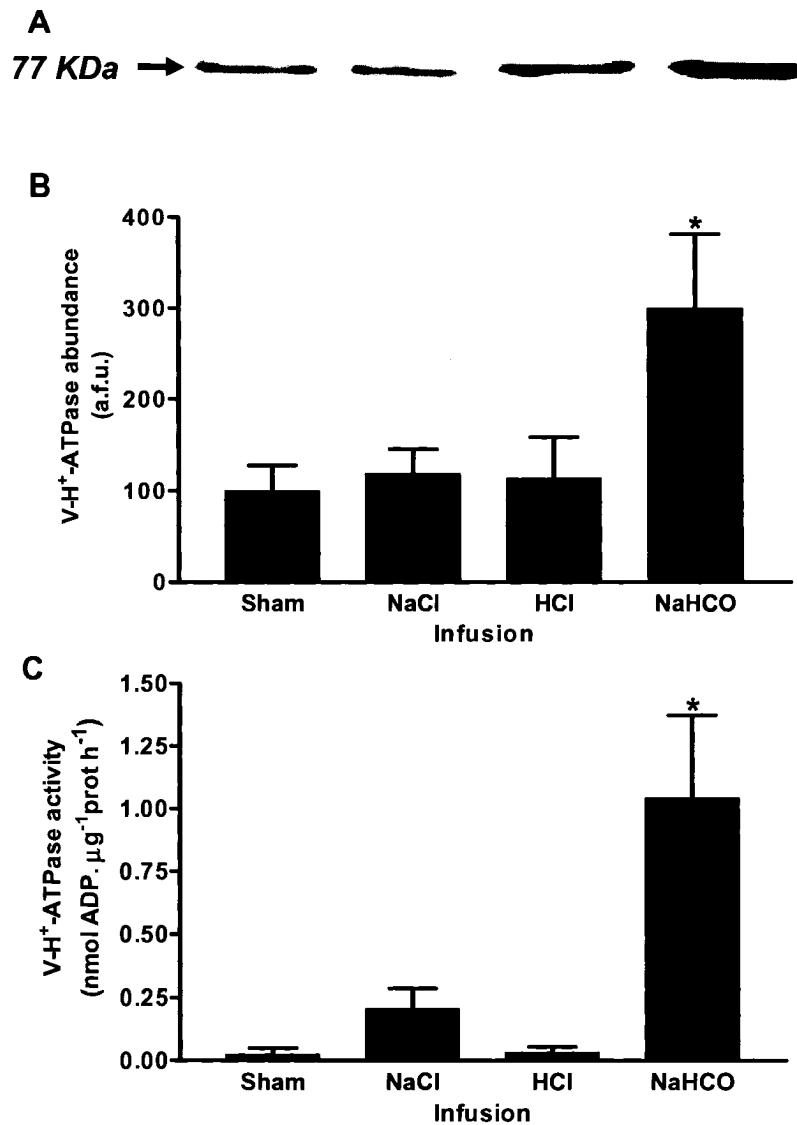


**Figure 2.5.** V-H<sup>+</sup>-ATPase in the membrane fraction of gills of sham-operated, NaCl-, acid- and base-infused fish. **A:** Representative quantitative immunoblotting against the A-subunit of the V-H<sup>+</sup>-ATPase: a distinct band of ~77 kDa was obtained. **B:** Fluorometric analysis revealed that the abundance of the A-subunit of the V-H<sup>+</sup>-ATPase in base-infused fish increased to 300 ± 81 % of sham-operated fish (100 ± 28 %) (N=4). **C:** V-H<sup>+</sup>-ATPase activity increased in concert with **B** (N=4). \**P*<0.05 (1-way ANOVA, Dunnet's post test). Results are mean ± s.e.m. a.f.u.: arbitrary fluorometric units.

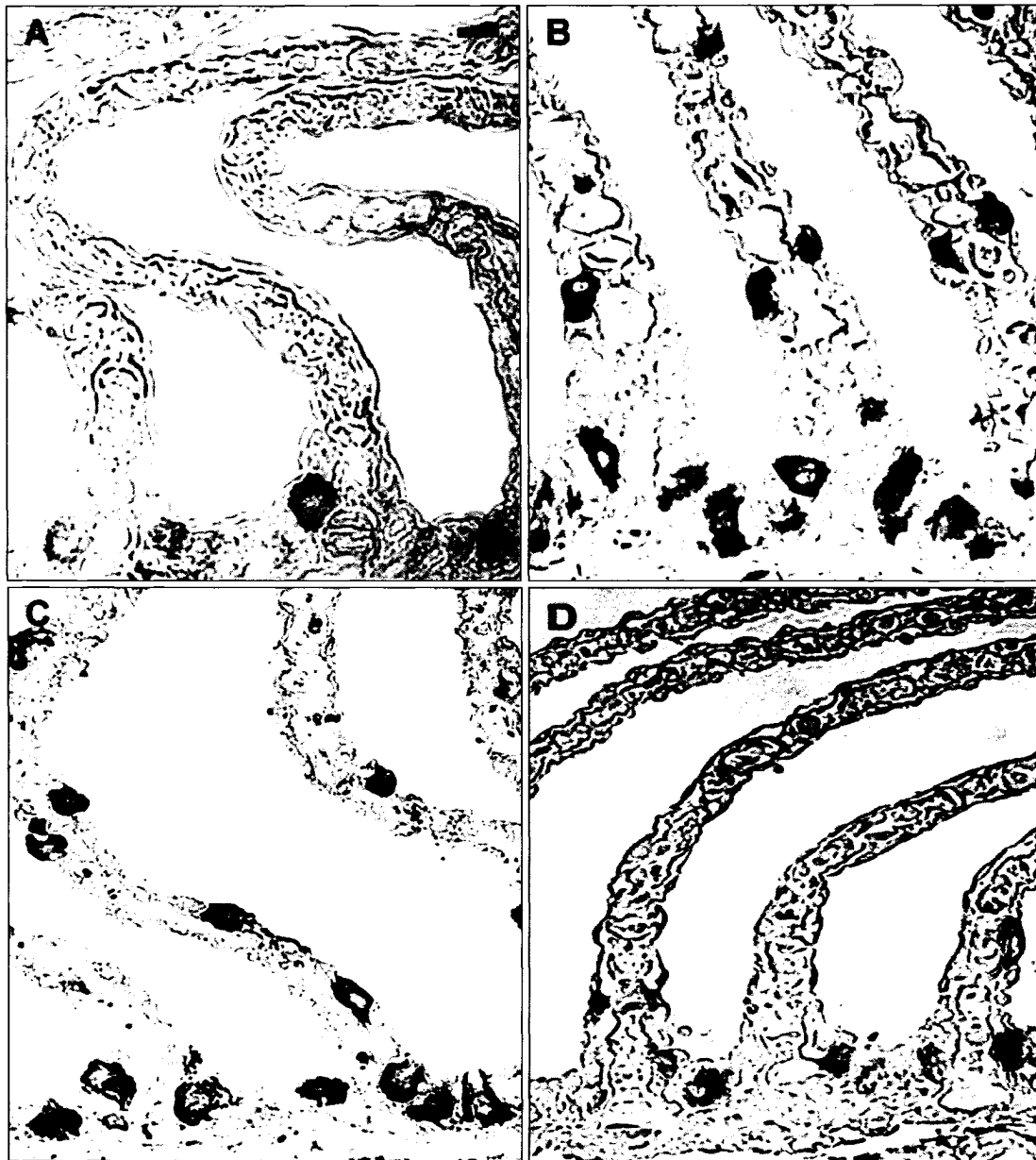


**Figure 2.6.** Representative images of V-H<sup>+</sup>-ATPase immunostaining in gills from sham-operated (A), acid-infused (B), base-infused (C), and NaCl-infused (D) fish. The sections were from equivalent regions in the gill filament, near the trailing edge. Scale bar: 10  $\mu$ m.



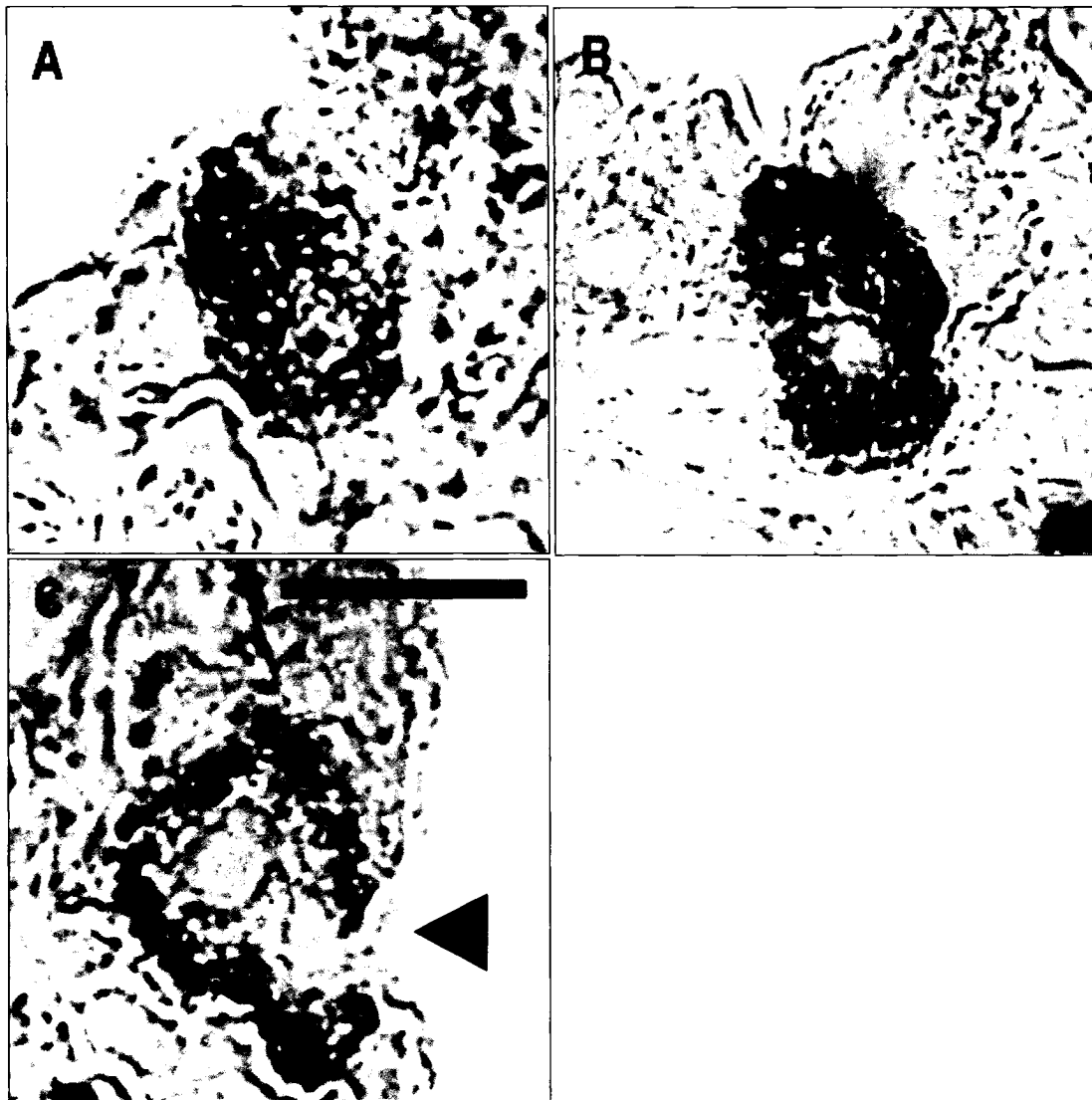


**Figure 2.7.** High magnification LM micrographs showing the V-H<sup>+</sup>-ATPase subcellular localization in control (A), acid- (B), and base-infused (C) fish. Note the distinct immunostaining at the basolateral region and the absence of staining on the apical membrane (arrowhead) in C. Scale bar: 10  $\mu$ m.

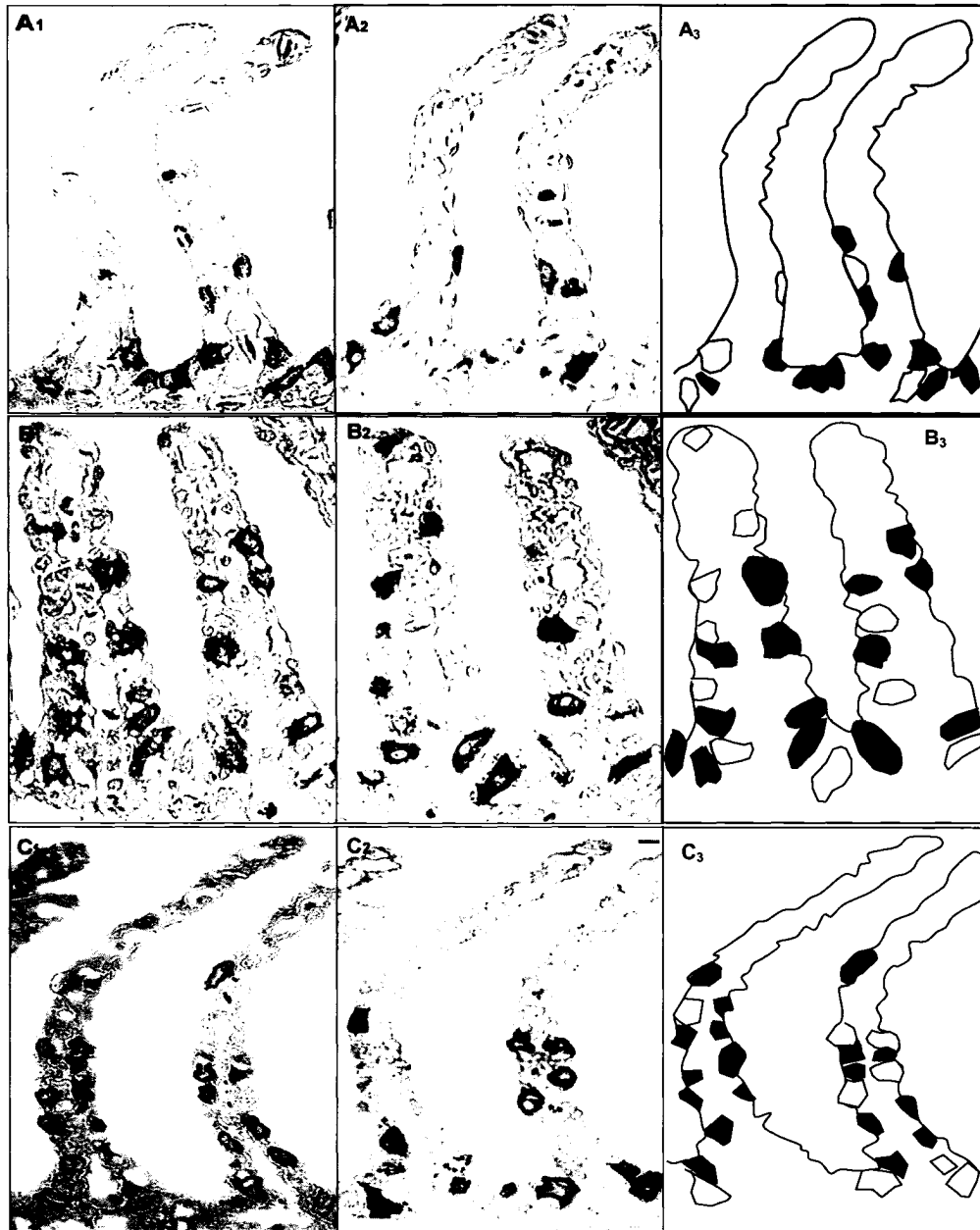


**Figure 2.8.** Immunohistochemistry of consecutive sections from the gill trailing edge from sham operated fish (A), acid-infused fish (B), and base-infused fish (C). The left panel ( $A_1$ ,  $B_1$ ,  $C_1$ ) shows  $\text{Na}^+/\text{K}^+$ -ATPase immunoreactivity, the centre panel ( $A_2$ ,  $B_2$ ,  $C_2$ ) shows  $\text{V-H}^+$ -ATPase immunoreactivity. The third panel ( $A_3$ ,  $B_3$ ,  $C_3$ ) demonstrates the approximate location of each immunostained cell. Cells that labeled positive for  $\text{Na}^+/\text{K}^+$ -ATPase only are in black,  $\text{V-H}^+$ -ATPase only are in white, and cells that labeled positive for both transporters are in grey. Scale bar: 10  $\mu\text{m}$ .

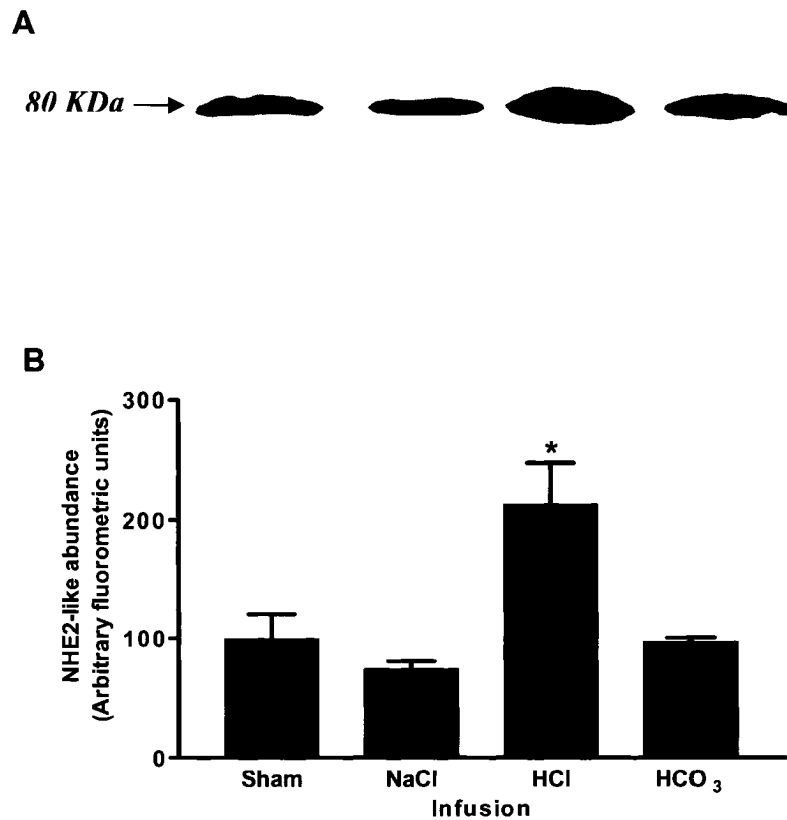


**Figure 2.9.** Quantitative immunoblotting of the membrane fraction of gills of sham-operated, NaCl-, acid- and base-infused fish. *A*: representative immunoblot incubated with anti-NHE2 antibody, showing a distinct band at ~80 KDa. *B*: flourometric analysis showed that the abundance of NHE2 in acid infused fish was  $213 \pm 5$  % of sham-operated fish ( $100 \pm 21$  %).  $N=4$ ;  $*P<0.05$  (1-way ANOVA, Dunnet's post test).

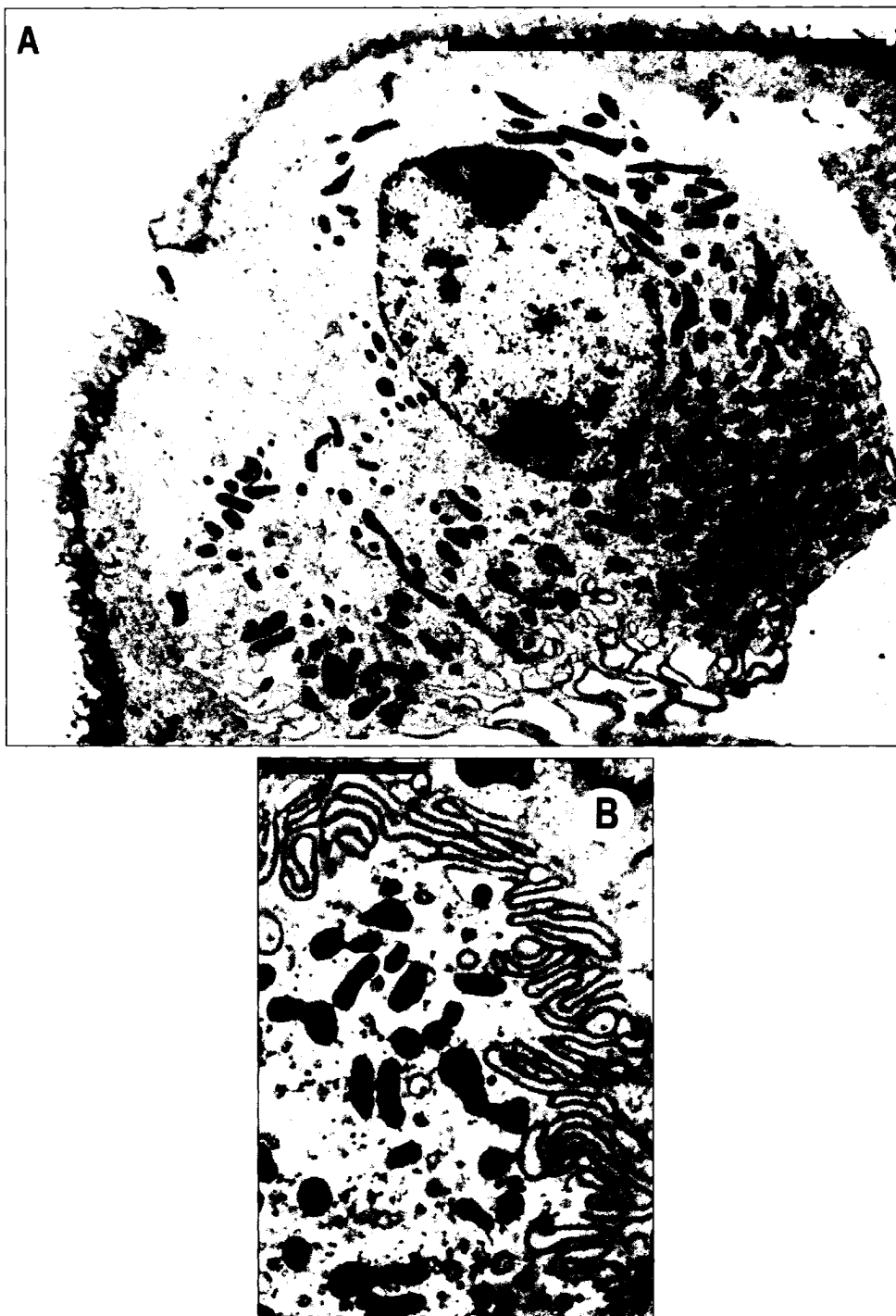


**Figure 2.10.** A: TEM picture of a Mitochondria-Rich (MR) cell located on the lamella of a base infused fish. A detail of the basolateral infoldings is shown in *B*. Scales bars: 10 and 2  $\mu\text{m}$ , respectively.

## References

- Brown, D. and Breton, S.** (1996). Mitochondria-rich, proton-secreting epithelial cells. *J. Exp. Biol.* 199, 2345-2358.
- Burger, J.W. and Hess, W.N.** (1960). Function of the rectal gland in the spiny dogfish. *Science* **131**, 670-671.
- Choe, K. P., Morrison-Shetlar, A. I., Wall, B. P. and Claiborne, J. B.** (2002). Immunological detection of  $\text{Na}^+/\text{H}^+$  exchangers in the gills of a hagfish, *Myxine glutinosa*, an elasmobranch, *Raja erinacea*, and a teleost, *Fundulus heteroclitus*. *Comp. Biochem. Physiol. A.* 131, 375-385.
- Claiborne, J., Blackston, C., Choe, K., Dawson, D., Harris, S., Mackenzie, L. and Morrison-Shetlar, A.** (1999). A mechanism for branchial acid excretion in marine fish: identification of multiple  $\text{Na}^+/\text{H}^+$  antiporter (NHE) isoforms in gills of two seawater teleosts. *J. Exp. Biol.* 202, 315-324.
- Claiborne, J. B., Edwards, S. L. and Morrison-Shetlar, A. I.** (2002). Acid-base regulation in fishes: cellular and molecular mechanisms. *J. Exp. Zool.* 293, 302-319.
- Claiborne, J. B. and Evans, D. H.** (1992). Acid-base balance and ion transfers in the spiny dogfish (*Squalus acanthias*) during hypercapnia: a role for ammonia excretion. *J. Exp. Zool.* 261, 9-17.
- Edwards, S. L., Donald, J. A., Toop, T., Donowitz, M. and Tse, C. M.** (2002). Immunolocalisation of sodium/proton exchanger-like proteins in the gills of elasmobranchs. *Comp. Biochem. Physiol. A.* 131, 257-265.

**Féaille, E. and Doucet, A.** (2001). Sodium-Potassium-Adenosinetriphosphatase-Dependent Sodium Transport in the Kidney: Hormonal Control. *Physiol Rev* 81, 345-418.

**Gilmour, K. M., Perry, S. F., Bernier, N. J., Henry, R. P. and Wood, C. M.** (2001). Extracellular Carbonic Anhydrase in the Dogfish, *Squalus acanthias*: A Role in CO<sub>2</sub> Excretion. *Physiol. Biochem. Zool.* 74, 477-492.

**Gluck, S., Nelson, R., Lee, B., Wang, Z., Guo, X., Fu, J. and Zhang, K.** (1992). Biochemistry of the renal V-ATPase. *J. Exp. Biol.* 172, 219-229.

**Hawkings, G. S., Galvez, F. and Goss, G. G.** (2004). Seawater acclimation causes independent alterations in Na<sup>+</sup>/K<sup>+</sup>- and H<sup>+</sup>-ATPase activity in isolated mitochondria-rich cell subtypes of the rainbow trout gill. *J. Exp. Biol.* 207, 905-912.

**Heisler, N.** (1988). Acid-base regulation. In *Physiology of Elasmobranch Fishes.*, (ed. T. J. Shuttleworth), pp. 215-252. Berlin: Springer-Verlag.

**Kato, F., Hyodo, S. and Kaneko, T.** (2003). Vacuolar-type proton pump in the basolateral plasma membrane energizes ion uptake in branchial mitochondria-rich cells of killifish *Fundulus heteroclitus*, adapted to a low ion environment. *J. Exp. Biol.* 206, 793-803.

**Kato, F. and Kaneko, T.** (2003). Short-term transformation and long-term replacement of branchial chloride cells in killifish transferred from seawater to freshwater, revealed by morphofunctional observations and a

newly established 'time-differential double fluorescent staining' technique. *J. Exp. Biol.* 206, 4113-4123.

**Katoh, F., Shimizu, A., Uchida, K. and Kaneko, T.** (2000). Shift of chloride cell distribution during early life stages in seawater-adapted killifish, *Fundulus heteroclitus*. *Zool. Sci.* 17, 11-18.

**Kirschner, L. B.** (2004). The mechanism of sodium chloride uptake in hyperregulating aquatic animals. *J. Exp. Biol.* 207, 1439-1452.

**Laemmli, U. K.** (1970). Cleavage of structural proteins during the assembly of the head of the bacteriophage T4. *Nature* 227, 680-685.

**Laurent, P.** (1984). Gill internal morphology. In *Fish Physiology*, vol. 10A eds. H. W. S. and D. W. Randall), pp. 73-183. New York: Academic Press.

**McCormick, S. D.** (1993). Methods for non-lethal gill biopsy and measurements of Na<sup>+</sup>/K<sup>+</sup>-ATPase activity. *Can. J. Fish Aquat. Sci.*, 656-658.

**Piermarini, P. M. and Evans, D. H.** (2001). Immunochemical analysis of the vacuolar proton-ATPase B-subunit in the gills of a euryhaline stingray (*Dasyatis sabina*): effects of salinity and relation to Na<sup>+</sup>/K<sup>+</sup>-ATPase. *J. Exp. Biol.* 204, 3251-3259.

**Piermarini, P. M., Verlander, J. W., Royaux, I. E. and Evans, D. H.** (2002). Pendrin immunoreactivity in the gill epithelium of a euryhaline elasmobranch. *Am. J. Physiol. Regulatory Integrative Comp. Physiol.* 283, R983-992.

**Richards, J., Heigenhauser, G. and Wood, C. (2003).** Exercise and recovery metabolism in the Pacific spiny dogfish (*Squalus acanthias*). *J. Comp. Physiol. B* 173, 463-474.

**Shuttleworth, T. J. (1988).** Salt and water balance. Extrarenal mechanisms. In *Physiology of elasmobranch fishes*, (ed. T. J. Shuttleworth), pp. 171-199. Berlin: Springer-Verlag.

**Swenson, E. R. and Maren, T. H. (1987).** Roles of gill and red cell carbonic anhydrase in elasmobranch  $\text{HCO}_3^-$  and  $\text{CO}_2$  excretion. *Am. J. Physiol. Regulatory Integrative Comp. Physiol.* 253, R450-458.

**Wilson, J. M., Morgan, J. D., Vogl, A. W. and Randall, D. J. (2002).** Branchial mitochondria-rich cells in the dogfish *Squalus acanthias*. *Comp. Biochem. Physiol., A*. 132, 365-374.

**Wilson, J., Randall, D., Donowitz, M., Vogl, A. and Ip, A. (2000a).** Immunolocalization of ion-transport proteins to branchial epithelium mitochondria-rich cells in the mudskipper (*Periophthalmodon schlosseri*). *J Exp Biol* 203, 2297-2310.

**Wilson, J. M., Randall, D. J., Vogl, A. W., Harris, J., Sly, W. S. and Iwama, G. K. (2000b).** Branchial carbonic anhydrase is present in the dogfish, *Squalus acanthias*. *Fish Physiol. Biochem.* 22, 329-336.

**Wilson, J. M., Randall, D. J., Vogl, A. W. and Iwama, G. K. (1997).** Immunolocalization of proton-ATPase in the gills of the elasmobranch, *Squalus acanthias*. *J. Exp. Zool.* 278, 78-86.



**Wood, C. M., Part, P. and Wright, P. A.** (1995). Ammonia and urea metabolism in relation to gill function and acid-base balance in a marine elasmobranch, the spiny dogfish (*Squalus acanthias*). *J. Exp. Biol.* 198, 1545-1558.

**Wood, C.M., Kajimura, M., Mommsen, T.P. and Walsh, P.J.** (2005). Alkaline tide and nitrogen conservation after feeding in an elasmobranch (*Squalus acanthias*). *J. Exp. Biol.* 208, 2693-2705.

**Zall, D. M., Fischer, M. D., and Garner, Q. M.** (1956). Photometric determination of chloride in water. *Anal. Chem.* 28, 1665-1678.

## Chapter III

### **Microtubule-dependent relocation of branchial V-H<sup>+</sup>-ATPase to the basolateral membrane in the Pacific spiny dogfish (*Squalus acanthias*): a role in base secretion<sup>1</sup>**

<sup>1</sup>A version of this chapter has been published. **Tresguerres, M.**, Parks, S.K., Katoh, F. and Goss, G.G. (2006). *The Journal of Experimental Biology* 209, 599-609. Reproduced with permission of the Company of Biologists and the co-authors of the manuscript.

## Introduction

The gills of marine elasmobranchs account for over 97% of the acid/base relevant ion fluxes between the animal and the environment (Heisler, 1988). Recently, distinct  $\text{Na}^+/\text{K}^+$ -ATPase- and  $\text{H}^+$ -ATPase-rich cells have been described in the gill epithelia of seawater and seawater-acclimated Atlantic stingrays (*Dasyatis sabina*) (Piermarini and Evans, 2001) and of the Pacific spiny dogfish (*Squalus acanthias*) (Tresguerres *et al.*, 2005; chapter II). Based on analogies to the mammalian kidney,  $\text{Na}^+/\text{K}^+$ -ATPase-rich cells were proposed to be involved in net acid secretion, while V- $\text{H}^+$ -ATPase-rich cells were thought to participate in net base secretion (Piermarini and Evans, 2001). The proposed model for base secretion predicts that  $\text{CO}_2$  from the blood diffuses into the cell, where it is hydrated into  $\text{H}^+$  and  $\text{HCO}_3^-$  by the enzyme carbonic anhydrase (CA).  $\text{HCO}_3^-$  leaves the cell across the apical membrane in exchange for  $\text{Cl}^-$  from the water through an anion exchanger. The  $\text{H}^+$  is then pumped back to the blood by the V- $\text{H}^+$ -ATPase. The coordinated action of these proteins would result in net base secretion (reviewed by Evans *et al.*, 2005). Immunodetection of a Pendrin-like protein, a putative  $\text{Cl}^-/\text{HCO}_3^-$  exchanger, in the apical membrane of the V- $\text{H}^+$ -ATPase-rich cells of the Atlantic stingray provided with the first solid evidence for the involvement of these cells in base secretion (Piermarini *et al.*, 2002). More recently, Pendrin immunoreactivity was also detected in the apical membrane of gill cells of *S. acanthias* (Evans *et al.*, 2004), suggesting that the model may be more widespread among marine elasmobranchs.

However, as explained above, the model for base secretion requires the V-H<sup>+</sup>-ATPase to be located in the basolateral membrane, yet the previous studies on marine elasmobranchs demonstrated a distinct cytoplasmic staining pattern (Piermarini and Evans, 2001; Piermarini *et al.*, 2002; Wilson *et al.*, 1997). Although it was suggested that V-H<sup>+</sup>-ATPase would be recycled between a cytoplasmic pool of vesicles and the basolateral membrane (Piermarini and Evans, 2001), definitive evidence was lacking. In the previous chapter (see also Tresguerres *et al.*, 2005), I demonstrated that induction of blood alkalosis by intravenous infusion of NaHCO<sub>3</sub> for 24h produces a dramatic cellular remodeling in the V-H<sup>+</sup>-ATPase-rich cells involving a switch in the V-H<sup>+</sup>-ATPase localization from primarily cytoplasmic to distinctly basolateral. My results support the hypotheses that the V-H<sup>+</sup>-ATPase-rich cells mediate net base secretion and suggest that trafficking of V-H<sup>+</sup>-ATPase between the cytoplasm and the basolateral membrane indeed exists and it is especially active during blood alkalosis. The current study was designed to investigate whether the cytoskeleton mediated movement of V-H<sup>+</sup>-ATPase from the cytoplasm to the basolateral membrane under alkaline stress is necessary for increased capacity for base secretion. To address this possibility, I repeated my base-infusion protocol (Tresguerres *et al.*, 2005; chapter II) with the addition of colchicine, a plant alkaloid extract that disrupts microtubule assembly and inhibits processes that require an intact cytoskeleton for the relocation of proteins within the cell (Brown, 2000; Stephens and Edds, 1976).

## Materials and methods

### *Animals*

Pacific spiny dogfish (*Squalus acanthias* L) from the Trevor Channel, Vancouver Island, BC, Canada were caught by hook and bait and transferred immediately to the Bamfield Marine Research Centre. Dogfish were held in a 288 m<sup>3</sup> tank provided with flowing seawater (11°C, 31 ppt salinity). The 6 h- and 24 h-infusion experiments were conducted in June and September 2005, respectively. Fish were fed once a week with pieces of dead flounder and squid while being housed in this tank, except for at least one day previous to the experiment.

### *Antibodies and reagents*

The  $\alpha$ -V-H<sup>+</sup>-ATPase antibody and other reagents were the same as in the previous chapter.

### *Surgery and acid-base infusions*

A total of 27 animals (2.31 ± 0.14 kg) were removed from the housing tank and cannulated for this study. Surgery and saline infusions were performed as described in the previous chapter. Animals infused with 500 mmol l<sup>-1</sup> NaCl and treated with colchicine (col-NaCl IF) served as an additional control. Table 3.1 shows the HCO<sub>3</sub><sup>-</sup> and NaCl loads in the 6 and 24 h infusions.

### *Blood samples and analytical procedures on plasma samples*

Arterial blood samples (400 µl) were taken at time 0 and subsequently every 1 hour in the 6 h infusions (N=4), and at times 0, 1, 3, 6, 9, 12, 18 and

24 h in the 24 h infusion experiments (N=5). After the blood extraction, an equal volume of heparanized 500 mmol l<sup>-1</sup> NaCl saline was injected into the fish to minimize changes in blood volume and prevent clotting. A ~50 µl aliquot of blood sample was used for haematocrit analysis. Blood pH was measured using calibrated electrodes (Radiometer G299A, Copenhagen, Denmark or Accumet micro-size pH electrode model 13-620-94, Fisher Scientific, USA). Blood samples were centrifuged at 12000 g to obtain plasma. Plasma total CO<sub>2</sub> (TCO<sub>2</sub>) was measured immediately in samples from the 6 h infusions, while samples from the 24 h experiments were frozen and shipped in a dry-shipper to the University of British Columbia, Vancouver, BC, Canada. TCO<sub>2</sub> was analyzed using a Corning 965 carbon dioxide analyzer (Ciba Corning Diagnostic, Halstead, Essex, England. A plasma aliquot was preserved at -80° C for later analysis of osmolarity (Precision Systems Inc., Natick, MA, USA), Na<sup>+</sup> concentration (atomic absorption spectrophotometer Perkin-Elmer model 3300, Norwalk, CT, USA), and Cl<sup>-</sup> concentration (Zall et al., 1956).

#### *Colchicine treatment*

A fresh colchicine stock solution (10 mg ml<sup>-1</sup>) in 500 mmol l<sup>-1</sup> NaCl was made just before each injection time. Colchicine-treated fish were injected with a bolus dose of 15 mg kg<sup>-1</sup> of colchicine at t=0. A nominal concentration of 10<sup>-4</sup> mmol l<sup>-1</sup> (cf. Maetz and Pic, 1976) in the plasma was targeted. However, colchicine has a half-life in plasma of ~1 h (Moffat, 1986) and therefore we followed the protocol by Gilmour *et al.*, (1998) and injected half

the initial dose every 6 h (at t=6, 12, 18 h). This protocol was applied to the colchicine-treated, base-infused fish (col-BIF) and col-NaCl infused fish. Fish infused with base alone were injected with an equivalent volume of 500 mmol l<sup>-1</sup> NaCl at the same experimental times.

#### *Terminal sampling*

After the blood sample at either 6 or 24 h of infusion, fish were anaesthetized and killed by injection of 5 ml of a saturated KCl solution. Gill samples were immediately excised and either snap frozen in liquid nitrogen for later western blot analyses or placed in fixative (see below) for immunohistochemistry.

#### *Immunohistochemistry*

Immunohistochemistry was performed as described in the previous chapter, with the following modifications. Three consecutive gill filaments were embedded together into paraffin blocks and sectioned every 4 µm. Sections from each block from the trailing edge of the filaments were immunostained and analyzed. For most sections, the secondary antibody and developing method was performed using the Vectastain ABC kit (Vector laboratories, CA, USA), following the manufacture's directions. Some sections were stained using a goat anti-rabbit antibody bound to 5 nm gold particles (BBInternational, Llanislen, Cardiff, UK) for 60 min, followed by silver enhancement method (10 min, same supplier), and a 30 second incubation in Harry's hematoxilin to stain nuclei. Since no qualitative differences were found, results from both methods were combined. Gill sections incubated

without the primary antibody never showed specific staining, regardless of the staining method used.

To detect potential changes in the number of V-H<sup>+</sup>-ATPase-rich cells in the different treatments, we counted the number of labeled cells per intralamellar space (#cells/IL). This was done by analyzing micrographs taken at 400x from randomly selected ILs from at least two gill filaments per fish. The total number of ILs analyzed was 40 in the 6 h infusion experiments, and 50 in the 24 h-infusions. The cellular distribution analysis was performed on 2000x micrographs from around 200 cells per treatment.

#### *Western blot analysis*

Western blotting was performed as described in the previous chapter, with the following modifications. After tissue homogenization and sonication, debris was removed by low speed centrifugation (3000 *g* for 10 min, 4°C), and an aliquot of the supernatant (whole gill homogenate) was stored at -80°C. The rest of the sample was then subjected to a medium speed centrifugation (20800 *g* for 60 min, 4°C) and the pellet was resuspended in homogenization buffer and stored at -80°C as the plasma membrane fraction. This fraction contains almost all the Na<sup>+</sup>/K<sup>+</sup>-ATPase activity as a marker of the basolateral membrane. However, it is unlikely that much of the microsomal fraction is pelleted in this medium speed fraction, because microsomal vesicles are typically not pelleted until much higher forces (~100000 *g*) are encountered. The gill membrane sample from one NaCl-infused, colchicine-treated fish was loaded in every gel and it was used to standardize samples



from different gels. Values are given as arbitrary fluorometric units (a.f.u.). NC membranes incubated with blocking buffer without the primary antibody served as controls, and did not show any labeling.

### *Statistics*

All data are given as means  $\pm$  s.e.m. Differences between groups were tested using one way analysis of variance (1-way ANOVA) or repeated-measures analysis of variance (RM-ANOVA) when appropriate. When RM-ANOVA was used, differences at each sampling time were tested using 1-way ANOVA. For analysis of blood pH and TCO<sub>2</sub> we used Dunnet's post test, using the BIF as the control treatment. In the western blotting and immunohistochemistry analyses I used Bonferroni's post test to compare all treatments. Statistical analysis of H<sup>+</sup>-ATPase cellular staining was performed using the Kruskal-Wallis and Dunns' tests. In all cases, the fiducial level of significance was set at  $P < 0.05$ .

## Results

### *i- 6h-infusions. Blood pH and plasma total CO<sub>2</sub>*

To control for potential effects of colchicine on basal acid/base regulatory processes, I monitored blood pH hourly in dogfish infused with NaCl for 3 h previous to and 6 h after the colchicine injection. As seen in figure 3.1, blood pH in the colchicine-treated, NaCl-infused fish (col-NaCl IF) remained between 7.80 and 7.90, while plasma TCO<sub>2</sub> ranged between 3.38 and 4.20 mmol l<sup>-1</sup> (N=4). I did not find any significant differences in plasma osmolarity, [Na<sup>+</sup>] or [Cl<sup>-</sup>], nor did we notice any changes in fish activity.

Figure 3.1A shows blood pH for the base-infused fish (BIF) and the colchicine-treated, base-infused fish (col-BIF). Both treatments induced a sharp increase in blood pH of ~0.25 pH units after 1 h of infusion, from ~7.90 to ~8.16 pH units. Although blood pH in the BIF had a tendency to drop by 6h (8.07 ± 0.07 pH units), it was not significantly lower than in the col-BIF (8.21 ± 0.03 pH units) (N=4). During t=1-6 h, blood pH in both BI treatments were significantly higher than in the col-NaCl IF (7.82 ± 0.05 pH units at t=6 h).

The TCO<sub>2</sub> graph (Fig. 3.1B) displayed a temporal pattern similar to blood pH: a rapid increase in both BIF and col-BIF followed by plateaus at values significantly higher than in the col-NaCl fish. However, unlike blood pH, TCO<sub>2</sub> in the col-BIF was significantly higher than in the BIF at t=4 and 6 h (11.31 ± 1.41 vs. 6.72 ± 0.44 and 10.34 ± 1.23 vs. 6.42 ± 0.33 mmol l<sup>-1</sup>, respectively).

I did not find any significant differences in any other plasma variables at any of the times analyzed. Osmolarity ranged between 880 and 940 mosmol l<sup>-1</sup>, [Na<sup>+</sup>] was between 230 and 286 mmol l<sup>-1</sup>, and [Cl<sup>-</sup>] values were between 211 and 286 mmol l<sup>-1</sup>.

*ii- 6h-infusions. V-H<sup>+</sup>-ATPase abundance*

In agreement with the previous chapter of this thesis (also see Tresguerres *et al.*, 2005), western analysis for V-H<sup>+</sup>-ATPase revealed a distinct band of ~80 kDA. Fluorometric analysis on whole gill homogenates showed no significant differences in V-H<sup>+</sup>-ATPase abundance between treatments (Fig. 3.2A). However, when the gill membrane fraction was assessed (Fig. 3.2B), I found a significant increase in V-H<sup>+</sup>-ATPase abundance in the BIF (344 ± 125 a.f.u.). The effect of the colchicine treatment on V-H<sup>+</sup>-ATPase migration to the basolateral membrane is apparent at this stage in the col-BIF, since V-H<sup>+</sup>-ATPase abundance in gill membranes from col-BIF and col-NaCl IF were not significantly different from each other (117 ± 22 vs. 72 ± 29 a.f.u., respectively).

*iii) 6h-infusions. Number of V-H<sup>+</sup>-ATPase-rich cells and cellular distribution*

The number of V-H<sup>+</sup>-ATPase-labeled cells in the gill epithelium of dogfish from the different treatments was estimated from low power micrographs (Fig. 3.3 A-C). The number of V-H<sup>+</sup>-ATPase-rich cells per interlamellar space was 4.42 ± 0.77 in the BIF, 4.32 ± 0.92 in the col-BIF, and 3.15 ± 0.37 in the col-NaCl IF. However, the differences were not significant (Fig. 3.3D). Analysis of V-H<sup>+</sup>-ATPase cellular distribution was performed

using high power micrographs (Fig. 3.4 A-C). The cellular distribution of V-H<sup>+</sup>-ATPase was classified into one of three arbitrary patterns: (1) distinct cytoplasmic staining, (2) distinct basolateral staining, and (3) a state intermediate between the former two. Examples of each of these patterns can be found in figure 3.4 A-C. Most cells ( $86.03 \pm 7.72 \%$ ) from col-NaCl IF had cytoplasmic V-H<sup>+</sup>-ATPase staining, a percentage significantly higher than both BIF and col-BIF. The intermediate staining pattern was found in 45% of the cells from col-BIF, 30% of cells from BIF, and only ~9% of cells from col-NaCl IF. Almost 57% of the cells from BIF showed a distinct basolateral location, significantly higher than the ~24% found in the col-BIF, and the scarce ~5% in the col-NaCl IF. Table 3.2 shows the average percentages for the three groups, together with a detailed statistical analysis. These results are in agreement with the general trend for greater V-H<sup>+</sup>-ATPase abundance found in gill membranes from BIF.

*iv- 24h-infusions. Blood pH and plasma total CO<sub>2</sub>*

Figure 3.5A shows blood pH in the 24h infusion experiments. In the first 6 h of the 24 h-infusions, blood pH in all the treatments behaved identically to the 6 h infusions described above. Even by t=9 h, pH in the col-BIF was higher than in the BIF, although not statistically significant. However, from t=12 h onward, blood pH from the col-BIF was found to be significantly more alkalotic than in the BIF, an effect that was greatest at t=24 h ( $8.33 \pm 0.06$  vs.  $8.02 \pm 0.03$  pH units). Blood pH in the col-NaCl IF was relatively stable throughout the infusions, with values between  $7.78 \pm 0.02$  and  $7.91 \pm$

0.03 pH units. These values were significantly lower than the BIF and col-BIF from t=1 until the end of the experiments.

In this experimental series,  $\text{TCO}_2$  from col-BIF was significantly higher than in BIF at 3 h ( $11.80 \pm 1.99$  vs.  $6.90 \pm 0.93$  mmol  $\text{l}^{-1}$ ), and 6 h ( $13.12 \pm 3.10$  vs.  $5.60 \pm 0.84$  mmol  $\text{l}^{-1}$ ). While the difference in  $\text{TCO}_2$  between col-BIF and BIF was reduced at t=9 and 12h, it became statistically significant again at t=18 and 24 h. At 24 h,  $\text{TCO}_2$  in the col-BIF was  $15.72 \pm 3.29$  mmol  $\text{l}^{-1}$ , compared to  $6.74 \pm 1.34$  mmol  $\text{l}^{-1}$  in the BIF. Col-NaCl IF had lower and very stable  $\text{TCO}_2$  values, which ranged between  $3.52 \pm 0.40$  and  $4.16 \pm 0.39$  mmol  $\text{l}^{-1}$ . Importantly,  $\text{TCO}_2$  from BIF and col-NaCl IF did not significantly differ at 24h (Fig. 3.5B). Plasma osmolarity,  $[\text{Na}^+]$  and  $[\text{Cl}^-]$  remained stable for the experimentation period (not shown).

*v- 24h-infusions. V-H<sup>+</sup>-ATPase abundance*

V-H<sup>+</sup>-ATPase from BIF gill samples was more abundant than in col-NaCl IF, both in whole gill homogenates ( $198.4 \pm 38.9$  vs.  $68.5 \pm 17.0$  a.f.u.) and in the gill membrane-enriched fraction ( $574.6 \pm 168.1$  vs.  $49.0 \pm 10.6$  a.f.u.). This suggests an additional response (i.e. protein synthesis) to the V-H<sup>+</sup>-ATPase translocation to the basolateral membrane observed in BIF from the 6 h infusion experiments. Whole gill samples from col-BIF showed a response that was intermediate between BIF and col-NaCl IF. Similar to the 6 h infusions, colchicine prevented the movement of V-H<sup>+</sup>-ATPase to the basolateral membrane in the col-BIF, since V-H<sup>+</sup>-ATPase abundance in the

gill membrane fraction was not significantly different than in the col-NaCl IF ( $155.5 \pm 51.3$  vs.  $49.0 \pm 10.6$  a.f.u., respectively) (Fig. 3.6).

*vi- 24h-infusions. Number of V-H<sup>+</sup>-ATPase-rich cells and cellular distribution*

Figure 3.7 shows representative images of gill sections from the three experimental groups. While we found a tendency for roughly one more V-H<sup>+</sup>-ATPase-immunoreactive cell per interlamellar space in the BIF and col-BIF compared to the col-NaCl IF ( $5.01 \pm 0.73$ ,  $4.97 \pm 0.32$ , and  $3.75 \pm 0.82$  cells/IL, respectively) (Fig. 3.7D), the difference was not significant.

The cellular V-H<sup>+</sup>-ATPase staining pattern was fairly homogeneous in the col-NaCl IF, where over 91% of the cells had cytoplasmic staining, and in the BIF, with 84% of cells showing a distinctly basolateral staining pattern. The staining pattern in the col-BIF was unique, with an in-between percentage of cells with cytoplasmic and basolateral staining patterns, but with more cells displaying the intermediate pattern (~44% of cells vs. ~10% in both the BIF and col-NaCl IF). Representative pictures and a summary of the staining patterns are shown in figure 3.8 and table 3.3, respectively.

## Discussion

Microtubule-dependent translocation of V-H<sup>+</sup>-ATPase from the cytoplasm to the cell membrane has been demonstrated for a variety of mammalian ion-transporting epithelia, most notably the kidney (reviewed by Wagner *et al.*, 2004). In particular, microtubules have been shown to mediate the translocation of V-H<sup>+</sup>-ATPase to the apical membrane of renal tubule intercalated cells (IC) in response to a variety of stimuli, including acid incubation (Schwartz *et al.*, 2002), angiotensin II (Wagner *et al.*, 1998), and aldosterone (Winter *et al.*, 2003). Microtubules also determine the constitutive apical and basolateral localization of V-H<sup>+</sup>-ATPase in the acid-secreting (A-type) and in the base-secreting (B-type) IC, respectively (Brown *et al.*, 1991). Contrary to the mammalian kidney, information about ion-transporting processes that rely on an intact cytoskeleton to mediate V-H<sup>+</sup>-ATPase relocation is much scarcer in other animal taxonomic groups. Some exceptions include urinary acidification in the turtle bladder (Gluck *et al.*, 1982) and ammonia excretion across crustacean gills (Weihrauch *et al.*, 2002). I could not find any references specifically linking V-H<sup>+</sup>-ATPase translocation to microtubules in any group of fishes (teleosts, elasmobranchs, etc.). However, the use of colchicine in fish transport physiology includes salt secretion in the seawater adapted grey mullet *Mugil capito* (Maetz and Pic, 1976), urea excretion in the Gulf toadfish *Opsanus beta* (Gilmour *et al.*, 1998), and calcium uptake in larvae of tilapia, *Oreochromis mossambicus* (Tsay and Hwang, 1998).

My results suggest that upregulation of branchial base secretion in the dogfish depends on the microtubule-dependent translocation of V-H<sup>+</sup>-ATPase to the basolateral membrane. When this process is prevented by colchicine, it correlates with increased blood pH and TCO<sub>2</sub>, indicating an impaired capacity to secrete excess base. The sections immunostained against V-H<sup>+</sup>-ATPase confirmed the inhibitory effect of colchicine on V-H<sup>+</sup>-ATPase translocation to the basolateral membrane. Originally, I intended to classify the staining patterns into either cytoplasmic or basolateral. Although most of the cells from the col-NaCl IF fit into the first and the majority of cells from BIF fit into the second category, some cells displayed an intermediate staining pattern and were classified into a third category. I believe that this nicely illustrates the dynamic aspects of the V-H<sup>+</sup>-ATPase translocation process, whereby there is a continuum of staining patterns between cytoplasmic and distinctly basolateral.

If the effect the colchicine was completely effective, I would expect a predominant cytoplasmic staining in the col-BIF. However, I found that the intermediate pattern showed the highest frequency. Also, based on the infusion rates, I might predict higher elevations in pH and TCO<sub>2</sub> if base secretion was totally impaired. Put together, these data suggest that colchicine only had a partial effect on blocking the V-H<sup>+</sup>-ATPase translocation to the basolateral membrane. Interestingly, microtubule-disrupting drugs only inhibit between 50 and 70% of acid and base secretion by A-type and B-type Ics (Brown and Stow, 1996). These authors suggested that random vesicle



movement resulted in fusion of V-H<sup>+</sup>-ATPase-containing vesicles to the appropriate target membrane.

Western blotting and immunohistochemistry analyses indicate that the base secretory mechanism that allows BIF to regulate blood pH and TCO<sub>2</sub> despite continuous infusion of HCO<sub>3</sub><sup>-</sup> includes two components. In the short term (6 h), the pool of V-H<sup>+</sup>-ATPase already present in cytoplasmic vesicles moves to the basolateral membrane in a microtubule-dependent manner. In the longer term (24 h), there is an additional upregulation in the synthesis of V-H<sup>+</sup>-ATPase as demonstrated by increased abundance in the whole gill homogenates. Since the number of V-H<sup>+</sup>-ATPase-rich cells per interlamellar space did not differ between treatments, I suggest that this increase takes place in already existing V-H<sup>+</sup>-ATPase-rich cells rather than being due to the appearance of new base-secreting cells. However, the samples used for V-H<sup>+</sup>-ATPase-rich cell enumeration were only from the trailing edge of gill filaments. I cannot discount the possibility that the number of V-H<sup>+</sup>-ATPase-rich cells in other parts of the filament increases after 24 h of infusion, which could be contributing to the steep increase in V-H<sup>+</sup>-ATPase abundance found in 24 h BIF.

The presence of specialized base-secreting cells in the gill epithelium of marine elasmobranchs is well supported by this and other studies. Gill V-H<sup>+</sup>-ATPase-rich cells have the apical anion exchanger Pendrin (Piermarini *et al.*, 2002; Evans *et al.*, 2004) and cytoplasmic V-H<sup>+</sup>-ATPase-containing vesicles (Wilson *et al.*, 1997; Piermarini and Evans, 2001; Piermarini *et al.*,

2002, Choe *et al.*, 2005; Tresguerres *et al.*, 2005; chapter II). When blood gets alkalotic, V-H<sup>+</sup>-ATPase inserts to the basolateral membrane in a microtubule-dependent manner to mediate base secretion, thus contributing to restore blood pH to normal values. In this configuration, the V-H<sup>+</sup>-ATPase-rich cells closely resemble the B-type IC from the mammalian kidney. Continuous alkalotic stress induces an upregulation in the synthesis of V-H<sup>+</sup>-ATPase units. The model for the V-H<sup>+</sup>-ATPase-rich cell also includes cytoplasmic carbonic anhydrase (CA) to catalyze the conversion of CO<sub>2</sub> into HCO<sub>3</sub><sup>-</sup> and H<sup>+</sup>, the substrates for V-H<sup>+</sup>-ATPase and Pendrin, respectively. The involvement of CA in branchial base secretion has been documented as early as 1955 by Hodler *et al.*, and confirmed by later studies (e.g. Swenson and Maren, 1987). Furthermore, CA II-like immunoreactivity has been detected in mitochondria-rich (MR) cells of the dogfish gill epithelium (Wilson *et al.*, 2000), although it has not been demonstrated if CA colocalizes with V-H<sup>+</sup>-ATPase and/or Pendrin in the same type of MR cells. I predict that V-H<sup>+</sup>-ATPase-rich cells should also have a chloride channel in the basolateral membrane to move Cl<sup>-</sup> that enters the cell through the apical membrane into the blood. This Cl<sup>-</sup> current would be essential to compensate for the inside-negative transmembrane potential generated by the V-H<sup>+</sup>-ATPase (c.f. Wagner *et al.*, 2004). A model for base secretion in V-H<sup>+</sup>-ATPase-rich cells is illustrated in figure 3.9.

The correlation between V-H<sup>+</sup>-ATPase localization and recovery from the alkalotic stress found in the current study is very strong. However, we

must also consider that colchicine might also affect other cellular components that might act directly or indirectly on the base secreting properties of the animal. An example of a possible direct effect would be that microtubule disruption affects the trafficking of the apical anion exchanger. Alternatively, our results may be explained by a non-target effect on a cell type elsewhere in the body whereby colchicine affects hormone release which in turn alters the mechanism of base secretion. Unfortunately, nothing is known about the hormonal pathways involved in acid/base regulation in fish, so I am unable to either control for or discuss this topic further. Nonetheless, it must be kept in mind that factors other than microtubule-dependent V-H<sup>+</sup>-ATPase redistribution might be responsible for the reduced ability to recover for an alkalotic load. Nonetheless, my results demonstrate that microtubule-dependent translocation of V-H<sup>+</sup>-ATPase from the cytoplasm to the cell membrane is associated with enhanced secretion of HCO<sub>3</sub><sup>-</sup> across the gills of dogfish.

In summary, my results strongly suggest that blood alkalosis induces the translocation of gill V-H<sup>+</sup>-ATPase from cytoplasmic vesicles to the basolateral membrane in a microtubule-dependent manner. Based on the effect of colchicine on blood pH and plasma total CO<sub>2</sub> from base-infused fish, and on the predominant role that the gills have on dogfish base secretion over other organs (Hodler *et al.*, 1955; Heisler, 1988) I propose that this process is essential for branchial transepithelial base secretion and maintenance of blood pH within homeostatic limits.

**Table 3.1.** Base and NaCl infusion rates in each of the infusion treatments. The values are expressed as  $\mu\text{mol kg}^{-1} \text{h}^{-1}$ .

	Infusion	[HCO <sub>3</sub> <sup>-</sup> ]	[Na <sup>+</sup> ]	[Cl <sup>-</sup> ]
6h N=4	Col-NaCl	-	2546 ± 501	2546 ± 501
	BIF	964 ± 63	1928 ± 107	964 ± 63
	Col-BIF	1055 ± 69	2111 ± 139	1055 ± 69
24h N=5	Col-NaCl	-	2415 ± 417	2415 ± 417
	BIF	1081 ± 108	2162 ± 216	1081 ± 108
	Col-BIF	1152 ± 124	2304 ± 248	1152 ± 124

**Table 3.2.** 6 h-infusions. V-H<sup>+</sup>-ATPase staining patterns in gills from colchicine-treated, NaCl infused (col-NaCl IF), base-infused (BIF) and colchicine-treated, base-infused fish (col-BIF). The letters indicate difference levels of statistical significance (Kruskal-Wallis test, Dunns' post test). Results are mean  $\pm$  s.e.m.

	<b>Cells (n)</b>	<b>Cytoplasmic (%)</b>	<b>Intermediate (%)</b>	<b>Basolateral (%)</b>
Col-NaCl	202	86.03 $\pm$ 7.72 <sup>a</sup>	8.62 $\pm$ 5.26 <sup>a</sup>	5.36 $\pm$ 3.42 <sup>a</sup>
BIF	241	13.42 $\pm$ 5.13 <sup>b</sup>	29.63 $\pm$ 11.07 <sup>a,b</sup>	56.95 $\pm$ 13.42 <sup>b</sup>
Col-BIF	208	31.47 $\pm$ 5.51 <sup>b</sup>	44.90 $\pm$ 5.42 <sup>b</sup>	23.63 $\pm$ 6.30 <sup>a</sup>

**Table 3.3.** 24 h infusions. V-H<sup>+</sup>-ATPase staining patterns in gills from colchicine-treated, NaCl infused (col-NaCl IF), base-infused (BIF) and colchicine-treated, base-infused fish (col-BIF). The letters indicate difference levels of statistical significance (Kruskal-Wallis test, Dunns' post test). Results are mean  $\pm$  s.e.m.

	<b>Cells (n)</b>	<b>Cytoplasmic (%)</b>	<b>Intermediate (%)</b>	<b>Basolateral (%)</b>
Col-NaCl	212	90.9 $\pm$ 4.49 <sup>a</sup>	9.72 $\pm$ 5.09 <sup>a</sup>	3.33 $\pm$ 3.33 <sup>a</sup>
BIF	393	4.94 $\pm$ 1.06 <sup>b</sup>	10.83 $\pm$ 1.54 <sup>a</sup>	84.22 $\pm$ 2.29 <sup>b</sup>
Col-BIF	324	32.50 $\pm$ 4.03 <sup>c</sup>	43.69 $\pm$ 6.92 <sup>b</sup>	23.82 $\pm$ 4.97 <sup>c</sup>

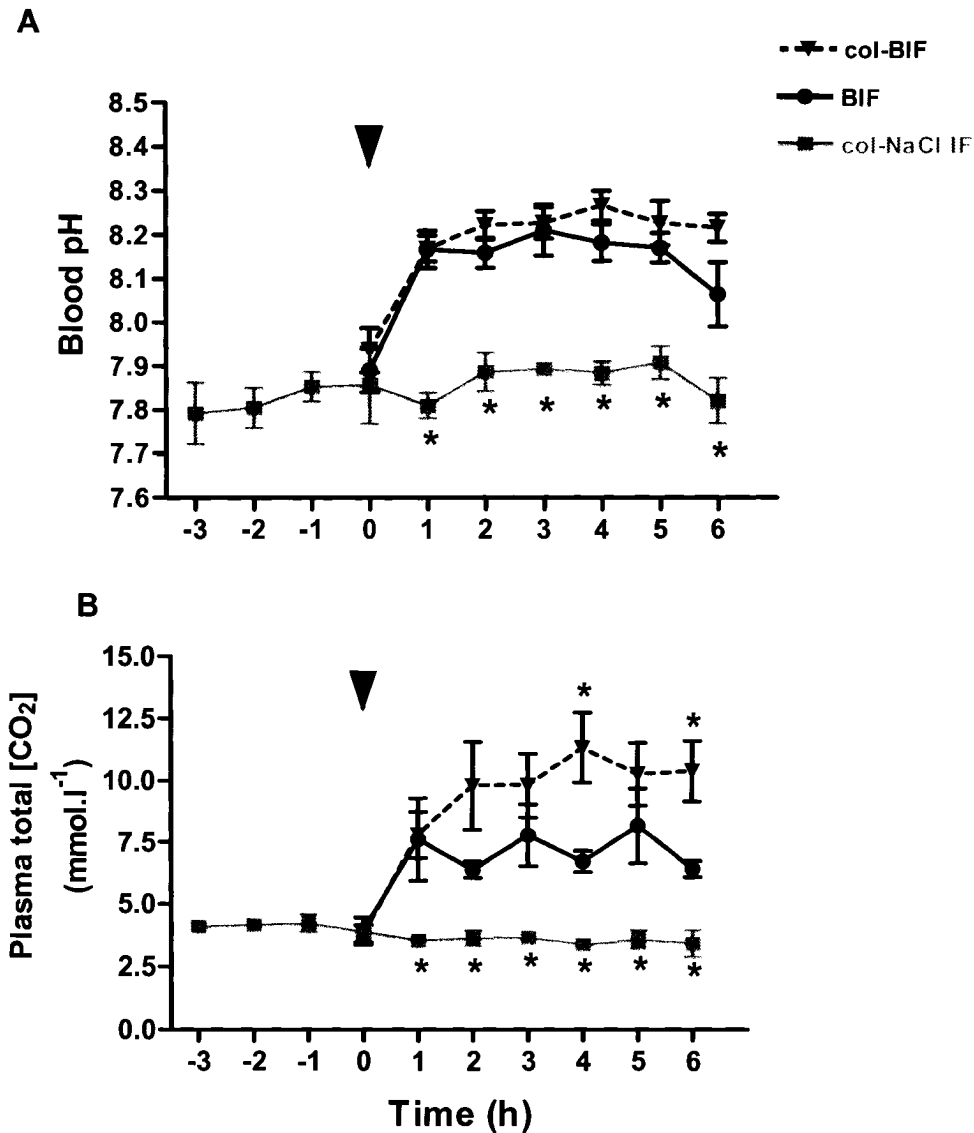


**Figure 3.1.** 6 h infusions. Blood parameters of colchicine-treated NaCl-infused fish, HCO<sub>3</sub><sup>-</sup> infused fish, and colchicine-treated HCO<sub>3</sub><sup>-</sup> infused fish (mean ± s.e.m.). *A*: Arterial blood pH. *B*: Total CO<sub>2</sub> in plasma from arterial blood samples. The arrowhead indicates injection of colchicine (15 mg kg<sup>-1</sup>). \**P*<0.05 compared to base-infused fish of the respective time (RM-ANOVA, 1-way ANOVA, Dunnet's post test). (N=4).

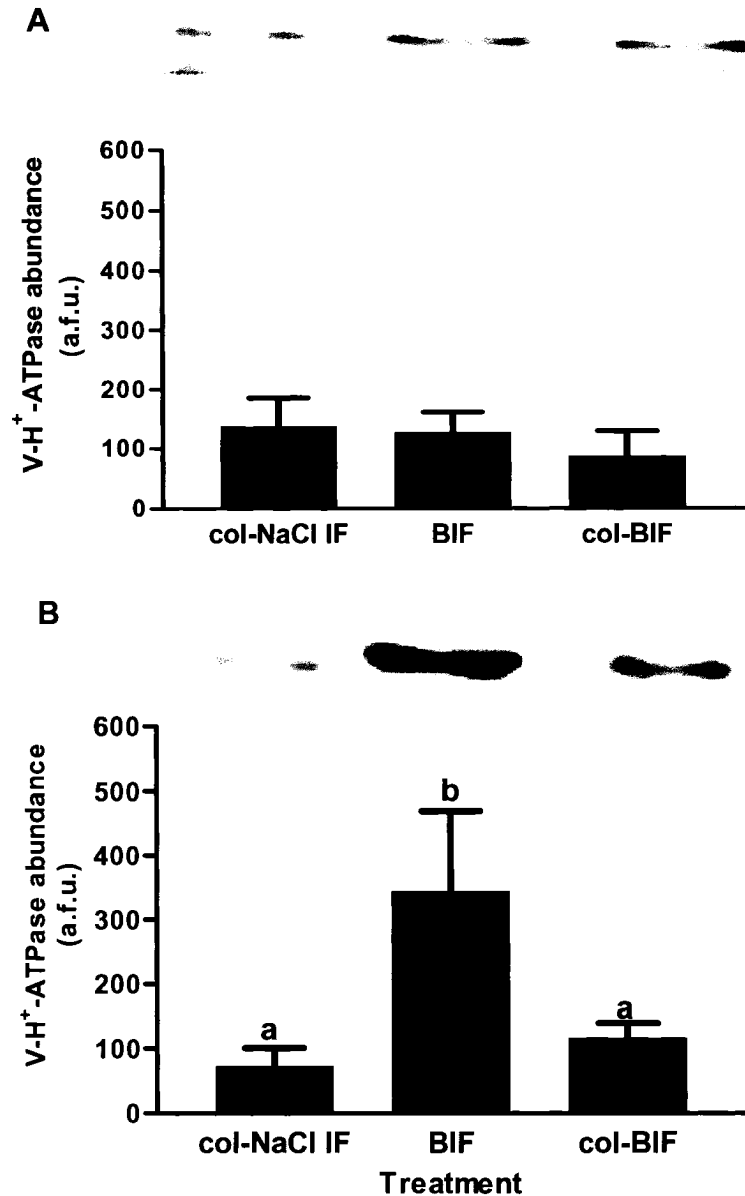


**Figure 3.2.** 6 h infusions. Quantitative analysis of V-H<sup>+</sup>-ATPase in gills from colchicine-treated, NaCl infused (col-NaCl IF), base-infused (BIF) and colchicine-treated, base-infused fish (col-BIF). *A*: Whole gill homogenates. *B*: Membrane fraction. V-H<sup>+</sup>-ATPase abundance was significantly greater only in the membrane fraction of BIF (N=4). Representative immunoblots are shown above each panel. The letters indicate difference levels of statistical significance (1-way ANOVA, Bonferroni's post test). Results are mean  $\pm$  s.e.m. a.f.u.: arbitrary fluorometric units.



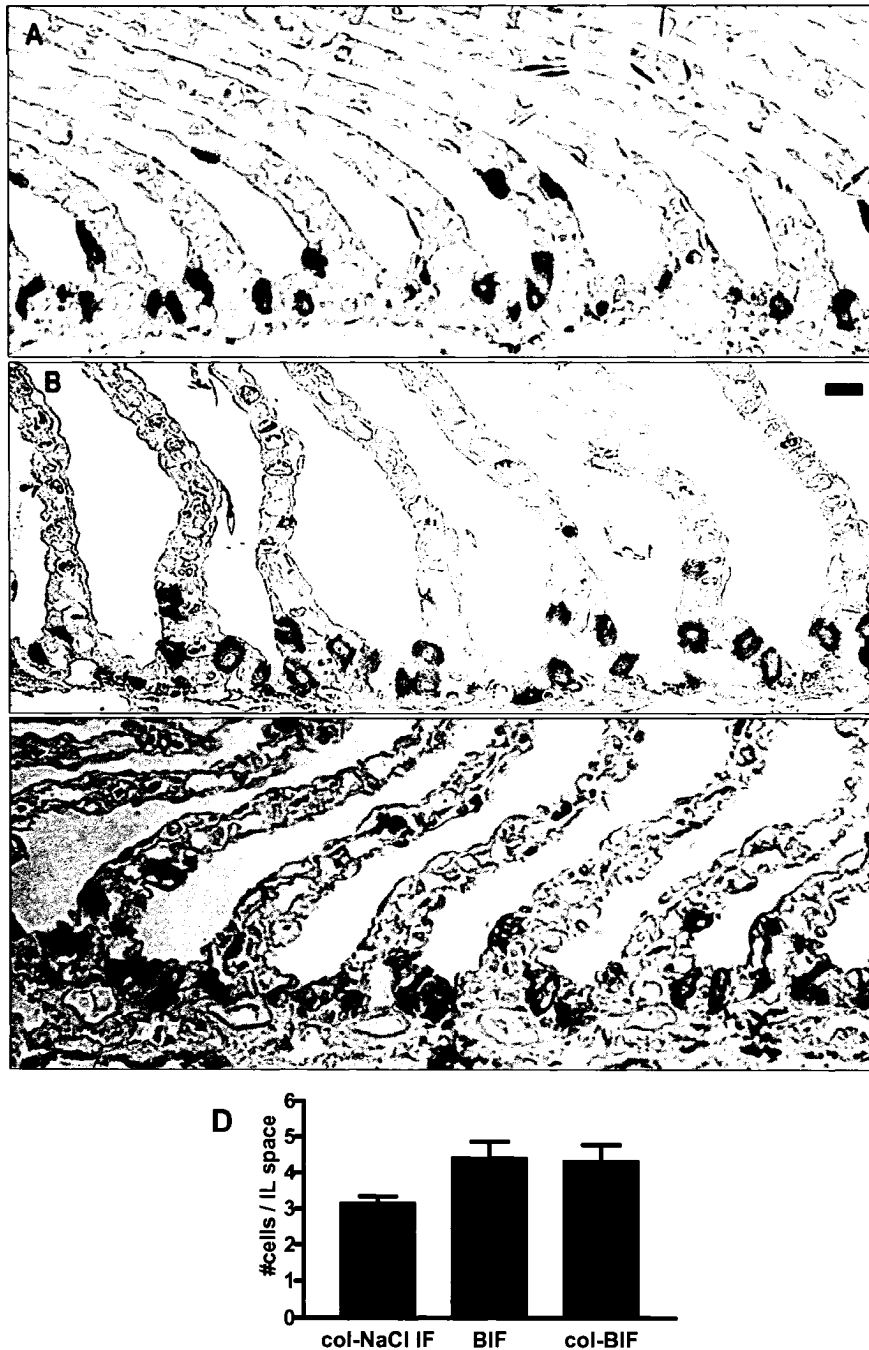


**Figure 3.3.** 6 h infusions. Representative images of V-H<sup>+</sup>-ATPase immunostaining in gills from colchicine-treated, NaCl infused (A), base-infused (B) and colchicine-treated, base-infused fish (C). Average number of V-H<sup>+</sup>-ATPase positive cells per interlamellar space (#cells/IL) (D) (mean ± s.e.m.) (N=4). No significant differences were found between treatments (1-way ANOVA, Bonferroni's post test). Mean ± s.e.m. Scale bar: 10  $\mu$ m.



**Figure 3.4.** 6 h infusions. High magnification (2000x) light micrographs showing V-H<sup>+</sup>-ATPase staining in gills from colchicine-treated, NaCl-infused (A), base-infused (B) and colchicine-treated, base-infused fish (C). c=cytoplasmic, b=basolateral, i=intermediate staining pattern.

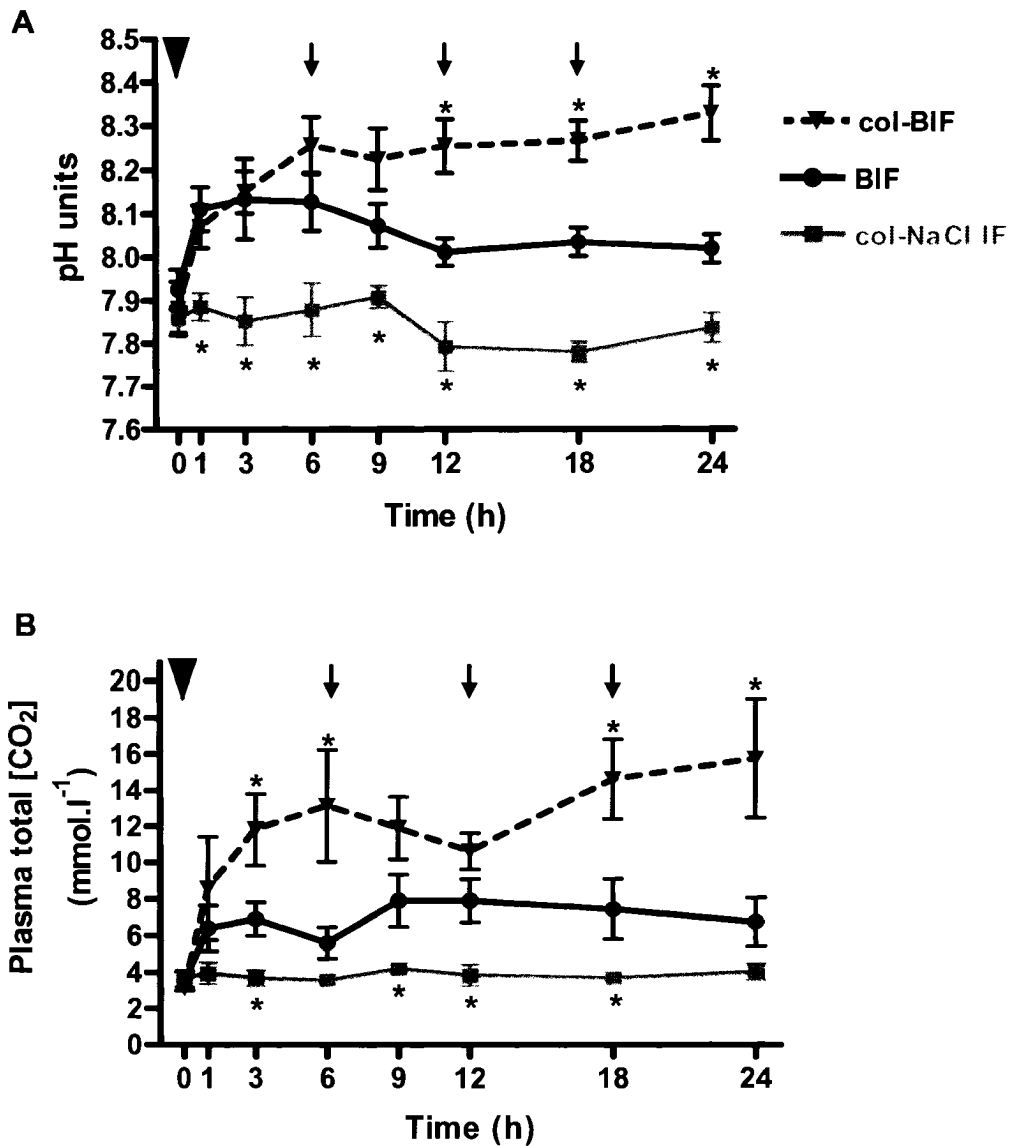


**Figure 3.5.** 24 h infusions. Blood parameters of colchicine-treated NaCl-infused fish, NaHCO<sub>3</sub>-infused fish, and colchicine-treated NaHCO<sub>3</sub>-infused fish (mean  $\pm$  s.e.m.). *A*: Arterial blood pH. *B*: Total CO<sub>2</sub> in plasma from arterial blood samples. The arrowhead indicates a bolus injection of colchicine (15 mg kg<sup>-1</sup>). Subsequent arrows indicate injection of half doses (7.5 mg kg<sup>-1</sup>). \**P* < 0.05 compared to base-infused fish of the respective time (RM-ANOVA, 1-way ANOVA, Dunnet's post test). (N=4).

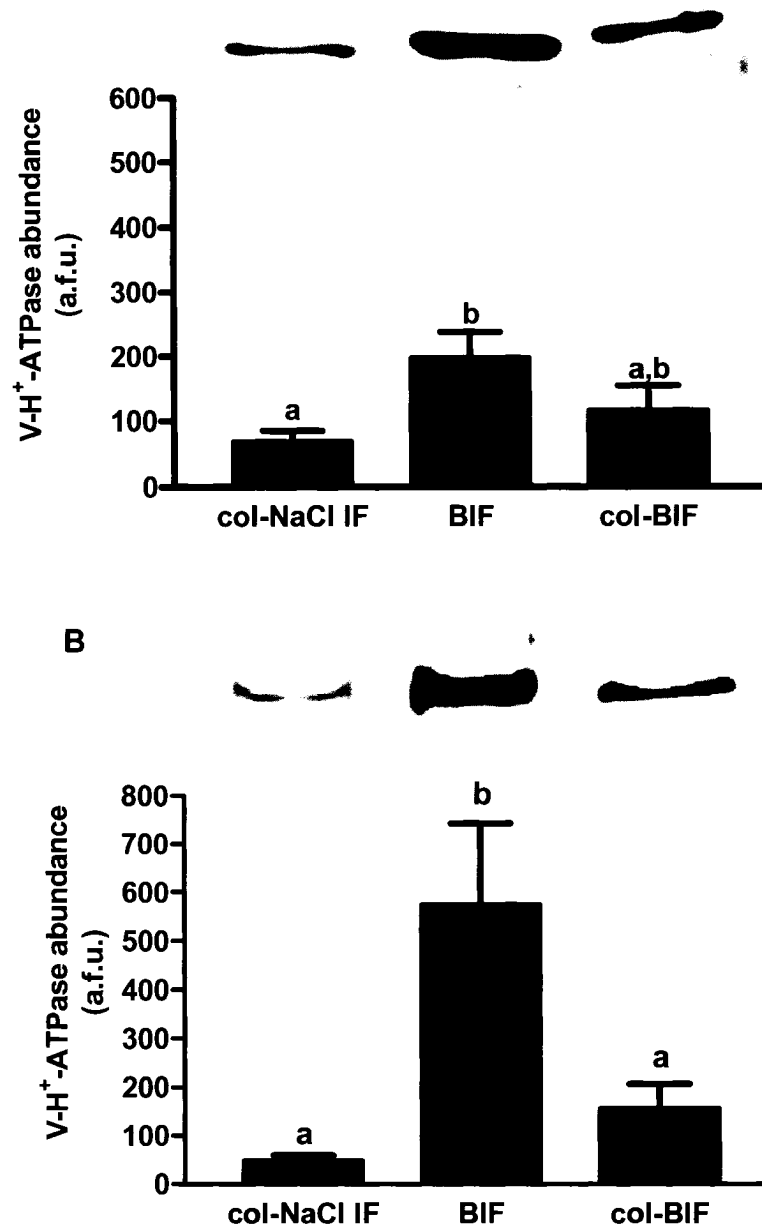


**Figure 3.6.** 24 h infusions. Quantitative analysis of V-H<sup>+</sup>-ATPase in gills from colchicine-treated, NaCl infused (col-NaCl IF, N=4), base-infused (BIF, N=5) and colchicine-treated, base-infused fish (col-BIF, N=5). *A*: Whole gill homogenates *B*: Membrane fraction. Representative immunoblots are shown above each panel. The letters indicate difference levels of statistical significance (1-way ANOVA, Bonferroni's post test). Results are mean  $\pm$  s.e.m. a.f.u.: arbitrary fluorometric units.

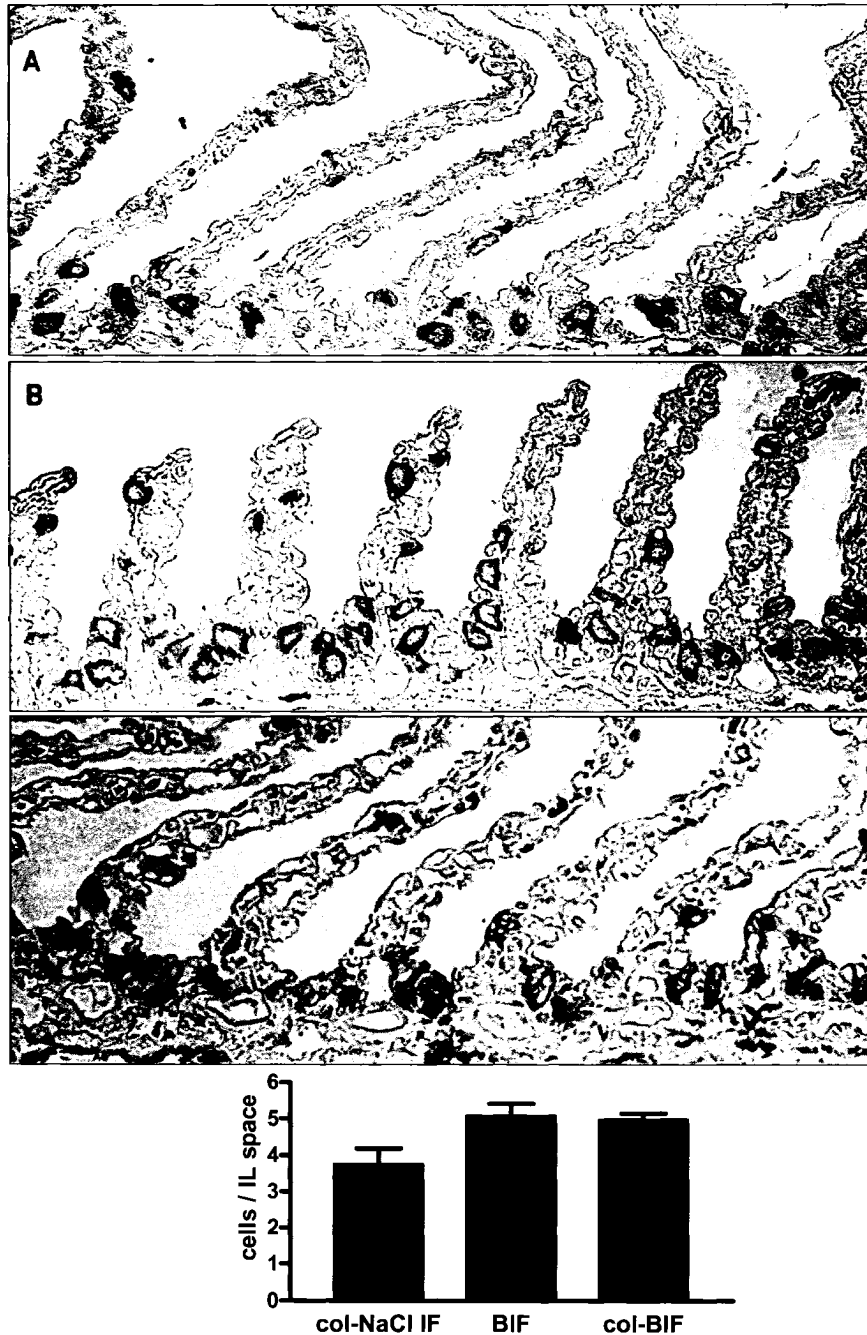


**Figure 3.7.** 24 h infusions. Representative images of V-H<sup>+</sup>-ATPase immunostaining in gills from colchicine-treated, NaCl infused (A), base-infused (B) and colchicine-treated, base-infused fish (C). Average number of V-H<sup>+</sup>-ATPase positive cells per interlamellar space (#cells/IL) (D) (mean ± s.e.m.) (n=4-5). No significant differences were found between treatments (1-way ANOVA, Bonferroni's post test). Mean ± s.e.m. Scale bar: 10 µm.

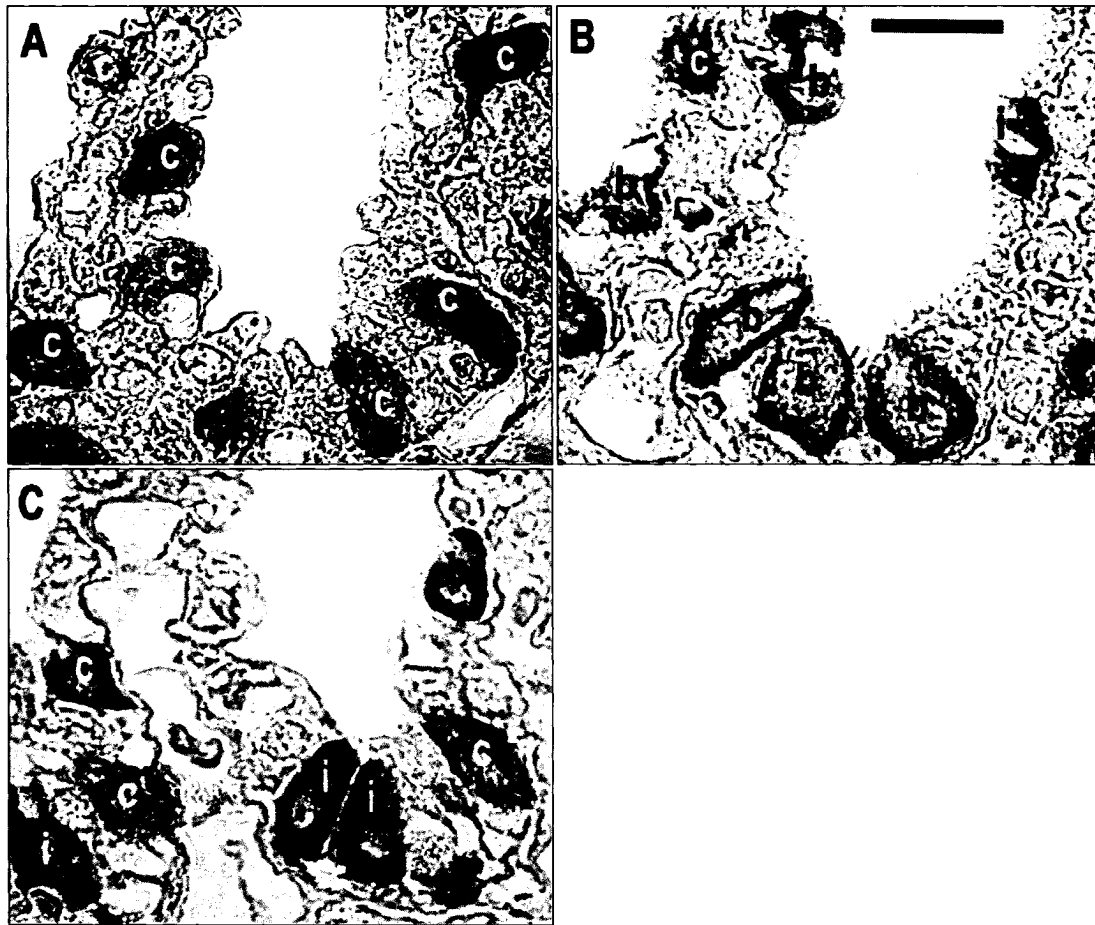


**Figure 3.8.** 24 h infusions. High magnification (2000x) light micrographs showing V-H<sup>+</sup>-ATPase staining in gills from colchicine-treated, NaCl-infused (A), base-infused (B) and colchicine-treated, base-infused fish (C). c=cytoplasmic, b=basolateral, i=intermediate staining pattern.

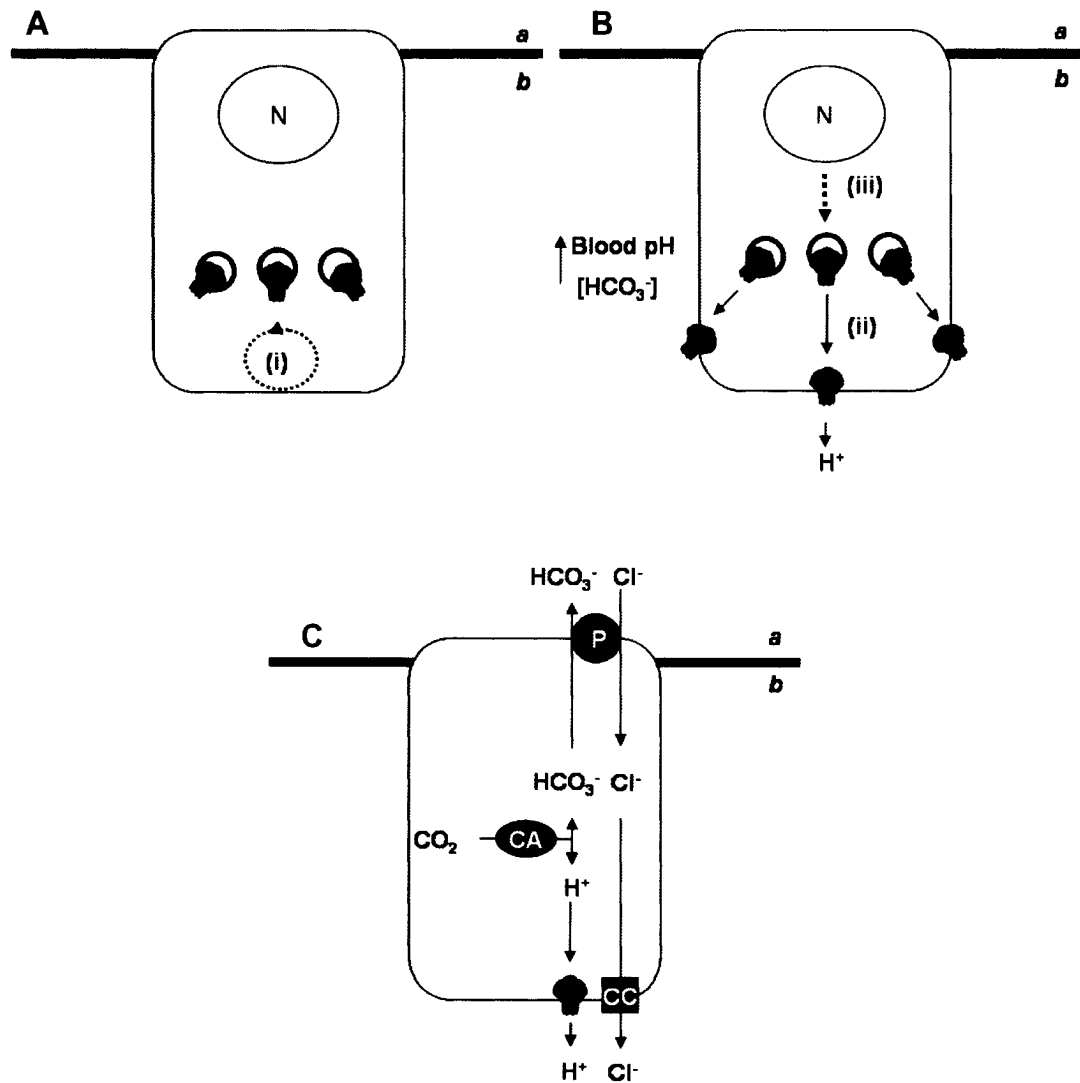


**Figure 3.9.** V-H<sup>+</sup>-ATPase-dependent base secretion in V-H<sup>+</sup>-ATPase-rich cells. (A) Basal base secretion. Most of the V-H<sup>+</sup>-ATPase is in cytoplasmic vesicles. (i) indicates the continuous recycling with the basolateral membrane. (B) Upregulation of base secretion under blood alkalosis. (ii) Short-term response: microtubule-dependent relocation of the pre-existent cytoplasmic pool to the basolateral membrane. (iii) In the longer term, there is also upregulation of V-H<sup>+</sup>-ATPase synthesis. (C) Model for base secretion in V-H<sup>+</sup>-ATPase-rich cells. P = Pendrin, CA = carbonic anhydrase, CC = chloride channel. a = apical side, b = basolateral side, N = nucleus.

## References

**Brown D.** (2000) Targeting of membrane transporters in renal epithelia: when cell biology meets physiology. *Am. J. Physiol. Renal Physiol.* 278, F192-201.

**Brown, D.I., Sabolic, I., and Gluck, S.** (1991). Colchicine-induced redistribution of proton pumps in the proximal tubule. *Kidney Int.* 40, Suppl. 33, S79-83.

**Brown D., and Stow, J.I.** (1996). Protein trafficking and polarity in kidney epithelium: from cell biology to physiology. *Physiol. Rev.* 76, 245-297.

**Choe, K.P., Kato, A., Hirose S., Plata, C., Sindic, A., Romero, M.F., Claiborne, J.B., and Evans, D.H.** (2005). NHE3 in an ancestral vertebrate: primary sequence, distribution, localization, and function in gills. *Am. J. Physiol. Reg. Integr. Comp. Physiol.* 289, 1520-1534.

**Evans, D.H., Piermarini, P.M. and Choe, K.P.** (2004). Homeostasis: osmoregulation, pH regulation, and nitrogen excretion. In *Biology of Sharks and their relatives*, (eds. J.C. Carrier, J.A. Musick and M.R. Heithaus), pp. 247-268. Boca Raton, FL, USA: CRC Press LLC.

**Evans, D.H., Piermarini, P.M. and Choe, K.P.** (2005). The multifunctional fish gill: dominant site of gas exchange, osmoregulation, acid-base regulation, and excretion of nitrogenous waste. *Physiol. Rev.* 85, 97-177.



**Gilmour, K.M., Perry, S.F., Wood, C.M., Henry, R.P., Laurent, P., Part, P. and Walsh, P.J.** (1998). Nitrogen excretion and the cardiorespiratory physiology of the gulf toadfish, *Opsanus beta*. *Physiol. Zool.* 71, 492-505.

**Gluck, S., Cannon, C., and Al-Awqati, Q.** (1982). Exocytosis regulates urinary acidification in turtle bladder by rapid insertion of H<sup>+</sup> pumps into the luminal membrane. *Proc. Natl. Acad. Sci. USA* 79, 4327–4331.

**Heisler, N.** (1988). Acid-base regulation. In *Physiology of Elasmobranch Fishes*, (ed. T. J. Shuttleworth), pp. 215-252. Berlin: Springer-Verlag.

**Hodler, J., Heinemann, H.O., Fishman, A.P., and Smith, H.W.** (1955). Urine pH and carbonic anhydrase activity in the marine dogfish. *Am. J. Physiol.* 183,155-162.

**Katoh, F., Hyodo, S. and Kaneko, T.** (2003). Vacuolar-type proton pump in the basolateral plasma membrane energizes ion uptake in branchial mitochondria-rich cells of killifish *Fundulus heteroclitus*, adapted to a low ion environment. *J. Exp. Biol.* 206, 793-803.

**Laemmli, U. K.** (1970). Cleavage of structural proteins during the assembly of the head of the bacteriophage T4. *Nature* 227, 680-685.

**Maetz, J. and Pic, P.** (1976). Microtubules in the 'chloride cell' of the gill and disruptive effects of colchicine on the salt balance of the seawater-adapted *Mugil capito*. *J. Exp. Zool.* **199**, 325–338.

**Moffat, A.C.** (1986). In *Clarke's isolation and identification of drugs*, 2<sup>nd</sup> ed. (eds. C.A Moffat, J.V. Jackson, M.S. Moss, and B. Widdop), p. 492. London, GB, The Pharmaceutical Press.

**Piermarini, P. M. and Evans, D. H.** (2001). Immunochemical analysis of the vacuolar proton-ATPase B-subunit in the gills of a euryhaline stingray (*Dasyatis sabina*): effects of salinity and relation to Na<sup>+</sup>/K<sup>+</sup>-ATPase. *J. Exp. Biol.* 204, 3251-3259.

**Piermarini, P. M., Verlander, J. W., Royaux, I. E. and Evans, D. H.** (2002). Pendrin immunoreactivity in the gill epithelium of a euryhaline elasmobranch. *Am. J. Physiol. Regulatory Integrative Comp. Physiol.* 283, R983-992.

**Schwartz G.J., Tsuruoka S., Vijayakumar, S., Petrovic, S., Mian, A., and Al-Awaqati, Q.** (2002). Acid incubation reverses the polarity of intercalated cell transporters, an effect mediated by hensin. *J. Clin. Invest.* 109, 89-99.

**Stephens, R.E. and Edds, K.T.** (1976). Microtubules: structure, chemistry, and function. *Physiol. Rev.* 56, 709-777.

**Swenson, E. R. and Maren, T. H.** (1987). Roles of gill and red cell carbonic anhydrase in elasmobranch HCO<sub>3</sub><sup>-</sup> and CO<sub>2</sub> excretion. *Am. J. Physiol. Regulatory Integrative Comp. Physiol.* 253, R450-458.

**Tresguerres, M., Katoh, F., Fenton, H., Jasinska, E., and Goss, G.G.** (2005). Regulation of branchial V-H<sup>+</sup>-ATPase, Na<sup>+</sup>/K<sup>+</sup>-ATPase and

NHE2 in response to acid and base infusions in the Pacific spiny dogfish (*Squalus acanthias*). *J. Exp. Biol.* 208, 345-354.

**Tsai, J.C., and Hwang, P.P.** (1998). Effects of wheat germ agglutinin and colchicine on microtubules of the mitochondria-rich cells and  $\text{Ca}^{2+}$  uptake in tilapia (*Oreochromis mossambicus*) larvae. *J. Exp. Biol.* 201, 2263-2272.

**Wagner, C.A., Finberg, K.E., Breton, S., Marshansky, V., Brown, D., and Geibel, J.P.** (2004). Renal vacuolar  $\text{H}^+$ -ATPase. *Physiol. Rev.* 84, 1263-1314.

**Wagner, C.A., Giebisch, G., Lang, F., and Geibel, J.P.** (1998). Angiotensin II stimulates vesicular  $\text{H}^+$ -ATPase in rat proximal tubular cells. *Proc. Natl. Acad. Sci. USA* 95, 9665–9668.

**Weihrauch, D., Ziegler, A., Siebers, D., and Towle, D.W.** (2002). Active ammonia excretion across the gills of the green shore crab *Carcinus maenas*: participation of  $\text{Na}^+/\text{K}^+$ -ATPase, V-type  $\text{H}^+$ -ATPase and functional microtubules. *J. Exp. Biol.* 205, 2765-2775.

**Wilson, J.M., Randall, D.J., Vogl, A.W., Harris, J., Sly, W.S. and Iwama, G.K.** (2000). Branchial carbonic anhydrase is present in the dogfish, *Squalus acanthias*. *Fish Physiol. Biochem.* 22, 329-336.

**Wilson, J. M., Randall, D. J., Vogl, A. W. and Iwama, G. K.** (1997). Immunolocalization of proton-ATPase in the gills of the elasmobranch, *Squalus acanthias*. *J. Exp. Zool.* 278, 78-86.

**Winter, C., Schulz, N., Giebisch, G., Geibel, J.P., and Wagner, C.A.**  
(2004). Nongenomic stimulation of vacuolar H<sup>+</sup>-ATPase in intercalated renal tubule cells by aldosterone. *Proc. Natl. Acad. Sci. USA* 101, 2636-2641.

**Zall, D. M., Fischer, M. D., and Garner, Q. M.** (1956). Photometric determination of chloride in water. *Anal. Chem.* 28, 1665-1678.

## Chapter IV

### **V-H<sup>+</sup>-ATPase translocation during blood alkalosis in dogfish gills: interaction with carbonic anhydrase and involvement in the post- feeding alkaline tide<sup>1</sup>**

<sup>1</sup>A version of this chapter has been published. **Tresguerres, M.**, Parks, S.K., Wood, C.M. and Goss, G.G. (2007). *American Journal of Physiology Integrative Regulatory Comparative Physiology* 292, 2012-2019. Reproduced with permission of the American Physiological Society and the co-authors of the manuscript.

## Introduction

The gills of marine elasmobranchs have a subpopulation of cells rich in V-H<sup>+</sup>-ATPase (Piermarini and Evans, 2001; Tresguerres *et al.*, 2005; chapter II). V-H<sup>+</sup>-ATPase is normally located in cytoplasmic vesicles but translocates to the basolateral membrane in a microtubule-dependent manner during blood alkalosis (Tresguerres *et al.*, 2006; chapter III). Impairment of the translocation process by colchicine reduces the fish's ability to excrete excess HCO<sub>3</sub><sup>-</sup> loaded by intravenous infusion, indicating that V-H<sup>+</sup>-ATPase translocation is involved in enhanced HCO<sub>3</sub><sup>-</sup> secretion to the external environment (Tresguerres *et al.*, 2006; chapter III). The proposed model for HCO<sub>3</sub><sup>-</sup> secretion included an intracellular carbonic anhydrase that serves to hydrate CO<sub>2</sub> into H<sup>+</sup> and HCO<sub>3</sub><sup>-</sup>. The basolaterally located V-H<sup>+</sup>-ATPase then reabsorbs the H<sup>+</sup> into the blood, thereby counteracting the blood alkalosis (Tresguerres *et al.*, 2006; chapter III), while the HCO<sub>3</sub><sup>-</sup> is most likely secreted to the surrounding seawater *via* an apical, Pendrin-like, anion exchanger (Evans *et al.*, 2004, Piermarini *et al.*, 2002).

In the current study, I have focused on identifying the nature of the stimulus that triggers the V-H<sup>+</sup>-ATPase translocation during NaHCO<sub>3</sub> infusion and evaluating whether a similar translocation occurs during a metabolic alkalosis of natural origin associated with feeding.

*A priori*, two major alternatives exist for the nature of the stimulus: (i) that blood alkalosis is detected by a specific pH or HCO<sub>3</sub><sup>-</sup> sensor in a place other than the V-H<sup>+</sup>-ATPase-rich cells, resulting in a hormonal or nervous

signal that ultimately results in V-H<sup>+</sup>-ATPase translocation; and (ii) that intracellular H<sup>+</sup> or HCO<sub>3</sub><sup>-</sup> produced by CA are sensed inside the V-H<sup>+</sup>-ATPase-rich cells which triggers the process. Recent research demonstrating that CA inhibition affects V-H<sup>+</sup>-ATPase cellular localization (Bagnis *et al.*, 2001; Breton and Brown, 2006; Pastor-Soler *et al.*, 2003) led me to investigate the potential involvement of CA in V-H<sup>+</sup>-ATPase translocation in dogfish gills. Under this second scenario, CA inhibition should prevent V-H<sup>+</sup>-ATPase translocation during blood alkalosis and also impair HCO<sub>3</sub><sup>-</sup> clearance from the blood.

Artificially induced A/B disturbances such as intravenous acid or base infusions (Arvedsen *et al.*, 2005; Galvez *et al.*, 2002; Goss and Wood, 1991; Goss and Perry, 1993; Tresguerres *et al.*, 2005, 2006; Wood *et al.*, 1995; chapters II and III), exposure to extreme hypercapnia (Georgalis *et al.*, 2006; Goss and Perry, 1993; Perry *et al.*, 2000), and acidic or alkaline diet regimes (Petrovic *et al.*, 2003; Frische *et al.*, 2003) are commonly used in fish and other animals in order to stimulate the A/B secretory mechanisms. The involvement of specific ion-transporting proteins is usually inferred based on changes in protein abundance or mRNA expression. One major criticism of results obtained from these studies is that it is unclear whether they are representative of the organism's normal physiology or if they only unveil mechanisms that are turned on upon extreme stresses.

Recently, Wood and colleagues (2005) found that a pronounced blood metabolic alkalosis occurs in dogfish after force-feeding *via* a stomach tube.

This phenomenon, known as “alkaline tide” (Niv and Fraser, 2002; Wang *et al.*, 2001), is the result of  $H^+$  secretion into the stomach during food digestion and simultaneous  $HCO_3^-$  reabsorption into the blood. The dogfish alkaline tide was characterized by significant rises in blood pH ( $\sim 0.20$  pH units) and plasma  $HCO_3^-$  ( $\sim 2.0$  mmol  $l^{-1}$ ) 3 to 6 h after feeding, which returned to control values approximately 17 h after feeding (Wood *et al.*, 2005). Very recently, similar results with a more pronounced rise in plasma  $[HCO_3^-]$  at 6 h were obtained after dogfish were allowed to feed naturally (Wood *et al.*, 2007). Since the gills are the main acid/base regulatory organ in marine elasmobranchs (Heisler, 1988), it was hypothesized that the excess base load is secreted by the gills (Wood *et al.*, 2005). Interestingly, the magnitude of the post-feeding metabolic alkaloses in these two feeding studies were broadly comparable to those induced by intravenous  $HCO_3^-$  infusion in my previous studies (Tresguerres *et al.*, 2005, 2006, chapters II and III). Therefore, I investigated if the branchial V- $H^+$ -ATPase translocation to the basolateral membrane takes place during the alkaline tide in naturally fed fish.



## Materials and Methods

### *Animals*

Pacific spiny dogfish (*Squalus acanthias* L.) were caught by hook and bait from the Trevor Channel (Vancouver Island, BC, Canada) and immediately transferred to the Bamfield Marine Sciences Centre, where they were held in batches of 20-60 animals in a 288 m<sup>3</sup> circular tank provided with flowing seawater (13 °C, 32 ppt salinity). Fish were fasted for at least 5 days before experimentation. All experiments were performed according to University of Alberta approved animal care protocols.

### *Surgery, NaHCO<sub>3</sub> infusion and acetazolamide injection*

Six dogfish (mean body mass  $1.72 \pm 0.11$  kg) were fitted with cannulae into the caudal artery and vein following the protocol described in detail in the previous chapters (see also Tresguerres *et al.*, 2005, 2006). After a 24 h recovery period, a 250 mmol l<sup>-1</sup> NaHCO<sub>3</sub>, 250 mmol l<sup>-1</sup> NaCl solution was infused *via* the venous cannulae using a peristaltic pump. The actual infusion rate was  $3.77 \pm 0.17$  ml kg<sup>-1</sup> h<sup>-1</sup>, resulting in a HCO<sub>3</sub><sup>-</sup> load of  $941.90 \pm 43.16$  μmol kg<sup>-1</sup> h<sup>-1</sup>. A stock acetazolamide solution (30 mg ml<sup>-1</sup> in DMSO) was prepared at the beginning of every experimentation day. Acetazolamide (30 mg kg<sup>-1</sup>) was injected *via* the venous cannulae 15 min before the start of the HCO<sub>3</sub><sup>-</sup> infusions, and an additional identical dose was injected after 6 h of infusion. Control fish were injected with an equivalent amount of DMSO alone (1 ml kg<sup>-1</sup>).

### *Blood sampling, analytical procedures on plasma samples*

The arterial cannulae was used to withdraw blood samples (200  $\mu$ l) at  $t=0$ , 1, 3, 6, 9 and 12 h. Blood pH was immediately measured using a thermostatted Accumet micro-size pH electrode model 13-620-94 (Fisher Scientific, Pittsburgh, PA, USA). The blood samples were then centrifuged at 12000  $g$  for 3 min to obtain plasma. 40  $\mu$ l of plasma were used for total  $\text{CO}_2$  ( $\text{TCO}_2$ ) determination by the method of Cameron (1971) in a thermostatted chamber (37°C) equipped with a  $\text{CO}_2$  electrode (Radiometer, Copenhagen, Denmark). Carbon dioxide tensions ( $\text{PCO}_2$ ) and bicarbonate concentrations ( $[\text{HCO}_3^-]$ ) were calculated using the solubility of carbon dioxide ( $\alpha_{\text{CO}_2}$ ), the apparent  $pK$  ( $pK_{\text{app}}$ ) for dogfish at the experimental temperature, and rearrangements of the Henderson-Hasselbalch equation according to Boutilier et al. (1984).

#### *Terminal sampling*

In the  $\text{NaHCO}_3$  infusion series, cannulated dogfish were anesthetized with tricaine methanesulphonate (TMS, 0.2  $\text{g l}^{-1}$ , AquaLife, Syndel Laboratories Ltd. Vancouver, BC, Canada) and injected with 5 ml of a saturated KCl solution after 12 h of  $\text{HCO}_3^-$  infusion, which killed the fish instantly. Gill samples were immediately excised and placed in fixative or were snap-frozen in liquid nitrogen for immunohistochemical and western blot analyses, respectively. In the feeding series, non-cannulated dogfish were terminally anaesthetized in their isolation boxes (see below) by stopping the water flow, lowering the water level to 6 l, and adding an overdose of TMS (0.2  $\text{g l}^{-1}$ ), a procedure which took about 3 minutes.

### *Feeding experiments*

An entire batch of about 30 dogfish in the 288 m<sup>3</sup> holding tank were placed on a feeding regime where they were fed every fifth day with freshly thawed whole hake (*Merluccius productus*) from which the heads had been removed. This is one of the most common natural preys of dogfish in British Columbia coastal waters (Jones and Gee, 1977). A feeding frenzy ensued, and all the food was consumed within 30 min. The ration supplied at each feeding was about 3% of body mass, based on the estimated mass of all the dogfish in the group tank. However, not all dogfish ate, and in a separate trial, the average mass of food consumed by those dogfish which had fed was 5-6% of body weight, based on autopsy at 24 h post-feeding. With practice, it was possible to discern which dogfish had fed by the bulging profile of the abdomen, and at 1 h after feeding, five of these animals were caught by dip-net and removed to isolation enclosures. The enclosures were individual 40 L polyurethane-coated wooden boxes (seawater flow = 1 l min<sup>-1</sup>) served with vigorous aeration (Wood *et al.*, 1995, 2005). Sham animals (N=5) were treated identically, but were removed from the holding tank immediately before feeding – i.e. after 5 days of fasting.

Based on a parallel series of experiments (Wood *et al.* , 2007), we knew that post-feeding excretion of base into the external seawater started on average at 6-12 h post-feeding, reached a maximum value at 12 -24 h, and continued through 48 h. Therefore, acid-base fluxes in fed and sham animals were measured overnight during the 12-24 h post-feeding period, and then

the animals were sacrificed for gill immunohistochemistry and western blotting within a further 2 h. At the start of the 12 h flux period, the water inflow to the box was stopped, and the volume set to a known level (about 35 l after subtraction of dogfish mass). Duplicate water samples were taken at 12 h and 24 h, and measured for titratable alkalinity and total ammonia. Titratable alkalinity was determined by titration of 10 ml water samples to pH = 4.00, using a Radiometer-Copenhagen GK2401C combination electrode, and a Gilmont microburette to dispense standardized acid (0.04 N HCl). Total ammonia concentration was measured by the indophenol blue method (Ivancic and Degobbi, 1984). Net acid-base fluxes were calculated as the difference between the change in ammonia concentration and the change in the concentration of titratable alkalinity in the water over the monitoring period, factored by weight, volume, and time, as outlined by McDonald *et al.* (1982).

#### *Immunohistochemistry*

Immunohistochemistry was performed as described in the previous chapters. V-H<sup>+</sup>-ATPase was immunolabeled in 4 µm paraffin sections using the antibody developed by Katoh *et al.* (2003) and the Vecstastain ABC kit (Vector Laboratories, Burlingame, CA, USA). Carbonic anhydrase (CA) immunostaining was performed in a similar manner using an anti-trout cytoplasmic CA antibody (Georgalis *et al.*, 2006). To investigate if CA is located in the same cells as V-H<sup>+</sup>-ATPase and Na<sup>+</sup>/K<sup>+</sup>-ATPase we

immunolabeled consecutive 4  $\mu\text{m}$  paraffin sections as described previously (Tresguerres *et al.*, 2005, 2006).

### *Western blotting*

Western blotting was performed as described in the previous chapter. Western blotting using the  $\alpha$ -CA antibody was done using 12 % polyacrylamide mini-gels.

### *Statistics*

All data are given as means  $\pm$  s.e.m. Differences between treatments were tested using Student's t-test. For the analyses of pH and  $\text{PCO}_2$  in the 12 h  $\text{NaHCO}_3$  infusion experiments, we used two-way repeated measures analysis of variance (2-way RM-ANOVA) followed by Bonferroni's post test to compare means at each experimental times ( $t=0$ , 1, 3, 6, 9 and 12 h). Statistical significance was set at  $P<0.05$ . All statistical analyses were performed on GraphPad Prism v.3.0 (GraphPad Software, San Diego California USA). Unless otherwise mentioned, the reagents used in this study were purchased from Sigma (St. Louis, MO, USA).

## Results

### *i- Carbonic anhydrase immunolabeling*

In accordance with previous reports from trout (Georgalis *et al.*, 2006), the anti-trout CA antibody recognized a 33 kDa band in dogfish gill samples subjected to SDS-PAGE-western blotting. The band disappeared when the anti-CA antibody was previously incubated with excess specific peptide demonstrating specificity of the antibody (Fig. 4.1). The CA antibody labeled most cells in the outer layer of the gill epithelium of fasted control dogfish (Fig. 4.2B). CA immunolabeling was stronger in cells that labeled for  $\text{Na}^+/\text{K}^+$ -ATPase (Fig 4.2A) and in  $\text{V-H}^+$ -ATPase-rich cells (Fig. 4.2C), but also in a minority of cells that did not label for any of the two ATPases.

### *ii- Effect of carbonic anhydrase inhibition on blood and plasma variables during $\text{NaHCO}_3$ infusion*

Blood pH of dogfish infused with  $\text{NaHCO}_3^-$  ( $946.90 \pm 43.16 \mu\text{mol kg}^{-1} \text{ h}^{-1}$ ) behaved as previously described (Tresguerres *et al.*, 2005; 2006; chapters II and III): an initial steep rise from  $7.68 \pm 0.04$  to  $7.91 \pm 0.04$  pH units followed by a plateau at  $\sim 8.04$  pH units despite the continuous infusion of base (N=3, Fig. 4.3A). Fish that were infused with base and also injected with acetazolamide ( $30 \text{ mg kg}^{-1}$ ) showed a similar pattern, except for  $t=1 \text{ h}$ . At this point, blood pH dropped by  $\sim 0.20$  pH units, although it was not significantly different from the control base-infused fish (Fig. 4.3A).

The inhibitory effect of acetazolamide on CA was apparent in plasma  $[\text{HCO}_3^-]$ . From  $t=3 \text{ h}$   $[\text{HCO}_3^-]$  was significantly higher than in base-infused

control fish, showing a continual increase to  $t = 12$  h ( $28.72 \pm 0.41$  vs.  $6.57 \pm 2.47$  mmol l<sup>-1</sup>, Fig. 4.3B) with no plateau noticed. Partial pressure of CO<sub>2</sub> (PCO<sub>2</sub>) was also significantly higher in acetazolamide-treated base-infused fish, reaching a maximum value by 9 h ( $6.36 \pm 0.14$  vs.  $1.51 \pm 0.29$  torr, Fig. 4.3C). By  $t = 12$  h PCO<sub>2</sub> reached a plateau in acetazolamide-treated fish, but it was still elevated compared to control base-infused fish ( $5.79 \pm 1.00$  vs.  $1.21 \pm 0.38$  torr).

*iii- Effect of carbonic anhydrase inhibition on V-H<sup>+</sup>-ATPase translocation and abundance*

Immunolabeling of gill sections from fish infused with NaHCO<sub>3</sub><sup>-</sup> revealed that V-H<sup>+</sup>-ATPase had translocated into the basolateral membrane (Fig. 4.4A), similar to our previous reports (Tresguerres *et al.*, 2005, 2006; chapters II and III). Acetazolamide clearly prevented V-H<sup>+</sup>-ATPase translocation (Fig. 4.4B), indicating that functional CA is required for the process to occur. The effect of acetazolamide on V-H<sup>+</sup>-ATPase translocation was also assessed from western blots (Fig. 4.5). There were no statistical differences in V-H<sup>+</sup>-ATPase abundance in whole gill homogenates from acetazolamide-treated fish compared to controls ( $1.00 \pm 0.13$  vs.  $1.43 \pm 0.34$  a.f.u.,  $N=3$ ,  $p>0.05$ ). However, V-H<sup>+</sup>-ATPase in cell membrane enriched samples from fish injected with acetazolamide was significantly lower compared to controls ( $0.24 \pm 0.08$  vs.  $1.00 \pm 0.28$  a.f.u.,  $N=3$ ,  $p<0.05$ ), providing further evidence for the CA involvement in V-H<sup>+</sup>-ATPase translocation.

*iv- Base efflux and V-H<sup>+</sup>-ATPase translocation and abundance during post-feeding alkalosis*

Dogfish (N=5) that had fed *ad libitum* in the housing tank and were transferred to individual boxes displayed a net efflux of metabolic base to the water at a rate of  $294.9 \pm 63.7 \mu\text{equiv l}^{-1} \text{ kg}^{-1} \text{ h}^{-1}$  between 12 and 24h after feeding. In comparison, sham fish (N=5) that had not fed exhibited no net acid/base fluxes at all at this time ( $-14.7 \pm 25.9 \mu\text{equiv l}^{-1} \text{ kg}^{-1} \text{ h}^{-1}$ ). The contribution of ammonia excretion, which is negative in the net base flux calculation, was identical in the two groups ( $-70.2 \pm 34.7 \mu\text{equiv l}^{-1} \text{ kg}^{-1} \text{ h}^{-1}$  in fed animals versus  $-70.8 \pm 30.6 \mu\text{equiv l}^{-1} \text{ kg}^{-1} \text{ h}^{-1}$  in shams). These data are very similar to a more extensive examination of post-feeding acid-base flux which demonstrated that this elevation of net base efflux continues for at least 48h after a meal (Wood *et al.*, 2007).

V-H<sup>+</sup>-ATPase immunolabeling in gills of fasted fish occurred in the cytoplasm (Fig. 4.6A) (also see Tresguerres *et al.*, 2005, 2006 and chapters II and III). However, V-H<sup>+</sup>-ATPase in gills of fed fish was distinctly located in the cell basolateral membrane of gill (Fig. 4.6B). To substantiate these findings, I quantified V-H<sup>+</sup>-ATPase in gill samples of both fed and fasted fish (Fig. 4.7). V-H<sup>+</sup>-ATPase abundance in whole gill homogenates was similar in samples from fasted ( $1.00 \pm 0.29 \text{ a.f.u.}$ ) and fed fish ( $1.18 \pm 0.16 \text{ a.f.u.}$ ) (n=4-5; p>0.05). However, the cell membrane enriched fraction from fed fish demonstrated increased V-H<sup>+</sup>-ATPase abundance compared to fasted fish ( $3.10 \pm 0.54$  vs.  $1.00 \pm 0.16 \text{ a.f.u.}$ , n=4-5; p<0.05).



## Discussion

I have previously shown that during blood alkalosis, V-H<sup>+</sup>-ATPase translocates to the basolateral membrane of specific gill cells of the Pacific dogfish (Tresguerres *et al.*, 2005, 2006; chapters II and III). This process is dependant on functional cytoskeleton microtubules, and correlates with the ability to recover from blood alkalosis (Tresguerres *et al.*, 2006; chapter III). Therefore, I proposed that branchial cellular remodeling involving V-H<sup>+</sup>-ATPase translocation into the basolateral membrane was necessary for H<sup>+</sup> reabsorption and HCO<sub>3</sub><sup>-</sup> secretion. Here I present novel findings about the cellular mechanism responsible for V-H<sup>+</sup>-ATPase translocation, its involvement in HCO<sub>3</sub><sup>-</sup> secretion and H<sup>+</sup> reabsorption, and the role of this mechanism under a normal physiological situation, the post-feeding alkaline tide.

### *Role of carbonic anhydrase (CA)*

Based on the estimated molecular size of the band from PAGE-western blotting and the peptide preabsorption experiment, the  $\alpha$ -CA antibody demonstrated good specificity in dogfish gills. CA seems to be widely distributed throughout the gill epithelium, but it is found in higher abundance in gill cells that are also rich in Na<sup>+</sup>/K<sup>+</sup>-ATPase and V-H<sup>+</sup>-ATPase. This localization is consistent with the previously proposed role of CA in branchial acid/base regulation (Perry and Gilmour, 2006; Tresguerres *et al.*, 2005, 2006; Wilson *et al.*, 2000; chapters II and III). This model predicted that CA hydrates CO<sub>2</sub> into H<sup>+</sup> and HCO<sub>3</sub><sup>-</sup> inside the Na<sup>+</sup>/K<sup>+</sup>-ATPase – and V-H<sup>+</sup>-

ATPase-rich cells. The  $\text{Na}^+/\text{K}^+$ -ATPase-rich cells are responsible for secreting  $\text{H}^+$  into the water in exchange for  $\text{Na}^+$ , probably via a  $\text{Na}^+/\text{H}^+$  exchanger (Tresguerres *et al.*, 2005; chapter II), while the V- $\text{H}^+$ -ATPase rich cells reabsorb  $\text{H}^+$  into the blood through basolateral V- $\text{H}^+$ -ATPases (Tresguerres *et al.*, 2005, 2006; chapters II and III) and apically located  $\text{Cl}^-/\text{HCO}_3^-$ , Pendrin-like anion exchangers (Evans *et al.*, 2004, Piermarini *et al.*, 2002).

The effect of CA inhibition by acetazolamide during blood alkalosis on blood pH, plasma  $[\text{HCO}_3^-]$  and plasma  $\text{PCO}_2$  mimicked previously reported results in dogfish using a similar CA inhibitor, methazolamide (Swenson and Maren, 1987). The lack of significant change in blood pH compared to fish infused with  $\text{HCO}_3^-$  alone is due to the simultaneous increase of plasma  $[\text{HCO}_3^-]$  and  $\text{PCO}_2$ , which counteract each other in acid-base terms. Here, I must mention that the acetazolamide treatment inhibits not only gill intracellular CA, but also other CA's in the body including red blood cell (rbc) CA and the extracellular CA IV recently reported to be present at the basolateral membrane of gill pillar cells (Gilmour *et al.*, 2007). Inhibition of rbc and type IV CA would slow down gaseous  $\text{CO}_2$  diffusion into the water, which is evident from the plasma  $\text{PCO}_2$  readings in our study. Thus, I can not rule out that the elevated  $\text{PCO}_2$  in the acetazolamide-treated  $\text{HCO}_3^-$ -infused fish inhibits V- $\text{H}^+$ -ATPase translocation. However, elevated  $\text{PCO}_2$  in the acetazolamide-treated  $\text{HCO}_3^-$  infused fish also indicates that delivery of  $\text{CO}_2$  to the cytoplasm of the V- $\text{H}^+$ -ATPase-rich cells is not a problem during rbc CA

inhibition. It would be extremely difficult to inhibit intracellular CA alone while also controlling for all the blood parameters during these prolonged whole animal  $\text{HCO}_3^-$  infusion experiments.

*A priori*, one of the alternatives was that V- $\text{H}^+$ -ATPase translocation was triggered by increased blood pH and/or  $[\text{HCO}_3^-]$ . However, when the gill samples were taken after 12 h of  $\text{HCO}_3^-$  infusion, acetazolamide-treated,  $\text{HCO}_3^-$ -infused fish had the same blood pH as and higher plasma  $[\text{HCO}_3^-]$  than fish that were infused with  $\text{HCO}_3^-$  alone. At this point, branchial V- $\text{H}^+$ -ATPase translocation was negligible in the acetazolamide-treated  $\text{HCO}_3^-$ -infused fish, suggesting that intracellular  $\text{H}^+$  or  $\text{HCO}_3^-$  generated by CA is the stimulus that triggers V- $\text{H}^+$ -ATPase translocation. Alternatively, it is also possible that CA is involved in the sensing mechanism somewhere else in the body.

Assuming that intracellular pH or  $[\text{HCO}_3^-]$  is the stimulus that triggers V- $\text{H}^+$ -ATPase translocation, the nature of the intracellular sensor remains to be determined. A distinct possibility is that the sensor is a soluble adenylyl cyclase (sAC). sAC is known to be activated by  $[\text{HCO}_3^-]$ , resulting in increased cAMP production (Buck *et al.*, 1999; Chen *et al.*, 2000; Mittag *et al.*, 1993). sAC has also been shown to mediate the translocation of V- $\text{H}^+$ -ATPase into the apical membrane of clear cells at the rat epididymis in response to increased luminal pH (Pastor-Soler *et al.*, 2003). This process is mediated by modulation of the actin cytoskeleton, and appears to result in  $\text{H}^+$  secretion into the lumen (Beaulieu *et al.*, 2005). Moreover, CA inhibition by

acetazolamide prevented the V-H<sup>+</sup>-ATPase translocation into the apical membrane (Pastor-Soler *et al.*, 2003). The results of these two studies on epididymis strongly suggest that intracellular HCO<sub>3</sub><sup>-</sup> generated by CA activates sAC resulting in increased cAMP production. This in turn modulates the actin cytoskeleton polymerization, which ultimately results in V-H<sup>+</sup>-ATPase accumulation in the apical region of clear cells and subsequent H<sup>+</sup> secretion into the lumen of the epididymis.

The similarities of this model with my results are evident. I hereby propose a role of sAC in the V-H<sup>+</sup>-ATPase translocation mechanism that takes place in gills of dogfish experiencing blood alkalosis. In order to further support this hypothesis, identification of dogfish sAC homologue using tools of molecular biology, biochemistry, or both, is absolutely required.

#### *Physiological role of the V-H<sup>+</sup>-ATPase translocation*

Although the alkalosis-induced V-H<sup>+</sup>-ATPase translocation is readily evident, it correlates well with recovery from alkalosis (Tresguerres *et al.*, 2006; chapter III), and it is in accordance with base secretory mechanisms from other physiological systems (see Breton and Brown, 2007), it was unclear whether or not this mechanism is of physiological relevance for normal (non-infused) dogfish. Recently it was demonstrated that dogfish show a characteristic alkaline tide whereby blood pH and [HCO<sub>3</sub><sup>-</sup>] are significantly elevated a few hours after feeding (Wood *et al.*, 2005; 2007). I took advantage of this situation to address if this naturally-induced blood alkalosis results in branchial V-H<sup>+</sup>-ATPase translocation.

Dogfish in the current study were sampled 24 -26 h after feeding. Between 12 and 24 h after feeding these fish were excreting net base (i.e.  $\text{HCO}_3^-$  equivalents) into the water. The measured rate was approximately 30% of the net  $\text{NaHCO}_3$  infusion rate used in the first set of experiments. I show using immunohistochemistry that  $\text{V-H}^+$ -ATPase has translocated to the basolateral membrane at  $t=24-26$  h.  $\text{V-H}^+$ -ATPase abundance in gill cell membranes was also significantly higher compared to fasted fish, which supports the histological results. These results strongly suggest that branchial  $\text{V-H}^+$ -ATPase insertion into the basolateral membrane is responsible for enhanced  $\text{HCO}_3^-$  secretion during the natural post-feeding period.

It is possible that the same factor that activates HCl secretion into the stomach lumen during digestion is also responsible for triggering the branchial  $\text{V-H}^+$ -ATPase translocation, or for enhancing the triggering signaling mechanism. Based on the mammalian system, some candidates would be histamine, acetylcholine and gastrin (Niv and Fraser, 2002). However, our  $\text{NaHCO}_3$  infusion experiments (Tresguerres *et al.*, 2005, 2006; chapters II and III; this chapter) clearly demonstrate that  $\text{V-H}^+$ -ATPase translocation can take place without the participation of any feeding-related hormone. While we cannot discount the possibility that base infusion results in release of an unknown hormone or factor, I propose that the elevated blood  $[\text{HCO}_3^-]$  during the post-feeding blood alkalosis results in elevated intracellular  $\text{PCO}_2$ , thus causing an intracellular increase in  $[\text{HCO}_3^-]$  inside the  $\text{V-H}^+$ -ATPase rich cells, which triggers branchial  $\text{V-H}^+$ -ATPase translocation.

Summarizing, I conclude that a physicochemical variable (probably  $[\text{HCO}_3^-]$ ) inside the V- $\text{H}^+$ -ATPase-rich cells triggers the translocation of V- $\text{H}^+$ -ATPase into the basolateral membrane to reabsorb the CA-generated  $\text{H}^+$  into the blood. This mechanism is important for maintaining blood acid/base balance during the naturally occurring post-feeding alkaline tide. If this model is confirmed it would be a clear example of two physiological functions (digestion and acid/base regulation) interacting with each other based on simple positive/negative feedback loops mediated by  $\text{CO}_2/\text{HCO}_3^-$ .

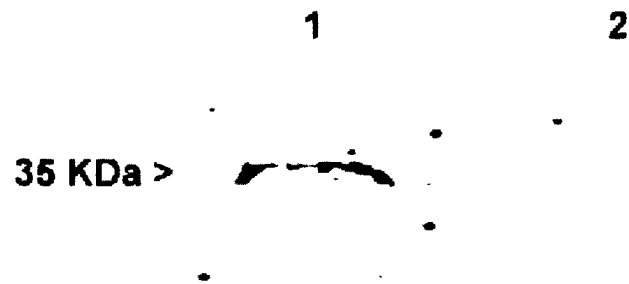


**Figure 4.1.** Western blotting of dogfish gills with the  $\alpha$ -CA antibody (lane 1). The band was eliminated after pre-incubating the primary antibody with excess peptide antigen (lane 2).

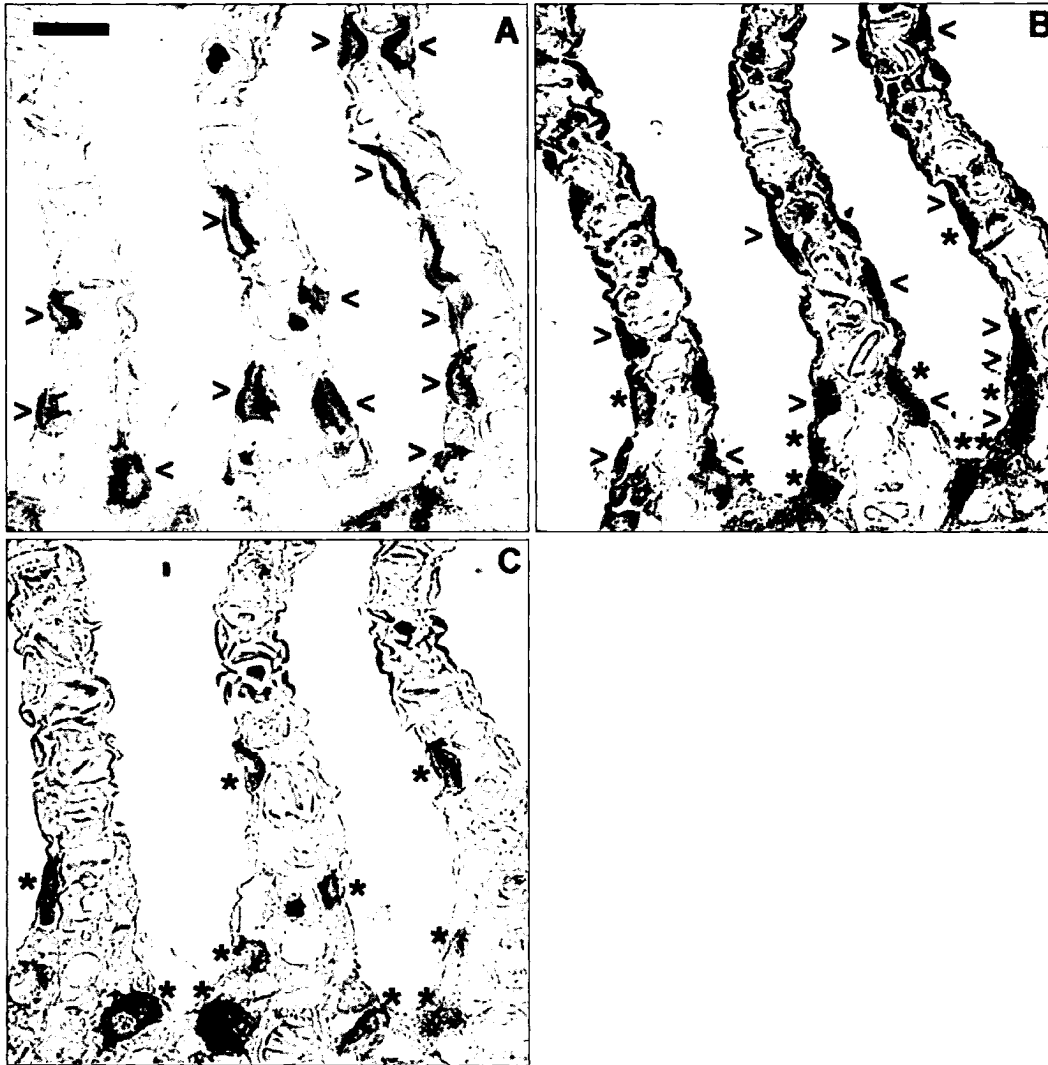


**Figure 4.2.** Representative micrographs of 4  $\mu\text{m}$  consecutive sections of dogfish gills immuno-labeled for  $\text{Na}^+/\text{K}^+$ -ATPase (A), carbonic anhydrase (CA) (B), and  $\text{V-H}^+$ -ATPase (C). Arrow heads indicate  $\text{Na}^+/\text{K}^+$ -ATPase labeling, and asterisks indicate  $\text{V-H}^+$ -ATPase labeling. Notice how CA-immunoreactivity takes place in cells that are positive for one or the other ATPase. Scale bar: 10  $\mu\text{m}$ .



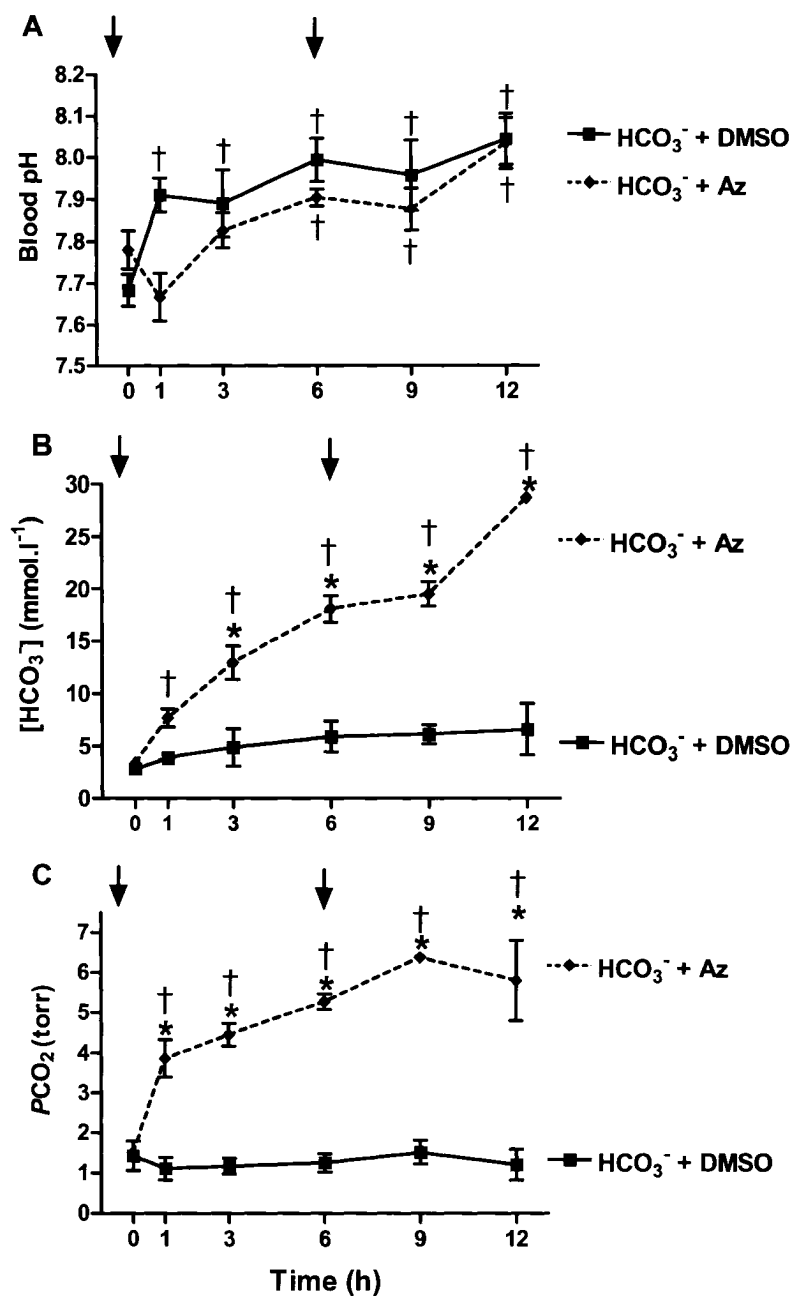


**Figure 4.3.** Blood parameters of fish infused intravenously with  $\text{NaHCO}_3$  ( $941.90 \pm 43.16 \mu\text{mol kg}^{-1} \text{h}^{-1}$ ) and injected with either DMSO (solid line) or acetazolamide (Az,  $30 \text{ mg kg}^{-1}$ -dash line-). The arrows indicate injection of DMSO or Az. (A) Arterial blood pH. (B) Arterial plasma  $[\text{HCO}_3^-]$ . (C) Arterial plasma  $\text{PCO}_2$ .  $N=3$ . \* $P<0.05$  compared to the control value ( $\text{HCO}_3^- + \text{DMSO}$ ) of the respective time. †  $P<0.05$  compared to  $t=0 \text{ h}$  within a same treatment. (2-way RM-ANOVA, Bonferroni's or Dunnett's post test).

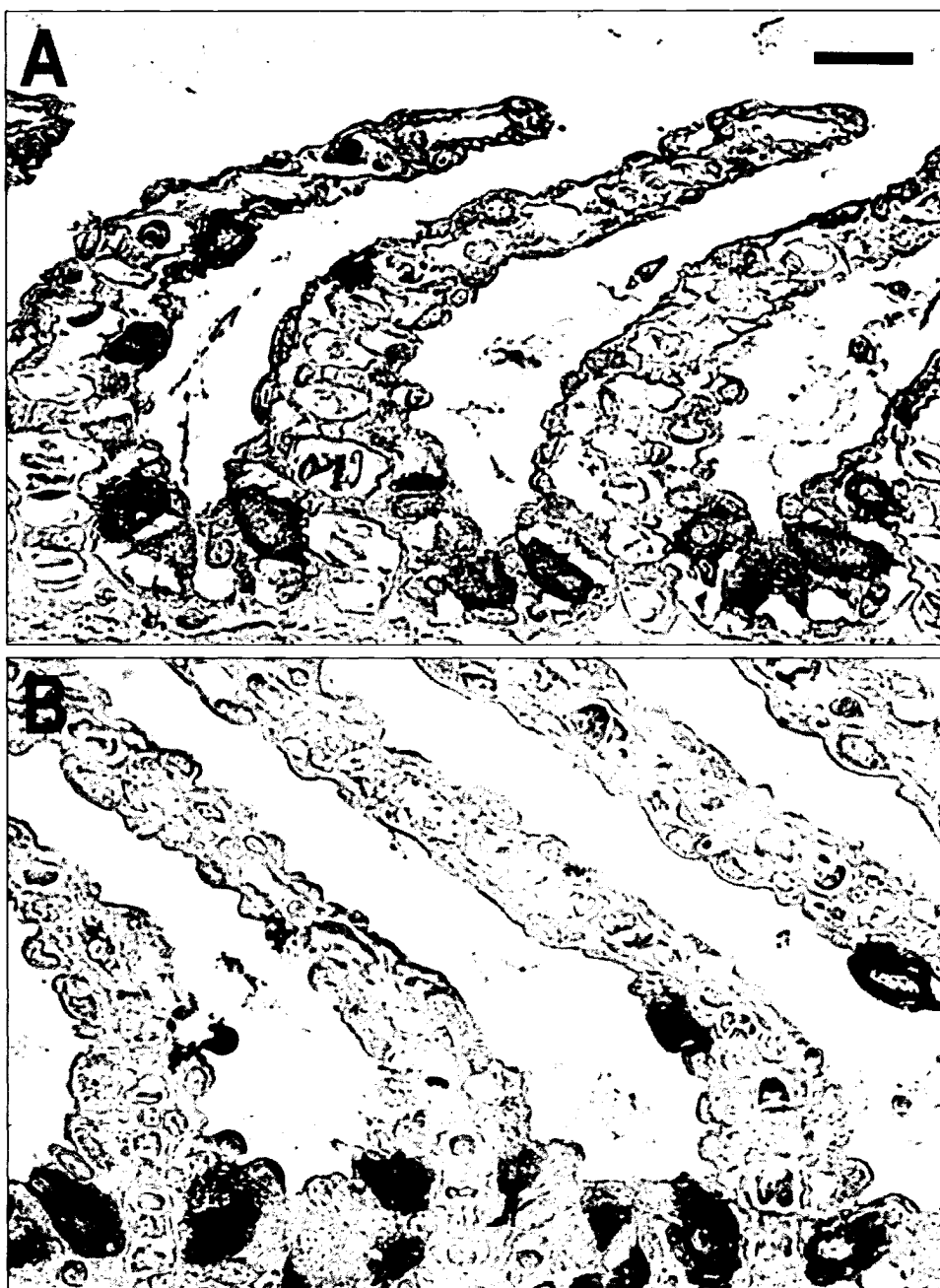


**Figure 4.4.** Representative micrographs of V-H<sup>+</sup>-ATPase immunolabeling in gills from fish infused with NaHCO<sub>3</sub> for 12 h. (A) Control fish (injected with DMSO). (B) Fish injected with acetazolamide (30 mg kg<sup>-1</sup>) at t=0 and 6 h. Scale bar: 10 µm.

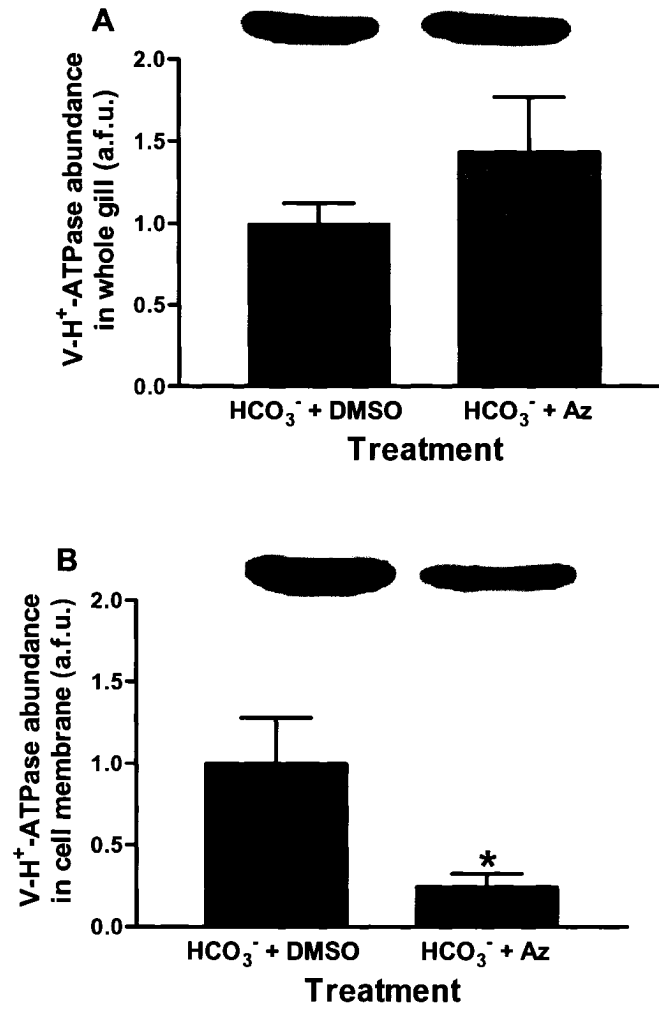


**Figure 4.5.** Fluorometric analysis of V-H<sup>+</sup>-ATPase abundance in gills from fish infused with NaHCO<sub>3</sub> for 12 h. (A) Whole gill homogenates. (B) Membrane fraction. The top panels show representative bands. HCO<sub>3</sub><sup>-</sup> + DMSO = control fish. HCO<sub>3</sub><sup>-</sup> + Az = fish injected with acetazolamide (30 mg kg<sup>-1</sup>). N=3. \**P*<0.05 (Student's t-test).

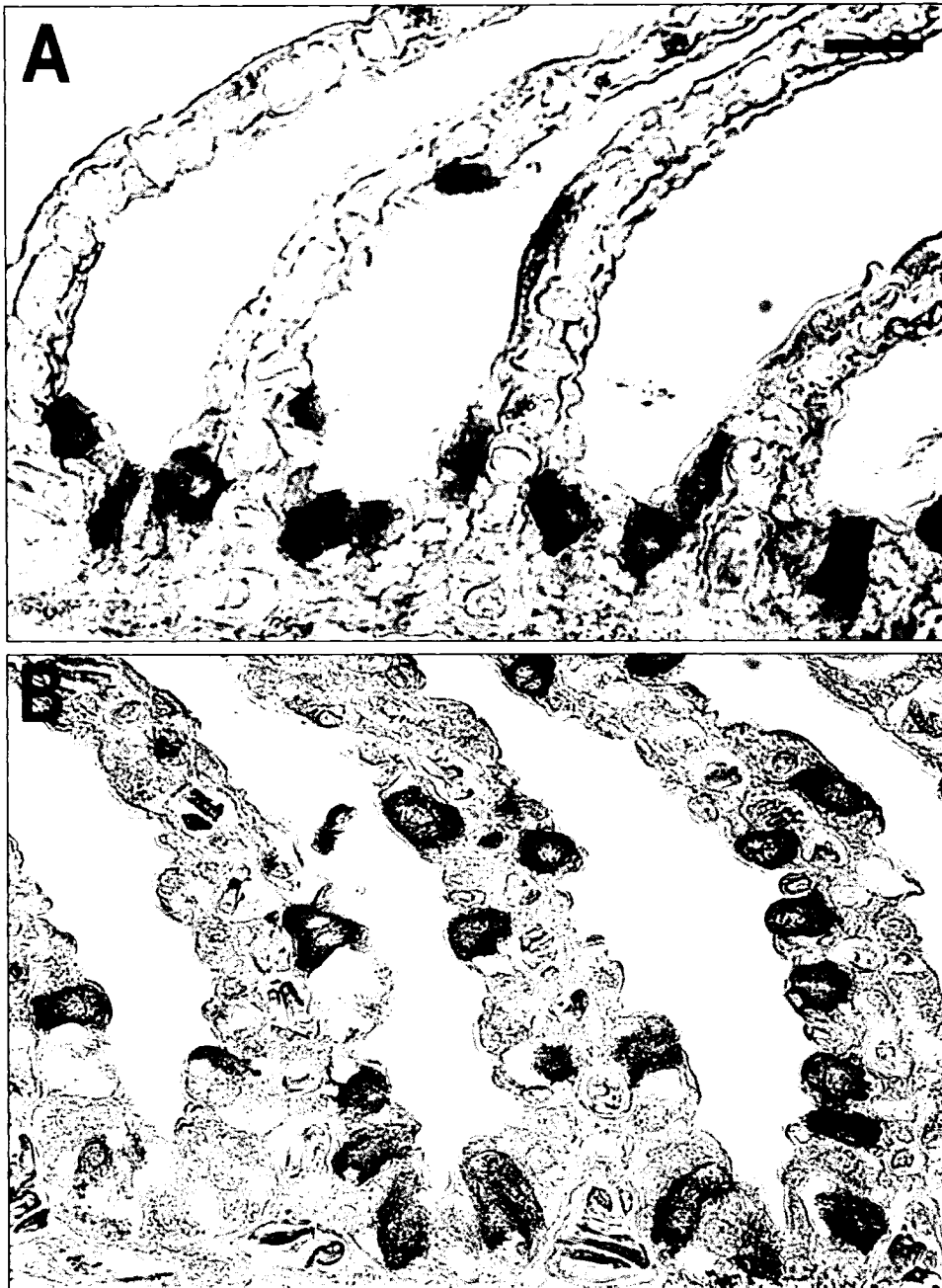


**Figure 4.6.** Representative micrographs of V-H<sup>+</sup>-ATPase immunolabeling in gills from fasted and fed fish. (A) Fasted fish. (B) Fish 24-26 h after feeding. Scale bar: 10  $\mu$ m.

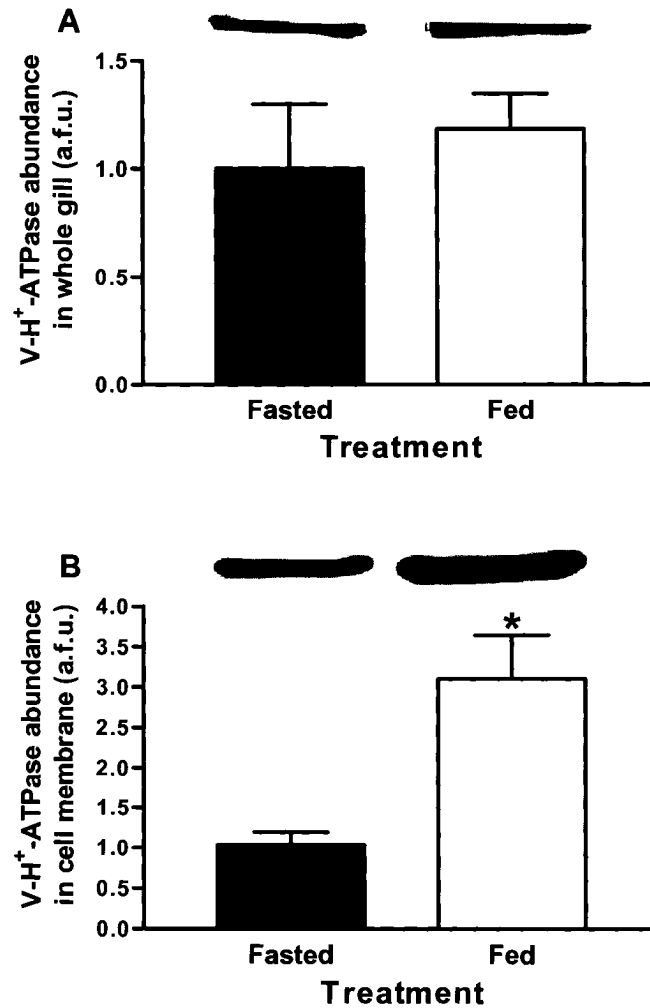


**Figure 4.7.** Fluorometric analysis of V-H<sup>+</sup>-ATPase abundance in gills from fasted and fed fish (24-26 h after feeding). (A) Whole gill homogenates. (B) Membrane fraction. The top panels show representative bands. N=4-5. \**P*<0.05 (Student's t-test).

## References

**Arvedsen, S.K., Andersen, J.B., Zaar, M., Andrade, D., Abe, A.S. and Wang, T.** (2005). Arterial acid-base status during digestion and following vascular infusion of NaHCO<sub>3</sub> and HCl in the South American rattlesnake, *Crotalus durissus*. *Comp. Biochem. Physiol. A* 142, 495-502.

**Bagnis, C., Marshansky, V., Breton, S. and Brown, D.** (2001) Remodeling the cellular profile of collecting ducts by chronic carbonic anhydrase inhibition. *Am. J. Physiol. Renal Physiol.* 280, F437-448.

**Beaulieu, V., Da Silva, N., Pastor-Soler, N., Brown, C.R., Smith, P.J.S., Brown, D. and Breton, S.** (2005) Modulation of the actin cytoskeleton via gelsolin regulates vacuolar H<sup>+</sup>-ATPase recycling. *J. Biol. Chem.* 280, 8452-8463.

**Boutilier, R.G., Heming, T.A. and Iwama, G.K.** (1984) Appendix: physicochemical parameters for use in fish respiratory physiology. In: *Fish Physiology, Vol. 10A*, (ed. W.S. Hoar and A.D. Randall) pp. 403-430. Orlando, FL, USA.: Academic Press,.

**Bradford, M.** (1976). A rapid and sensitive method for the quantitation of microgram quantities of protein utilizing the principle of protein-dye binding. *Anal. Biochem.* 72, 248-254.

**Breton, S. and Brown, D.** (2007). New insights into the regulation of V-ATPase-dependent proton secretion. *Am. J. Physiol. Renal Physiol.* 292: F1-10.

**Buck, J., Sinclair, M.L., Schapal, L., Cann, M.J. and Levin, L.R.**

(1999). Cytosolic adenylyl cyclase defines a unique signaling molecule in mammals. *PNAS* 96, 79-84.

**Cameron, J.N.** (1971). Rapid method for determination of total carbon dioxide in small blood samples. *J. Appl. Physiol.* 31, 632-634.

**Chen, Y., Cann, M.J., Litvin, T.N., Iourgenko, V., Sinclair, M.L., Levin, L.R. and Buck, J.** (2000). Soluble adenylyl cyclase as an evolutionarily conserved bicarbonate sensor. *Science* 289, 625-628.

**Evans, D.H., Piermarini, P.M. and Choe, K.P.** (2004). Homeostasis: osmoregulation, pH regulation, and nitrogen excretion. In *Biology of Sharks and their relatives*, (eds. J.C. Carrier, J.A. Musick and M.R. Heithaus), pp. 247-268. Boca Raton, FL, USA: CRC Press LLC.

**Frische, S., Kwon, T.-H., Frokiar, J., Madsen, K.M. and Nielsen, S.** (2003). Regulated expression of pendrin in rat kidney in response to chronic  $\text{NH}_4\text{Cl}$  or  $\text{NaHCO}_3$  loading. *Am. J. Physiol. Renal Physiol.* 284, F584-593.

**Galvez, F., Reid, S.D., Hawkings, G. and Goss, G.G.** (2002). Isolation and characterization of mitochondria-rich cell types from the gill of freshwater rainbow trout. *Am. J. Physiol. Reg. Integ. Comp. Physiol.* 282, R658-668.

**Georgalis, T., Perry, S.F. and Gilmour, K.M.** (2006). The role of branchial carbonic anhydrase in acid-base regulation in rainbow trout (*Oncorhynchus mykiss*). *J. Exp. Biol.* 209, 518-530.

**Gilmour, K., Bayaa, M., Kenney, L., McNeill, B. and Perry, S.** (2007). Type IV carbonic anhydrase is present in the gills of spiny dogfish

(*Squalus acanthias*). *Am. J. Physiol. Reg. Integr. Comp. Physiol.* 292: R556-567.

**Goss, G.G. and Wood, C.M.** (1991). Two-substrate kinetic analysis: A novel approach linking ion and acid-base transport at the gills of freshwater trout, *Oncorhynchus mykiss*. *J. Comp. Physiol. B* 161, 635-646.

**Goss, G.G. and Perry, S.F.** (1993) Physiological and morphological regulation of acid-base status during hypercapnia in rainbow trout (*Oncorhynchus mykiss*). *Can. J. Zool.* 71, 1673-1680.

**Heisler, N.** (1988). Acid-base regulation. In *Physiology of Elasmobranch Fishes.*, (ed. T. J. Shuttleworth), pp. 215-252. Berlin: Springer-Verlag.

**Ivancic, I. and Degobbis, D.** (1984). An optimal manual procedure for ammonia analysis in natural waters by the indophenol blue method. *Water Res.* 18: 1143-1147.

**Jones, B.C. and Geen, G.H.** (1977). Food and feeding of spiny dogfish (*Squalus acanthias*) in British Columbia waters. *J. Fish Res. Bd. Canada* 34, 2067-2078.

**Kato, F., Hyodo, S. and Kaneko, T.** (2003). Vacuolar-type proton pump in the basolateral plasma membrane energizes ion uptake in branchial mitochondria-rich cells of killifish *Fundulus heteroclitus*, adapted to a low ion environment. *J. Exp. Biol.* 206, 793-803.

**Laemmli, U.K.** (1970). Cleavage of structural proteins during the assembly of the head of the bacteriophage T4. *Nature* 227, 680-685.



**McDonald, D.G., Walker, R.L., Wilkes, P.R.H. and Wood, C.M.**  $H^+$  excretion in the marine teleost, *Parophrys vetulus*. *J. Exp. Biol.* 98, 403-414.

**Mittag, T.W., Guo, W.B. and Kobayashi, K.** (1993). Bicarbonate-activated adenylyl cyclase in fluid-transporting tissues. *Am. J. Physiol. Renal Physiol.* 264, F1060-1064.

**Niv, Y. and Fraser, G.M.** (2002). The alkaline tide phenomenon. *J. Clin. Gastroenterol.* 35, 5-8.

**Pastor-Soler, N., Beaulieu, V., Litvin, T.N., Da Silva, N., Chen Y., Brown, D., Buck, J., Levin, L.R. and Breton, S.** (2003). Bicarbonate-regulated adenylyl cyclase (sAC) is a sensor that regulates pH-dependent V-ATPase recycling. *J. Biol. Chem.* 278, 49523-49529.

**Perry, S., Beyers, M. and Johnson, D.** (2000). Cloning and molecular characterization of the trout (*Oncorhynchus mykiss*) vacuolar  $H^+$ -ATPase B subunit. *J. Exp. Biol.* 203, 459-470.

**Perry, S.F. and Gilmour, K.M.** (2007). Acid-base balance and  $CO_2$  excretion in fish: unanswered questions and emerging models. *Resp. Physiol. Neurobiol.* 154: 199-215.

**Petrovic, S., Wang, Z., Ma, L. and Soleimani, M.** (2003). Regulation of the apical  $Cl^-/HCO_3^-$  exchanger pendrin in rat cortical collecting duct in metabolic acidosis. *Am. J. Physiol. Renal. Physiol.* 284, F103-112.

**Piermarini, P.M. and Evans, D.H.** (2001). Immunochemical analysis of the vacuolar proton-ATPase B-subunit in the gills of a euryhaline stingray (*Dasyatis sabina*): effects of salinity and relation to  $Na^+/K^+$ -ATPase. *J. Exp.*

*Biol.* 204, 3251-3259.

**Piermarini, P.M., Verlander, J.W., Royaux, I.E. and Evans, D.H.** (2002). Pendrin immunoreactivity in the gill epithelium of a euryhaline elasmobranch. *Am. J. Physiol. Reg. Integr. Comp. Physiol.* 283, R983-992.

**Swenson, E.R. and Maren, T.H.** (1987). Roles of gill and red cell carbonic anhydrase in elasmobranch  $\text{HCO}_3^-$  and  $\text{CO}_2$  excretion. *Am. J. Physiol. Reg. Integr. Comp. Physiol.* 253, R450-458.

**Tresguerres, M., Katoh, F., Fenton, H., Jasinska, E. and Goss, G.G.** (2005). Regulation of branchial  $\text{V-H}^+$ -ATPase,  $\text{Na}^+/\text{K}^+$ -ATPase and NHE2 in response to acid and base infusions in the Pacific spiny dogfish (*Squalus acanthias*). *J. Exp. Biol.* 208, 345-354.

**Tresguerres, M., Parks, S.K., Katoh, F. and Goss, G.G.** (2006). Microtubule-dependent relocation of branchial  $\text{V-H}^+$ -ATPase to the basolateral membrane in the Pacific spiny dogfish (*Squalus acanthias*): a role in base secretion. *J. Exp. Biol.* 209, 599-609.

**Wang, T., Busk, M. and Overgaard, J.** (2001). The respiratory consequences of feeding in amphibians and reptiles. *Comp. Biochem. Physiol. A* 128, 533-547.

**Wilson, J.M., Randall, D.J., Vogl, A.W., Harris, J., Sly, W.S. and Iwama, G.K.** (2000). Branchial carbonic anhydrase is present in the dogfish, *Squalus acanthias*. *Fish Physiol. Biochem.* 22, 329-336.

**Wood, C.M., Part, P. and Wright, P.A.** (1995). Ammonia and urea metabolism in relation to gill function and acid-base balance in a marine

elasmobranch, the spiny dogfish (*Squalus acanthias*). *J. Exp. Biol.* 198, 1545-1558.

**Wood, C.M., Kajimura, M., Bucking, C., Walsh, P.J.** (2007)  
Osmoregulation, ionoregulation, and acid-base regulation by the gastrointestinal tract in the elasmobranch *Squalus acanthias*. *J Exp Biol* **210**, 1335-1349.

**Wood, C.M., Kajimura, M., Mommsen, T.P. and Walsh, P.J.** (2005).  
Alkaline tide and nitrogen conservation after feeding in an elasmobranch (*Squalus acanthias*). *J. Exp. Biol.* 208, 2693-2705.

## **Chapter V**

### **V-H<sup>+</sup>-ATPase translocation and HCO<sub>3</sub><sup>-</sup>-activated cAMP production in isolated gill fragments of the Pacific spiny dogfish (*Squalus acanthias*)**

## Introduction

My previous results show that V-H<sup>+</sup>-ATPase inserts into the basolateral membrane of specific gill cells of the dogfish when there is the necessity for enhanced base secretion (Tresguerres *et al.*, 2005, chapter II). Specifically, I have shown that blood alkalosis induced by intravenous infusion of NaHCO<sub>3</sub><sup>-</sup> results in a microtubule-dependent translocation of the V-H<sup>+</sup>-ATPase in gills of the Pacific spiny dogfish *Squalus acanthias* (Tresguerres *et al.*, 2006, chapter III). Moreover, this process is directly correlated to the fish's ability to excrete the excess HCO<sub>3</sub><sup>-</sup> from the blood, suggesting that this is a (the?) mechanism for systemic HCO<sub>3</sub><sup>-</sup> secretion (Tresguerres *et al.*, 2006; chapter III). Of note, V-H<sup>+</sup>-ATPase translocation also takes place during a post-feeding alkalosis and also correlates with net base secretion into the water during that period (Tresguerres *et al.*, 2007; chapter IV) supporting my hypothesis that V-H<sup>+</sup>-ATPase translocation is important for the normal physiology of dogfish.

The V-H<sup>+</sup>-ATPase-rich cells (and also the putative acid-secreting Na<sup>+</sup>/K<sup>+</sup>-ATPase-rich cells) have great amounts of carbonic anhydrase (CA) (Tresguerres *et al.*, 2007; chapter IV). Inhibition of CA by acetazolamide during NaHCO<sub>3</sub> infusion results in a lack of V-H<sup>+</sup>-ATPase translocation and increased plasma [HCO<sub>3</sub><sup>-</sup>] (Tresguerres *et al.*, 2007; chapter IV). However, these experiments have a limitation in that acetazolamide likely blocked other CAs present in the dogfish in addition to CA present inside the V-H<sup>+</sup>-ATPase-rich cells at the gills. Potential unwanted targets include CA inside the red

blood cells (rbc) and extracellular CA IV at the gills (Gilmour *et al.*, 2007). Another possibility is that CA elsewhere in the body is involved in sensing the alkaline stress and releasing an unknown factor which would ultimately trigger the V-H<sup>+</sup>-ATPase translocation at the gills.

Adenosine 3':5'-cyclic monophosphate (cyclic AMP, cAMP) is a prototypical intracellular second messenger in prokaryotes and eukaryotes (Buck *et al.*, 1999). Until recently, the only known way of cAMP production was *via* transmembrane adenylyl cyclases (tmACs), which are sensitive to protein G regulation and activated by the non-physiological molecule forskolin (Wuttke *et al.*, 2001). Soluble adenylyl cyclase (sAC) is a relatively newly discovered enzyme that is directly activated by HCO<sub>3</sub><sup>-</sup> ion to produce cAMP (Buck *et al.*, 1999). Importantly, tmACs are not activated by HCO<sub>3</sub><sup>-</sup>, at least in mammals (Chen *et al.*, 2000), and therefore activation by HCO<sub>3</sub><sup>-</sup> is a distinctive feature of sAC. Unlike the classic tmACs, sAC is not located in the cell membrane, but it is associated with microtubules, nucleus and mitochondria instead (Kamenetsky *et al.*, 2006). *In vitro* studies have determined that sAC activity is enhanced by Mn<sup>2+</sup>, although it is not clear if Mn<sup>2+</sup> is physiologically important *in vivo* due to its low concentration in tissues and cells (Buck *et al.*, 1999). Catechol estrogens (CE) are known to specifically inhibit sAC when used in low doses (Steebhorn *et al.*, 2005; Pastor-Soler *et al.*, 2003). More recently, the novel sAC inhibitor KH7 has been identified in a high-throughput chemical library screen (Hess *et al.*,

2005). However, one problem associated with these compounds is their high price, which makes whole animal experiments prohibitive and unviable.

In the previous chapter (see also Tresguerres *et al.*, 2007), I proposed that  $\text{HCO}_3^-$  generated by CA from hydrating  $\text{CO}_2$  inside the cells stimulates a sAC. The increased cAMP concentration would then signal the translocation of V- $\text{H}^+$ -ATPase from cytoplasmic vesicles into the basolateral membrane to mediate  $\text{H}^+$  reabsorption into the blood and facilitate  $\text{HCO}_3^-$  secretion to the surrounding seawater. This mechanism would be similar to the rat epididymis, where V- $\text{H}^+$ -ATPase is recruited to the apical membrane in a sAC dependent manner in response to alkaline luminal pH (Pastor-Soler *et al.*, 2003).

To both resolve the previous arguments about the potential non-target inhibition of CAs and examine the potential involvement of sACs in V- $\text{H}^+$ -ATPase translocation, I examined the effect of alkalosis on isolated gill fragments. I hypothesized that V- $\text{H}^+$ -ATPase translocation still would take place under these conditions, which would suggest that the components necessary for sensing alkaline stress are present in the gill and no additional extrinsic hormones or nervous inputs are needed. In addition, if sAC indeed acts as the sensor for alkalotic stress, I expect that increasing  $[\text{HCO}_3^-]$  will stimulate cAMP production in gill homogenates. With these premises in mind, I have designed and executed the preliminary experiments described in this chapter.

## Materials and methods

### *Animals*

Pacific spiny dogfish (*Squalus acanthias* L) were obtained, held and fed as described in chapters II and III.

### *Antibodies and reagents*

The  $\alpha$ -V-H<sup>+</sup>-ATPase antibody and other reagents were the same as in the previous chapters. Any additional reagent was purchased from Sigma (St. Louis, MO, USA). KH7 was a kind gift from Profs. J. Buck and L. Levin (Weill Medical College, Cornell University, New York, NY, USA).

### *Gill perfusion and isolation*

A total of 6 animals (~2.50 kg) were removed from the housing tank and used for this study. Fish were caught by hand, anesthetized with tricaine methanesulphonate (TMS, 0.2 g l<sup>-1</sup>, AquaLife, Syndel Laboratories Ltd. Vancouver, BC, Canada), and transferred to an operating table, where the gills were irrigated with aerated seawater containing TMS. The chest cavity was opened using a scalpel and power forceps, and the gills were perfused through the heart with dogfish saline (in mmol l<sup>-1</sup>, 280.0 NaCl, 6.0 KCl, 5.0 CaCl<sub>2</sub>, 3.0 MgCl<sub>2</sub>, 0.5 NaSO<sub>4</sub>, 1.0 NaHPO<sub>4</sub>, 4.0 NaHCO<sub>3</sub>, 350.0 urea, 70.0 TMAO, 5.0 glucose, pH 7.80; modified from Wilson *et al.*, 2000) (*Experiment I*, N=4). This procedure completely eliminated blood from the gills. Gill samples were removed from the arch (second to last gill) and snap frozen for the cAMP assays (right side of the dogfish head) or used in the incubation experiments (left side), as explained below. Gill perfusion was performed on



one additional dogfish, but in this case the dogfish saline contained an extra 50 mmol l<sup>-1</sup> NaHCO<sub>3</sub> (pH 8.50) (*Experiment II*, 6 filaments from 1 dogfish for each experimental time).

#### *Gill incubation*

Following the gill perfusion, gills were placed in ice-cold dogfish saline. Gill filaments (~2 mm) were cut from the gills using a scalpel. One sample was immediately immersed in fixative (t=0). In *Experiment I*, additional samples were placed in 20 ml tubes containing the experimental incubation solutions (Table 5.1). Tubes were placed in containers provided with flowing seawater, which kept the T° constant at 13.5°C while providing vigorous mixing. After 6 h of incubation, the gill samples were placed in fixative.

In *Experiment II*, gill fragments were incubated in the saline with additional 50 mmol l<sup>-1</sup> NaHCO<sub>3</sub> (pH 8.50) and samples were taken and placed in fixative at t=1, 2 and 6 h. During the incubation, gill samples were placed in a plastic basket suspended inside the container with the solution. The solution was continuously stirred by a magnetic bar.

#### *Incubation solutions*

pH of the solutions was measured using a thermostatted Accumet micro-size pH electrode model 13-620-94 (Fisher Scientific, Pittsburgh, PA, USA). Total CO<sub>2</sub> (TCO<sub>2</sub>) was determined in a chamber (37°C) equipped with a CO<sub>2</sub> electrode (Radiometer, Copenhagen, Denmark) following the method by Cameron (1971). PCO<sub>2</sub> and [HCO<sub>3</sub><sup>-</sup>] were calculated from pH and TCO<sub>2</sub> as

described in chapter IV. pH,  $PCO_2$  and  $[HCO_3^-]$  of the solutions at the time of commencement ( $t=0$ ) and end of experiments (6 h) are shown in table 5.1.

#### *Immunohistochemistry*

Gill fixation and immunohistochemistry for  $V-H^+$ -ATPase was performed as described in chapters II-IV.

#### *cAMP assay in gill homogenates*

Frozen gill samples from *Experiment I* (perfused with normal dogfish saline) were pulverized in liquid  $N_2$  using mortar and pestle and re-suspended in 20 volumes of ice cold homogenization buffer (250  $mmol\ l^{-1}$  sucrose, 1  $mmol\ l^{-1}$  EDTA, 30  $mmol\ l^{-1}$  Tris, 100  $mg/ml$  PMSF, 2  $mg\ ml^{-1}$  pepstatin, pH 7.40), and sonicated on ice for 20 seconds. Debris was removed by low speed centrifugation (3000  $g$  for 5 min,  $4^\circ C$ ). Samples of the supernatant were incubated at room temperature in the solutions listed in table 5.2. After 20 min, incubations were stopped by addition of concentrated HCl (1:100 v/v) and the samples were stored at  $-80^\circ C$ . The cAMP produced in each sample was assessed in duplicate 100  $\mu l$  aliquots using the Correlate Direct Cyclic AMP Enzyme Immunoassay Kit (Assay designs, Ann Arbor, MI, USA) following the manufacturer's directions.

## Results

### *i- V-H<sup>+</sup>-ATPase translocation in isolated gill fragments*

#### *Experiment I*

The majority of cells from gill filaments incubated in external media with different  $[\text{HCO}_3^-]$ ,  $\text{PCO}_2$  and pH displayed cytoplasmic V-H<sup>+</sup>-ATPase immunolabeling (N=4). However, there were a number of cells with basolateral V-H<sup>+</sup>-ATPase immunolabeling in the incubation with high  $[\text{HCO}_3^-]$  and  $\text{PCO}_2$ , normal pH of 7.82 (treatment #2) (Fig. 5.1). These cells were found in filaments from all four fish examined. A few cells in the incubation with high  $[\text{HCO}_3^-]$  and pH, "low"  $\text{PCO}_2$  and treated with 2-CE also had basolateral V-H<sup>+</sup>-ATPase immunolabeling (treatment #10) (Fig. 5.1). However, these cells were found in gill filaments from only two of the four fishes examined. There were no cells with basolateral V-H<sup>+</sup>-ATPase immunolabeling in any of the other treatments.

#### *Experiment II*

Gills from this experiment were internally perfused with a high  $[\text{HCO}_3^-]$  and pH solution prior to incubation in the same solution. V-H<sup>+</sup>-ATPase translocation occurred as soon as 1 h after incubation. The number of cells with basolateral V-H<sup>+</sup>-ATPase immunolabeling and the degree of the basolateral labeling increased proportionally with the incubation time. By t=6 h, the majority of cells had a distinct basolateral V-H<sup>+</sup>-ATPase staining pattern (Fig. 5.2).

### *ii- cAMP in gill homogenates*

An elevated  $[\text{HCO}_3^-]$  of  $50 \text{ mmol l}^{-1}$  significantly activated cAMP production in gill homogenates by almost 100%. This result shows that a  $\text{HCO}_3^-$ -sensitive adenylyl cyclase is present in dogfish gills. The effect was completely abolished when homogenates were incubated with  $50 \text{ mmol l}^{-1}$   $\text{HCO}_3^-$  in the presence of  $5 \text{ mmol l}^{-1}$   $\text{MnCl}_2$  (Fig. 5.3A). In a separate experiment,  $\text{HCO}_3^-$  had a similar stimulating effect on cAMP production (Fig. 5.3B). In this experiment, the  $\text{HCO}_3^-$ -activation was significantly reduced by addition of the specific sAC inhibitors KH7 and 2-CE ( $50 \text{ }\mu\text{mol l}^{-1}$  in both cases). To confirm that the effects of KH7 and 2-CE were specific for the  $\text{HCO}_3^-$ -stimulated cAMP production, the inhibitors were added to separate control (with extra  $50 \text{ mmol l}^{-1}$   $\text{NaCl}$ ). Neither KH7 nor 2-CE inhibited cAMP production under this condition (Fig. 5C).

## Discussion

The results presented in this chapter demonstrate that V-H<sup>+</sup>-ATPase translocation into the basolateral membrane of dogfish gill cells can take place in isolated gill fragments subjected to alkaline stress. In addition, cAMP production in gill homogenates is stimulated under similar conditions, an effect that is abolished by specific sAC inhibitors. This suggests a link between V-H<sup>+</sup>-ATPase translocation and cAMP, possibly mediated by sAC.

### *V-H<sup>+</sup>-ATPase translocation in isolated gill fragments*

Before drawing any further conclusions, I must list the limitations of the present study and state that these experiments are only preliminary and will need to be repeated with another field season at Bamfield and more concise quantification of the effects under each condition. In the first incubation series, gills were internally perfused with normal dogfish saline and then incubated in the different solutions. The rationale was that the physico-chemical parameters of the specific incubation solutions would be transferred to the gill cell cytoplasm. Specifically, CO<sub>2</sub> would simply diffuse inside the cells, while I hypothesized that HCO<sub>3</sub><sup>-</sup> would enter the cells across the apical anion exchanger (AE) Pendrin working in reverse (import HCO<sub>3</sub><sup>-</sup> into the cell in exchange for Cl<sup>-</sup>). In addition, the incubation solution could also enter the basolateral side of the epithelium directly through the blood vessels that are exposed after dissection. Even though these premises seem to have been fulfilled in certain cells, the V-H<sup>+</sup>-ATPase immunolabeling pattern remained cytoplasmic in the majority of cells during all the incubations. The only

incubation in which V-H<sup>+</sup>-ATPase translocation was noticed consisted of elevated [HCO<sub>3</sub><sup>-</sup>] and *PCO*<sub>2</sub>, and normal pH (treatment #2). Incubations in media in which only *PCO*<sub>2</sub> (treatment #1) or only pH (treatment #6) were elevated did not result in any appreciable V-H<sup>+</sup>-ATPase translocation. Neither was there V-H<sup>+</sup>-ATPase translocation in a condition with elevated [HCO<sub>3</sub><sup>-</sup>] and pH, but low *PCO*<sub>2</sub> (treatment #8). Unfortunately, since only some cells from this treatment demonstrated V-H<sup>+</sup>-ATPase translocation it was not appropriate to perform quantitative analyses of the effects of pH, [HCO<sub>3</sub><sup>-</sup>], *PCO*<sub>2</sub>, 2-CE and acetazolamide. Nonetheless, elevated [HCO<sub>3</sub><sup>-</sup>] and pH was the only treatment that consistently resulted in V-H<sup>+</sup>-ATPase translocation in at least some cells in all gill filaments analyzed. It is possible that this type of incubation indeed resulted in elevated [HCO<sub>3</sub><sup>-</sup>]<sub>i</sub> by AE transport, CA-generated HCO<sub>3</sub><sup>-</sup> from CO<sub>2</sub> or both. These results also suggest that [HCO<sub>3</sub><sup>-</sup>] and *PCO*<sub>2</sub> have synergistic effects. A somehow complicated hypothesis is that the elevated intracellular *PCO*<sub>2</sub> triggers the V-H<sup>+</sup>-ATPase translocation *via* the CA-HCO<sub>3</sub><sup>-</sup>-sAC pathway, while the elevated external [HCO<sub>3</sub><sup>-</sup>] prevents intracellular HCO<sub>3</sub><sup>-</sup> leaking to the external medium. This could potentially enhance the triggering stimulus for V-H<sup>+</sup>-ATPase translocation.

In gill filaments from two out of four fish some cells also demonstrated V-H<sup>+</sup>-ATPase translocation in the incubation with high [HCO<sub>3</sub><sup>-</sup>] and pH, a relatively low *PCO*<sub>2</sub> and 2-CE -a sAC inhibitor- (treatment #10) (Fig. 5.1) . No V-H<sup>+</sup>-ATPase translocation was detected in any cell from gill filaments incubated in the same conditions, but without 2-CE. The only logical

explanation for this result is that maybe  $\text{HCO}_3^-$  differentially entered into certain cells and 2-CE did not. This could be due to inefficient mixing during the incubation and problems with boundary layers, and requires further research.

Perfusing the gills with a solution with elevated  $[\text{HCO}_3^-]$ , pH and  $\text{PCO}_2$  prior to incubation in the same medium proved to be much more efficient in triggering the  $\text{V-H}^+$ -ATPase translocation. Unfortunately, the validity of these results is limited because all the gill filaments that I analyzed came from the same dogfish. As a consequence, the conclusions presented below must be confirmed by future additional experiments.

Of the three variables that were elevated during the incubations (extracellular  $[\text{HCO}_3^-]$ ,  $\text{PCO}_2$  and pH), I can probably rule out pH as the trigger for  $\text{V-H}^+$ -ATPase translocation. This decision is based on the results presented above, which show that  $\text{V-H}^+$ -ATPase translocation can take place under conditions where pH was unaltered. The permeability of the basolateral side of fish gill epithelia to  $\text{HCO}_3^-$  has been proposed to be very limited (Perry *et al.*, 1982; 1984; Gilmour *et al.* 2001; Wilson *et al.*, 2000). Therefore, it is  $\text{CO}_2$  that probably diffuses inside the cells and it is hydrated into  $\text{H}^+$  and  $\text{HCO}_3^-$  by CA (chapter IV, Tresguerres *et al.*, 2007). I propose that an elevation in intracellular  $\text{HCO}_3^-$  triggers  $\text{V-H}^+$ -ATPase translocation.

Interestingly, the increased  $\text{PCO}_2$  should result in a faster rate in  $\text{CO}_2$  diffusion into the cell no matter from which side (apical-basolateral) the gradient is applied. However,  $\text{V-H}^+$ -ATPase translocation was much more

efficient when the elevated  $PCO_2$  was present at both sides. This implies one or all of the following options: (1) there is a  $PCO_2$  sensing mechanism in the external side of the basolateral membrane, (2) the extracellular CA IV described by Gilmour *et al.* (2007) in the basolateral membrane of pillar cells is essential for the entrance of  $HCO_3^-$  (as  $CO_2$ ) into the V-H<sup>+</sup>-ATPase-rich cells, (3) the permeability of the basolateral membrane of dogfish gills to  $HCO_3^-$  is not really limited, or (4) the permeability of the V-H<sup>+</sup>-ATPase-rich cells basolateral membrane is increased during elevated blood  $[HCO_3^-]$  and/or  $PCO_2$  conditions. Any of these scenarios should result in further elevations of  $[HCO_3^-]_i$  during blood alkalosis, which could in turn trigger V-H<sup>+</sup>-ATPase translocation. It would be adaptive if V-H<sup>+</sup>-ATPase is only triggered by specific changes in the blood, and not in seawater. Future experiments to address this question should include gill perfusion using the solutions detailed in table 1, followed by incubation in normal seawater and V-H<sup>+</sup>-ATPase immunohistochemical analysis.

#### *cAMP in gill homogenates*

Elevating the  $[HCO_3^-]$  to 50 mmol l<sup>-1</sup> in vitro in gill homogenates resulted in a significant increase in cAMP production. To date, only two options for the generation of cAMP have been described. The traditional way involves transmembrane adenylyl cyclases (tmAC), of which nine isoforms have been identified (Antoni, 2000). cAMP production by tmAC is activated in response to G proteins,  $Ca^{2+}$  and/or protein phosphorylation (Cooper, 2003). However, tmAC are insensitive to  $[HCO_3^-]$ , or at least the mammalian



isoforms are (Chen *et al.*, 2000). This is a crucial point, because it indicates that the elevation in cAMP in my experiments is probably not explained by tmAC. A second way of generating cAMP is *via* soluble adenylyl cyclase (sAC). Research on sAC began almost forty years ago, when it was noticed that elevations in  $[\text{HCO}_3^-]$  resulted in increased cAMP production in rat testis (Braun and Dods, 1975; Garbers *et al.*, 1971). The physiological role of the cAMP increase was proposed to be in sperm maturation and motility prior to ejaculation (Braun and Dods, 1975; Garbers *et al.*, 1971). Recently, sAC was finally molecularly identified from rat testis (Buck *et al.*, 1999), and subsequently cloned from other tissues and organisms, including humans (Geng *et al.*, 2005). Interestingly, similar sAC has also been identified in bacteria, suggesting that sAC is a “conserved  $\text{HCO}_3^-$  sensor” (Chen *et al.*, 2000). It has been confirmed that sAC plays an important role in the processes of sperm maturation (Pastor-Soler *et al.*, 2003) and axonal development and neural differentiation (Stessin *et al.*, 2006; Wu *et al.*, 2006). It has also been proposed to play a role in A/B relevant ion transport at the mammalian kidney (Breton and Brown, 2007). Notably, V- $\text{H}^+$ -ATPase translocation into the apical membrane of rat testis cells has been demonstrated to depend on elevation in  $[\text{HCO}_3^-]$ , and mediated by intracellular CA and sAC (Pastor-Soler *et al.*, 2003). I have used the model from rat testis cells as a frame of reference for my dogfish experiments.

The  $\text{HCO}_3^-$ -dependent cAMP production in dogfish gill homogenates was totally abolished by KH7 and 2-hydroxy-estradiol (2-CE), further

supporting the presence of sAC in my system. While KH7 is a very specific inhibitor of sAC (Hess *et al.*, 2005), 2-CE has been shown to also inhibit tmAC at higher concentrations (Steegborn *et al.*, 2005). However, neither 2-CE nor KH7 inhibit basal cAMP production (without  $\text{HCO}_3^-$  stimulation) in gill homogenates, indicating that the inhibitors are only acting on the  $\text{HCO}_3^-$ -sensitive component (sAC?) in dogfish gill homogenates.

The enhanced cAMP production in response to  $\text{HCO}_3^-$  in my experiments was also totally abolished by  $5 \text{ mmol l}^{-1} \text{ Mn}^{2+}$ . *A priori* this was an unexpected result because it has been traditionally shown that  $\text{Mn}^{2+}$  activates cAMP production both in rat testis homogenates (Braun *et al.*, 1975) and in purified human and rat sAC (Litvin *et al.*, 2003). However, a search of the literature revealed that the sAC is inhibited by  $\text{HCO}_3^-$  and  $\text{Mn}^{2+}$  when applied together (Geng *et al.*, 2005). The authors proposed that  $\text{Mn}^{2+}$  might inhibit sAC by binding into a catalytic or allosteric site. The same explanation might be true for my results. Additionally, divalent metals are important in the catalytic mechanism of sAC (Kamenetsky *et al.*, 2006). Therefore, it is also possible that  $\text{Mn}^{2+}$  is complexed by  $\text{HCO}_3^-$ , which would leave no metal left to coordinate ATP hydrolysis by sAC. Future research in the area is necessary to clarify these questions.

Activation of cAMP production by  $\text{HCO}_3^-$  does not necessarily imply that the same mechanism is responsible for the V- $\text{H}^+$ -ATPase translocation. However, summing up the data presented in this and the previous chapters, together with the bibliography, I conclude that the sAC involvement in the V-

H<sup>+</sup>-ATPase translocation mechanism is highly probable. The definitive confirmation of the sAC presence in dogfish gills awaits molecular identification and cloning of a dogfish homologue. Complementary experiments should include a detailed kinetic and pharmacological analysis of the HCO<sub>3</sub><sup>-</sup>-activated cAMP production in gill homogenates, or better yet in purified dogfish sAC.

### *Integration*

With the precautions listed above, I suggest that V-H<sup>+</sup>-ATPase translocation can take place in isolated gill fragments subjected to alkaline stress. It is likely that the trigger for V-H<sup>+</sup>-ATPase translocation is CA-generated [HCO<sub>3</sub><sup>-</sup>]<sub>i</sub>, which in turns activates a putative sAC. According to this hypothesis, the increased cAMP is the final trigger for V-H<sup>+</sup>-ATPase translocation. This model predicts that all the components of the regulatory response to blood alkalosis occur entirely within the gill tissue and does not appear to require other input to occur. The components would include the sensing mechanism (sAC), accessory proteins (CA), signaling proteins (PKA?) and effector proteins (V-H<sup>+</sup>-ATPase and microtubule-related proteins). Moreover, this system has the potentiality of self-regulation *via* negative feedback because H<sup>+</sup> reabsorption counteracts the original blood alkalosis signal. This does not rule out that extrinsic factors could further regulate HCO<sub>3</sub><sup>-</sup> secretion and H<sup>+</sup> reabsorption in dogfish gills, but they could act by modulating a system that is already functional at the cell level. This is a highly novel hypothesis that could potentially have important implications for

theories about the evolution of physiological systems (see chapter X, General Discussion).

**Table 5.1.** pH,  $PCO_2$  and  $[HCO_3^-]$  of the incubation solutions.

	t=0			t=6h		
Treatment	pH	$PCO_2$ (torr)	$[HCO_3^-]$ (mmol l <sup>-1</sup> )	pH (torr)	$PCO_2$	$[HCO_3^-]$ (mmol l <sup>-1</sup> )
<b>1</b> -Low $[HCO_3^-]$ -High $PCO_2$	6.80 ± 0.04	23.5 ± 0.8	5.7 ± 0.4	6.88 ± 0.13	20.2 ± 7.8	4.8 ± 0.3
<b>2</b> -High $[HCO_3^-]$ -High $PCO_2$	7.82 ± 0.04	18.3 ± 2.1	56.1 ± 2.1	7.91 ± 0.12	17.0 ± 6.7	52.4 ± 0.9
<b>3</b> -High $[HCO_3^-]$ -High $PCO_2$ -AZ	7.82 ± 0.04	18.3 ± 2.1	56.1 ± 2.1	7.97 ± 0.10	13.8 ± 4.0	55.1 ± 1.3
<b>4</b> -High $[HCO_3^-]$ -High $PCO_2$ -2-CE	7.82 ± 0.04	18.3 ± 2.1	56.1 ± 2.1	7.99 ± 0.09	13.7 ± 3.8	57.7 ± 1.1
<b>5</b> -Low $[HCO_3^-]$ -Low $PCO_2$ -Ctrl pH	7.83 ± 0.04	0.5 ± 0.3	1.6 ± 0.4	7.87 ± 0.05	0.2 ± 0.0	0.9 ± 0.3
<b>6</b> -Low $[HCO_3^-]$ -Low $PCO_2$ -High pH	8.27 ± 0.02	0.2 ± 0.5	1.9 ± 0.5	8.28 ± 0.05	0.0 ± 0.0	0.1 ± 0.1
<b>7</b> -Low $[HCO_3^-]$ -Low $PCO_2$ -Low pH	6.86 ± 0.06	1.3 ± 0.0	0.4 ± 0.2	6.91 ± 0.06	0.0 ± 0.0	0.0 ± 0.0
<b>8</b> -High $[HCO_3^-]$ -Low $PCO_2$	8.38 ± 0.04	4.4 ± 0.5	53.7 ± 0.8	8.46 ± 0.05	3.9 ± 0.5	57.7 ± 0.4
<b>9</b> -High $[HCO_3^-]$ -Low $PCO_2$ -AZ	8.38 ± 0.04	4.4 ± 0.5	53.7 ± 0.8	8.50 ± 0.04	3.6 ± 0.4	58.6 ± 0.6
<b>10</b> -High $[HCO_3^-]$ -Low $PCO_2$ -2-CE	8.38 ± 0.04	4.4 ± 0.5	53.7 ± 0.8	8.51 ± 0.03	3.3 ± 0.3	57.4 ± 0.9

AZ: 100  $\mu\text{mol l}^{-1}$  acetazolamide; 2-CE: 100  $\mu\text{mol l}^{-1}$  2-hydroxy-estradiol.

N=4.

**Table 5.2.** Incubation solutions in the [cAMP] determination experiments.

Treatment	NaCl	MnCl <sub>2</sub>	DMSO	NaHCO <sub>3</sub>	KH7
NaCl (control)	55.0	-	1.0 µl	-	-
NaCl + Mn <sup>2+</sup>	50.0	5.0	1.0 µl	-	-
NaHCO <sub>3</sub>	5.0	-	1.0 µl	50.0	-
NaHCO <sub>3</sub> <sup>-</sup> + Mn <sup>2+</sup>	5.0	5.0	1.0 µl	50.0	-
NaHCO <sub>3</sub> <sup>-</sup> + 50 µmmol l <sup>-1</sup> KH7	5.0	-	-	50.0	1.0 µl
NaHCO <sub>3</sub> <sup>-</sup> + 50 µmmol l <sup>-1</sup> 2-CE	5.0	-	-	50.0	1.0 µl
NaCl + 50 µmmol l <sup>-1</sup> KH7	55.0	-	-	-	1.0 µl
NaCl + 50 µmmol l <sup>-1</sup> 2-CE	55.0	-	-	-	1.0 µl

Samples were in homogenization buffer (250 mmol l<sup>-1</sup> sucrose, 1 mmol l<sup>-1</sup> EDTA, 30 mmol l<sup>-1</sup> Tris, 100 mg ml<sup>-1</sup> PMSF, 2 mg ml<sup>-1</sup> pepstatin) prior to incubation. The table shows what was added to 100 µl subsamples. KH7 and 2-CE was added from a 5.0 mmol l<sup>-1</sup> stock in DMSO. 2-CE: 2-hydroxy-estradiol.

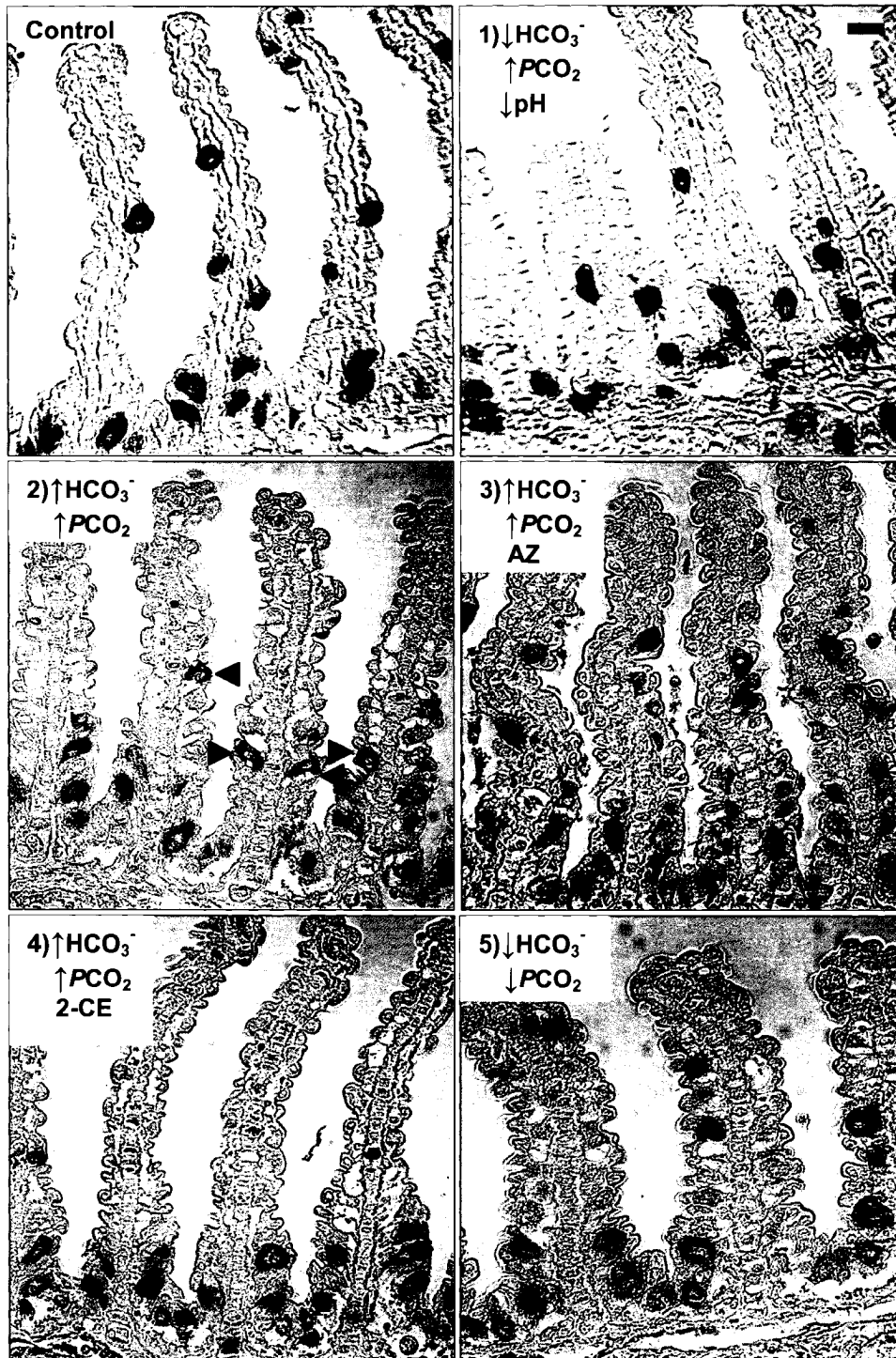


**Figure 5.1.**

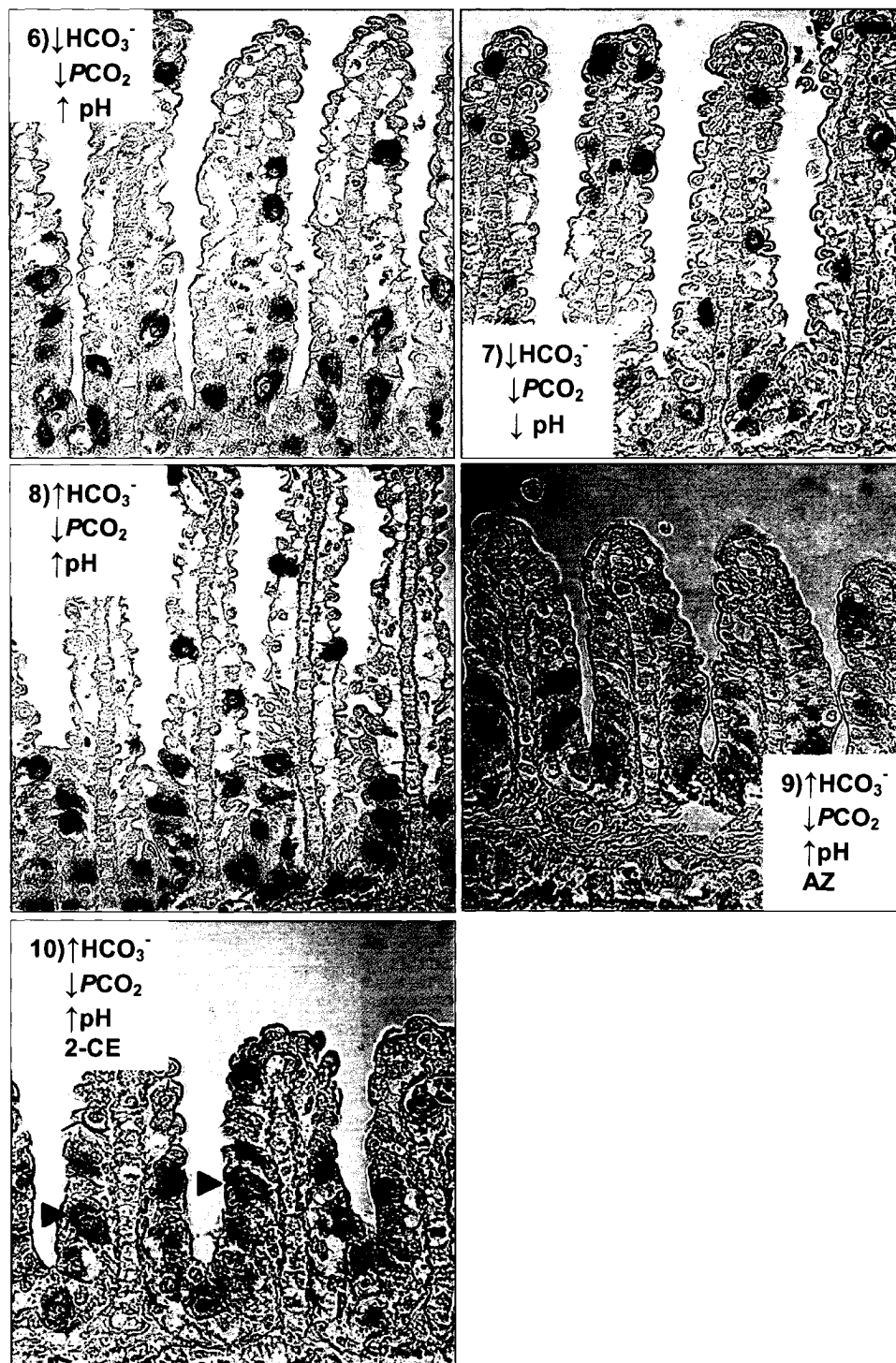


**Figure 5.1.** V-H<sup>+</sup>-ATPase immunolabeling in the isolated gill experiments (experiment I). The incubation parameters are listed in the box of each figure. For more details refer to table 5.1. Arrowheads in (2) and (10) indicate cells with basolateral V-H<sup>+</sup>-ATPase immunolabeling. Scale bar: 10  $\mu\text{m}$ .



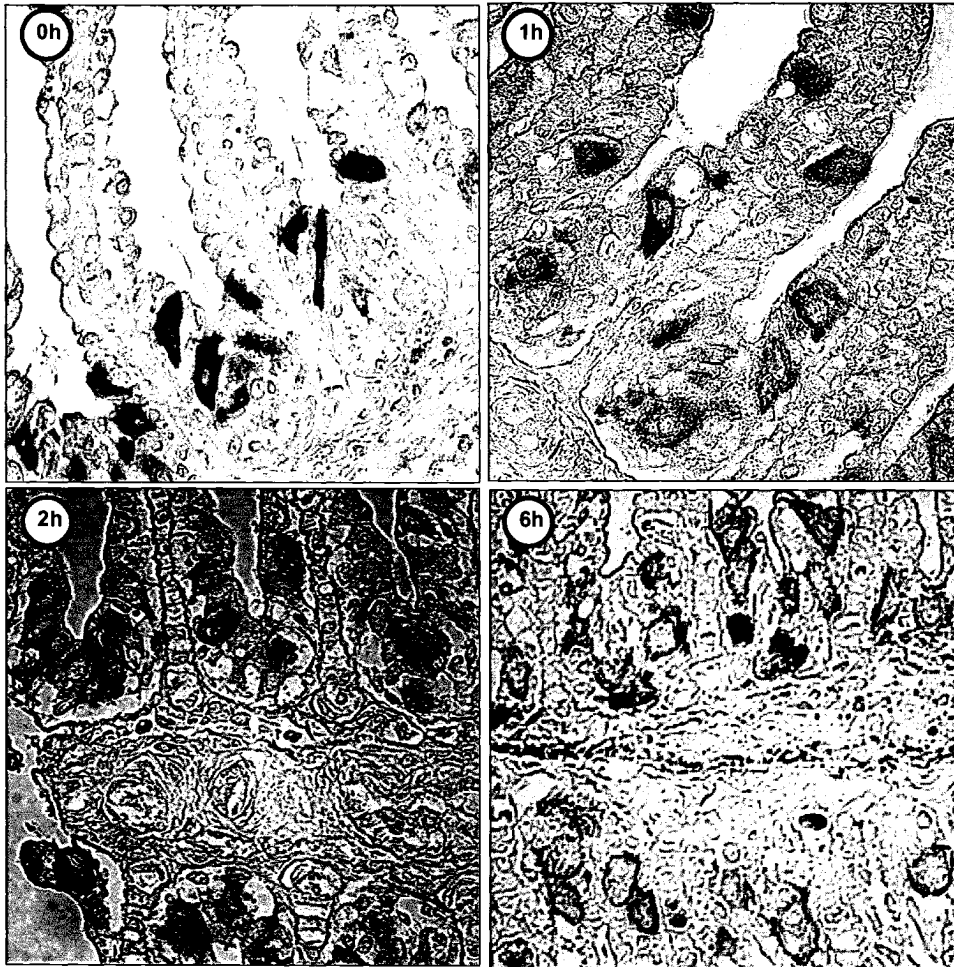


**Figure 5.2.** V-H<sup>+</sup>-ATPase immunolabeling in the isolated gill experiments (*experiment II*). Gills were perfused internally with dogfish saline containing an extra 50 mmol l<sup>-1</sup> [HCO<sub>3</sub><sup>-</sup>] (pH 8.50), and incubated for up to 6 h in the same medium. The incubation times are indicated in the circles. Magnification: 640x.

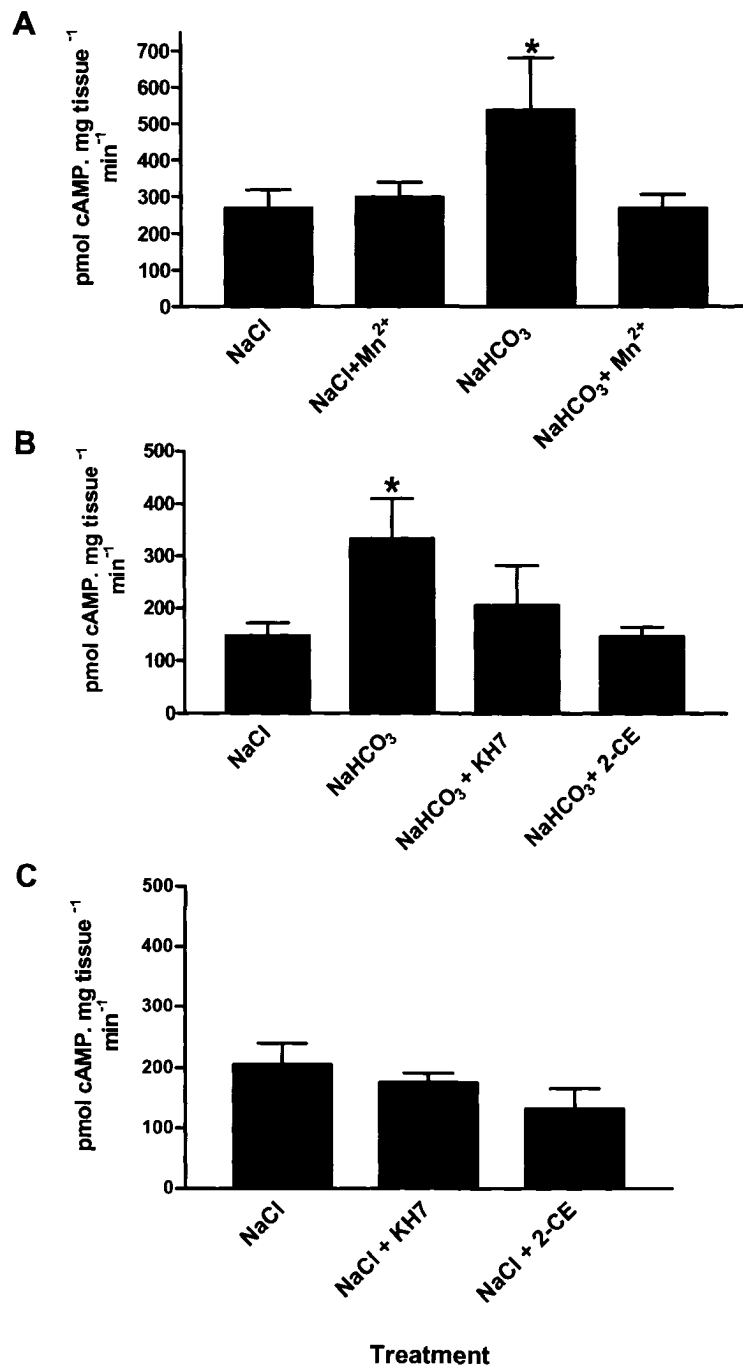


**Figure 5.3.**

**Figure 5.3.** [cAMP] in gill homogenates. Samples were dissolved in homogenization buffer and incubated in the solutions described in table 5.2. The asterisk indicates a significant difference compared to the NaCl control ( $p < 0.05$ , 1-way repeated-measures ANOVA, Dunnet's test,  $N=5$  in A and B;  $N=3$  in C). KH7, 2-CE (2-hydroxy-estradiol) are specific inhibitors of soluble adenylyl cyclase, and were added at a concentration of  $50 \mu\text{mol l}^{-1}$ .

## References

- Antoni, F.A.** (2000). Molecular diversity of cyclic AMP signaling. *Front. Neuroendocrinol.* **21**, 103-132.
- Braun, T. and Dods, R.F.** (1975). Development of a  $Mn^{2+}$ -sensitive, "soluble" adenylate cyclase in rat testis. *PNAS* **72**, 1097-1101.
- Breton, S. and Brown, D.** (2007). New insights into the regulation of V-ATPase-dependent proton secretion. *Am. J. Physiol. Renal Physiol.* **292**: F1-10.
- Buck, J., Sinclair, M.L., Schapal, L., Cann, M.J. and Levin, L.R.** (1999). Cytosolic adenylyl cyclase defines a unique signaling molecule in mammals. *PNAS* **96**, 79-84.
- Chen, Y., Cann, M.J., Litvin, T.N., Iourgenko, V., Sinclair, M.L., Levin, L.R. and Buck, J.** (2000). Soluble adenylyl cyclase as an evolutionary conserved bicarbonate sensor. *Science* **289**, 625-628.
- Cooper, D.M.** (2003). Regulation and organization of adenylyl cyclases and cAMP. *Biochem. J.* **375**, 517-529.
- Garbers, D.L., Lust, W.D., First, N.L. and Lardy, H.A.** (1971). Effect of phosphodiesterase inhibitors and cyclic nucleotides on sperm respiration and motility. *Biochem.* **10**, 1825-1831.
- Geng, W., Wang, Z., Zhang, J., Reed, B.Y. Pak, C.Y.C. and Moe, O.W.** (2005). Cloning and characterization of the human soluble adenylyl cyclase. *Am. J. Physiol. Cell Physiol.* **288**, C1305–1316.
- Gilmour, K., Bayaa, M., Kenney, L., McNeill, B. and Perry, S.**

(2007). Type IV carbonic anhydrase is present in the gills of spiny dogfish (*Squalus acanthias*). *Am. J. Physiol. Reg. Integr. Comp. Physiol.* 292: R556-567.

**Hess, K.C., Jones, B.H., Marquez, B., Chen, Y., Ord, T.S., Kamenetsky, M., Miyamoto, C., Zippin, J. H., Kopf, G.S., Suarez, S.S. et al.** (2005). The "Soluble" Adenylyl Cyclase in Sperm Mediates Multiple Signaling Events Required for Fertilization. *Dev. Cell* **9**, 249-259.

**Kamenetsky M., Middelhaufe S., Bank E.M., Levin L.R., Buck J., Steegborn, C.** (2006). Molecular details of cAMP generation in mammalian cells: a tale of two systems. *J. Mol. Biol.* **362**, 623-639.

**Litvin, T.N., Kamenetsky, M., Zaryfian, A., Buck, J. and Levin, L.R.** (2003). Kinetic properties of "soluble" adenylyl cyclase. *J. Biol. Chem.* **278**, 15922-1926.

**Pastor-Soler, N., Beaulieu, V., Litvin, T.N., Da Silva, N., Chen Y., Brown, D., Buck, J., Levin, L.R. and Breton, S.** (2003). Bicarbonate-regulated adenylyl cyclase (sAC) is a sensor that regulates pH-dependent V-ATPase recycling. *J. Biol. Chem.* **278**, 49523-49529.

**Steegborn, C., Litvin, T.N., Hess, K.C., Capper, A.B., Taussig, R., Buck, J. and Wu, H.** (2005). A novel mechanism for adenylyl cyclase inhibition from the crystal structure of its complex with catechol estrogen. *J. Biol. Chem.* **280**, 31754-31759.

**Tresguerres, M., Katoh, F., Fenton, H., Jasinska, E. and Goss, G.G.** (2005). Regulation of branchial V-H<sup>+</sup>-ATPase, Na<sup>+</sup>/K<sup>+</sup>-ATPase and

NHE2 in response to acid and base infusions in the Pacific spiny dogfish (*Squalus acanthias*). *J. Exp. Biol.* **208**, 345-354.

**Tresguerres, M., Parks, S.K., Katoh, F. and Goss, G.G.** (2006). Microtubule-dependent relocation of branchial V-H<sup>+</sup>-ATPase to the basolateral membrane in the Pacific spiny dogfish (*Squalus acanthias*): a role in base secretion. *J. Exp. Biol.* **209**, 599-609.

**Tresguerres, M., Parks, S. K., Wood, C.M. and Goss, G. G.** (2007). V-H<sup>+</sup>-ATPase translocation during blood alkalosis in dogfish gills: interaction with carbonic anhydrase and involvement in the post-feeding alkaline tide. *Am. J. Physiol. Int. Reg. Comp. Physiol.* **292**.

**Wilson, J.M., Randall, D.J., Vogl, A.W., Harris, J., Sly, W.S. and Iwama, G.K.** (2000). Branchial carbonic anhydrase is present in the dogfish, *Squalus acanthias*. *Fish Physiol. Biochem.* **22**, 329-336.

**Wu, K.Y., Zippin, J.H., Huron, D.R., Kamenetsky, M., Hengst, U., Buck, J., Levin, L.R. and Jaffrey, S.R.** (2006). Soluble adenylyl cyclase is required for netrin-1 signaling in nerve growth cones. *Nature Neuroscience* **9**, 1257-1254.

**Wuttke, M. S., Buck, J. and Levin, L. R.** (2001). Bicarbonate-regulated soluble adenylyl cyclase. *JOP. J. Pancreas* **2**, 154–158.

**Pacific hagfish *Eptatretus stoutii***

## Chapter VI

### **V-H<sup>+</sup>-ATPase, Na<sup>+</sup>/K<sup>+</sup>-ATPase and NHE2 immunoreactivity in the gill epithelium of the Pacific hagfish (*Eptatretus stoutii*)<sup>1</sup>**

<sup>1</sup>A version of this chapter has been published. **Tresguerres, M.**, Parks, S.K. and Goss, G.G. (2006). *Comparative Biochemistry and Physiology A* 145, 312-321. Reproduced with permission of Elsevier Inc. and the co-authors of the manuscript.



## Introduction

Hagfish are the most ancient group of living craniates. They are believed to have conserved several characteristics from the common ancestor with the vertebrates, an organism that presumably never entered into freshwater (Holland and Chen, 2001). For these reasons, hagfish are a very interesting case for comparative studies about vertebrate ionic and acid-base (A/B) regulation.

Hagfish are peculiar when compared to lampreys, elasmobranchs and teleosts in that they are exclusively marine osmoconformers. Since plasma  $[Cl^-]$  and  $[Na^+]$  are similar to seawater (SW) (Morris, 1965), they do not need to actively uptake or secrete NaCl to maintain ionic homeostasis. These functions are usually achieved by mitochondria-rich (MR) cells in the gill (teleosts) or rectal gland (elasmobranchs) epithelia. Nonetheless, the hagfish gill epithelium has numerous MR cells, often referred to as ionocytes (Elger and Hentschel, 1983; Mallat and Paulsen, 1986; Bartels, 1992). Based on the role of the MR cells in other physiological systems, it has been suggested that the hagfish MR cells are involved in systemic acid/base (A/B) regulation (Bartels, 1992).

Evans (1984) was the first to propose  $Na^+/H^+$  and  $Cl^-/HCO_3^-$  exchange systems for A/B regulation in hagfish. He found that placing hagfish in  $Na^+$ -free SW-like water inhibited the net secretion of acid, while  $Cl^-$ -free SW-like water inhibited the net secretion of base. Since the urinary output of hagfish is very small, the gills were proposed to be the place where these exchanges

take place (Evans, 1984). A first step to confirm this hypothesis is to look for ion-transporting proteins with known functions in better-studied systems. For example,  $\text{Na}^+/\text{K}^+$ -ATPase and carbonic anhydrase (CA), two A/B relevant enzymes, have been found in gill MR cells of the Pacific hagfish *Eptatretus stoutii* (Mallat *et al.*, 1986). The MR cells in the gills of the Atlantic hagfish *Myxine glutinosa* also have high levels of  $\text{Na}^+/\text{K}^+$ -ATPase (Choe *et al.*, 1999). In addition, the gills of *M. glutinosa* have at least one  $\text{Na}^+/\text{H}^+$  exchange-like (NHE) protein (Edwards *et al.* 2001; Choe *et al.*, 2002). Furthermore, hagfish NHE mRNA expression increases during metabolic acidosis, suggesting that it is an apical exchanger involved in acid secretion (Edwards *et al.*, 2001). However, the localization of the NHE in the hagfish gill epithelium was not examined in those studies since they were limited to western blotting (Choe) and quantitative PCR (Edwards).

Unlike acid secretion, nothing is known about the cellular mechanisms for base secretion in hagfish gills. Here, the gills of marine elasmobranchs serve as a better reference than teleosts, since they are involved in A/B regulation but not in salt secretion (Heisler, 1988). In marine elasmobranchs, a basolateral vacuolar-type  $\text{H}^+$ -ATPase (V- $\text{H}^+$ -ATPase) has been proposed to energize the secretion of  $\text{HCO}_3^-$  to SW across an apical  $\text{Cl}^-/\text{HCO}_3^-$  exchanger (Piermarini *et al.*, 2003, Evans *et al.*, 2005; Tresguerres *et al.*, 2005; 2006; chapters II and III). Moreover, V- $\text{H}^+$ -ATPase and  $\text{Na}^+/\text{K}^+$ -ATPase take place in different cells, suggesting that marine elasmobranchs have distinct acid- and

base-secreting cells (Piermarini *et al.*, 2003; Tresguerres *et al.*, 2005; chapter II).

The present study is designed to elucidate the role of the hagfish MR cells. Using heterologous antibodies, V-H<sup>+</sup>-ATPase, Na<sup>+</sup>/K<sup>+</sup>-ATPase and NHE2 immunoreactivity in the gill epithelium of the Pacific hagfish was examined.

## Materials and methods

### *Animals*

Pacific hagfish (*Eptatretus stoutii* L) from the Trevor Channel, Vancouver Island, BC, Canada, were attracted with bait to a bottom-dwelling net. Hagfish were held in a 20 m<sup>3</sup> tank with flowing seawater (10°C, 31 ppt salinity) at the Bamfield Marine Sciences Centre. Fish were not fed while being housed in this tank. After 7 days, 4 individuals were removed from the tank, anesthetized and sacrificed by decapitation. Gill pouches were immediately excised and either frozen in liquid nitrogen for later western blot analyses or placed in fixative (see below) for immunohistochemistry.

### *Antibodies and reagents*

I used the rabbit  $\alpha$ -V-H<sup>+</sup>-ATPase antibody developed by Katoh *et al.* (2003), which was raised against a synthetic peptide based on the highly conserved and hydrophilic region in the A-subunit. The rabbit  $\alpha$ -Na<sup>+</sup>/K<sup>+</sup>-ATPase antibody recognizes a part of a highly conserved region of the  $\alpha$ -subunit (Katoh *et al.*, 2000; Katoh and Kaneko, 2003). The rabbit  $\alpha$ -NHE2 antibody was designed against a fragment of the C-terminal region of mammalian NHE2 by Dr Mark Donowitz (National Institutes of Health, Bethesda, Maryland, MD, USA). All of these antibodies have been successfully used in the gill epithelia from a variety of teleost and elasmobranch fishes. A donkey anti-rabbit fluorescent secondary antibody (Li-Cor Inc., Lincoln, NE, USA) was used for Western analysis. Unless otherwise

mentioned, the reagents used in this study were purchased from Sigma (St. Louis, MO, USA).

#### *Western blotting*

Western blotting analyses in whole hagfish gill pouches was performed as described in the previous chapters. 20 µg of total protein were separated in a 7.5 % polyacrylamide mini-gel and transferred to a nitrocellulose (NC) membrane using a wet transfer cell (Bio-Rad Laboratories, Inc., USA).

#### *Immunohistochemistry*

Gill pouches for immunohistochemistry were fixed in 3% paraformaldehyde, 0.1 mmol l<sup>-1</sup> cacodylate buffer (pH 7.40) overnight at 4°C. After incubation in 50% ethanol for 6h, samples were immersed in 70% ethanol and preserved at 4°C until their final processing for immunohistochemistry. Serial sections (4 µm) were cut from pouches embedded into paraffin blocks. Different pairs of consecutive sections from each pouch were immunostained for V-H<sup>+</sup>-ATPase and Na<sup>+</sup>/K<sup>+</sup>-ATPase, V-H<sup>+</sup>-ATPase and NHE2, or Na<sup>+</sup>/K<sup>+</sup>-ATPase and NHE2. Sections were deparaffinated in toluene, hydrated in a decreasing ethanol series and double distilled water, incubated in 0.6% H<sub>2</sub>O<sub>2</sub> for 30 min to devitalize endogenous peroxidase activity, and subsequently blocked with 2% normal goat serum (NGS) for 30 min. Sections were incubated overnight at 4°C with antibody against V-H<sup>+</sup>-ATPase (1:500), NHE2 (1:1000) or Na<sup>+</sup>/K<sup>+</sup>-ATPase (1:3000) diluted in 2% NGS, 0.1% bovine serum albumin, 0.02% keyhole limpet haemocyanin, 0.01% NaN<sub>3</sub> in 10 mmol l<sup>-1</sup> PBS, pH 7.40. Secondary antibody

incubation and signal developing were performed using the Vectastain ABC kit (Vector laboratories, CA, USA), according to the manufacture's directions.

Sections were viewed using a Leica LMRXA compound microscope (Leica Microsystems, Wetzlar, Germany) and images were captured and digitalized with an Optronics MacroFire 1.0 digital camera and its associated software Picture Frame (Optronics, Goleta, CA, USA). Micrographs were cropped and adjusted for brightness and contrast using Adobe Photoshop 7.0 (Adobe Systems Inc., USA).

## Results

### *i- Antibody specificity*

The three antibodies each recognized proteins of appropriate size, as estimated from western blots in whole gill samples and also in cell membrane enriched samples. The bands corresponding to the Na<sup>+</sup>/K<sup>+</sup>-ATPase  $\alpha$  subunit (105 kDA), the V-H<sup>+</sup>-ATPase A subunit (70 kDA) and NHE2 (63 kDa) were sharp and distinct, and were absent in control blots in which the primary antibody was omitted (Fig. 6.1).

### *ii- Immunohistochemistry in gill pouches*

To help with interpretation of the immunostained sections we have included a figure illustrating the gross anatomy of the gill pouches and the unique structure of their filamental and lamellar epithelia (Fig. 6.2). The density of immunopositive cells appeared to be larger at the afferent side of the gill pouch for all three transporter proteins analyzed. Na<sup>+</sup>/K<sup>+</sup>-ATPase-like immunoreactivity (NKA-LIR) was mostly restricted to epithelial cells in contact with the lumen of the gill pouch (water side), although some sections also showed labeling in the outer muscular wall of the pouch. The number of labeled cells was greater in the gill primary filaments (Fig. 6.3A) and decreased towards the lamella (Fig. 6.3B).

V-H<sup>+</sup>-ATPase- and NHE2-like immunoreactivity (VKA-LIR and NHE2-LIR) (Fig. 6.3C, D and E, F respectively) was virtually identical to NKA-IR. Sections probed for NHE2 presented a higher background compared to NKA and VHA, but still certain cells in the outer layer of the epithelium showed an

evidently stronger signal. Interestingly, NHE2-LIR was also strong in red blood cells (not shown). Sections incubated with no primary antibody showed no staining (Fig. 6.3H).

*iii- Na<sup>+</sup>/K<sup>+</sup>-ATPase, V-H<sup>+</sup>-ATPase and NHE2 subcellular localization*

The subcellular staining of Na<sup>+</sup>/K<sup>+</sup>-ATPase, V-H<sup>+</sup>-ATPase and NHE2 was analyzed from higher magnification (1600x) micrographs. When NKA-LIR was demonstrated, it was found to be distributed throughout the cell (Fig. 6.4A), including many with heavier staining in the supranuclear area (Fig. 6.4B). However, VHA-LIR was more variable. Some cells showed a staining pattern similar to Na<sup>+</sup>/K<sup>+</sup>-ATPase (Fig. 4C), while other cells had slightly heavier signal either in the supra-nuclear (denoted by #) or the infra-nuclear (denoted by \*) region (Fig. 6.4D). NHE-2-LIR was generally found throughout the cell cytoplasm, although in some cells the staining was stronger in the apical region (Fig. 6.4E).

*iv- Co-localization study*

To determine if the three ion-transporting proteins were localized in the same cells, we immunostained pairs of consecutive sections using the three possible combinations NKA-VHA (Fig. 6.5A), NKA-NHE2 (Fig. 6.5B), and VHA-NHE2 (Fig. 6.5C). We focused on gill filaments and lamella that due to their particular shape were easily recognizable in both sections. For every combination, the majority (>75 %) of the cells were positive for both transporters analyzed, both in filaments and in lamella. Rather than label all cells that co-localize with both transporters, we have labeled those cells



(arrows) that are immunopositive for only one of the transporters to demonstrate that these represent a small proportion of cells. Representative examples are shown in figure 6.5.

## Discussion

My results indicate that V-H<sup>+</sup>-ATPase, Na<sup>+</sup>/K<sup>+</sup>-ATPase and NHE2 homologous proteins are present in the MR cells of the Pacific hagfish gill epithelium. This is the first time that V-H<sup>+</sup>-ATPase-like immunoreactivity (L-IR) is reported for any species of hagfish, and the first report of any Na<sup>+</sup>/H<sup>+</sup> exchanger in *Eptatretus stoutii*. Moreover, we have conducted co-localization of the proteins in pairs of consecutive sections by labeling for the three possible combinations of two antibodies. In general, and for each of the transporters, cells that were labeled as positive for one transporter also were labeled by the second antibody. While we do find that there is a small proportion of cells that only appear to label with one antibody, we conclude that in general, the three proteins are located in the same cells suggesting that there are not separate populations of MR cells in *E. stoutii* as has been demonstrated in gills of the Atlantic stingray *Dasyatis sabina* (Piermarini and Evans, 2001) and the Pacific spiny dogfish *Squalus acanthias* (Tresguerres *et al.*; 2005; chapter II), and also in the skin of zebrafish larvae (Lin *et al.*, 2006). The exceptions, where there appear to be only staining with one antibody, are likely due to an artifact of using consecutive 4 µm sections where a small proportion of cells will not be represented in serial section. This could be especially problematic in hagfish gill pouches because of its very intricate morphology, which makes it difficult to identify the same cell in consecutive sections. However, it is also possible that the negative cells had lower levels of antigen protein, which would explain the lack of labeling by the antibodies.

This does not discount the possibility that there exists sub-types of MR cells in *E. stoutii* gills, but based on these specific transporters that have been used in previous studies to subtype MR cells (Piermarini and Evans, 2001; Tresguerres *et al.*, 2005; Lin *et al.*, 2006; chapter II), this does not appear to be the case.

#### *Cellular localization of the transporters*

At first glance,  $\text{Na}^+/\text{K}^+$ -ATPase,  $\text{V-H}^+$ -ATPase and NHE2 seem to be localized in the cytoplasm of cuboidal cells in the outer layer of the gill epithelium, which have their apical openings in contact with the lumen of the gill pouch (seawater). However, examination of high magnification micrographs, together with previous reports about the ultrastructure of the hagfish MR cell (Bartels and Welsch, 1986; Mallat and Paulsen, 1986; Bartels, 1992), suggest otherwise.

One of the distinctive morphological features of the hagfish gill MR cells is that the basolateral membrane penetrates deep into the cell cytoplasm in the form of a tubular system (Bartels and Welsch, 1986). The gill MR cells of SW and FW teleosts also have a well developed tubular system, which has been shown to be associated with  $\text{Na}^+/\text{K}^+$ -ATPase (Karnaky *et al.*, 1976; Hootman and Philpott, 1980; Philpott, 1980; Sardet, 1980). Therefore, I believe that the  $\text{Na}^+/\text{K}^+$ -ATPase staining in the hagfish gill MR cells is likely due to a similar association with the tubular system resulting in apparent cytoplasmic and sub-apical staining patterns (fig. 6.6).

Although I expected NHE2 to be predominantly apical given its proposed role in acid-base regulation in hagfish (Edwards *et al.*, 2001), a cytoplasmic staining pattern is common for  $\text{Na}^+/\text{H}^+$  exchangers for marine fish during resting A/B conditions. At least that is the case for the blue-throated wrasse *Pseudolabrus tetrourus* (Edwards *et al.*, 1999), the dogfish *S. acanthias* (Weakley *et al.*, 2003) and the longhorn sculpin *Myoxocephalus octodecimspinosus* (Catches and Claiborne, 2004). It is worth noting that the last two studies used species-specific antibodies, suggesting that my results are not due to inadequate specificity of the heterologous antibody but to a characteristic of NHE itself. A distinct possibility is that NHE2 is located in cytoplasmic vesicles that insert into the apical membrane depending on the A/B status of the animal (fig. 6.6). In support of this hypothesis, I have detected some cells with stronger NHE2 L-IR in the apical region. I expect this condition would be exacerbated during blood acidosis, a compensatory mechanism that would be complemented by increased expression of NHE (see Edwards *et al.* 2001). An apical NHE could take advantage of the inward directed  $\text{Na}^+$  gradient to secrete  $\text{H}^+$  into SW, similar to what has been proposed for marine elasmobranchs and teleosts (reviewed by Claiborne *et al.*, 2002).

The V- $\text{H}^+$ -ATPase cellular distribution found is more controversial. The observed cytoplasmic staining could be due to V- $\text{H}^+$ -ATPase-containing vesicles, to its presence in the tubular system, or both. I did find cells displaying either stronger supranuclear or infranuclear immunoreactivity (see

fig. 4D). I propose that, like NHE2, V-H<sup>+</sup>-ATPase redistribution of vesicles might depend on the A/B status of the blood (fig. 6.6). For example, I have recently shown that V-H<sup>+</sup>-ATPase moves from the cytoplasm to the basolateral membrane of dogfish gill cells upon induction of blood alkalosis (Tresguerres *et al.*, 2005; 2006; chapters II and III). However, the more complex structure of the basolateral membrane of hagfish MR cells compared to dogfish will likely make it harder to test for this model in hagfish.

Insertion into the apical membrane for acid secretion in hagfish gill cells may be also possible (fig. 6.6), although the use of an ATPase for H<sup>+</sup> excretion in SW does not make much sense thermodynamically. Alternatively, the hagfish branchial V-H<sup>+</sup>-ATPase could also be involved in other ion transporting processes, like active NH<sub>4</sub><sup>+</sup> excretion as it has been demonstrated in some crustaceans (Weihrauch *et al.*, 2002), or in the Ca<sup>+</sup> secretory mechanism that takes place in hagfish gills (Forster and Fenwick, 1994).

Due to their peculiar ecological characteristics, hagfish are likely to experience acid/base disturbances in the wild. Hagfish regularly use anaerobic metabolism, a trait probably related to the low-oxygen partial pressure of the deep sea environments they inhabit. Hagfish also endure sudden bursts of swimming related to their opportunistic feeding. These characteristics can result in extreme metabolic blood acidosis, as discussed in Mallatt *et al.* (1986). In most vertebrates, including elasmobranchs (Wood *et al.*, 2005), the post-prandial period is associated with blood alkalosis

resulting from net acid secretion into the stomach with proposed compensatory upregulation of base secretion at the gills. Whether or not the hagfish experiences a similar response remains to be determined.

*Comparison to MR cells from lampreys, elasmobranchs and teleosts*

In addition to  $\text{Na}^+/\text{K}^+$ -ATPase,  $\text{V-H}^+$ -ATPase and NHE2, hagfish gill MR cells also possess carbonic anhydrase (CA) (Mallat *et al.*, 1986). Therefore, these cells have all the machinery present in cells involved in A/B and ionic regulation from lampreys, elasmobranch and teleost gills (see Evans *et al.* 2005).

The gills of marine lampreys and teleosts are involved not only in A/B regulation, but also in salt secretion. As a result of the overlapping of these two processes, the A/B regulatory mechanisms at the cellular level are more difficult to study and the existence of cell subtypes for A/B regulation is unknown. On the other hand, marine elasmobranchs excrete the excess salt *via* the rectal gland, leaving the gills as a predominantly A/B regulatory organ (Heisler, 1988). Similarly, hagfish do not actively secrete significant amounts of salt across the gills, making a comparison between gill cell subtypes from hagfish and marine elasmobranchs more appropriate. The gills of marine elasmobranchs have distinct  $\text{Na}^+/\text{K}^+$ -ATPase- and  $\text{V-H}^+$ -ATPase-rich cells, which are presumably involved in acid and base secretion, respectively (Piermarini and Evans, 2001; Piermarini *et al.*, 2002; Tresguerres *et al.*, 2005; 2006). The situation is different for the hagfish gill epithelium, as it appears to lack evident ion-transporting cell subtypes. If we look into FW species,

stingrays and lampreys also have distinct  $\text{Na}^+/\text{K}^+$ -ATPase- and  $\text{V-H}^+$ -ATPase-rich cells (Piermarini and Evans, 2001; Choe *et al.*, 2004). The situation in FW teleosts is more variable, but at least salmonids also have MR cells subtypes (Goss *et al.*, 2001; Galvez *et al.*, 2002), one of which is responsible for  $\text{Na}^+$  uptake and  $\text{H}^+$  secretion (Reid *et al.*, 2003). This suggests that from an ion-transporting perspective the hagfish epithelium is less specialized compared to lampreys, elasmobranches and teleosts, and that the hagfish MR cells are multifunctional units that alternatively perform net acid or net base secretion depending on the physiological needs of the animal. Whether the appearance of distinct cell subtypes took place later during the evolution of vertebrates, or the condition in hagfish is derived due to its scavenger and deep-sea burrowing habit, are fascinating questions, although difficult to address.

Clearly, more studies are necessary, and looking at changes in the expression and/or redistribution of  $\text{Na}^+/\text{K}^+$ -ATPase,  $\text{V-H}^+$ -ATPase, NHE2, CA and anion exchangers during acid/base disturbances would be especially helpful.

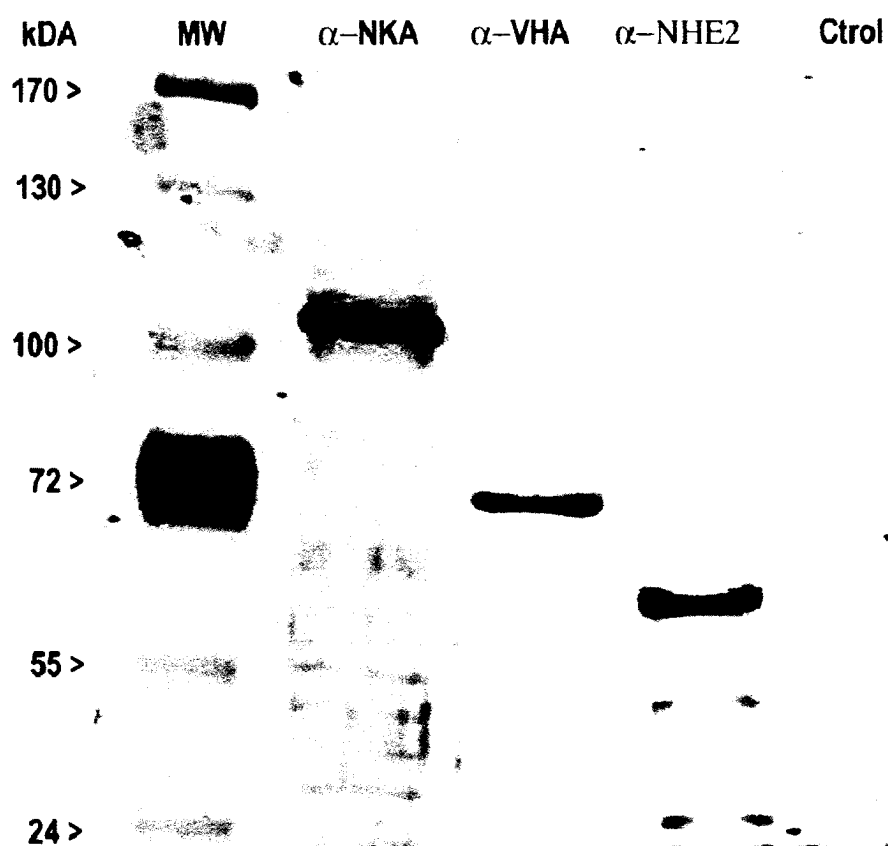


**Figure 6.1.** Western blotting in hagfish gill homogenates using antibodies against  $\text{Na}^+/\text{K}^+$ -ATPase ( $\alpha$ -NKA),  $\text{V-H}^+$ -ATPase ( $\alpha$ -VHA) and  $\text{Na}^+/\text{H}^+$  exchanger 2 ( $\alpha$ -NHE2). MW = molecular weight marker. Control = blot incubated with secondary antibody alone.



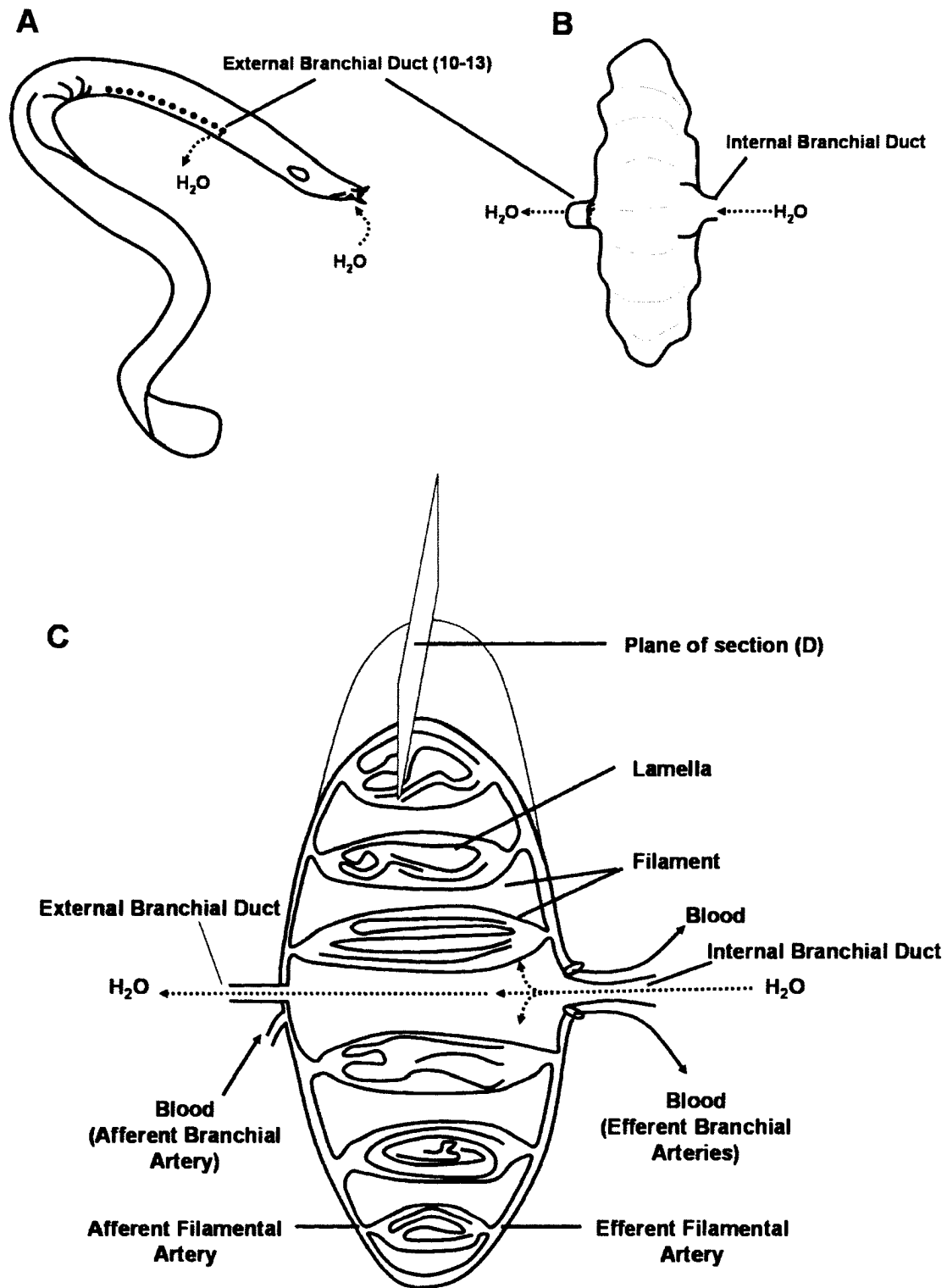
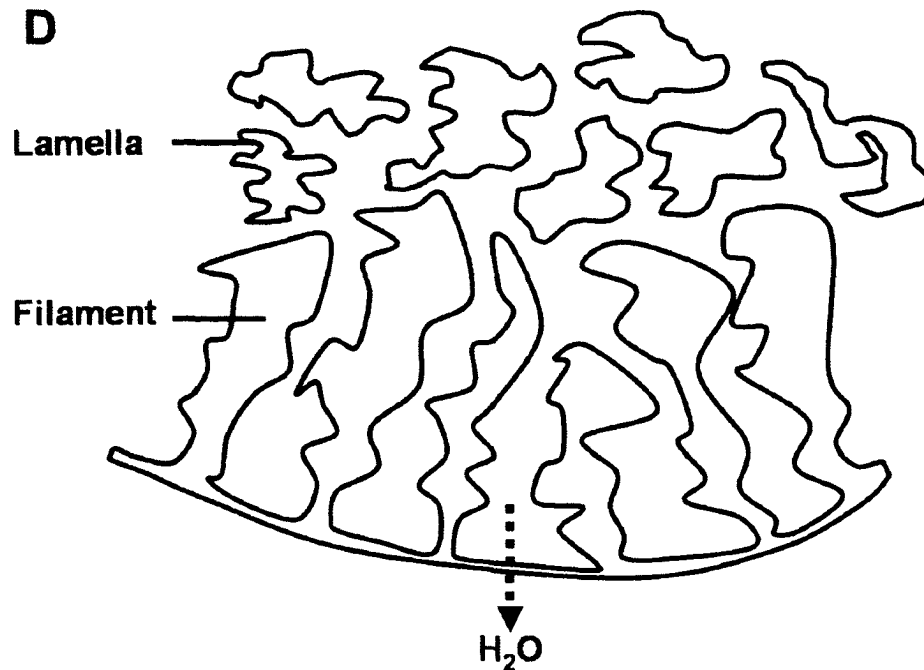


Figure 6.2.



**Figure 6.2.** Schematic of the hagfish gill pouch gross anatomy and fine structure. *A*: Water enters the hagfish through the nasopharyngeal duct, and it leaves across the 10 to 13 pairs of gill pouches located at each side of the body. *B*: External morphology of a gill pouch. *C*: Cross section of a gill pouch (modified from Mallat and Paulsen, 1986). Water and blood flow in counter-current fashion. The surface area of filaments and lamella is enlarged by radial infoldings, as opposed to the typical structures found in lampreys, elasmobranchs and teleosts. The plane of section used in the immunohistochemistry study is illustrated on top of the pouch, which is also shown in more detail in *D*. *D*: Section across the gill pouch in the orientation indicated in *C*. The gill filaments and lamella are shown in the same view as the immunohistochemistry sections of figures 3-5. Notice how the radial infolding of the lamella results in an apparent separation from the filaments in this plane of section.

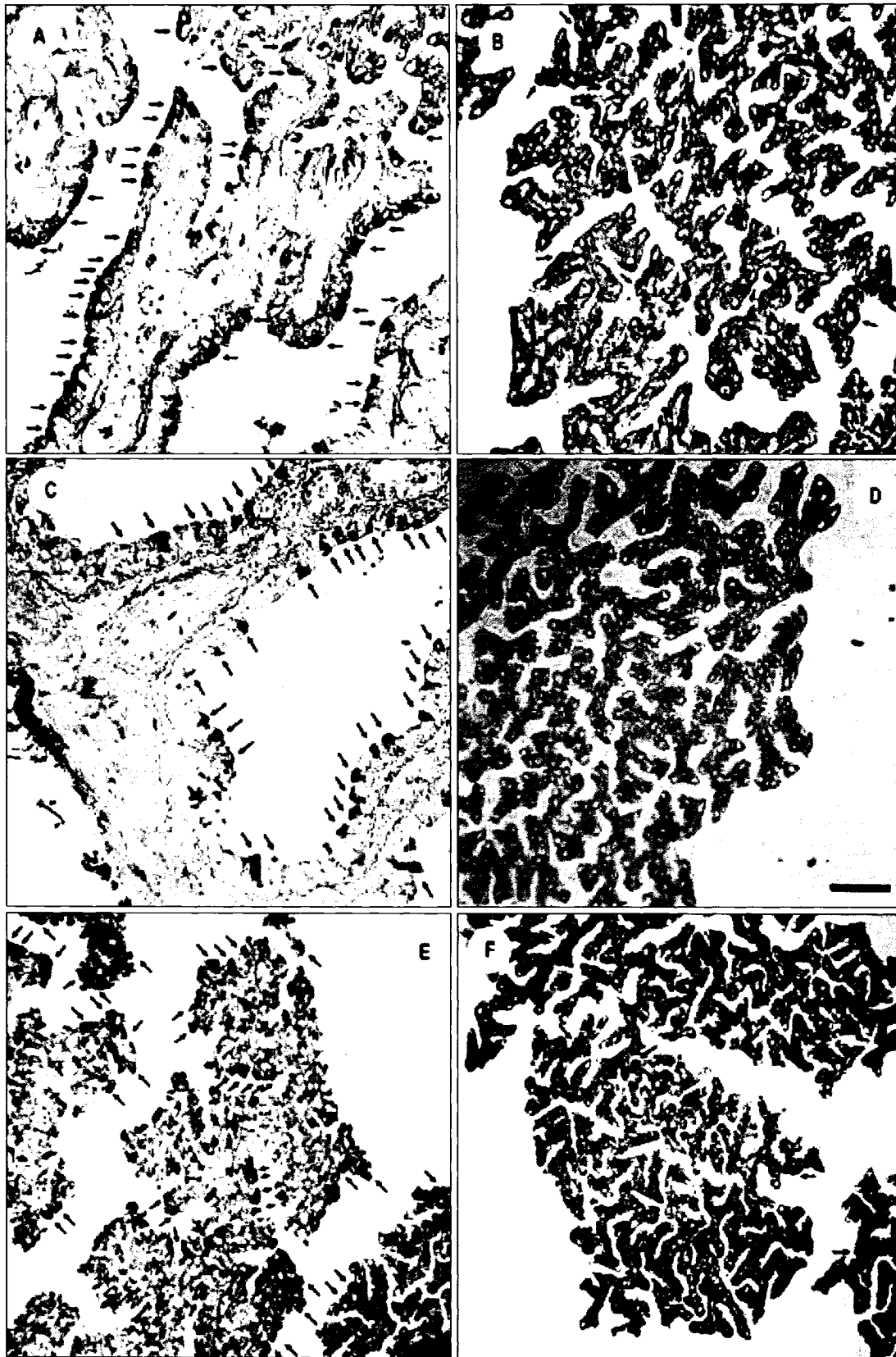
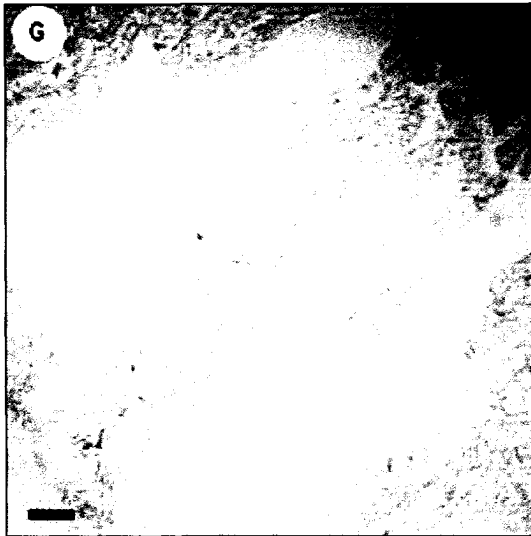
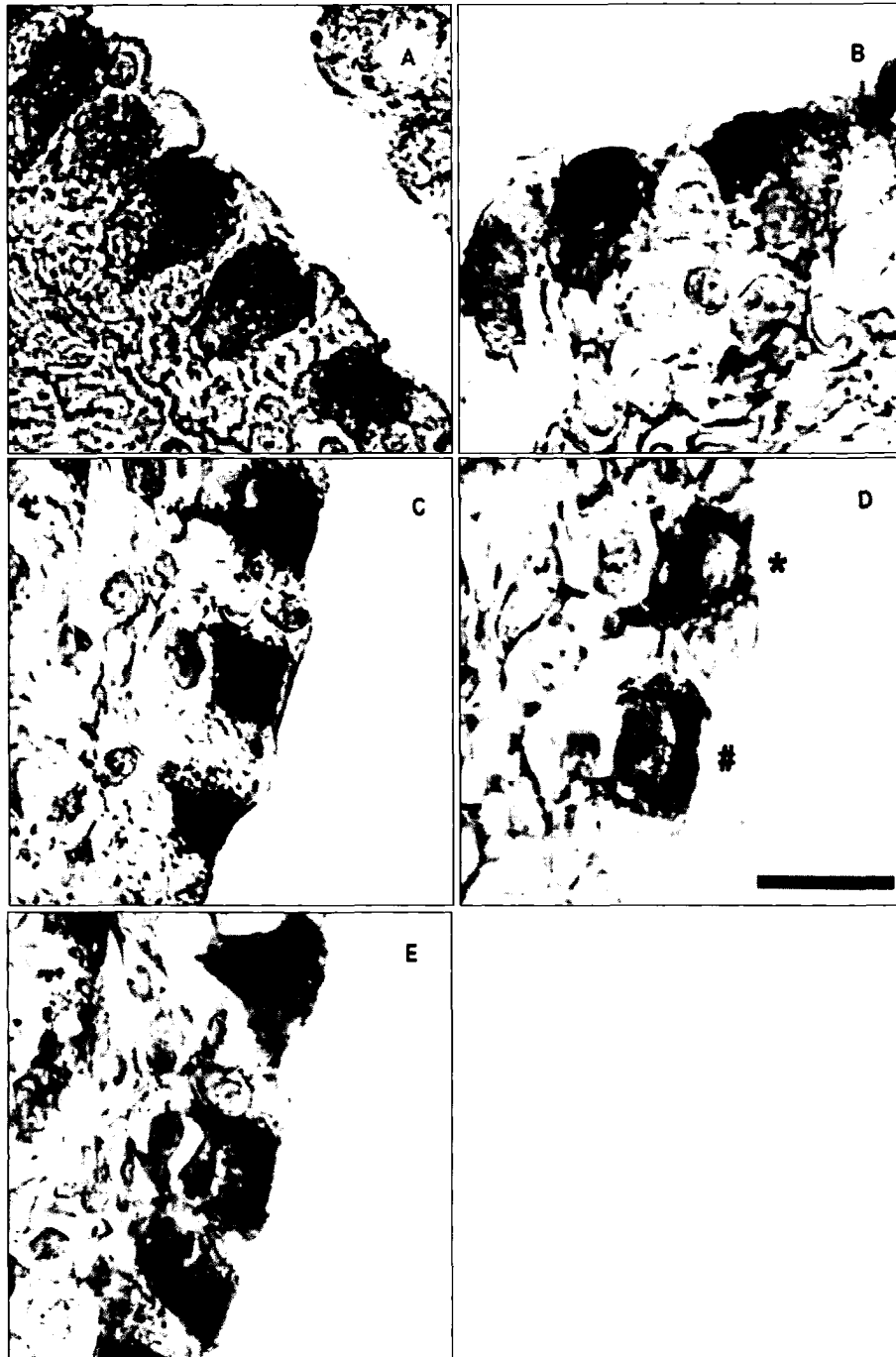


Figure 6.3.



**Figure 6.3.**  $\text{Na}^+/\text{K}^+$ -ATPase (*A, B*),  $\text{V-H}^+$ -ATPase (*C, D*) and NHE2 (*E, F*) like-immunoreactivity in sections from hagfish gill filaments (*A, C, E*) and lamella (*B, D, F*). A section incubated with secondary antibody alone is shown in *G*. Some of the positive cells are indicated with arrows. Scale bar = 50  $\mu\text{m}$ .



**Figure 6.4.** High magnification micrographs of sections immunostained for  $\text{Na}^+/\text{K}^+$ -ATPase (A, B),  $\text{V-H}^+$ -ATPase (C, D) and NHE2 (E). Note that  $\text{V-H}^+$ -ATPase immunoreactivity is diffuse (C), supra-nuclear (#), or infra-nuclear (\*) (D). The cell in the middle of the field in (E) shows apical NHE2 immunoreactivity. Scale bar = 10  $\mu\text{m}$ . (C) and (E) are consecutive sections.

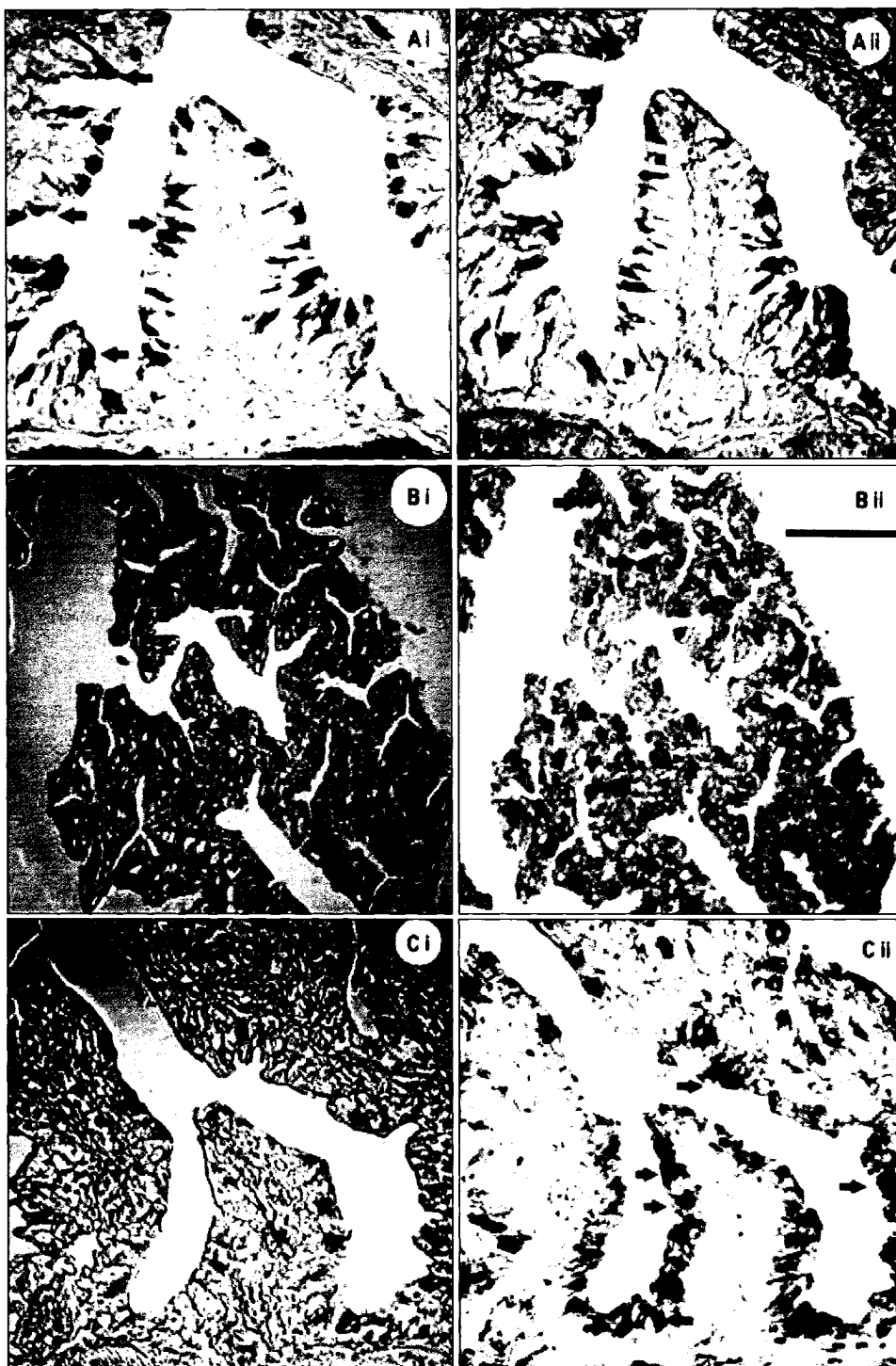


**Figure 6.5.** Co-localization  $\text{Na}^+/\text{K}^+$ -ATPase (NKA) and  $\text{V-H}^+$ -ATPase (VHA) (*Ai, Aii*), NKA and NHE2 (*Bi, Bii*) and VHA and NHE2 (*Ci, Cii*). For each pair of micrographs, the arrows indicate cells that are immunoreactive with only one of the antibodies (NKA = black arrows, VHA = white arrows, NHE2 = grey arrows). Scale bar = 50  $\mu\text{m}$ .

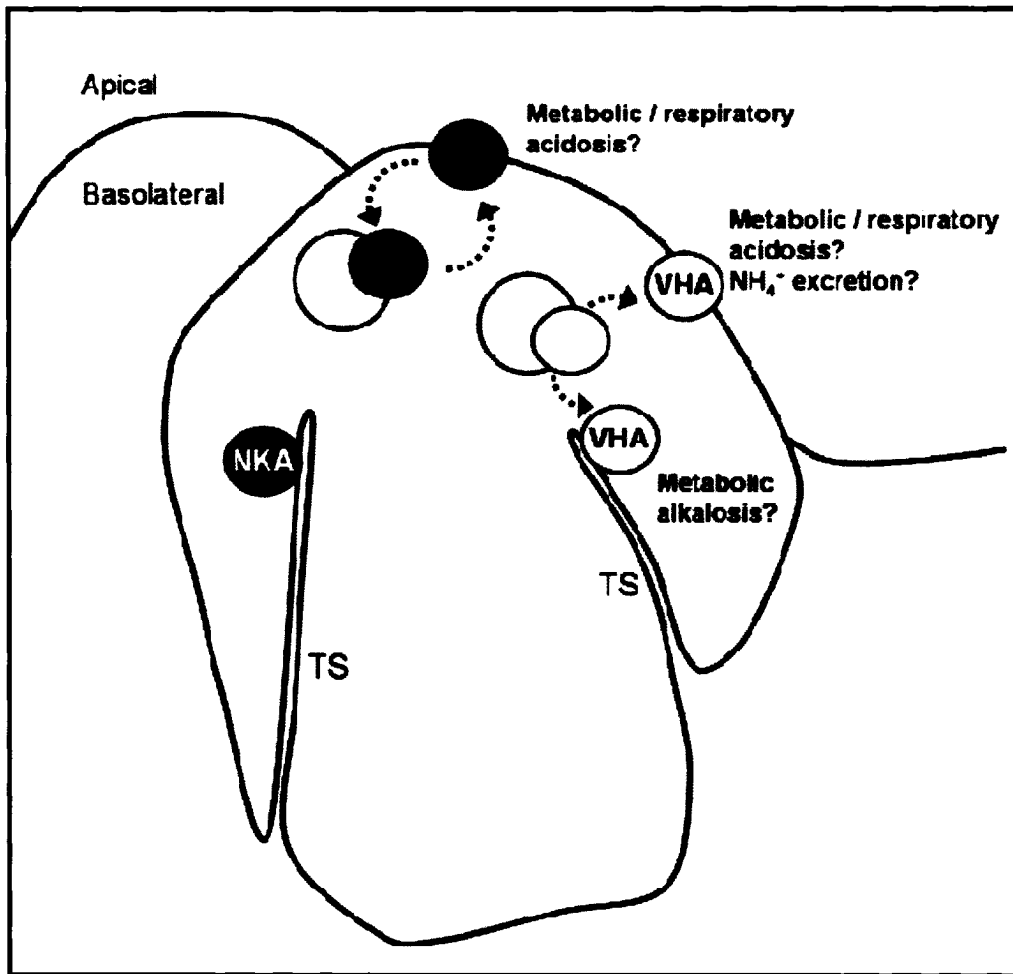


**Figure 6.6.** Working model of ion-transporting cell in hagfish gills. NKA = Na<sup>+</sup>/K<sup>+</sup>-ATPase, VHA = V-H<sup>+</sup>-ATPase, NHE = Na<sup>+</sup>/H<sup>+</sup> exchanger, TS = tubular system. I propose that under blood acidosis, NHE-containing vesicles insert into the apical membrane for H<sup>+</sup> secretion in exchange for Na<sup>+</sup>. NKA in the TS works in series with NHE2. VHA-containing vesicles insert into the TS during blood alkalosis, thus pumping H<sup>+</sup> back into the blood, and potentially also into the apical membrane during other conditions.

## References

- Bartels, H.** (1992). The gills of hagfishes. In: *The Biology of Hagfishes* (eds. J. Jørgensen, J. Lomholt, R. Weber and R. Malte). Chapman and Hall, London, pp 205-222.
- Bartels, H. and Welsch, U.** (1986). Mitochondria-rich cells in the gill epithelium of cyclostomes. A thin section and freeze fracture study. In: *Indo-Pacific Fish Biology: Proceedings of the Second International Conference on Indo-Pacific Fishes*, Ichthyological Society of Japan, Tokyo. (eds. T. Uyeno, T. Taniuchi and K. Matsuura), pp. 58-72.
- Catches, J. S. and Claiborne, J. B.** (2004). NHE2 and Na<sup>+</sup>/K<sup>+</sup>-ATPase immunoreactivity in *Myxocephalus octodecimspinosus*. *Bull. Mt. Desert Isl. Biol. Lab* 43, 22-23.
- Choe, K. P., Edwards, S., Morrison-Shetlar, A. I., Toop, T. and Claiborne, J. B.** (1999). Immunolocalization of Na<sup>+</sup>/K<sup>+</sup>-ATPase in mitochondrion-rich cells of the atlantic hagfish (*Myxine glutinosa*) gill. *Comp. Biochem. Physiol. A* 124, 161-168.
- Choe, K. P., O'Brien, S., Evans, D. H., Toop, T. and Edwards, S. L.** (2004). Immunolocalization of Na<sup>+</sup>/K<sup>+</sup>-ATPase, carbonic anhydrase II, and vacuolar H<sup>+</sup>-ATPase in the gills of freshwater adult lampreys, *Geotria australis*. *J. Exp. Zool. A* 301, 654-665.
- Claiborne, J. B., Edwards, S. L. and Morrison-Shetlar, A. I.** (2002). Acid/base regulation in fishes: cellular and molecular mechanisms. *J. Exp. Zool.* 293, 302-319.



**Edwards, S.L., Claiborne, J.B., Morrison-Shetlar A. I. and Toop, T.** (2001). Expression of Na<sup>+</sup>/H<sup>+</sup> exchanger mRNA in the gills of the Atlantic hagfish (*Myxine glutinosa*) in response to metabolic acidosis. *Comp. Biochem. Physiol. A* 130, 81-91.

**Edwards, S.L., Tse, C.M. and Toop, T.** (1999). Immunolocalization of NHE3-like immunoreactivity in the gills of the rainbow trout (*Oncorhynchus mykiss*) and the blue-throated wrasse (*Pseudolabrus tettrious*). *J. Exp. Biol.* 195: 465-469.

**Elger, M. and Hentschel, H.** (1983). Morphological evidence for ionocytes in the gill epithelium of the hagfish *Myxine glutinosa* L. *Bull. Mt. Desert Isl. Biol. Lab.* 23: 4-8.

**Evans, D.H., Piermarini, P.M. and Choe, K.P.** (2004). Homeostasis: osmoregulation, pH regulation, and nitrogen excretion. In *Biology of Sharks and their relatives*, (eds. J.C. Carrier, J.A. Musick and M.R. Heithaus), pp. 247-268. Boca Raton, FL, USA: CRC Press LLC.

**Evans, D.H., Piermarini, P.M. and Choe, K.P.** (2005). The multifunctional fish gill: dominant site of gas exchange, osmoregulation, acid-base regulation, and excretion of nitrogenous waste. *Physiol. Rev.* 85, 97-177.

**Forster, M. E. and Fenwick, J. C.** (1994). Stimulation of calcium efflux from the hagfish, *Eptatretus cirrhatus*, gill pouch by an extract of corpuscles of Stannius from an Eel (*Anguilla dieffenbachii*): teleostei. *Gen. Comp. Endocrinol.* 94, 92-103.

**Galvez, F., Reid, S. D., Hawkings, G. and Goss, G. G.** (2002). Isolation and characterization of mitochondria-rich cell types from the gill of freshwater rainbow trout. *Am. J. Physiol. Reg. Integr. Comp. Physiol.* 282, 658-668.

**Goss, G. G., Adamia, S. And Galvez, F.** (2001). Peanut lectin binds to a subpopulation of mitochondria-rich cells in the rainbow trout gill epithelium. *Am. J. Physiol. Reg. Integr. Comp. Physiol.* 281, 1718-1725.

**Heisler, N.** (1988). Acid-base regulation. In *Physiology of Elasmobranch Fishes.*, (ed. T. J. Shuttleworth), pp. 215-252. Berlin: Springer-Verlag.

**Holland, N.H. and Chen, J.** (2001). Origin and early evolution of the vertebrates: new insights from advances in molecular biology, anatomy, and palaeontology. *BioEssays* 23, 142-151.

**Hootman, S. R. and Philpott C. W.** (1979). Ultracytochemical localization of Na<sup>+</sup>, K<sup>+</sup> - activated ATPase in chloride cells from the gills of a euryhaline teleost. *Anat. Rec.* 193, 99-130.

**Karnaky, Jr., K. J. Kinter, L. B., Kinter, W. B. And Stirling C. E.** (1976). Teleost chloride cell. II. Autoradiographic localization of gill Na,K-ATPase in killifish *Fundulus heteroclitus* adapted to low and high salinity environments. *J. Cell Biol.* 70, 157-177.

**Katoh, F., Hyodo, S. and Kaneko, T.** (2003). Vacuolar-type proton pump in the basolateral plasma membrane energizes ion uptake in branchial

mitochondria-rich cells of killifish *Fundulus heteroclitus*, adapted to a low ion environment. *J. Exp. Biol.* 206, 793-803.

**Laemmli, U. K.** (1970). Cleavage of structural proteins during the assembly of the head of the bacteriophage T4. *Nature* 227, 680-685.

**Lin, L. Y., Horng, J. L., Kunkel, J. G. And Hwang, P. P.** (2006). Proton pump- rich cell secretes acid in skin of zebrafish larvae. *Am. J. Physiol. Cell Physiol.* 290, C371-378.

**Mallat, J., Conley, D.M. and Ridgway, R.L.** (1987). Why do hagfish have gill “chloride cells” when they need not regulate plasma NaCl concentration? *Can. J. Zool.* 65, 1956-1965.

**Mallat, J. and Paulsen, C.** (1986). Gill ultrastructure of the Pacific hagfish *Eptatretus stouti*. *Am. J. Anat.* 177, 243-269.

**Morris, R.** (1965). Studies on salt and water balance in *Myxine glutinosa* (L.). *J. Exp. Biol.* 42, 359-371.

**Philpott, C. W.** (1980). Tubular system membranes of teleost chloride cells: osmotic response and transport sites. *Am. J. Physiol. Regul. Integr. Comp. Physiol.* 238, 171-184.

**Piermarini, P. M. and Evans, D. H.** (2001). Immunochemical analysis of the vacuolar proton-ATPase B-subunit in the gills of a euryhaline stingray (*Dasyatis sabina*): effects of salinity and relation to Na<sup>+</sup>/K<sup>+</sup>-ATPase. *J. Exp. Biol.* 204, 3251-3259.

**Piermarini, P. M., Verlander, J. W., Royaux, I. E. and Evans, D. H.** (2002). Pendrin immunoreactivity in the gill epithelium of a euryhaline elasmobranch. *Am. J. Physiol. Reg. Integr. Comp. Physiol.* 283, R983-992.

**Reid, S. D., Hawkings, G. S., Galvez, F. and Goss, G. G.** (2003). Localization and characterization of phenamil-sensitive  $\text{Na}^+$  influx in isolated rainbow trout gill epithelial cells. *J. Exp. Biol.* 206, 551-559.

**Sardet, C.** (1980). Freeze fracture of the gill epithelium of euryhaline teleost fish. *Am. J. Physiol. Regul. Integr. Comp. Physiol.* 238, 207-212.

**Tresguerres, M., Katoh, F., Fenton, H., Jasinska, E., and Goss, G.G.** (2005). Regulation of branchial  $\text{V-H}^+$ -ATPase,  $\text{Na}^+/\text{K}^+$ -ATPase and NHE2 in response to acid and base infusions in the Pacific spiny dogfish (*Squalus acanthias*). *J. Exp. Biol.* 208, 345-354.

**Tresguerres, M., Parks, S.K., Katoh, F. and Goss, G.G.** (2006). Microtubule-dependent relocation of branchial  $\text{V-H}^+$ -ATPase to the basolateral membrane in the Pacific spiny dogfish (*Squalus acanthias*): a role in base secretion. *J. Exp. Biol.* 209, 599-609.

**Weakley, J., Choe, P. K. and Claiborne, J. B.** (2003). Immunological detection of gill NHE2 in the dogfish (*Squalus acanthias*). *Bull. Mt. Desert Isl. Biol. Lab.* 42, 81-82.

**Weihrauch, D., Ziegler, A., Siebers, D., and Towle, D.W.** (2002). Active ammonia excretion across the gills of the green shore crab *Carcinus maenas*: participation of  $\text{Na}^+/\text{K}^+$ -ATPase, V-type  $\text{H}^+$ -ATPase and functional microtubules. *J. Exp. Biol.* 205, 2765-2775.

**Wood, C. M., Kajimura, M., Mommsen, T. P. and Walsh, P. J.**  
(2005). Alkaline tide and nitrogen conservation after feeding in an  
elasmobranch (*Squalus acanthias*). *J. Exp. Biol.* 208, 2693-2705.

## Chapter VII

### **Recovery from blood alkalosis in the Pacific hagfish (*Eptatretus stoutii*): involvement of gill V-H<sup>+</sup>-ATPase and Na<sup>+</sup>/K<sup>+</sup>-ATPase<sup>1</sup>**

<sup>1</sup>A version of this chapter has been accepted for publication. **Tresguerres, M.**, Parks, S.K. and Goss, G.G. *Comparative Biochemistry and Physiology A* DOI j.cbpa.2007.03.032. Reproduced with permission of Elsevier Inc. and the co-authors of the manuscript.

## Introduction

The hagfish gill epithelium has abundant mitochondria-rich (MR) cells (Bartels, 1992; Elger and Hentschel, 1983; Mallat and Paulsen, 1986), where ion transport-related proteins such as  $\text{Na}^+/\text{K}^+$ -ATPase, carbonic anhydrase (CA),  $\text{Na}^+/\text{H}^+$  exchanger (NHE) and vacuolar proton ATPase (V- $\text{H}^+$ -ATPase) (Choe *et al.*, 1999; 2002; Edwards *et al.*, 2001; Mallat *et al.*, 1987; Tresguerres *et al.*, 2006b; chapter VI) are located. Based on the role of these proteins in fish (see Evans *et al.*, 2005), and the fact that hagfish are osmoconformers (Morris 1965), it is likely that the role of the MR cells is the transport of acid/base relevant ions between the blood and seawater.

To date, the role of hagfish gills in acid/base regulation has mostly been limited to the study of acid secretion. In particular, acid infusions have been used to induce blood acidosis in order to study acid secretion at the whole animal (McDonald *et al.* 1991) and molecular levels (Edwards *et al.* 2001). These studies concluded that hagfish have a substantial capacity for overcoming an acidic load, and that a  $\text{Na}^+/\text{H}^+$  exchanger (NHE) protein is probably involved in the branchial mechanism for acid secretion. Further evidence for NHE presence in hagfish gills have been provided from immunohistochemistry and western blot experiments (Choe *et al.*, 2002; Tresguerres *et al.*, 2006b; chapter VI). On the other hand, I am aware of only one study on base secretion in hagfish (Evans 1984). This study reported that the Atlantic hagfish *Myxine glutinosa* was unable to secrete base when placed in  $\text{Cl}^-$ -free seawater, suggesting the existence of a  $\text{Cl}^-/\text{HCO}_3^-$  exchange

system. More recently, I found V-H<sup>+</sup>-ATPase immunoreactivity in the gill epithelium of the Pacific hagfish *Eptatretus stoutii* (Tresguerres *et al.*, 2006b; chapter VI) Based on current models for base secretion in gills of marine elasmobranchs (Piermarini and Evans 2001, Tresguerres *et al.*, 2005; 2006c; chapters II-IV), I have proposed that V-H<sup>+</sup>-ATPase is involved in reabsorbing protons to the blood and in energizing HCO<sub>3</sub><sup>-</sup> secretion to the water (Tresguerres *et al.*, 2006c; chapter VI).

In order to study the responses to blood alkalosis, hagfish were injected with NaHCO<sub>3</sub> (6000 mmol kg<sup>-1</sup>) into the subcutaneous sinus and blood pH and total CO<sub>2</sub> (TCO<sub>2</sub>) were monitored for 6 h. I also induced long-term alkalosis by repeated infusions of NaHCO<sub>3</sub> (6000 mmol kg<sup>-1</sup>) over a 24 h experiment. My results show that hagfish restore their blood pH by 6 h after each alkaline load, and suggest that basolateral V-H<sup>+</sup>-ATPase plays a role in the base-secretory mechanism.



## Materials and methods

### *Animals*

Pacific hagfish (*Eptatretus stoutii* L) were caught with bait and a bottom-dwelling net from the Trevor Channel, Vancouver Island, BC, Canada. Hagfish were transported to the Bamfield Marine Sciences Centre, where they were held in a 20 m<sup>3</sup> tank with flowing seawater (14 °C). Fish were not fed at any time, and were used for experimentation within 2 weeks after capture. The experiments were conducted during September 2005 (6 h-infusions) and July 2006 (24 h-infusions).

### *Antibodies and reagents*

Antibodies and reagents were the same as in the previous chapter.

### *NaHCO<sub>3</sub> infusions*

Hagfish (mean body mass 96.29 ± 8.42 g) were anesthetized in seawater containing 1:1000 tricaine methanesulfonate (TMS; AquaLife, Syndel Laboratories Ltd, Vancouver, BC, Canada). Hagfish were suspended by the head, which causes blood to accumulate in the caudal subcutaneous sinus. After taking a 200 µl blood sample (t=0 h), base (250 mmol l<sup>-1</sup> NaHCO<sub>3</sub>, 250 mmol l<sup>-1</sup> NaCl) was injected using a heparinized 21G syringe to achieve a HCO<sub>3</sub><sup>-</sup> load of 6000 mmol kg<sup>-1</sup>. A similar infusion protocol has been used by McDonald et al. (1991) and Edwards et al. (2001). Hagfish were placed in individual containers (20 l) provided with flowing seawater. In the 24 h experiments, this infusion procedure was repeated after blood sampling at t=6, 12 and 18 h. Based on the high blood volume in hagfish (estimated at

~14% body weight: Forster et al. 2001), this sampling regime would remove ~10% of the total blood volume. The main aim of the long term infusions was to maintain the alkaline stress to ensure ample time for the putative upregulation in the synthesis of the ion-transporting proteins related to acid/base balance.

#### *Blood samples and analytical procedures on plasma samples*

Blood samples (200 µl) were obtained as described above. Blood pH was measured immediately in a thermo-jacketted Accumet micro-size pH electrode model 13-620-94 (Fisher Scientific, Pittsburgh, PA, USA). Blood samples were then centrifuged (12 000 g for 2 min) to obtain plasma. Plasma aliquots from the 6h experiments were frozen (-80 °C) and shipped in a dry-shipper to the University of British Columbia, Vancouver, BC, Canada, where total CO<sub>2</sub> (TCO<sub>2</sub>) was analyzed using a Corning 965 carbon dioxide analyzer (Ciba Corning Diagnostic, Halstead, Essex, UK). Plasma aliquots from the 24 h experiments were used for immediate TCO<sub>2</sub> determination in a Cameron chamber equipped with a CO<sub>2</sub> electrode (Radiometer, Copenhagen, Denmark). In both cases, the remaining plasma was kept frozen (-80 °C) for later [Na<sup>+</sup>] (atomic absorption spectrophotometer; model 3300; Perkin-Elmer, Norwalk, CT, USA) and [Cl<sup>-</sup>] concentration (Zall *et al.*, 1956).

#### *Terminal sampling*

At the end of each experiment, hagfish were anesthetized in seawater containing TMS for 5 min and subsequently terminated by decapitation. Gill pouches were dissected and immediately snap-frozen in liquid N<sub>2</sub> for later western blot analyses or placed in fixative for immunohistochemistry.

### *Immunohistochemistry*

Immunohistochemistry was performed as described in the previous chapter. A schematic of the hagfish gill pouch structure and the exact orientation of the gill sections can be found in chapter VI and in Tresguerres *et al.* (2006b).

### *Western blot analysis*

Frozen gill samples were immersed in liquid nitrogen and pulverized in a porcelain grinder. The resultant powder was resuspended in 1:10 w/v of ice-cold homogenization buffer (250 mmol l<sup>-1</sup> sucrose, 1 mmol l<sup>-1</sup> EDTA, 30 mmol l<sup>-1</sup> Tris, 100 mg ml<sup>-1</sup> PMSF and 2 mg ml<sup>-1</sup> pepstatin, pH 7.40), and sonicated on ice (3 x 5 sec). Debris, and nuclei were removed by low speed centrifugation (3000 g for 10 min, 4 °C). An aliquot of the supernatant was stored at -80°C (whole gill homogenate), and the remaining was centrifuged at medium speed (20800 g for 30 min, 4 °C). The resulting pellet was resuspended in homogenization buffer and stored at -80 °C. The pelleted fraction should contain large fragments of plasma membrane (both apical and basolateral) along with membrane from the Golgi and the endoplasmic reticulum, but no small cytoplasmic vesicles as they typically do not pellet down unless greater forces (100000 g for >1 h) are applied (Alberts *et al.*, 1994). Therefore, this fraction is referred to as “cell membrane enriched”. Aliquots of both the whole gill and cell membrane enriched fractions were saved for protein determination analysis (Pierce, IL, USA).

SDS-PAGE, blotting, visualization and quantification of the bands was performed as described in the previous chapters.

### *Statistics*

All data are given as means  $\pm$  s.e.m. Differences between groups were tested using one way analysis of variance (1-way ANOVA), Student's t-test or one- or two-way repeated measures analysis of variance (1- or 2-way-RM-ANOVA) followed by Bonferroni's or Dunnet's post test when appropriate. Statistical significance was set at  $P < 0.05$ . All statistical analyses were performed on GraphPad Prism v.3.0 (GraphPad Software, San Diego California USA).

## Results

### *i- 6 h. Blood and plasma variables*

At  $t=0$ , blood pH was  $7.78 \pm 0.04$  and  $7.69 \pm 0.03$  pH units in NaCl-infused (control) and base-infused hagfish (BIH), respectively ( $p > 0.05$ ,  $N=6$ ). The NaCl injection did not significantly affect blood pH in control hagfish ( $7.82 \pm 0.03$  and  $7.81 \pm 0.05$  pH units at  $t=1$  and 6 h, respectively). In contrast, the  $6000 \text{ mmol kg}^{-1} \text{ HCO}_3^-$  injection produced an increase in blood pH at  $t=1$  h ( $8.05 \pm 0.05$  pH units), which was significantly higher compared to control, NaCl-injected fish ( $p < 0.05$ ,  $N=6$ ). Blood pH in BIH returned to control values by  $t=6$  h ( $7.85 \pm 0.08$  pH units). These results are shown in figure 7.1A.

Plasma total  $\text{CO}_2$  ( $\text{TCO}_2$ ) essentially followed the same pattern as blood pH (Fig. 7.1B). Control hagfish had  $\text{TCO}_2$  values of  $7.32 \pm 0.57$ ,  $6.26 \pm 0.71$  and  $5.92 \pm 1.19 \text{ mmol CO}_2 \text{ l}^{-1}$  at  $t=0$ , 1 and 6 h, respectively ( $N=6$ ).  $\text{TCO}_2$  in BIH started at a significantly lower value at  $t=0$  ( $5.48 \pm 0.52 \text{ mmol CO}_2 \text{ l}^{-1}$ ). However, the effect of the  $\text{HCO}_3^-$  injection was evident at  $t=1$  h ( $21.82 \pm 2.91 \text{ mmol CO}_2 \text{ l}^{-1}$ ), when  $\text{TCO}_2$  was significantly higher compared to control hagfish. Similar to blood pH,  $\text{TCO}_2$  in BIH had returned to control values by  $t=6$  h ( $8.85 \pm 1.83 \text{ mmol CO}_2 \text{ l}^{-1}$ ) ( $p > 0.05$ ,  $N=6$ ). Plasma  $[\text{Na}^+]$  and  $[\text{Cl}^-]$  did not differ between treatments or times.

### *ii- 6 h. $\text{Na}^+/\text{K}^+$ -ATPase and V- $\text{H}^+$ -ATPase gill immunohistochemistry*

$\text{Na}^+/\text{K}^+$ -ATPase and V- $\text{H}^+$ -ATPase gill immunolabeling patterns 6h after the injections were similar in control and BIH (Fig. 7.2). Most cells that were labeled by one antibody also were labeled by the other antibody, indicating

that both transporters exist in the same cells, or at least in a majority of cells. At the cellular level, both  $\text{Na}^+/\text{K}^+$ -ATPase and  $\text{V-H}^+$ -ATPase immunolabeling occurred throughout the cell. These results are similar to those obtained for non-injected hagfish (Tresguerres *et al.*, 2006b; chapter VI). Sections incubated with no primary antibody showed no staining (not shown, but see previous chapter).

*iii- 6 h.  $\text{Na}^+/\text{K}^+$ -ATPase and  $\text{V-H}^+$ -ATPase gill abundance*

The  $\alpha\text{-Na}^+/\text{K}^+$ -ATPase antibody recognized a single band of ~105 kDa, while staining with the  $\alpha\text{-V-H}^+$ -ATPase antibody resulted in a single band of ~70 kDa. Both bands were absent in control blots that were incubated without primary antibody (not shown, see Tresguerres *et al.*, 2006b; chapter VI). There were no significant differences in  $\text{Na}^+/\text{K}^+$ -ATPase or  $\text{V-H}^+$ -ATPase abundance between gills from control and BIH, neither in whole gill homogenates (not shown) nor in the fraction enriched in cell membranes (Fig. 7.3).

*iv- 24 h. Blood and plasma variables*

In this experimental series, four bolus  $6000 \text{ mmol kg}^{-1} \text{ HCO}_3^-$  doses were injected into the subcutaneous sinus at  $t=0$ , 6, 12 and 18 h. During the first 12 h, blood pH showed a pattern similar to the 6 h experiment described in the previous section. There were significant increases in blood pH of BIH compared to control fish 3 h after each injection ( $8.13 \pm 0.06$  vs.  $7.84 \pm 0.03$  pH units at  $t=3\text{h}$ ;  $8.16 \pm 0.04$  vs.  $7.94 \pm 0.03$  pH units at  $t=9\text{h}$ ,  $p<0.05$ ;  $N=7$  in both cases), but they were fully compensated 3 h later ( $8.07 \pm 0.04$  vs.  $7.97 \pm$

0.03 pH units at t=6 h;  $8.01 \pm 0.03$  vs.  $7.98 \pm 0.04$  pH units at t=12 h,  $p > 0.05$  in both cases). Between 12 and 24 h, blood samples were withdrawn every 6 h instead of every 3 h. While this impaired the temporal resolution of the study, it was done in an effort to prevent anemia. Blood pH did not statistically differ between BIH and controls at t=18 h ( $7.99 \pm 0.05$  vs.  $7.97 \pm 0.05$  pH units) and t=24 h ( $8.05 \pm 0.05$  vs.  $7.92 \pm 0.08$  pH units). Blood pH as a function of time is shown in figure 7.4A.

TCO<sub>2</sub> in control fish remained between a minimum of  $2.80 \pm 1.10$  mmol CO<sub>2</sub> l<sup>-1</sup> at t=18 h and a maximum of  $7.00 \pm 1.80$  mmol CO<sub>2</sub> l<sup>-1</sup> at t=12 h. TCO<sub>2</sub> in BIH was maximum 3 h after the first HCO<sub>3</sub><sup>-</sup> infusion, when it reached  $13.26 \pm 2.90$  mmol CO<sub>2</sub> l<sup>-1</sup> ( $p < 0.05$  compared to controls at the same time). In the remaining sampling times TCO<sub>2</sub> from BIH was not significantly different compared to controls (Fig. 7.4B). Importantly, this includes t=9 h (3h after the second injection) ( $6.13 \pm 0.08$  vs.  $3.07 \pm 1.12$  mmol CO<sub>2</sub> l<sup>-1</sup>,  $p > 0.05$ ).

Plasma [Na<sup>+</sup>] and [Cl<sup>-</sup>] are shown in table 7.1. [Na<sup>+</sup>] from control and BIH were not different from each other at any sampling time. However, [Na<sup>+</sup>] at t= 9 and 12 h were significantly higher compared to t = 0 for both control and BIH, probably due to the higher [Na<sup>+</sup>] concentration of the infusion solutions compared to hagfish plasma. [Cl<sup>-</sup>] values were more variable than [Na<sup>+</sup>], and did not differ significantly between treatments or times.

#### *v- 24 h. Na<sup>+</sup>/K<sup>+</sup>-ATPase and V-H<sup>+</sup>-ATPase gill immunohistochemistry*

Na<sup>+</sup>/K<sup>+</sup>-ATPase and V-H<sup>+</sup>-ATPase immunoreactivity patterns after the 24 h experiments were similar to those from the 6 h experiments. Both

proteins were localized mostly in the same cells, and the immunolabeling occurred throughout the cell (Fig. 7.5).

*vi- 24 h. Na<sup>+</sup>/K<sup>+</sup>-ATPase and V-H<sup>+</sup>-ATPase gill abundance*

Control and BIH had similar Na<sup>+</sup>/K<sup>+</sup>-ATPase levels in whole gill homogenates ( $1.28 \pm 1.19$  vs.  $1.87 \pm 0.34$  a.f.u., respectively, N=7), as estimated from western blots. However, V-H<sup>+</sup>-ATPase abundance was higher in BIH compared to control hagfish ( $2.83 \pm 0.65$  vs.  $1.24 \pm 0.21$  a.f.u.,  $p < 0.05$ , N=7), indicating that blood alkalosis had produced an upregulation of V-H<sup>+</sup>-ATPase synthesis (Fig. 7.6).

When samples enriched in gill cell membranes were used for western blotting, I found that membrane-bound Na<sup>+</sup>/K<sup>+</sup>-ATPase had decreased in BIH compared to controls ( $0.63 \pm 0.08$  vs.  $0.98 \pm 0.10$  a.f.u.), while membrane-bound V-H<sup>+</sup>-ATPase abundance had increased in the same group ( $1.82 \pm 0.26$  vs.  $1.08 \pm 0.13$  a.f.u.) ( $p < 0.05$ , N=7 in both cases) (Fig. 7.7).

*vii- 24 h. NHE2-like protein (lp) abundance and cellular localization*

The abundance and cellular localization of a putative NHE2 was analyzed using the heterologous NHE2 antibody described in the previous chapter. There were no changes in the abundance of the NHE2-lp in whole gill homogenates or in the fraction enriched in cell membranes (not shown). The cellular distribution of the NHE2-lp was cytoplasmic in all cells analyzed (not shown, but see chapter VI for representative pictures).



## Discussion

These results show that hagfish can readily recover from acute (6 h experiments) and repeated (24 h experiments) blood alkalosis events. Some of the possible routes for reducing blood  $[\text{HCO}_3^-]$  are production of alkaline urine, accumulation in body tissues or red blood cells (rbc), simple diffusion to seawater, and intestinal or branchial secretion. If we consider the low urinary output of hagfish (Morris 1965) and their almost non-existent rbc permeability to  $\text{HCO}_3^-$  (Peters *et al.*, 2000), these two options can be discounted. Although  $\text{HCO}_3^-$  diffusion to seawater cannot be fully discounted, some characteristics of the blood pH and plasma  $\text{TCO}_2$  profiles argue against it. In particular, if diffusion was the main component of the  $\text{HCO}_3^-$  clearance, I would expect the repeated  $\text{HCO}_3^-$  injections to exert similar changes in blood pH and plasma  $\text{HCO}_3^-$ . For example, the first injection elevated blood pH from  $7.80 \pm 0.07$  to  $8.13 \pm 0.02$  pH units at  $t=3$  h ( $\Delta\text{pH}=0.33 \pm 0.07$  pH units), while the second injection only elevated blood pH from  $8.07 \pm 0.04$  to  $8.16 \pm 0.04$  pH units ( $\Delta\text{pH}=0.09 \pm 0.03$  pH units). The effect is most evident in the lack of significant change in  $\text{TCO}_2$  3h after the second  $\text{HCO}_3^-$  injection ( $t=9$  h). These results indicate that an active mechanism for  $\text{HCO}_3^-$  secretion had been upregulated and remained active to prevent greater changes in blood parameters after the subsequent  $\text{HCO}_3^-$  loads.

I have no data to refute the possible transport of  $\text{HCO}_3^-$  into the intracellular compartment, for example the muscle. However, this mechanism would likely affect intracellular pH and  $[\text{HCO}_3^-]$  enormously. Regulation of

blood pH like we observed in our study does not seem to be adaptive if it comes at the expense of dramatic changes in those intracellular parameters.

Given the established role of gills in acid/base regulation in elasmobranch and teleost fishes (Evans *et al.*, 2005), and the changes in branchial  $\text{Na}^+/\text{K}^+$ -ATPase and  $\text{V-H}^+$ -ATPase reported in this study, it is likely that branchial  $\text{HCO}_3^-$  secretion plays a major role in the recovery from blood alkalosis. However, the putative role of intestinal  $\text{HCO}_3^-$  secretion (see Grosell 2006; Taylor and Grosell 2006) deserves further investigation.

Current evidence suggest that  $\text{Na}^+/\text{K}^+$ -ATPase,  $\text{V-H}^+$ -ATPase (this study) and also an NHE2-like protein (-lp) (Tresguerres *et al.* 2006*b*; chapter VI) are located in the same cells. However, there is a minority of cells that are not immunolabeled for all the transporters. This is likely an artifact of using the various antibodies in consecutive sections as explained in detail in Tresguerres *et al.* (2005, 2006*b*; chapters II and VI). Despite these technical difficulties, the majority of cells that label for one transporter also label for the other two, indicating that the vast majority (if not all) of cells have  $\text{Na}^+/\text{K}^+$ -ATPase,  $\text{V-H}^+$ -ATPase and NHE2-lp.

In the short-term (6 h), there were no significant changes in  $\text{Na}^+/\text{K}^+$ -ATPase or  $\text{V-H}^+$ -ATPase abundance in whole gill or cell membranes. However, blood pH and  $\text{TCO}_2$  fully recovered by the end of the experimentation period. This indicates that the already present base-secretory machinery was sufficient and in place to handle the  $\text{HCO}_3^-$  load. Possible short term activation of base secretory mechanisms includes direct

activation by an increase in substrate concentration ( $[\text{HCO}_3^-]$ ) and/or post-translational modification such as phosphorylation/de-phosphorylation. However, I was unable to accurately measure  $\text{Na}^+/\text{K}^+$ -ATPase activity and  $\text{V-H}^+$ -ATPase activity in hagfish gills using the method of McCormick (1993). Optimization of the assay for hagfish specific conditions is required to complete this type of analysis.

The long-term (24 h) experiments give more insights into the cellular mechanism for base secretion. The increase in  $\text{V-H}^+$ -ATPase abundance in whole gill homogenates is indicative of upregulation of this enzyme in response to  $\text{HCO}_3^-$  load. In addition, increased  $\text{V-H}^+$ -ATPase abundance in the gill cell membrane enriched fraction demonstrates that this ATPase inserts into the cell membrane in response to  $\text{HCO}_3^-$  load. The centrifugation protocol used in the current study would not separate the apical from the basolateral membrane. However, the immunolabeled sections suggest that  $\text{V-H}^+$ -ATPase labeling does not occur on the apical membrane. Therefore, it is likely that  $\text{V-H}^+$ -ATPase insertion under my experimental conditions is into the basolateral membrane. At first sight, this seems to be in contradiction with the immunohistochemistry results, which show a cytoplasmic-like  $\text{V-H}^+$ -ATPase immunolabeling. However, hagfish gill MR cell basolateral membrane forms a tubular system that occupies most of the cell cytoplasm (Bartels and Welsch, 1986). Therefore, combining the western blotting, immunohistochemistry and ultrastructure data, we believe that  $\text{V-H}^+$ -ATPase is inserting into the basolateral tubular system during blood alkalosis. However, immunogold

experiments are required in order to definitely confirm if V-H<sup>+</sup>-ATPase indeed inserts into the basolateral membrane. The function of this insertion would be to reabsorb H<sup>+</sup> to the blood and help with the extrusion of HCO<sub>3</sub><sup>-</sup> to seawater via an apical anion exchanger yet to be identified. This putative anion exchanger could be subjected to additional activation mechanisms in order to increase HCO<sub>3</sub><sup>-</sup> secretion.

A complementary explanation for the increased V-H<sup>+</sup>-ATPase abundance in the membrane-enriched fraction would be that the newly synthesized units of the enzyme (or of the V<sub>o</sub> complex) are assembled together in the endoplasmic reticulum (ER) like it has been demonstrated in yeast (Graham et al. 1998). In that case, we predict that the holoenzyme would subsequently migrate and insert into the basolateral membrane. Unfortunately, separation of the plasma membrane from Golgi or ER by differential centrifugation is extremely difficult and hampered by the fact that specific markers (e.g. antibodies) to detect those compartments are not available.

Na<sup>+</sup>/K<sup>+</sup>-ATPase abundance is reduced in the cell membrane enriched fraction of HCO<sub>3</sub><sup>-</sup> infused hagfish. Since Na<sup>+</sup>/K<sup>+</sup>-ATPase abundance does not change in whole gill samples, this is likely due to removal of Na<sup>+</sup>/K<sup>+</sup>-ATPase from the basolateral membrane during blood alkalosis. Similar insertion and removal of Na<sup>+</sup>/K<sup>+</sup>-ATPase units has been proposed to regulate Na<sup>+</sup> absorption in the mammalian kidney (Beltowsky et al. 2003, 2004). In fish gills, Na<sup>+</sup>/K<sup>+</sup> ATPase is involved in acid secretion (for review see Evans *et al.*,

2005). Therefore, removal of  $\text{Na}^+/\text{K}^+$ -ATPase from the basolateral membrane during blood alkalosis is likely related to a concomitant reduction in  $\text{H}^+$  secretion to the water, which would help in counteracting alkalosis. Moreover, the NHE2-lp is located in the same cells as  $\text{Na}^+/\text{K}^+$ -ATPase and  $\text{V-H}^+$ -ATPase (Tresguerres *et al.*, 2006b; chapter VI). The cellular localization of the NHE2-lp was exclusively cytoplasmic during blood alkalosis. Combining all the evidence, it is likely that blood acid-base regulation in the hagfish is achieved by differential insertion of the relevant ion-transporting proteins into either the apical or the basolateral membrane of the MR cells.

The  $\text{NaHCO}_3$  loads in my experiments were rather abrupt. For example, in similar experiments in dogfish, the  $\text{HCO}_3^-$  load was infused gradually and continuously over the experimentation period (Tresguerres *et al.*, 2005, 2006c; chapters II and III). It is unclear whether or not hagfish in the wild experience blood alkalosis of this magnitude. However, the robust regulatory mechanism described in our study suggests that hagfish may experience periods of significant blood alkalosis naturally. Some possible sources of alkaline stress include respiratory disturbances related to conditions found in the deep-sea waters or a blood post-feeding alkaline tide as has been reported for elasmobranchs (Wood *et al.*, 2005). Regarding this last possibility, I have recently shown that  $\text{V-H}^+$ -ATPase translocates into the basolateral membrane of dogfish gill cells during a post-feeding alkalosis (Tresguerres *et al.*, 2007; chapter IV).

An evolutionary comparison to the branchial acid/base regulatory mechanisms from fish relatives is almost unavoidable when discussing results obtained from hagfish. Briefly, a basolateral V-H<sup>+</sup>-ATPase acting for HCO<sub>3</sub><sup>-</sup> secretion and H<sup>+</sup> reabsorption matches the proposed models for acid-base and ionic regulation in freshwater lampreys (Choe *et al.*, 2004), marine (Piermarini and Evans 2001; Tresguerres *et al.*, 2005, 2006c; chapters II and III) and freshwater elasmobranchs (Piermarini and Evans 2001), and some marine (Catches *et al.*, 2006) and freshwater (Tresguerres *et al.*, 2006a; chapter VIII) teleosts. I conclude that hagfish have gill MR cells for systemic acid-base regulation (see Mallat *et al.*, 1987), and that at least some of the components of the gill Cl<sup>-</sup>/HCO<sub>3</sub><sup>-</sup> exchange systems present in existing fish (namely, V-H<sup>+</sup>-ATPase) indeed evolved before the vertebrates entered freshwater (see Evans 1984), since they are present in the primitive hagfish.

**Table 7.1.** Plasma [Na<sup>+</sup>] and [Cl<sup>-</sup>] of the experimental hagfish at the sampling times.

Time (h)	[Na <sup>+</sup> ] (mmol l <sup>-1</sup> )	[Cl <sup>-</sup> ] (mmol l <sup>-1</sup> )
0	440.10 ± 8.17	451.17 ± 27.11
3	429.11 ± 9.95	479.14 ± 53.33
6	436.89 ± 11.34	481.56 ± 36.36
9	488.59 ± 7.93 *	501.52 ± 30.86
12	477.29 ± 9.94 *	491.93 ± 29.30
18	460.07 ± 7.94	439.28 ± 28.60
24	463.66 ± 9.90	452.94 ± 31.20

Values are means ± s.e.m (N=14) from the combination of NaCl- and NaHCO<sub>3</sub>-infused hagfish. The asterisks indicate significant differences compared to t= 0 (1-way RM-ANOVA, Dunnett's post-test)

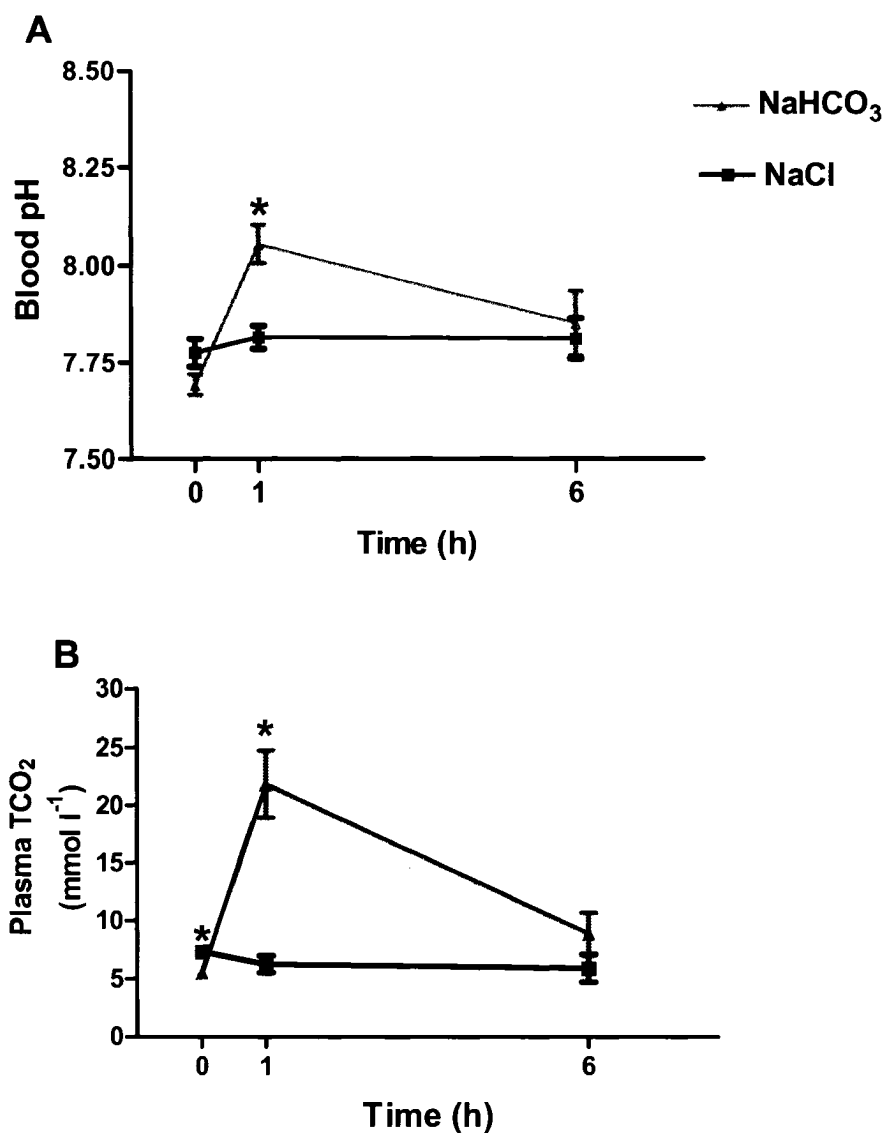


**Figure 7.1.** 6 h experiments. Blood parameters of hagfish injected with either 250 mmol l<sup>-1</sup> NaHCO<sub>3</sub><sup>-</sup> (6000 mmol kg<sup>-1</sup>) or an equivalent volume of 500 mmol l<sup>-1</sup> NaCl (Mean ± s.e.m., N=6). (A) Blood pH. (B) Plasma total [CO<sub>2</sub>]. \*P<0.05 compared to the control value (NaCl) of the respective time (2-way-RM-ANOVA, Bonferroni's post test).



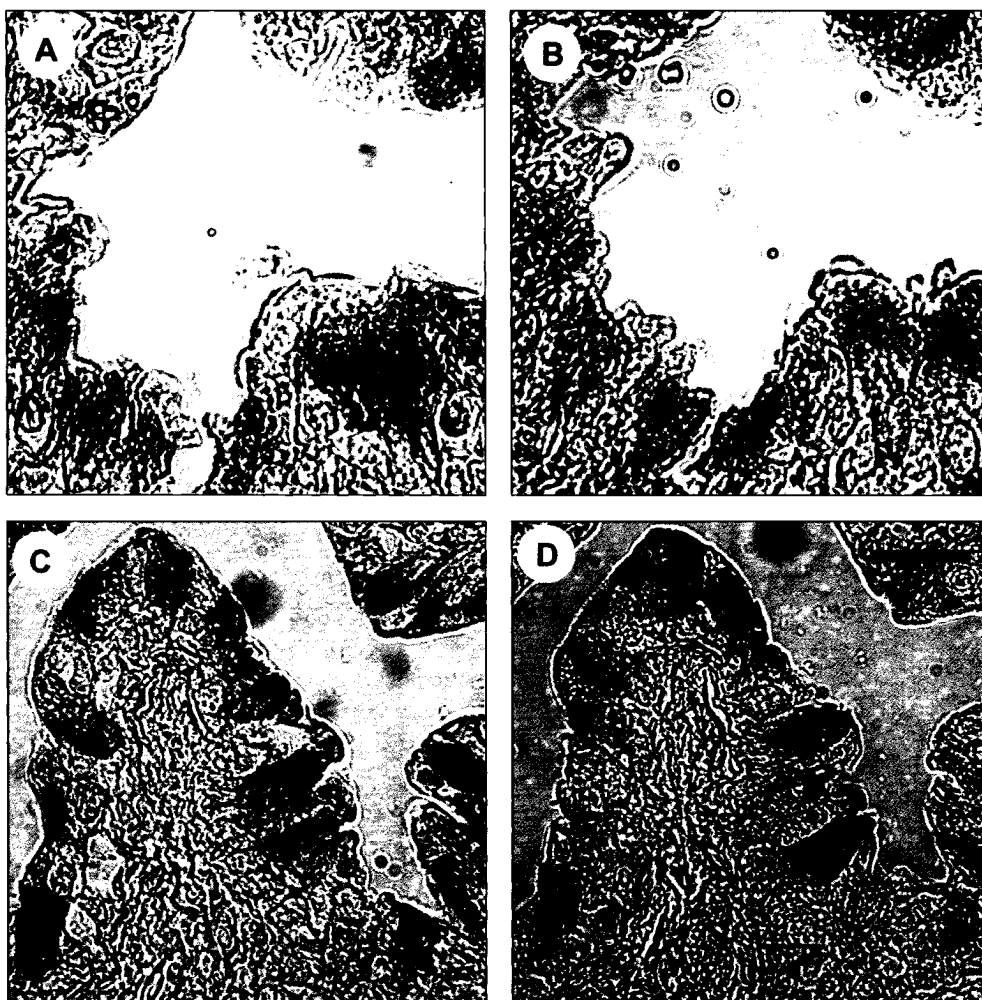


**Figure 7.2.** 6 h experiments.  $\text{Na}^+/\text{K}^+$ -ATPase (A, C) and  $\text{V-H}^+$ -ATPase (B, D) immunoreactivity (IR) in gill consecutive sections from NaCl-injected (A, B) and  $\text{NaHCO}_3$ -injected (C, D) hagfish. A, C =  $\text{Na}^+/\text{K}^+$ -ATPase IR. B, D =  $\text{V-H}^+$ -ATPase IR. Scale bar = 10  $\mu\text{m}$ .

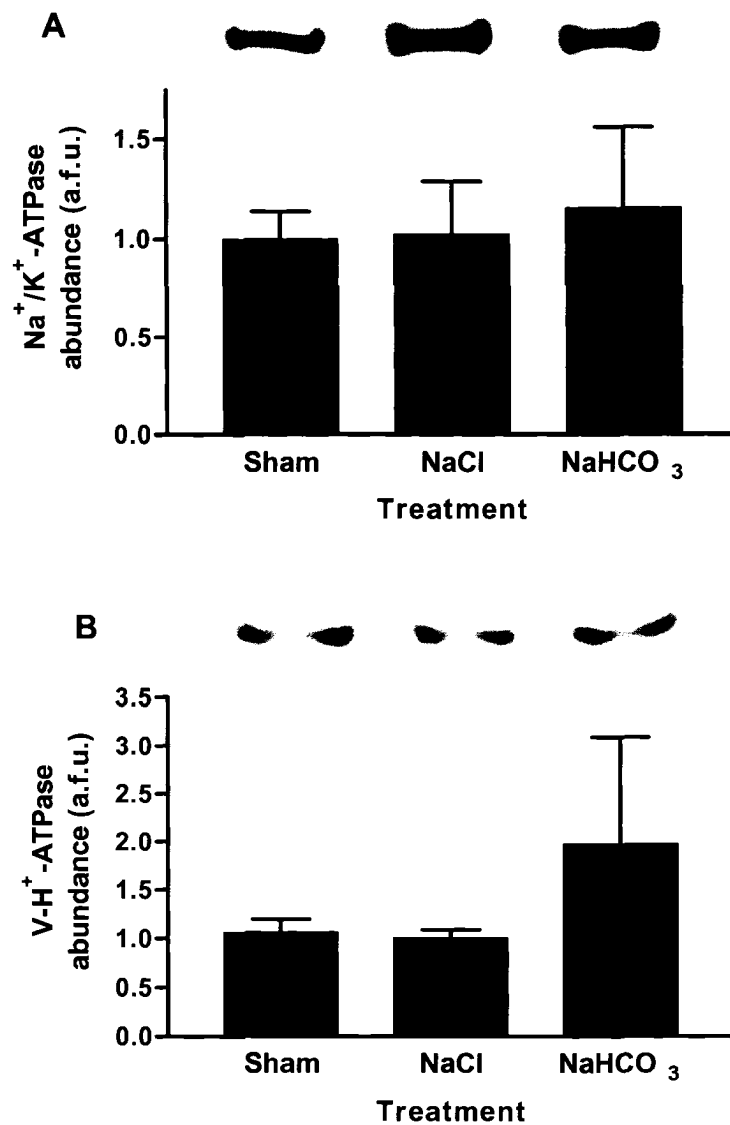


**Figure 7.3.** 6 h experiments. Na<sup>+</sup>/K<sup>+</sup>-ATPase (A) and V-H<sup>+</sup>-ATPase (B) abundance in gills from sham (not-infused), NaCl- and NaHCO<sub>3</sub>-infused hagfish. These data are from cell membranes, but whole gill homogenates showed the same trend. No significant differences were found between treatments (1-way ANOVA) (N=4-6).

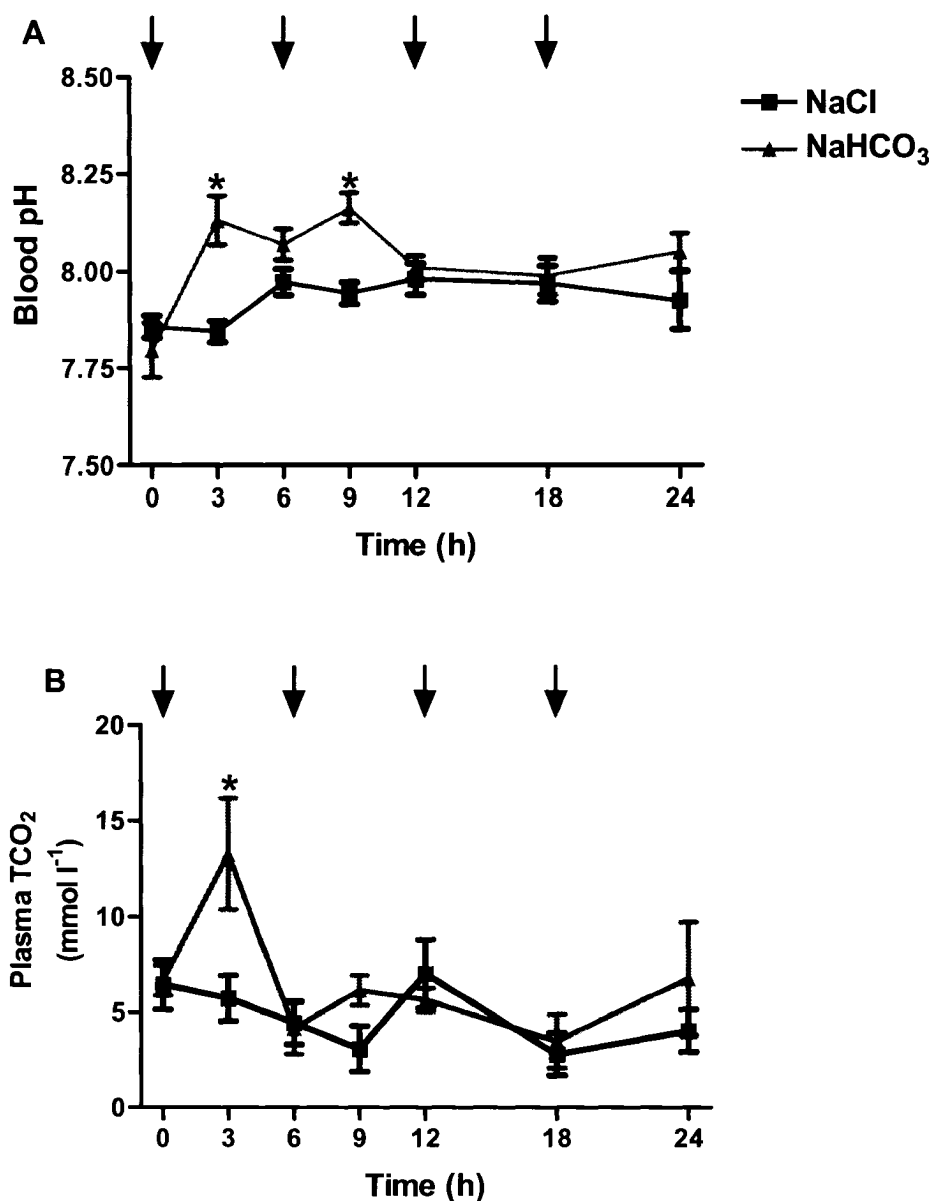


**Figure 7.4.** 24 h experiments. Blood parameters of hagfish injected with either 250 mmol l<sup>-1</sup> NaHCO<sub>3</sub><sup>-</sup> or 500 mmol l<sup>-1</sup> NaCl (Mean ± s.e.m., N=6). The arrows indicate 6000 mmol kg<sup>-1</sup> injections of HCO<sub>3</sub><sup>-</sup> or equivalent volume or NaCl (A) Blood pH. (B) Plasma total [CO<sub>2</sub>]. \**P*<0.05 compared to the control value (NaCl) of the respective time (2-way-RM-ANOVA, Bonferroni's post test).

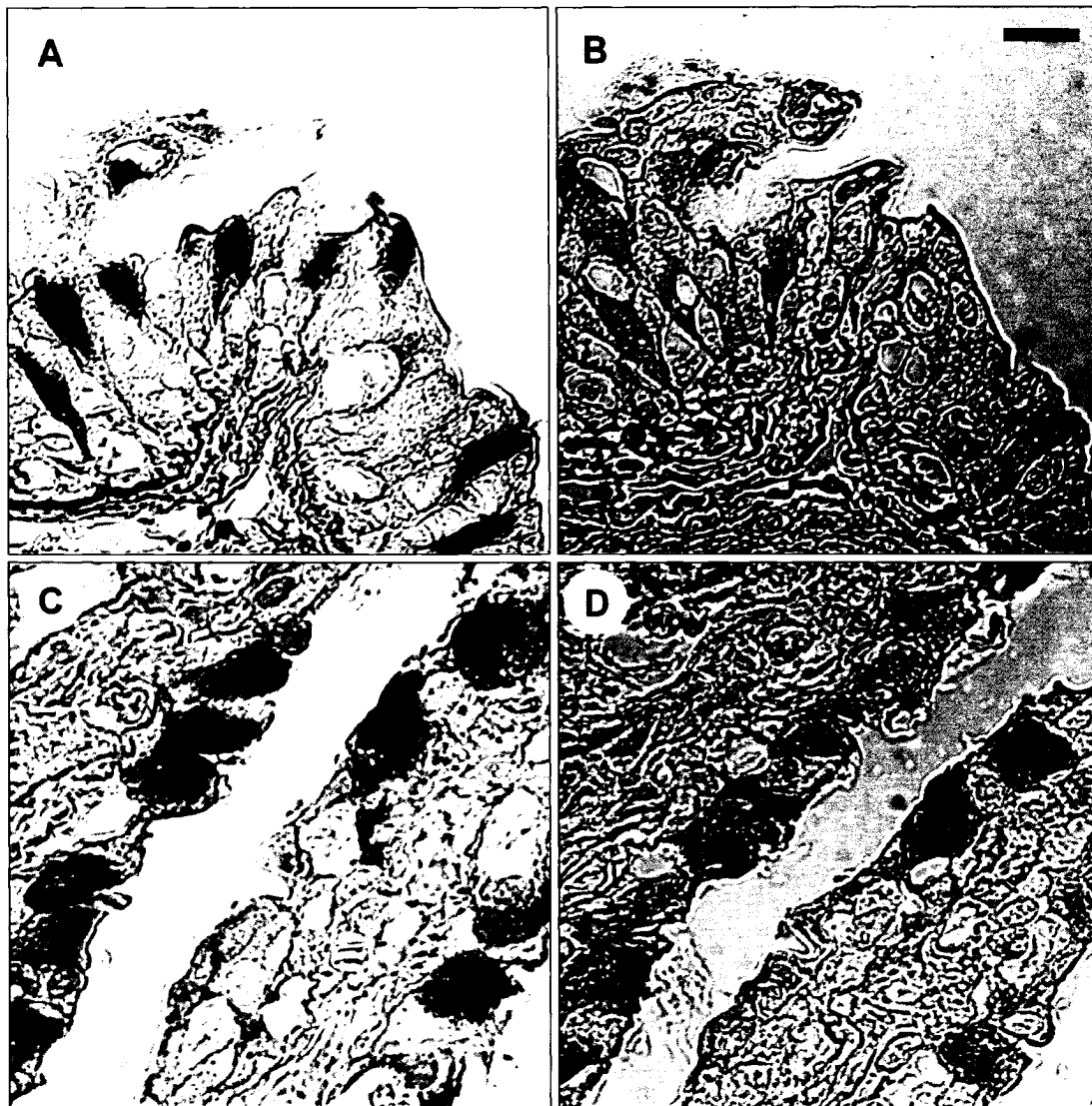


**Figure 7.5.** 24 h experiments.  $\text{Na}^+/\text{K}^+$ -ATPase and  $\text{V-H}^+$ -ATPase immunoreactivity (IR) in gill consecutive sections from NaCl-injected (A, B) and  $\text{NaHCO}_3$ -injected (C, D) hagfish. A, C =  $\text{Na}^+/\text{K}^+$ -ATPase IR. B, D =  $\text{V-H}^+$ -ATPase IR. Scale bar = 10  $\mu\text{m}$ .

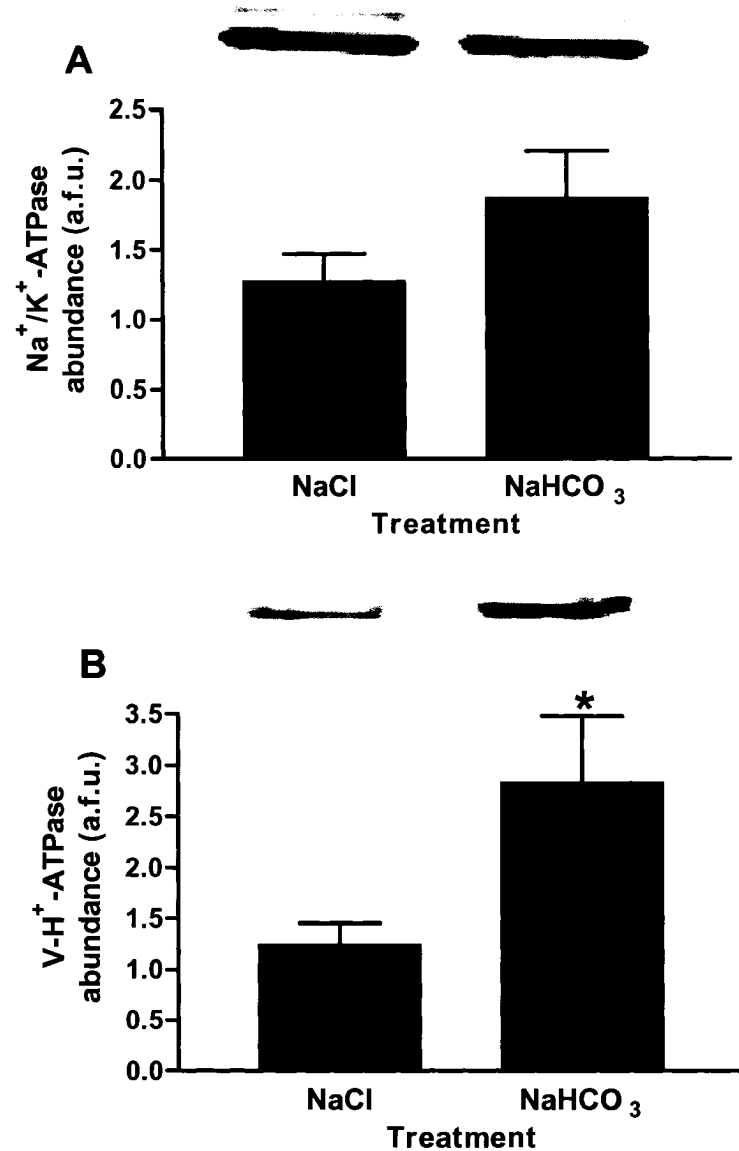


**Figure 7.6.** 24 h experiments.  $\text{Na}^+/\text{K}^+$ -ATPase (A) and  $\text{V-H}^+$ -ATPase (B) abundance in whole gill homogenates from NaCl- and  $\text{NaHCO}_3$ -infused hagfish. \* $P < 0.05$  compared to the control value (NaCl) (Student's t-test) (N=7).

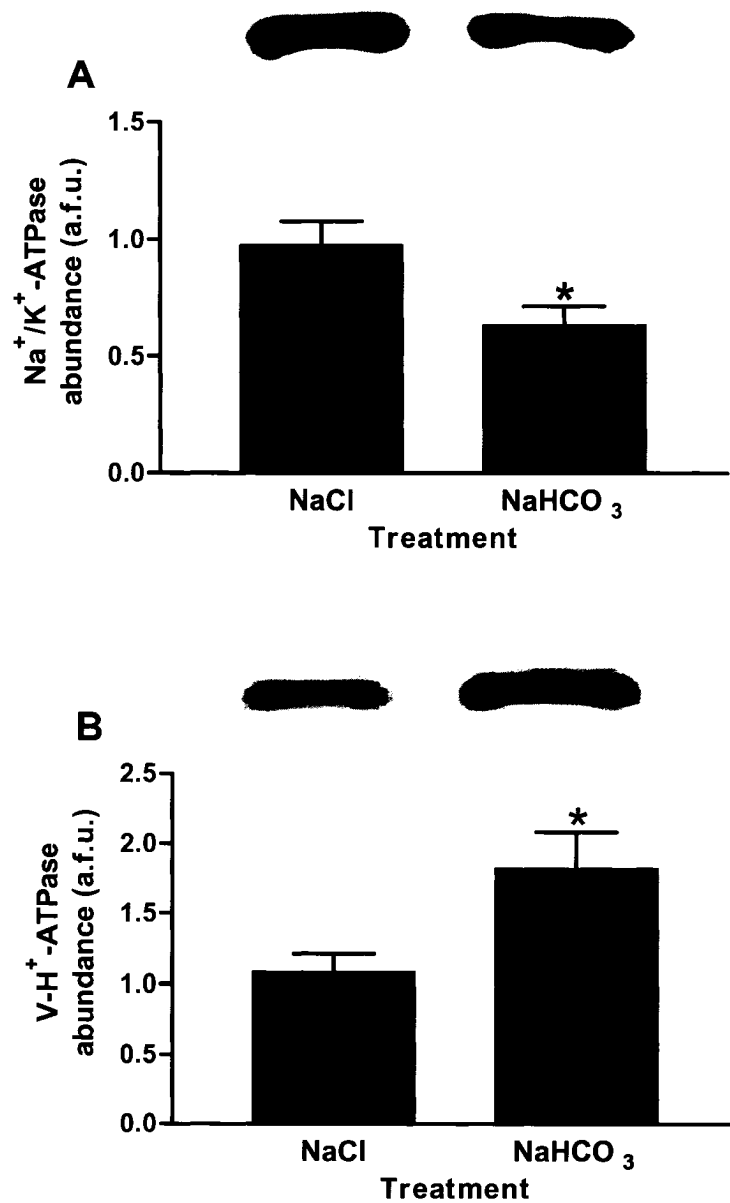


**Figure 7.7.** 24 h experiments. Na<sup>+</sup>/K<sup>+</sup>-ATPase (A) and V-H<sup>+</sup>-ATPase (B) abundance in gill cell membranes from NaCl- and NaHCO<sub>3</sub>-infused hagfish. \**P*<0.05 compared to the control value (NaCl) (Student's t-test) (N=7).

## References

- Alberts, B., Bray, D., Lewis, J., Raff, M., Roberts, K. and Watson, J.D.** (1994). *Molecular biology of the cell*. 3<sup>rd</sup> ed. Garland Publishing, New York and London.
- Bartels, H.** (1992). The gills of hagfishes. In: *The Biology of Hagfishes* (eds. J. Jørgensen, J. Lomholt, R. Weber and R. Malte). Chapman and Hall, London, pp 205-222.
- Bartels, H. and Welsch, U.** (1986). Mitochondria-rich cells in the gill epithelium of cyclostomes. A thin section and freeze fracture study. In: *Indo-Pacific Fish Biology: Proceedings of the Second International Conference on Indo-Pacific Fishes*, Ichthyological Society of Japan, Tokyo. (eds. T. Uyeno, T. Taniuchi and K. Matsuura), pp. 58-72.
- Beltowsky, J., Marciniak, A., Jamroz-Wiśniewska, A., Borkowska, E. and Wójcicka, G.** (2004). Bidirectional regulation of renal cortical Na<sup>+</sup>, K<sup>+</sup>-ATPase by protein kinase C. *Acta Biochim. Pol.* **51**, 757-772.
- Beltowsky, J., Marciniak, A., Wójcicka, G. and Górny, D.** (2003). Regulation of renal Na<sup>+</sup>, K<sup>+</sup>-ATPase and ouabain sensitive H<sup>+</sup>, K<sup>+</sup>-ATPase by the cyclic AMP-protein kinase A signal transduction pathway. *Acta Biochim. Pol.* **50**, 103-114.
- Catches, J.S., Burns, J.M., Edwards, S.L. and Claiborne, J.B.** (2006). Na<sup>+</sup>/H<sup>+</sup> antiporter, V-H<sup>+</sup>-ATPase and Na<sup>+</sup>/K<sup>+</sup>-ATPase immunolocalization in a marine teleost (*Myoxocephalus octodecemspinosus*). *J. Exp. Biol.* **209**, 3440-3447.

**Choe, K. P., Edwards, S., Morrison-Shetlar, A. I., Toop, T. and Claiborne, J. B.** (1999). Immunolocalization of  $\text{Na}^+/\text{K}^+$ -ATPase in mitochondrion-rich cells of the atlantic hagfish (*Myxine glutinosa*) gill. *Comp. Biochem. Physiol. A* 124, 161-168.

**Choe, K.P., Morrison-Shetlar, A.I., Wall, B.P. and Claiborne, J.B.** (2002). Immunological detection of  $\text{Na}^+/\text{H}^+$  exchangers in the gills of a hagfish, *Myxine glutinosa*, an elasmobranch, *Raja erinacea*, and a teleost, *Fundulus heteroclitus*. *Comp. Biochem. Physiol. A* 131, 375-385.

**Choe, K. P., O'Brien, S., Evans, D. H., Toop, T. and Edwards, S. L.** (2004). Immunolocalization of  $\text{Na}^+/\text{K}^+$ -ATPase, carbonic anhydrase II, and vacuolar  $\text{H}^+$ -ATPase in the gills of freshwater adult lampreys, *Geotria australis*. *J. Exp. Zool. A* 301, 654-665.

**Edwards, S.L., Claiborne, J.B., Morrison-Shetlar A. I. and Toop, T.** (2001). Expression of  $\text{Na}^+/\text{H}^+$  exchanger mRNA in the gills of the Atlantic hagfish (*Myxine glutinosa*) in response to metabolic acidosis. *Comp. Biochem. Physiol. A* 130, 81-91.

**Elger, M. and Hentschel, H.** (1983). Morphological evidence for ionocytes in the gill epithelium of the hagfish *Myxine glutinosa* L. *Bull. Mt. Desert Isl. Biol. Lab.* 23: 4-8.

**Evans, D.H.** (1984). Gill  $\text{Na}^+/\text{H}^+$  and  $\text{Cl}^-/\text{HCO}_3^-$  exchange systems evolved before the vertebrates entered freshwater. *J. Exp. Biol.* 113, 465-469.

**Evans, D.H., Piermarini, P.M. and Choe, K.P.** (2005). The multifunctional fish gill: dominant site of gas exchange, osmoregulation, acid-



base regulation, and excretion of nitrogenous waste. *Physiol. Rev.* 85, 97-177.

**Forster, M.E., Russell, M.J., Hambleton, D.C. and Olson, K.R.** (2001). Blood and extracellular fluid volume in whole body and tissues of the Pacific hagfish, *Eptatretus stouti*. *Physiol. Biochem. Zool.* 74, 750-756.

**Graham, L.A., Hill, K.J. and Stevens, T.H.** (1998). Assembly of the yeast vacuolar H<sup>+</sup>-ATPase occurs in the endoplasmic reticulum and requires a Vma12p/Vma22p assembly complex. *J. Cell. Biol.* 142, 39-49.

**Grosell, M.** (2006) Intestinal anion exchange in marine fish osmoregulation. *J. Exp. Biol.* 209, 2813-2827.

**Katoh, F. and Kaneko, T.** (2003). Short-term transformation and long-term replacement of branchial chloride cells in killifish transferred from seawater to freshwater, revealed by morphofunctional observations and a newly established 'time-differential double fluorescent staining' technique. *J. Exp. Biol.* 206, 4113-4123.

**Katoh, F., Hyodo, S. and Kaneko, T.** (2003). Vacuolar-type proton pump in the basolateral plasma membrane energizes ion uptake in branchial mitochondria-rich cells of killifish *Fundulus heteroclitus*, adapted to a low ion environment. *J. Exp. Biol.* 206, 793-803.

**Katoh, F., Shimizu, A., Uchida, K. and Kaneko, T.** (2000). Shift of chloride cell distribution during early life stages in seawater-adapted killifish, *Fundulus heteroclitus*. *Zool. Sci.* 17, 11-18.

**Laemmli, U. K.** (1970). Cleavage of structural proteins during the assembly of the head of the bacteriophage T4. *Nature* 227, 680-685.

**Mallat, J., Conley, D.M. and Ridgway, R.L.** (1987). Why do hagfish have gill “chloride cells” when they need not regulate plasma NaCl concentration? *Can. J. Zool.* 65, 1956-1965.

**Mallat, J. and Paulsen, C.** (1986). Gill ultrastructure of the Pacific hagfish *Eptatretus stouti*. *Am. J. Anat.* 177, 243-269.

**McCormick, S.D.** (1993). Methods for non-lethal gill biopsy and measurements of Na<sup>+</sup>/K<sup>+</sup>-ATPase activity. *Can. J. Fish Aquat. Sci.*, 656-658.

**McDonald, D.G., Cavdek, V., Calvert L. and Milligan, C.L.** (1991). Acid-base regulation in the Atlantic hagfish *Myxine glutinosa*. *J. Exp. Biol.* 161, 201-215.

**Morris, R.** (1965). Studies on salt and water balance in *Myxine glutinosa* (L.). *J. Exp. Biol.* 42, 359-371.

**Peters, T., Forster, R. and Gros, G.** (2000). Hagfish (*Myxine glutinosa*) red cell membrane exhibits no bicarbonate permeability as detected by <sup>18</sup>O exchange. *J. Exp. Biol.* 203, 1551-1560.

**Piermarini, P. M. and Evans, D. H.** (2001). Immunochemical analysis of the vacuolar proton-ATPase B-subunit in the gills of a euryhaline stingray (*Dasyatis sabina*): effects of salinity and relation to Na<sup>+</sup>/K<sup>+</sup>-ATPase. *J. Exp. Biol.* 204, 3251-3259.

**Taylor, J.R. and Grosell, M.** (2006). Evolutionary aspects of intestinal bicarbonate secretion in fish. *Comp. Biochem. Physiol. A* 143, 523-529.

**Tresguerres, M., Katoh, F., Fenton, H., Jasinska, E., and Goss, G.G.** (2005). Regulation of branchial V-H<sup>+</sup>-ATPase, Na<sup>+</sup>/K<sup>+</sup>-ATPase and NHE2 in response to acid and base infusions in the Pacific spiny dogfish (*Squalus acanthias*). *J. Exp. Biol.* 208, 345-354.

**Tresguerres, M., Katoh, F., Orr, E., Parks, S.K. and Goss, G.G.** (2006a). Chloride uptake and base secretion in freshwater fish: a transepithelial ion-transport metabolon? *Physiol. Biochem. Zool.* 79, 981-996.

**Tresguerres, M., Parks, S.K. and Goss, G.G.** (2006b). V-H<sup>+</sup>-ATPase, Na<sup>+</sup>/K<sup>+</sup>-ATPase and NHE2 immunoreactivity in the gill epithelium of the Pacific hagfish (*Eptatretus stoutii*). *Comp. Biochem. Physiol. A.* 145, 312-321.

**Tresguerres, M., Parks, S.K., Katoh, F. and Goss, G.G.** (2006c). Microtubule-dependent relocation of branchial V-H<sup>+</sup>-ATPase to the basolateral membrane in the Pacific spiny dogfish (*Squalus acanthias*): a role in base secretion. *J. Exp. Biol.* 209, 599-609.

**Tresguerres, M., Parks, S.K., Wood, C.M. and Goss, G.G.** (2007). V-H<sup>+</sup>-ATPase translocation during blood alkalosis in dogfish gills: interaction with carbonic anhydrase and involvement in the post-feeding alkaline tide. *Am. J. Physiol. Reg. Int. Comp. Physiol.* 292.

**Wood, C. M., Kajimura, M., Mommsen, T. P. and Walsh, P. J.** (2005). Alkaline tide and nitrogen conservation after feeding in an elasmobranch (*Squalus acanthias*). *J. Exp. Biol.* 208, 2693-2705.

**Zall, D. M., Fischer, M. D., and Garner, Q. M.** (1956). Photometric determination of chloride in water. *Anal. Chem.* 28, 1665-1678.

**Rainbow trout *Oncorhynchus mykiss***

## Chapter VIII

### Chloride uptake and base secretion in freshwater fish: a transepithelial ion-transport metabolon?<sup>1,2</sup>

<sup>1</sup>A version of this chapter has been published. **Tresguerres, M.**, Katoh, F., Orr, E., Parks, S.K. and Goss, G.G. (2006). *Physiological and Biochemical Zoology* 79 (6): 981-996. Reproduced with permission of Chicago University Press and the co-authors of the manuscript.

<sup>2</sup>This manuscript is an invited review for *Physiological and Biochemical Zoology*. As such, it has a specific format that does not include a “Materials and Methods” section. Details about the Materials and Methods, absent in the manuscript published in *Physiol. Biochem. Zool.*, have been included at the end of this chapter.

## Introduction

### *Historical background*

Freshwater (FW) fish passively lose ions to the more dilute environment, most importantly across the gills and in the urine (Evans *et al.*, 2005). In order to maintain homeostasis, this is compensated by active uptake of  $\text{Na}^+$  and  $\text{Cl}^-$  across the gills (Motaïs and Garcia-Romeu, 1972; McDonald and Wood, 1981). Originally, it was proposed that the mechanism for NaCl absorption coupled  $\text{Na}^+$  influx with  $\text{NH}_4^+$  secretion and  $\text{Cl}^-$  uptake with  $\text{HCO}_3^-$  extrusion (Krogh, 1939). Therefore, an intimate linkage between salt and acid/base regulation in fish gill ion transport was established early on.

Over the last 40 years, there has been extensive debate about the branchial cellular mechanisms responsible for these ionic fluxes. Kerstetter *et al.* (1970) first suggested that  $\text{Na}^+$  was in fact exchanged for  $\text{H}^+$  instead of  $\text{NH}_4^+$ , a hypothesis that was later confirmed by Avella and Bornancin (1989) and Wilson *et al.* (1994). For decades, the proposed mechanism for  $\text{Na}^+$  uptake in FW fish gills consisted of apical electroneutral  $\text{Na}^+/\text{H}^+$  exchangers (NHE), with basolateral  $\text{Na}^+/\text{K}^+$ -ATPase providing the electromotive force (Kerstetter *et al.* 1970; Motaïs and Garcia-Romeu 1972). However, this model was challenged based on further analyses of thermodynamic parameters for electroneutral exchange. As first noticed by Avella and Bornancin (1989), external  $\text{Na}^+$  concentration  $[\text{Na}^+]_{\text{FW}}$  is in the micromolar range, while intracellular  $\text{Na}^+$  concentration  $[\text{Na}^+]_i$  in the gill epithelium is a few millimoles. Thus, it seemed unlikely that the  $\text{Na}^+$  uptake in FW could take place *via* an apical electroneutral exchanger. As a result, an alternative model was

developed, and it is now generally accepted that, at least in the rainbow trout in very dilute FW, the apical entry of  $\text{Na}^+$  into the cell depends on apical vacuolar proton ATPases ( $\text{V-H}^+$ -ATPase) electrochemically coupled to  $\text{Na}^+$  channels (Fenwick *et al.*, 1999; Grosell and Wood 2002; Reid *et al.*, 2003). For an excellent review in this topic I suggest consulting the recent paper by Kirschner (2004) which discusses variations of the model for  $\text{Na}^+$  uptake in a number of FW animals.

On the other hand, elucidating the branchial cellular mechanism(s) for  $\text{Cl}^-$  uptake has been more obscure than for  $\text{Na}^+$  (De Renzis and Bornancin, 1984; Motaïs and Garcia-Romeu, 1972; Perry, 1997). Although the original hypothesis by Krogh for  $\text{Cl}^-/\text{HCO}_3^-$  exchange has remained unchallenged, a model including a viable energizing step is still lacking. The proposed involvement of active  $\text{Cl}^-$  transporters in the basolateral (Maetz and Garcia-Romeu, 1964) or apical membrane (De Renzis and Bornancin, 1984) has not garnered widespread support both theoretically and experimentally as evidenced by few supporting publications. However, if we consider the  $[\text{Cl}^-]$  and  $[\text{HCO}_3^-]$  both in FW and inside the gill cells, it is not clear how an apical electroneutral  $\text{Cl}^-/\text{HCO}_3^-$  exchanger can be operational. In this chapter, I discuss a viable mechanism for branchial  $\text{Cl}^-$  uptake in FW fish based on structure-function analysis of the MR cells, new information on homologous anion exchangers and their properties and re-interpretation of previously published results. I propose that  $\text{Cl}^-$  uptake across the FW fish gill takes place via an apical anion exchanger (AE) functionally linked to carbonic anhydrase

(CA) and to basolateral V-H<sup>+</sup>-ATPases (Fig. 8.1). In this model, basolateral V-H<sup>+</sup>-ATPases provide the necessary driving force to overcome the unfavorable gradient for Cl<sup>-</sup> uptake. I propose to name this arrangement of proteins the “freshwater chloride-uptake metabolon”. The term “metabolon” has been extensively used in biochemistry (Srere 1987; 1993) to define complexes of metabolic enzymes, or any group of proteins that act together to accomplish a singular metabolic function. The functional significance of a metabolon is that the close proximity between enzymes allows for the rapid movement of metabolites from one active site to the next, which is also known as substrate channeling (Miles et al. 1999). Some of the advantages of this process are to limit the loss of metabolites by diffusion and to create specific pools of substrates at high concentrations (Sterling et al. 2001). In my model, the ultimate result of the combined action of AE, CA and V-H<sup>+</sup>-ATPase would be to create a local [HCO<sub>3</sub><sup>-</sup>]<sub>i</sub> high enough to drive Cl<sup>-</sup> uptake from FW via an anion exchanger.

#### *Evidence for linkage between Cl<sup>-</sup> uptake and HCO<sub>3</sub><sup>-</sup> secretion*

The relationship between Cl<sup>-</sup> uptake and base secretion in FW teleosts was first suggested by August Krogh. He found that Cl<sup>-</sup> could be absorbed without the simultaneous transfer of an accompanying cation, and proposed that internal HCO<sub>3</sub><sup>-</sup> was exchanged for Cl<sup>-</sup> in order to maintain electrical neutrality (Krogh 1939). Many studies have examined this hypothesis since then. For example, Maetz and Garcia-Romeu (1964) reported that increasing HCO<sub>3</sub><sup>-</sup> in the water inhibited Cl<sup>-</sup> uptake in the goldfish *Carassius auratus*, and



that intraperitoneal injection of  $\text{NaHCO}_3$  produced the opposite effect. Furthermore, injection of acetazolamide, an inhibitor of CA, significantly reduced  $\text{Cl}^-$  uptake. Manipulation of internal and external  $\text{HCO}_3^-$  produced virtually identical effects in artificially irrigated gills of the rainbow trout (Kerstetter and Kirschner, 1972). Although these authors did not find any significant effect of acetazolamide on  $\text{Cl}^-$  uptake, the difference might be due to the fact that in the goldfish experiments, the initial ion uptake rate was stimulated by injecting a hypotonic solution. It is thus possible that the role of CA in  $\text{Cl}^-/\text{HCO}_3^-$  exchange is only significant when the  $\text{Cl}^-$  uptake mechanism is stimulated.

Over the next few decades, the relationship between  $\text{Cl}^-$  uptake and  $\text{HCO}_3^-$  secretion was extended to several fish species. In particular, experimental induction of metabolic and respiratory alkalosis by either  $\text{NaHCO}_3$  injection or recovery from environmental hypercapnia demonstrated the importance of  $\text{Cl}^-/\text{HCO}_3^-$  exchange for regulation of blood pH. Using both procedures, Goss and Wood (1991) found that  $\text{Cl}^-$  uptake and base secretion in rainbow trout have a direct 1:1 linkage. Moreover, they presented evidence that gill anion exchange follows a two-substrate model, whereby the fluxes of those ions across the gill epithelium is limited by the availability of not only external  $\text{Cl}^-$ , but also of intracellular  $\text{HCO}_3^-$ .  $K_m$  for  $\text{Cl}^-$  was  $135 \mu\text{equiv.L}^{-1}$ , far below the water  $[\text{Cl}^-]$  of  $600 \mu\text{M}$ , while *apparent*  $K_m^{\text{HCO}_3^-}$  was  $33 \text{ mequiv.L}^{-1}$ , far higher than the estimated  $[\text{HCO}_3^-]_i$  of  $\sim 2 \text{ mmol l}^{-1}$ . Since  $K_m$  is the concentration of substrate that results in half-maximal rate of transport (Voet

and Voet, 1995), it is evident that the putative apical anion exchanger could not efficiently function with the gill  $[\text{HCO}_3^-]_i$  than can be accounted for by standard bulk measurement. In addition, the estimated  $K_m$  value suggests that a change of a few millimoles in  $[\text{HCO}_3^-]_i$  can greatly alter rates of  $\text{Cl}^-$  uptake (Goss and Wood, 1991).

*Apical electroneutral anion exchange: thermodynamic considerations*

In order to understand why the classic model of an apical electroneutral anion exchanger would not work for  $\text{Cl}^-$  uptake in most FW fishes, it is imperative to review some characteristics of the environment and how they might affect anion exchange.

Typical FW systems have  $[\text{Cl}^-]$  between 0.01 and 1  $\text{mmol l}^{-1}$  and total carbonate concentration ranging from 0.1 to 3  $\text{mmol l}^{-1}$  (Table 8.1). Inside fish gill cells, the available set of data from several trout species points to  $[\text{Cl}^-]_i$  between 40 and 90  $\text{mmol l}^{-1}$  (Wood and LeMoigne, 1991; Eddy and Chang, 1993; Morgan *et al.*, 1994; Morgan and Potts, 1995). On the other hand,  $\text{pH}_i$  in trout gill cells has been estimated to be around 7.2-7.5 (Wood and LeMoigne, 1991; Goss and Wood, 1991). This value translates into a bulk  $[\text{HCO}_3^-]_i$  of around 2  $\text{mmol l}^{-1}$  (at  $P_{\text{CO}_2} = 2.5 \text{ torr} = 0.33 \text{ kPa}$ ;  $T = 10^\circ \text{C}$ ), not much different from the surrounding FW and far lower than the *apparent*  $K_m^{\text{HCO}_3^-}$  of 33.3  $\text{mmol l}^{-1}$  as predicted by Goss and Wood (1991). However, all these calculations estimate the bulk  $[\text{HCO}_3^-]$  and do not discriminate between areas of localized higher or lower concentrations within the cells, a key point in my model.

In order for  $\text{Cl}^-$  uptake and base secretion to rely on an electroneutral exchange of  $\text{Cl}^-$  and  $\text{HCO}_3^-$  across the apical membrane, the  $\text{HCO}_3^-$  concentration gradient between the cytosol and FW must be larger than the tendency for  $\text{Cl}^-$  movement in the same direction (Jensen *et al.*, 2003). According to the ion concentrations provided above, the net gradient for  $\text{Cl}^-$  favors efflux (cytosol $\rightarrow$ FW) rather than uptake (FW $\rightarrow$ cytosol). In order to counteract this tendency for efflux, the gradient for  $\text{HCO}_3^-$  must be of similar magnitude but of opposite direction. Although  $[\text{HCO}_3^-]_i$  present a small tendency for outward movement (cytosol $\rightarrow$ FW) in most FW situations, this net driving force for  $\text{HCO}_3^-$  secretion is not sufficient to overcome the large net gradient opposing  $\text{Cl}^-$  uptake. The only mechanisms available to allow electroneutral  $\text{Cl}^-/\text{HCO}_3^-$  exchange under these conditions are to increase  $[\text{HCO}_3^-]_i$  and/or to decrease  $[\text{Cl}^-]_i$  significantly. A reduction in  $[\text{Cl}^-]_i$  to the levels required is unlikely; for example at an external  $[\text{Cl}^-]$  of  $0.1 \text{ mmol l}^{-1}$ ,  $[\text{Cl}^-]_i$  would have to be substantially less than  $1 \text{ mmol l}^{-1}$  (Table 8.1). Since envisioning a mechanism for reducing  $[\text{Cl}^-]_i$  to such levels is difficult, the only option at this point therefore is to increase  $[\text{HCO}_3^-]_i$  to a value which would allow for electroneutral anion exchange under these conditions. However, the increase in  $[\text{HCO}_3^-]_i$  must be substantial. Even assuming conservative values of  $[\text{Cl}^-]_i = 40 \text{ mmol l}^{-1}$ ,  $[\text{Cl}^-]_o = 1 \text{ mmol l}^{-1}$ , and  $[\text{HCO}_3^-]_o = 0.5 \text{ mmol l}^{-1}$ , intracellular  $[\text{HCO}_3^-]$  should be higher than  $20 \text{ mmol l}^{-1}$  in order for electroneutral exchange to be viable. Furthermore, if we consider the actual water

parameters from selected places where fish research is conducted,  $[\text{HCO}_3^-]_i$  must be even higher (Table 8.1).

*What is the mechanism for elevating  $[\text{HCO}_3^-]_i$  to high enough levels to allow for transport?*

As pointed out above, bulk  $[\text{HCO}_3^-]_i$  in trout gill cells has been estimated to be around  $2 \text{ mmol l}^{-1}$ , which is theoretically insufficient to drive  $\text{Cl}^-$  uptake from FW. However, these values are based on extracellular A/B data and/or mean gill  $\text{pH}_i$  measurements, which are representative of the whole gill tissue (Goss and Wood, 1991). Since the ion-transporting cells represent a small proportion of the total cells in the gill epithelium (Laurent, 1984), it is possible that their actual  $\text{pH}_i$  and  $[\text{HCO}_3^-]_i$  values are masked by those from the most abundant pavement (PV) cells. For example, our lab has recently found two subpopulations of MR cells with different resting  $\text{pH}_i$ , as estimated from intracellular measurements using the pH-sensitive dye BCECF-AM (Parks *et al.*, 2007). This suggests that cell types with different ion-transporting functions have internal environments with different physical-chemical properties. Moreover, the concept of molarity is based on the solute being distributed homogeneously throughout the solution. But what would happen if there exists local environments (microdomains) with higher  $[\text{HCO}_3^-]_i$  within the same cell? Such a scenario has been established for other ions, most notably calcium (reviewed in Rizzuto and Pozzan, 2006).

To illustrate how the concept of microdomains can be applied to  $\text{HCO}_3^-$ , I will perform some simple hypothetical calculations. To begin, I assume that

the area underneath any transporter can be represented by a cylinder with a specific volume that can be determined according to the following mathematical equation:

$$(1) V = \pi \times r^2 \times h$$

where  $r$  equals the radius of the area under the protein and  $h$  equals the distance away from the membrane. To illustrate my model, I have chosen a variety of different scenarios ranging from the equivalent of a  $[\text{HCO}_3^-]_i$  in bulk solution of approximately  $2 \text{ mmol l}^{-1}$  down to dimensions comparable to the size of the transport site of AE1, as predicted from its crystal structure (Wang *et al.*, 1994).

Using Avogadro's number ( $6.023 \times 10^{23} \text{ molecules mol}^{-1}$ ) I then calculate that the number of molecules of  $\text{HCO}_3^-$  per liter at  $2 \text{ mmol l}^{-1}$  would be approximately  $12.046 \times 10^{20}$ . This allows me to determine the chance (%) for a particular space to be occupied by a molecule of  $\text{HCO}_3^-$  using the following equation:

$$(2) \text{ Theoretical occupancy} = \text{volume} \times (12.046 \times 10^{20}) \times 100\%$$

where volume is expressed in liters.

Theoretical scenarios are represented in table 8.2, and their implications are numerous. The first implication that is apparent is that the chance of

occupancy of a particular  $\text{HCO}_3^-$  transport site is quite low. In particular, if  $\text{HCO}_3^-$  is distributed randomly and homogeneously throughout the cell, the chance for one  $\text{HCO}_3^-$  molecule to be in a volume equivalent to a cylinder of 1 nm in diameter and radius is approximately 0.4 %. Since such a volume is comparable to the transport site of an apical anion exchanger (using values for AE1 size from Wang *et al.*, 1991), under those conditions  $\text{HCO}_3^-$  would not be available as a substrate most of the time.

Similarly, we can calculate the effective  $[\text{HCO}_3^-]$  if we place a single molecule of  $\text{HCO}_3^-$  within that hypothetical cylinder of set dimensions. Molarity is defined as the moles solute divided by the volume of the solution expressed in liters. Since one molecule is equal to the inverse of Avogadro's number, then

$$(3) \text{ Effective } [\text{HCO}_3^-] = (\text{Avogadro's number} \times \text{volume})^{-1}$$

I represent a variety of scenarios in figure 8.2, ranging from the dimensions given for the crystal structure of the membrane domain for AE1 (Wang *et al.*, 1994) down to the volume of the transport site of the  $[\text{HCO}_3^-]$  molecule. Figure 8.2 shows that placing a  $\text{HCO}_3^-$  molecule within close proximity to the transporting region substantially increases the local  $[\text{HCO}_3^-]$ . This is important as it has been demonstrated that CA is located in the sub-apical region of fish gill cells (Rahim *et al.* 1988) (see next sections). CA facilitates the hydration of  $\text{CO}_2$  into primarily  $\text{H}^+$  and  $\text{HCO}_3^-$ , which would

place a  $\text{HCO}_3^-$  directly in the vicinity of the transporter. Finally, given that placing a  $\text{HCO}_3^-$  near the transport site can raise the effective concentration above  $500 \text{ mmol l}^{-1}$ , it would be sufficient to drive an electroneutral  $\text{Cl}^-/\text{HCO}_3^-$  exchange (see Table 8.1). This agrees with the two-substrate model proposed by Goss and Wood (1991), where increasing  $[\text{HCO}_3^-]_i$  acts to significantly increase the maximum influx rate of  $\text{Cl}^-$  ( $J_{\text{Max}}^{\text{Cl}^-}$ ) with constant  $[\text{Cl}^-]_{\text{FW}}$ . Under such a scenario, increasing  $[\text{HCO}_3^-]_i$  would increase theoretical occupancy and increase  $\text{Cl}^-$  transport rate.

However, a problem exists with the generation of excess  $\text{H}^+$  in this region as a product of CA activity. In order to prevent severe acidosis and  $\text{HCO}_3^-$  dehydration, the  $\text{H}^+$  must be either rapidly buffered, immediately removed from the area, or both. The next few sections of this chapter will deal with cellular, structural and functional considerations that are relevant to my proposed model, and could explain the necessary increase in local  $[\text{HCO}_3^-]_i$  and the  $\text{H}^+$  removal to the blood.

#### *Cellular and molecular components involved in branchial $\text{Cl}^-/\text{HCO}_3^-$ exchange*

##### *Nomenclature of ion transporting cells in the gill*

The actual site where the majority of transepithelial ion transport takes place in the gill epithelium is attributed to the mitochondria-rich (MR) cells, also known as chloride cells. The former name illustrates the most recognizable characteristic of these cells, the great number of mitochondria present in the cytoplasm, a trait that is indicative of the large supply of ATP required to fuel active ion transport against the steep concentration gradients

found both in FW and SW. On the other hand, the name “chloride cell” derives from the pioneering study by Keys and Wilmer (1932), who hypothesized that a group of large ovoid cells located at the base of the lamella in gills from SW eels (*Anguilla vulgaris*) were responsible for branchial chloride secretion. Therefore, those cells were named “chloride secreting cells”. Later evidence supported the chloride secreting function of these cells (e.g.  $\text{Ag}^+$  precipitate in the apical crypt after incubation with  $\text{AgNO}_3$ ), and the name was shortened to simply “chloride cells”, probably by Copeland (1948) (c.f. Laurent 1984). Although the term chloride cell has been used profusely in the literature and it has a vast tradition, it does not reflect any morphological or physiological characteristic of the MR cell from FW fish. Therefore, I will only use MR cell throughout the text, even when citing literature where chloride cell was originally used.

#### *MR cell subtypes*

The morphology and cell composition of the gill epithelium has been extensively reviewed (e.g. Laurent and Dunel, 1980; Laurent, 1984; Pisam and Rambourg, 1991; Goss *et al.*, 1995; Perry, 1997; Evans *et al.*, 2005). Hence, here I will only refer to some ultrastructural characteristics of the MR cells from FW fishes that are relevant to this particular chapter. The presence of different FW MR cell morphologies has been noted as early as the 60's (Doyle and Gorecki, 1961). However, it was Pisam and co-workers (1987; 1990; 1995) who described this phenomenon in detail. These authors used some characteristics of the cells such as shape, their localization within the



gill filament, their light or dark staining, the mitochondria distribution and the morphology of the basolateral tubular system, to distinguish two types of MR cells in the gill epithelium of a variety of FW-adapted fish (reviewed by Pisam and Rambourg, 1991). However, they made no attempt to identify the physiological functions of the subtypes. More recently, Goss *et al.* (2001) also detected two subtypes of MR cells, this time based on the differential labeling by peanut lectin agglutinin (PNA). Isolated MR cells that bound PNA (PNA<sup>+</sup>) were similar in morphology to the  $\alpha$ -MR cells described in the study by Pisam and Rambourg (1991), e.g., they are lighter in color and had a more developed tubular system (Goss *et al.*, 2001; Galvez *et al.*, 2002). These morphologic characteristics also match those of the classic MR cells (“Chloride cells”).

Importantly, only the PNA<sup>-</sup> MR cells were shown to have a Na<sup>+</sup> influx mechanism of similar characteristics to whole-animals (Reid *et al.*, 2003), thus establishing a separation of function between the subtypes. By analogy to the base-secreting MR intercalated cells in the mammalian kidney, which also bind PNA (Satlin *et al.*, 1992), the fish gill PNA<sup>+</sup> MR cells were hypothesized to be involved in Cl<sup>-</sup> uptake/HCO<sub>3</sub><sup>-</sup> secretion (Goss *et al.*, 2001; Galvez *et al.*, 2002; Perry *et al.*, 2003). However, the evidence linking PNA<sup>+</sup> MR cell and Cl<sup>-</sup>/HCO<sub>3</sub><sup>-</sup> exchange is scarce and indirect. Figure 8.3 demonstrates the preferential localization of PNA<sup>+</sup> MR cells in the interlamellar region of the gill filament and at the base of the lamella in FW rainbow trout. As described in the following section, localization to the base

of the lamella is typical of MR cells that appear to be involved in  $\text{Cl}^-$  uptake/ $\text{HCO}_3^-$  secretion.

#### *MR cell and $\text{Cl}^-/\text{HCO}_3^-$ exchange*

The available evidence strongly suggests that the cells responsible for  $\text{Cl}^-/\text{HCO}_3^-$  exchange are the MR cells located at the base of the gill lamella and in the interlamellar region. However, care must be taken in interpretation of results from different species and animals of the same species raised in slightly different environments (see Kirschner 2004, who makes a similar case for  $\text{Na}^+$  uptake). Regardless, there is a strong relationship between the gill filament total MR cell Apical Surface Area (MRC ASA) and  $\text{Cl}^-$  uptake in a variety of species of normal (Perry *et al.*, 1992) and  $\text{NaHCO}_3$  infused fish (Goss *et al.*, 1994). In these studies, there also does not appear to be a strong correlation between  $\text{Na}^+$  uptake and MRC ASA during respiratory acidosis. During acidosis, when MRC ASA is reduced by 40-90 % in the rainbow trout and the brown bullhead catfish (*Ictalurus nebulosa*),  $\text{Na}^+$  uptake either increases or is unchanged suggesting that filamental MR cells are not the place of  $\text{H}^+$  secretion/ $\text{Na}^+$  uptake (Goss *et al.*, 1992; Goss and Perry, 1993, reviewed by Goss *et al.*, 1998). Although in some studies MRC ASA also correlates positively with  $\text{Na}^+$  influx (Perry and Laurent, 1989; Perry *et al.*, 1992), this is likely due to a required linkage between net base and net acid secretion under control (non-stimulated) conditions.

Further evidence for the involvement of MR cells in  $\text{Cl}^-/\text{HCO}_3^-$  exchange derives from the x-ray micro-analyses of  $[\text{Cl}^-]_i$  by Morgan *et al.*

(1994) and Morgan and Potts (1995) in isolated gill cells of the brown trout *Salmo trutta*.  $[Cl^-]_i$  in the MR cells increased during exposure to elevated external  $[Cl^-]$ , while acetazolamide and thiocyanate, a non-specific inhibitor of  $Cl^-$  uptake, reduced  $[Cl^-]_i$  in the same cells. None of these treatments produced changes in  $[Cl^-]_i$  in the respiratory PV cells. Unfortunately, the existence of  $PNA^-$  and  $PNA^+$  MR cells was unknown at the time, but since the cells analyzed were chosen on the basis of the apical membrane morphology and location in the gill filament they likely were  $PNA^+$  MR cells.

*Structure-function relationships: importance of MR cell ultrastructure*

The first transmission electron microscopy (TEM) pictures of FW fish MR cells were published by Doyle and Gorecki (1961). These authors identified cells with large numbers of mitochondria which also possessed what they thought was an extensively developed endoplasmic reticulum in close association with the mitochondria. Later studies determined that this structure was in fact part of the cell basolateral membrane and not the endoplasmic reticulum, and it was named the tubular system (Philpott 1980).

The structure of the tubular system is of key importance for our model. Its continuity with the basolateral plasma membrane of the MR cell from both SW and FW fish has been demonstrated using a variety of methods, including the use of extracellular markers such as horseradish peroxidase (Philpott, 1966; reviewed in Philpott, 1980) and specific TEM staining techniques (Pisam, 1981). However, the most compelling evidence for the continuity of the basolateral membrane in the tubular system is the freeze-fracture study

on the gill epithelium by Sardet *et al.* (1979). In that work the organization and structure of the tubular system is clearly revealed. Abundant intramembranous particles were found in the walls of the tubular system, which were suggested to be ion pumps and/or channels. Importantly for my model, the tubular system reaches within close proximity of the apical membrane of the MR cells (Sardet *et al.*, 1979). Although the actual distance between the tubular system and the apical membrane was not measured in the original study, values between 0.3 and 1  $\mu\text{m}$  can be estimated from the pictures provided in Sardet *et al.* (1979) and Sardet (1980). Figure 8.4 shows a TEM picture of a MR cell from FW rainbow trout along with a representative diagram that illustrates the structure of the tubular system as suggested by Sardet *et al.* (1979).

Several authors have hypothesized about the physiological meaning of this structure. The tubular system in MR cells from SW fish has been proposed to concentrate  $\text{Na}^+$ , thus facilitating  $\text{Na}^+$  secretion through the leaky paracellular junctions following the outside negative potential created by transcellular  $\text{Cl}^-$  flux (Sardet, 1980). However, the role of the tubular system in MR cells from FW fish is less clear. We propose that it might have a role in bringing ion-transporting proteins from the apical and basolateral membrane into close proximity. Clearly, structure-function relationships play an important role in physiological processes. However, the very intricate ultrastructural arrangement of the MR cells from FW fish has not been considered at length.

*Molecular identity of the apical  $\text{Cl}^-/\text{HCO}_3^-$  exchanger*

The tight 1:1 linkage between  $\text{Cl}^-$  uptake and  $\text{HCO}_3^-$  secretion is most likely indicative of the involvement of an apical AE. The strong inhibition of chloride uptake by the disulfonic stilbene derivatives SITS (Perry and Randall, 1981) and DIDS (Chang and Hwang, 2004) further supports this hypothesis. Prior to 1999, the only known family of  $\text{Cl}^-/\text{HCO}_3^-$  exchangers in vertebrates were those homologous to the red blood cell anion exchanger AE1 originally cloned by Kopito and Lodish (1985). The AE family of proteins has three members, AE1-3, and are now part of the solute carrier 4 (SLC4) designation. Repeated and significant attempts to identify SLC4 (AE family) anion exchangers in the apical membrane of the fish gill MR cells using a variety of methods have failed so far (Greg Goss, personal observation).

A few papers demonstrated apparent apical AE1 immunoreactivity in the gills of tilapia and Coho salmon (Wilson *et al.*, 2000; 2002b). However, the antibody that was used was generated using trout red blood cells proteins extracted from a region of the SDS gel around 100 Kda (Cameron *et al.*, 1996). As a consequence, a cocktail of proteins could have been present in the region against which many different antibodies could have been raised. Since contaminating antibodies would not be eliminated with the affinity protocol used (Cameron *et al.*, 1996), the supposedly anti-AE1 antibody likely has significant non-specific cross-reactivity and any result obtained using it must be interpreted with caution.

The discovery of a new family of anion exchangers, SLC26, has opened new avenues for investigation of the molecular identity of the gill

anion exchanger in FW fish. This family was discovered when several proteins suspected of causing genetic diseases were cloned and showed great similarity in amino acid sequence. The original members (SAT1, DTDST, DRA) were first identified as sulfate transporters (Bissig *et al.*, 1994; Hästbacka *et al.*, 1994; Silberg *et al.*, 1995). Soon after, it was published that both Pendrin (SLC26a4) and the congenital chloride diarrhea anion exchanger DRA (SLC26a3) could also transport  $\text{Cl}^-$  (Moseley *et al.*, 1999; Scott *et al.*, 1999). It was then that it was realized that this new family of anion exchangers could fulfill the role of  $\text{Cl}^-/\text{HCO}_3^-$  exchange in a variety of tissues. Through database mining of the human genome, subsequent members of this family were quickly discovered, bringing the current total up to eleven paralogues, termed SLC26a1-11 (Lohi *et al.*, 2000; 2002; Vincourt *et al.*, 2003). Currently, within the members of this family, it has been demonstrated that different paralogues may transport a range of anions, including  $\text{SO}_4^{2-}$ ,  $\text{OH}^-$ ,  $\text{HCO}_3^-$ ,  $\text{NO}_3^-$ ,  $\text{Cl}^-$ ,  $\text{I}^-$ ,  $\text{Br}^-$ , formate, hexose, oxalate and multiple organic ions. They are occasionally electrogenic, and anion specificity varies between members, between isoforms, and between orthologs (Silberg *et al.*, 1995; Mosley *et al.*, 1999; Scott *et al.*, 1999; Lohi *et al.*, 2000; 2002; Xie *et al.*, 2002; Chambard and Ashmore 2003; Vincourt *et al.*, 2003; Chernova *et al.*, 2005). The SLC26s contain three major conserved areas, one of which is the STAS domain at the carboxy-terminal of the protein (Mount and Romero, 2004). The STAS domain is an ancient conserved domain common to most sulfate transporters including those from bacteria (Aravind and Koonin, 2000). Many

SLC26 family members also contain a PDZ domain within the STAS domain that allows specific binding to other proteins (Lohi *et al.*, 2003, Ko *et al.*, 2004). Importantly for my model, CA II is known to bind to the STAS domain in some SLC26 family members (Vince *et al.*, 2000; Sterling and Casey, 2002).

In the fish gill, the SLC26 family has several potential candidates for fulfilling the role of the apical anion exchanger in MR cells. Currently the most favored candidate is a Pendrin homologue (SLC26a4) based on the study by Piermarini *et al.* (2002). These authors used a heterologous SLC26a4 antibody on the gills of a euryhaline elasmobranch, revealing apical staining only in cells rich in basolateral V-H<sup>+</sup>-ATPase. Immunoreactivity of this antibody was stronger in FW stingrays when compared to the SW-acclimated or marine stingrays. In mammals, SLC26a4 has been localized to the apical membrane of the PNA<sup>+</sup> MR B-type intercalated cells (IC) within the cortical collecting duct of the kidney (Royaux *et al.*, 2001). In addition, the expression of SLC26a4 is regulated based on acid-base balance and chloride balance in the body (Wagner *et al.*, 2002; Quentin *et al.*, 2004). Regardless of the exact molecular identity of the anion exchanger in the fish gill, its functional properties should allow for electroneutral exchange of Cl<sup>-</sup> and HCO<sub>3</sub><sup>-</sup>.

#### *Carbonic anhydrase (CA) in trout gill cells*

The importance of CA for acid/base and ion regulation in freshwater fish gills has been long established (see Introduction). CA catalyzes the hydration of CO<sub>2</sub> into H<sup>+</sup> and HCO<sub>3</sub><sup>-</sup> (Maren, 1967), which act as the

counterions for  $\text{Na}^+$  and  $\text{Cl}^-$  uptake, respectively (reviewed in Perry and Laurent, 1990). In agreement with both ion-transporting processes, CA is localized in MR cells both at the lamellae and in the interlamellar space of the gill epithelium (Rahim *et al.*, 1988; Georgalis *et al.*, 2006). CA is also found in pavement and mucus cells, which was interpreted as evidence for an additional CA involvement in gas exchange (Rahim *et al.*, 1988).

In the MR cells, CA is more concentrated in the apical region, as demonstrated by immunogold TEM immunohistochemistry (Rahim *et al.*, 1988). CA signal is found both in the apical membrane and in the subapical space, where numerous vesicles and also the (basolateral) tubular system are located (Rahim *et al.*, 1988). This suggests that  $[\text{HCO}_3^-]$  and  $[\text{H}^+]$  should be substantially higher in that region of the cell.

It was not until very recently that a cytoplasmic CA isoenzyme present in rainbow trout gills (TCAc) was successfully cloned (Esbaugh *et al.*, 2005). Compared to mammalian CAs sequences, TCAc most closely resembles human CAII. However, the amino acid identity is a relatively low 62% (Esbaugh *et al.*, 2005), implicating that some of the mammalian CA II characteristics might not apply to TCAc. From preliminary analyses of the amino acid sequence it is not clear whether or not TCAc is able to have physical interactions with other proteins in an analogue manner to mammalian CA II and SLCs 4 and 26 (Esbaugh *et al.*, 2005). In addition, other yet unidentified CA isoforms might also be present in the fish gill.



In order to explore a putative physical interaction between CA and anion exchanger in fish gills, it is imperative to identify the anion exchanger(s) involved in apical  $\text{Cl}^-/\text{HCO}_3^-$  exchange in fish gills. Nonetheless, there is a distinct subcellular CA localization in the MR cells described by Rahim *et al.* (1988) that fits with our model and provides a mechanism for the interaction of the enzyme and its catalyzed products with ion-transporting proteins in both the apical and basolateral membranes.

*Basolateral V-H<sup>+</sup>-ATPases moving H<sup>+</sup> from the MR cells into the blood*

The large amount of  $\text{HCO}_3^-$  produced by CA for apical  $\text{Cl}^-/\text{HCO}_3^-$  exchange is accompanied by an equally large production of  $\text{H}^+$  which must be rapidly neutralized in order to avoid a reduction in the rate or even a reversal of the CA catalyzed reaction. In my model, I propose that the  $\text{H}^+$  are exported into the tubular system by V-H<sup>+</sup>-ATPases located at the basolateral membrane.

In trout, V-H<sup>+</sup>-ATPase has been localized to the pavement cells (Sullivan *et al.*, 1995), or to both the pavement and the MR cells (Lin *et al.*, 1994; Wilson *et al.*, 2000). This discrepancy is likely explainable by the abovementioned existence of two subpopulations of MR cells, the PNA<sup>-</sup> MR cells being similar in morphology to the PV cells, but with more mitochondria (Goss *et al.*, 2001). Immunogold staining revealed that V-H<sup>+</sup>-ATPase is mainly located on the apical membrane and the subapical region of the cells, although there was also labeling towards the basolateral side of the MR cells (Wilson *et al.*, 2000). The cytoplasmic staining has often been interpreted as

V-H<sup>+</sup>-ATPase-containing vesicles that are recycled into the apical membrane for acid secretion (Lin *et al.*, 1994; Sullivan *et al.*, 1995). However, recent results have prompted me to suggest that the staining pattern might also be related to a subpopulation of cells with basolateral V-H<sup>+</sup>-ATPase that could then function to perform net base secretion. In my experiments, light microscopy micrographs did show cells located high in the lamella with distinct apical/sub-apical labeling (consistent with a role in H<sup>+</sup> secretion and Na<sup>+</sup> uptake) as has been previously published. However, there are also cells located at the base of the lamellae and in the primary filament with cytoplasmic staining (Fig. 8.5A, B). Moreover, these cells are often completely lacking staining in the apical pole, which argues against apical vesicle recycling. In addition, immunolocalization of Na<sup>+</sup>/K<sup>+</sup>-ATPase and staining of the cell membrane using the Champy-Maillet technique (Garcia-Romeu and Masoni, 1970) show a staining pattern that is similar to filamental V-H<sup>+</sup>-ATPase positive cells (Fig. 8.5C, D). It is well documented that Na<sup>+</sup>/K<sup>+</sup>-ATPase is closely associated to the MRC tubular system in all species of fish studied so far (Karnaky *et al.*, 1976; Hootman and Philpott, 1979; reviewed in De Renzis and Bornancin, 1984; McCormick, 1995), which is continuous with the basolateral membrane (see previous sections).

To substantiate my immunocytochemistry LM observations, I performed immunogold TEM using the V-H<sup>+</sup>-ATPase antibody developed by Katoh *et al.* (2003) and focused my attention on the association between V-H<sup>+</sup>-ATPase and the tubular system in MR cells found only in the interlamellar

regions. The immunogold TEM pictures are shown in figure 8.6. Most of the MR cells located at the base of the lamella label for V-H<sup>+</sup>-ATPase in the cytoplasm and not in the apical membrane. When these cells are analyzed at higher magnification, it can be seen that the signal is found in darker (membrane?) elements in the proximity of mitochondria, which is consistent with being associated with the tubular system. Unfortunately, the immuno TEM technique requires the use of a soft fixation protocol in order to preserve the epitopes that are recognized by the antibodies, and it does not allow for optimum preservation of cellular membranous structures such as the tubular system. Nevertheless, the combined results from LM and TEM suggest that V-H<sup>+</sup>-ATPase is present in the tubular system of some MR cells, preferentially those located at the base of the gill filaments and in the interlamellar spaces.

Alternatively, it has been suggested that an apical V-H<sup>+</sup>-ATPase could act to produce a local acidification in the apical region of the MR cell, thus lowering HCO<sub>3</sub><sup>-</sup> activity and facilitating Cl<sup>-</sup>/HCO<sub>3</sub><sup>-</sup> exchange (Marshall, 2002). Such a mechanism would be similar to the frog skin (Larsen, 1991; Ehrenfeld and Klein, 1997), and also to gills of euryhaline crustaceans (Onken and Putzenlechner, 1991; Genovese *et al.*, 2005). However, this mechanism is not viable for the gill fish because by secreting both H<sup>+</sup> and HCO<sub>3</sub><sup>-</sup> to the external medium Cl<sup>-</sup> uptake becomes uncoupled from *net* HCO<sub>3</sub><sup>-</sup> secretion and from acid-base regulation because an acidic and a basic equivalent are being transported in the same direction simultaneously. This is directly

opposite of the direct 1:1 linkage between  $\text{Cl}^-$  uptake and  $\text{HCO}_3^-$  excretion that has been experimentally demonstrated numerous times.

From a physiological point of view, a basolateral  $\text{V-H}^+$ -ATPase would have two major advantages over other transporters (i.e. NHE). Firstly,  $\text{V-H}^+$ -ATPase would be able to pump  $\text{H}^+$  out of the MR cell despite the very low pH that is expected to be created inside the tubular system. Secondly, the inside negative membrane potential created by the  $\text{V-H}^+$ -ATPase could drive  $\text{Cl}^-$  across the basolateral membrane, (cf. Wagner *et al.*, 2004). The rapid clearing of  $\text{H}^+$  and  $\text{Cl}^-$  from the cell cytoplasm into the blood space is essential to prevent  $\text{Cl}^-/\text{HCO}_3^-$  exchange from slowing down or even be reversed.

Even in seawater, it is apparent that  $\text{V-H}^+$ -ATPases are important in regulation of base secretion. In the gills of elasmobranch an apical anion exchanger and basolateral  $\text{V-H}^+$ -ATPases mediate  $\text{HCO}_3^-$  secretion for acid base regulation (Piermarini *et al.*, 2002; Tresguerres *et al.*, 2005, 2006; chapters II and III). Another similar  $\text{HCO}_3^-$ -secreting system is the extensively studied B-type intercalated cells (IC) from the mammalian kidney (Brown and Breton, 2000; Wagner *et al.*, 2003) where apical SLC26a4 (Pendrin) and basolateral  $\text{V-H}^+$ -ATPase mediate base secretion. Clearly, the involvement of a basolateral  $\text{V-H}^+$ -ATPase in  $\text{Cl}^-/\text{HCO}_3^-$  exchange in the gills of FW teleosts follows established models and would act as an energizing step to allow for  $\text{Cl}^-$  uptake against an apparent concentration gradient.

To support my contention that basolateral  $\text{V-H}^+$ -ATPase is an important and required component of the  $\text{Cl}^-$  uptake metabolon, I have closely

examined the literature where re-interpretation of the results in light of this new hypothesis may explain results that were difficult to interpret originally. For example, bafilomycin -a specific V-H<sup>+</sup>-ATPase inhibitor- has been shown to inhibit both Na<sup>+</sup> and Cl<sup>-</sup> uptake in FW tilapia (Fenwick *et al.*, 1999), a result similarly noted recently in zebrafish by Boisen *et al.* (2003). The effect on Na<sup>+</sup> uptake was explained by the involvement of apical V-H<sup>+</sup>-ATPases. On the other hand, the effect on Cl<sup>-</sup> was not as clear at the time and a convoluted argument was proposed whereby inhibition of V-H<sup>+</sup>-ATPase would produce a decrease in blood pH, which in turn would result in a compensatory decrease in HCO<sub>3</sub><sup>-</sup> secretion, and therefore also in Cl<sup>-</sup> uptake. However, under my model, bafilomycin would act to directly inhibit Cl<sup>-</sup> uptake by inhibiting the function of the metabolon.

Recently, Chang and Hwang (2004) demonstrated that V-H<sup>+</sup>-ATPase is directly involved in Cl<sup>-</sup> uptake in FW tilapia, since acclimation to an artificial medium with a reduced [Cl<sup>-</sup>]<sub>FW</sub> of 0.002 mmol l<sup>-1</sup> induced a 140% increase in V-H<sup>+</sup>-ATPase abundance. Furthermore, [Na<sup>+</sup>]<sub>FW</sub> was kept at a relative high concentration of 10 mmol l<sup>-1</sup>, so the increase in V-H<sup>+</sup>-ATPase was not related to upregulation of Na<sup>+</sup> uptake. Acclimation to the medium with reduced [Cl<sup>-</sup>] produced a similar increase in CA abundance. In their study, addition of NEM, acetazolamide or DIDS (inhibitors of V-H<sup>+</sup>-ATPase, CA and Cl<sup>-</sup>/HCO<sub>3</sub><sup>-</sup> exchanger, respectively) to the bath produced reductions in Cl<sup>-</sup> influx of 52-82 %, with NEM having the greatest effect. However, apical ouabain treatment also produced a significant inhibition in Na<sup>+</sup>/K<sup>+</sup>-ATPase activity and a

reduction in  $\text{Cl}^-$  uptake, likely through a run-down of the membrane potential in MR cells. However, we know that  $\text{Na}^+/\text{K}^+$  ATPase is not expressed on the apical surface of the MR cell. This finding itself illustrates that caution should be exercised in interpretation of apical and basolateral localization of specific proteins based on site of drug application. This is because many drugs (e.g. NEM and bafilomycin) can penetrate effectively and affect ion-transporting proteins located on the basolateral membrane even if they are applied from the apical side of the epithelium or *vice-versa*. For example, Genovese *et al.* (2005) showed that bafilomycin can inhibit the apical  $\text{V-H}^+$ -ATPase in crab gills even when it is dissolved in the solution bathing the basolateral side. Chang and Hwang (2004) did interpret their results with caution and proposed the involvement of either apical or basolateral  $\text{V-H}^+$ -ATPases as energizers for  $\text{Cl}^-$  uptake.

### *Perspectives*

Elucidating the mechanism for  $\text{Cl}^-$  uptake/ $\text{HCO}_3^-$  secretion and ion-transporting processes in general across gills of FW fish requires a multi-disciplinary approach as many of the specifics of this model remain to be defined. For example, molecular identification and functional characterization of the apical AE, followed by studies about potential domains involved in the interaction with other proteins, CA in particular are required. Following this, co-localization studies of AE, CA and  $\text{V-H}^+$ -ATPase are absolutely required. This may be done with traditional immunocytochemical staining techniques. However, I feel that better resolution is needed in order to find the exact

cellular localization and degree of interaction between the proteins. The use of semiconducting nanocrystals (quantum dots) is a relatively new imaging tool (Lidke and Arndt-Jovin, 2004) that holds promise in this regard.

A prediction from my model is that the tubular system would be the recipient of large amounts of protons and that these protons must return to the blood via the tubular system. Therefore, this predicts a pH gradient within the MR cell tubular system. Unfortunately, the current technology for pH imaging does not give enough spatial or temporal resolution to examine individual tubules in the tubular system, which are ~70 nM in diameter and highly branched so this hypothesis awaits future technological innovation.

Finally, I would like to stress the importance of exploring new hypothesis and models as a basis for scientific inquiry. For example, the involvement of apical  $\text{Na}^+/\text{NH}_4^+$  or  $\text{Na}^+/\text{H}^+$  exchange for  $\text{Na}^+$  uptake (Krogh, 1939; Kerstetter *et al.*, 1970) was considered dogma for almost 40 years. However, many investigators in the mid-1980s began to question the feasibility of the model and this has resulted in significant impetus for research in the past two decades. It is clear now that, at least for some species of fish, the mechanism for  $\text{Na}^+$  uptake and  $\text{H}^+$  secretion includes apical  $\text{V-H}^+$ -ATPases and some type of  $\text{Na}^+$  channel, as yet unidentified. Here, I propose that basolateral  $\text{V-H}^+$ -ATPases are also involved in  $\text{Cl}^-$  uptake as part of a complex of enzymes –a metabolon- that also includes apical Aes physically linked to CA. The body of evidence supporting this hypothesis is strong, and includes both theoretical ( $\text{Cl}^-$  and  $\text{HCO}_3^-$  concentrations in the cell

and in FW), empirical (effects of ion-transporting protein inhibitors, upregulation of expression of ion-transporting proteins in low  $[Cl]_o$ , LM and TEM immunohistochemistry), and comparative/evolutionary evidence (cellular co-localization of apical SLC26A4 and basolateral V-H<sup>+</sup>-ATPase in elasmobranch gills, B-type Ics in the mammalian kidney). I recognize that a large part of the model depends on speculative evidence (interaction domains between proteins, local ion concentrations, etc.) However, with the development of new technologies, the relationships between the structure of the tubular system of the MR cell and metabolon-type interactions will form a significant advancement in our understanding of fundamental properties of ion transport.



## Materials and Methods

All images shown are from freshwater rainbow trout kept at the aquatic facilities of the Department of Biological Sciences, University of Alberta, Edmonton, AB, Canada. The water chemistry in these facilities is shown in table 8.1. Figure 8.3 is a fluorescence image of a live gill filament. Reagents and incubation times were as described in Goss *et al.* (2001). I used a water immersion microscope equipped with a camera (Richardson's Technologies Inc., Calgary, AB, Canada). Figure 8.4A is a representative transmission electron micrograph of a gill mitochondria-rich cell. Samples were processed as described in Katoh *et al.*, (2003). The micrographs of immunolabeled sections shown in figures 8.5A-C were obtained as described in the previous chapters. Details about the Champy-Maillet technique (Fig. 8.5D), which stains lipids, can be found in Garcia-Romeu and Masoni (1970) and Wilson *et al.* (2002a). Finally, the immunogold technique (Fig. 8.6) was performed as described in Katoh *et al.* (2003).

**Table 8.1.** Theoretical requirements for electroneutral  $\text{Cl}^-/\text{HCO}_3^-$  exchange in typical freshwater systems.

	$[\text{Cl}^-]_{\text{FW}}$	$[\text{HCO}_3^-]_{\text{FW}}^1$	$[\text{HCO}_3^-]_{\text{i needed}}$ to drive apical AE <sup>2</sup>	$[\text{Cl}^-]_{\text{i needed}}^3$
Vancouver <sup>4</sup>	0.01 mmol l <sup>-1</sup>	0.10 mmol l <sup>-1</sup>	> 400 mmol l <sup>-1</sup>	<0.20 mmol l <sup>-1</sup>
Edmonton <sup>5</sup>	0.50 mmol l <sup>-1</sup>	1.60 mmol l <sup>-1</sup>	> 128 mmol l <sup>-1</sup>	<0.63 mmol l <sup>-1</sup>
Hamilton <sup>6</sup>	0.80 mmol l <sup>-1</sup>	2.10 mmol l <sup>-1</sup>	> 105 mmol l <sup>-1</sup>	<0.76 mmol l <sup>-1</sup>
Ottawa <sup>7</sup>	0.15 mmol l <sup>-1</sup>	0.45 mmol l <sup>-1</sup>	> 120 mmol l <sup>-1</sup>	<0.15 mmol l <sup>-1</sup>

<sup>1</sup> Assuming that most of the total carbonate is in the form of  $\text{HCO}_3^-$ .

<sup>2</sup> Assuming  $[\text{Cl}^-]_{\text{i}}$  of 40 mmol l<sup>-1</sup>

<sup>3</sup> Assuming  $[\text{HCO}_3^-]_{\text{i}}$  of 2 mmol l<sup>-1</sup>

<sup>4</sup> Wilson et al. (2000)

<sup>5</sup> Hawkings et al. (2004), personal observation

<sup>6</sup> Goss and Wood (1991)

<sup>7</sup> Greco et al. (1995)

**Table 8.2.** Theoretical occupancy for arbitrary volumes inside the mitochondria-rich cells.

	Height	Radius	Volume	T.O.
	(nm)	(nm)	(liters)	(%)
1) Size of the Anion exchanger <sup>1</sup>	10	10	$3.14 \times 10^{-21}$	380.0
2) Bulk Solution	6.5	6.5	$8.63 \times 10^{-22}$	100
3) Binding pocket	2.0	2.0	$2.51 \times 10^{-23}$	3.0
4) AE HCO <sub>3</sub> <sup>-</sup> transporting site	1.0	1.0	$3.14 \times 10^{-24}$	0.4

<sup>1</sup>From Wang *et al.*, 1994.

Based on the assumption of a [HCO<sub>3</sub><sup>-</sup>]<sub>i</sub> of 2 mmol l<sup>-1</sup> distributed homogeneously throughout the cell. Theoretical occupancy (T.O) represents the chance for the given volumes to contain at least one HCO<sub>3</sub><sup>-</sup> molecule. A T.O. of 100 % indicates that at least one HCO<sub>3</sub><sup>-</sup> molecule will be present in that given volume at any given time. Under these conditions, the chance for any single HCO<sub>3</sub><sup>-</sup> molecule to be in the proximity of the HCO<sub>3</sub><sup>-</sup> transporting site of the apical anion exchanger (AE) is extremely low.

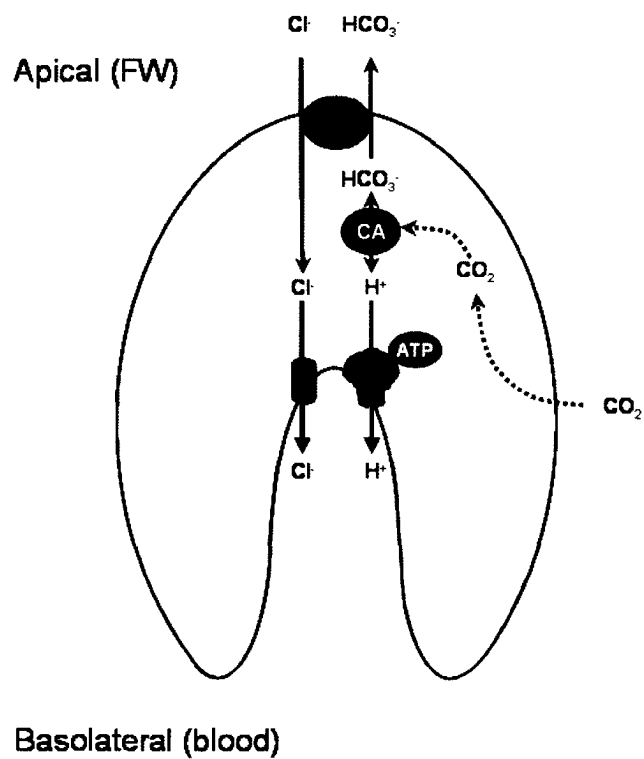


**Figure 8.1.** Schematic diagram of the freshwater  $\text{Cl}^-$  uptake metabolon model in mitochondria-rich cells. AE = anion exchanger; CA = carbonic anhydrase; blue icon =  $\text{V-H}^+$ -ATPase, black icon = chloride channel.

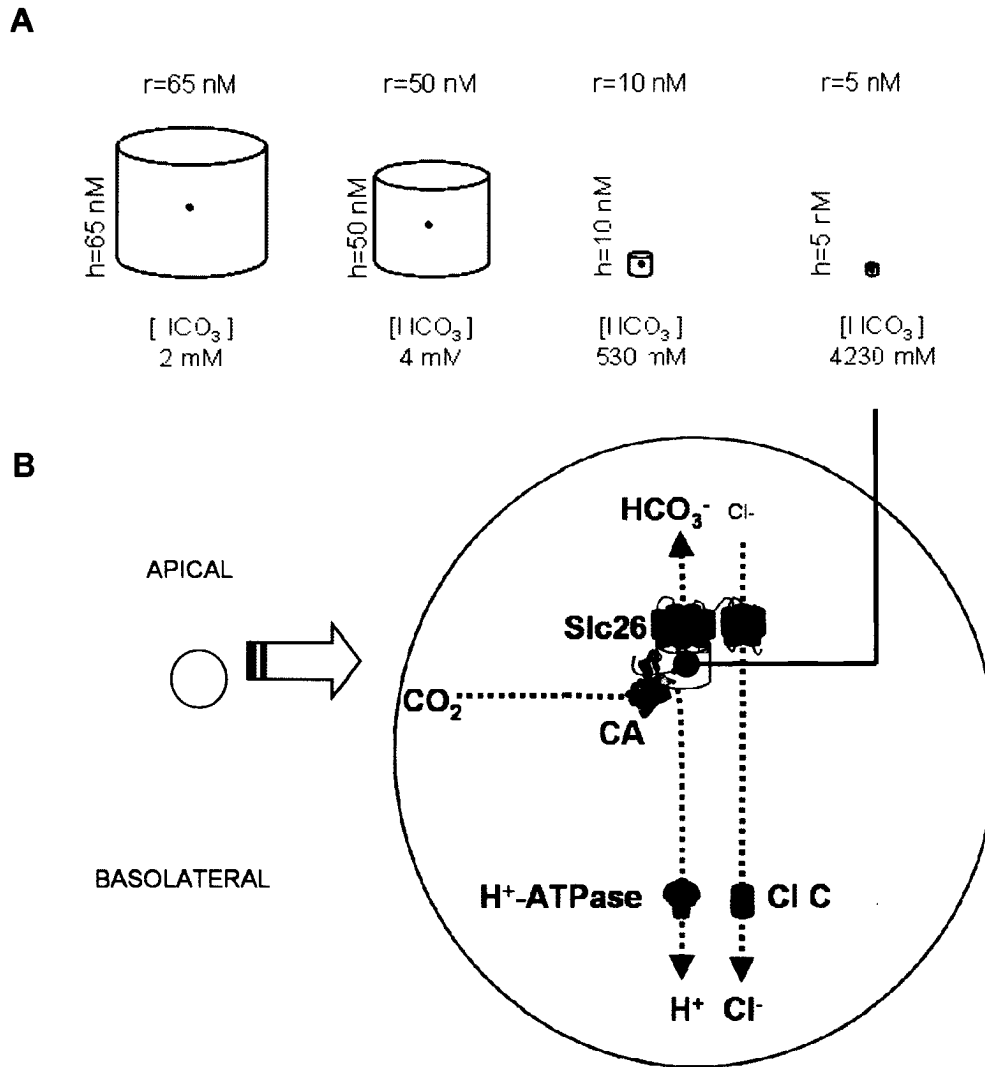


**Figure 8.2.** The freshwater chloride uptake metabolon. **A:**  $\text{HCO}_3^-$  concentrations resulting from placing a single  $\text{HCO}_3^-$  molecule in hypothetical cylinders with different volumes ranging from the equivalent of the bulk solution of a mitochondria-rich (MR) cell to the  $\text{HCO}_3^-$  binding site of the anion exchanger 1 (see text for details). **B:** Region of an MR cell containing the apical membrane and a portion of the tubular system (TS). The elevated  $[\text{HCO}_3^-]$  resulting in this area from CA activity is enough to drive chloride uptake from the much diluted FW.  $\text{H}^+$  exit the cell to the blood through a basolateral V- $\text{H}^+$ -ATPase located in the TS. CA = carbonic anhydrase; Cl C: chloride channel.

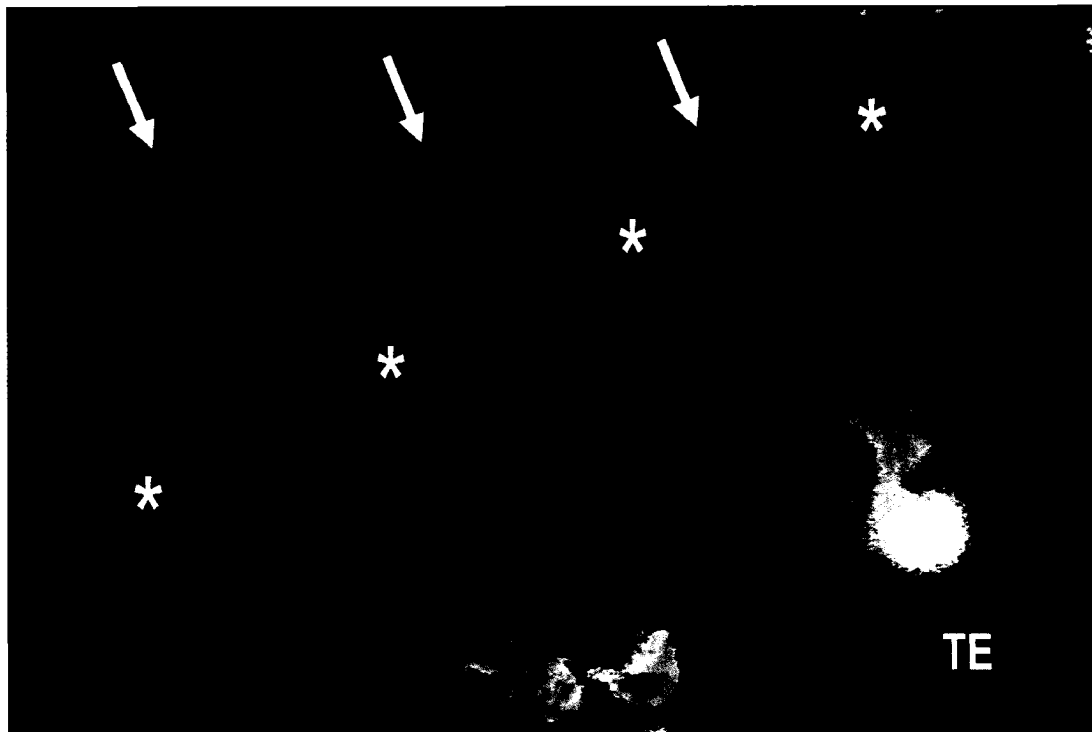


**Figure 8.3.** Overlay image of the trailing edge of a gill filament from a rainbow trout acclimated to freshwater showing the localization of PNA<sup>+</sup> cells. Green: gill auto fluorescence. Red: TRITC-conjugated Peanut lectin agglutinin, labeling the apical surface of PNA<sup>+</sup> mitochondria-rich (MR) cells. The asterisks mark the position of lamella, arrows point at the inter-lamellar spaces (ILS); TE = trailing edge of the filament. Note that the PNA<sup>+</sup> MR cells are either in ILS or at the base of the lamella. Scale bar = 10  $\mu$ m.

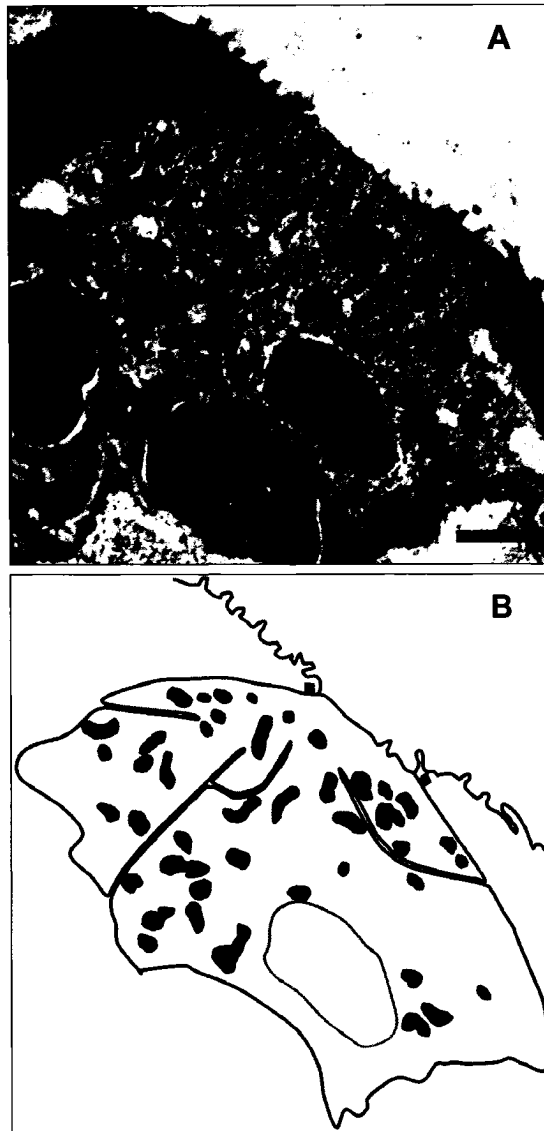


**Figure 8.4.** The tubular system of mitochondria-rich (MR) cells. A) TEM picture of a MR cell. B) Schematic representation of the same MR cell depicting the structure of a few branches of the tubular system (TS), which cannot be identified at the magnification shown in (A). The cell nucleus and mitochondria are depicted in light and dark grey, respectively. Notice how the TS penetrates deep into the cell cytoplasm. Adapted from Sardet et al. (1979). Scale bar: 1  $\mu\text{m}$ .

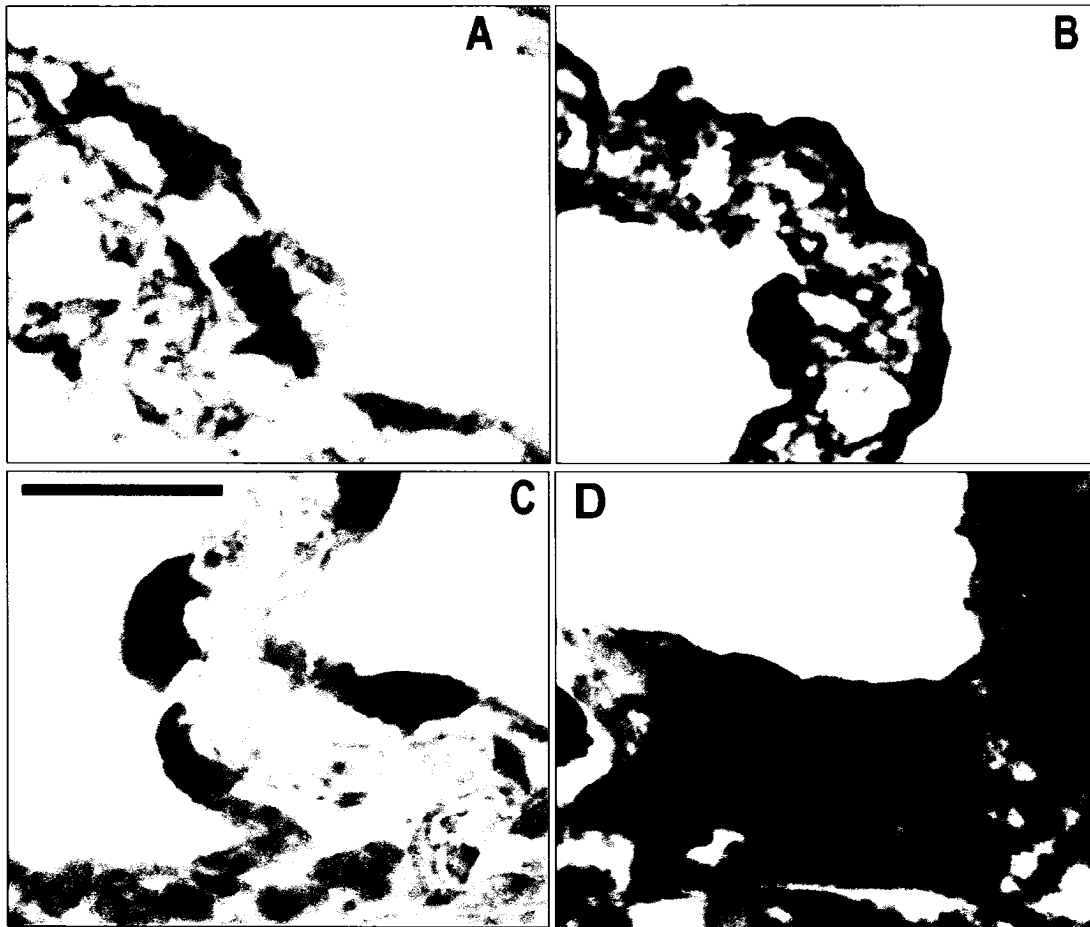


**Figure 8.5.** V-H<sup>+</sup>-ATPase and Na<sup>+</sup>/K<sup>+</sup>-ATPase immunoreactivity in the gills of freshwater trout. *A*: Cells near the base of lamellae showing V-H<sup>+</sup>-ATPase staining, with no signal in apical region. *B*: cells on gill lamellae showing apical V-H<sup>+</sup>-ATPase staining. *C*: Na<sup>+</sup>/K<sup>+</sup>-ATPase staining. Notice how it appears to be cytoplasmic, although it is known to be located in the basolateral tubular system (TS). *D*: Champy-Maillet technique, which stains cellular membranes black. Completely dark cells are indicative of the TS occupying most of the cytoplasm. Notice the similarity to *A* and *C*.



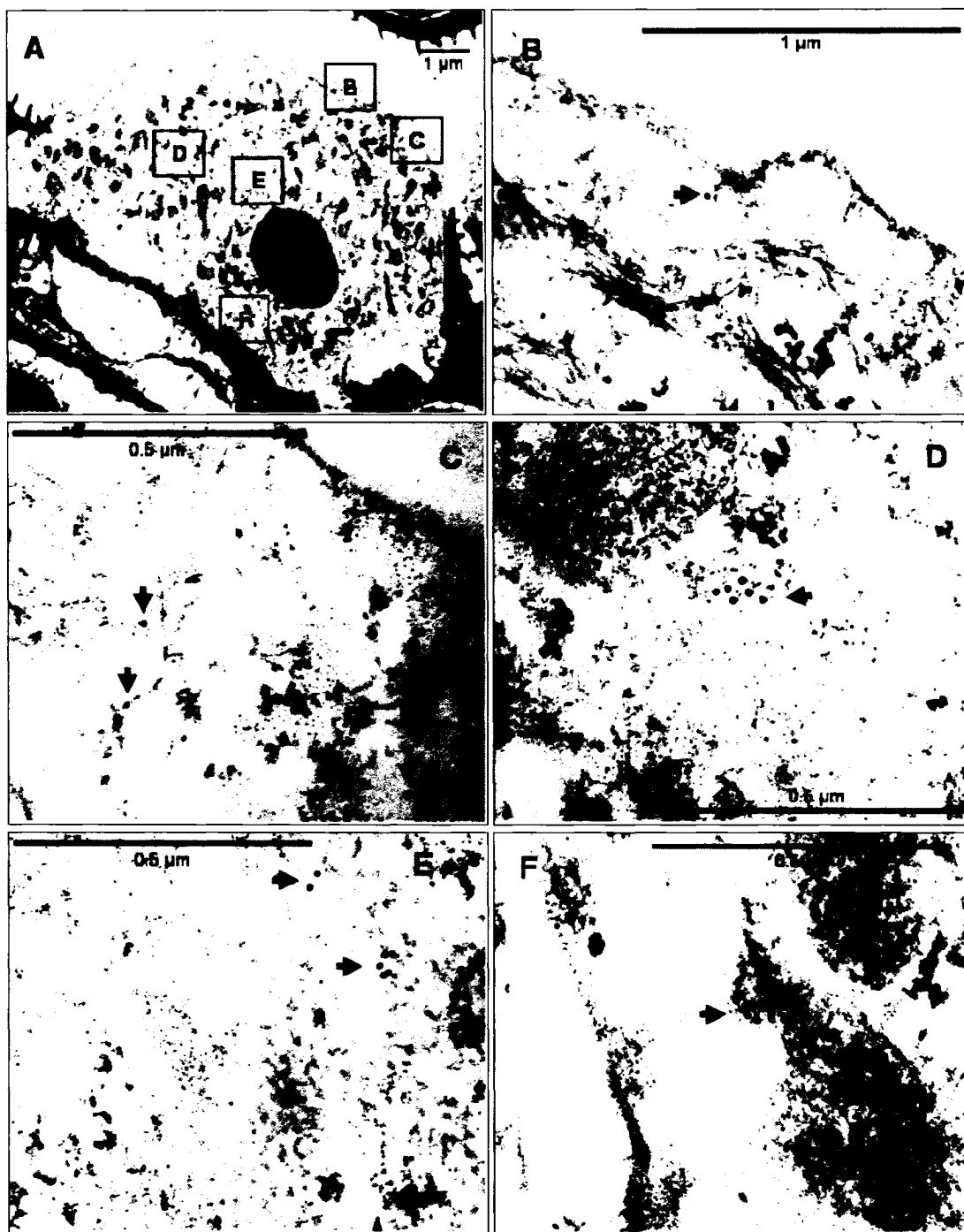


**Figure 8.6.**

**Figure 8.6.** Transmission electron microscopy (TEM) immuno-gold against V-H<sup>+</sup>-ATPase. The immunoreactive 10 nm gold particles are indicated by arrows. *A*: Mitochondria-rich cell located at the base of a gill lamellae. The marked regions are shown in greater detail in the rest of the pictures. *B*: The apical membrane is devoid of signal. *C*: There is some labeling in the sub-apical region (see also *B*), probably in elements of the cytoskeleton and the tubular system (TS). *D, E, F*: examples of V-H<sup>+</sup>-ATPase labeling in elements located in the cytoplasm. Notice how the immuno-gold particles are found in darker elements of the cytoplasm, probably the TS.

## References

**Aravind, L. and Koonin, E.V.** (2000) The STAS domain - a link between anion transporters and antisigma-factor antagonists. *Curr. Biol.* 10, R53-55.

**Avella, M. and Bornancin, M.** (1989). A new analysis of ammonia and sodium transport through the gills of the freshwater rainbow trout (*Salmo gairdneri*). *J. Exp. Biol.* 142, 155-175.

**Bissig, M., Hagenbuch, B., Stieger, B., Koller, T., and Meier P.J.** (1994). Functional expression cloning of the canalicular sulphate transport system of rat hepatocytes. *J. Biol. Chem.* 269, 3017-21.

**Boisen, A. M. Z., Amstrup, J., Novak, I., and Grosell, M.** (2003). Sodium and chloride transport in soft water and hard water acclimated zebrafish (*Danio rerio*). *Biochim. Biophys. Acta* 1618, 207-218.

**Brown, D. and Breton., S.** (2000). Structure, function and cellular distribution of the vacuolar H<sup>+</sup>-ATPase (H<sup>+</sup>V-ATPase/ proton pump). In: *The Kidney: Physiology and Pathophysiology* (3<sup>rd</sup> ed.), (e.d. D.W. Seldin and G. Giebisch). Pp. 171–191. Philadelphia, PA, USA: Lippincott Williams & Wilkins.

**Cameron, B.A., Perry II, S.F., Wu, C., Ko, K. and Tufts, B.L.** (1996). Bicarbonate permeability and immunological evidence for an anion exchanger-like protein in the red blood cells of the sea lamprey, *Petromyzon marinus*. *J. Comp. Physiol. B* 166, 197-204.

**Chambard, J.M. and Ashmore, J.F.** (2003). Sugar transport by mammalian members of the SLC26 superfamily of anion-bicarbonate exchangers. *J. Physiol.* 550, 667-677.

**Chang, I.-C. and Huang, P.P.** (2004). Cl<sup>-</sup> uptake mechanism in freshwater-adapted tilapia (*Oreochromis mossambicus*). *Physiol. Biochem. Zool.* 77, 406-414.

**Chernova, M.N., Jiang, L., Friedman, D.J., Darman, R.B., Lohi, H., Kere, J., Vadorpe, D.H. and Alper, S.L.** (2005). Functional comparison of mouse slc26a6 anion exchanger with human SLC26A6 polypeptide variants: Differences in anion selectivity, regulation, and electrogenicity. *J. Biol. Chem.* 280, 8564-8580.

**Copeland, D.E.** (1948). The cytological basis of chloride transfer in the gills of *Fundulus heteroclitus*. *J. Morphol.* 82, 201-228.

**De Renzis, G. and Bornancin, M.** (1984). Ion transport and gill ATPases. In: *Fish Physiology*, vol. 10A. (ed. H. S. Hoar and D. W. Randall). Pp. 65-104. New York, NY, USA: Academic Press.

**Doyle, W.L. and Gorecki, D.** (1961). The so-called chloride cell of the fish gill. *Physiol. Zool.* 34, 81-85.

**Eddy, F.B. and Chang, Y.-J.** (1993). Effects of salinity in relation to migration and development in fish. In: *The Vertebrate Gas Transport Cascade* (ed. J. E. P. W. Bicudo), pp. 35-42. Boca Raton, FL, USA : CRC Press.

**Ehrenfeld, J. and Klein, U.** (1997). The key role of the H<sup>+</sup> V-ATPase in acid-base balance and Na<sup>+</sup> transport processes in frog skin. *J. Exp. Biol.* 200, 247-256.

**Esabaugh, A.J., Perry, S.F., Bayaa, M., Georgalis, T., Nickerson, J., Tufts, B.L. and Gilmour, K.M.** (2005). Cytoplasmic carbonic anhydrase isoenzymes in rainbow trout *Oncorhynchus mykiss*: comparative physiology and molecular evolution. *J. Exp. Biol.* 208, 1951-1961.

**Evans, D.H., Piermarini, P.M. and Choe, K.P.** (2005). The Multifunctional Fish Gill: Dominant Site of Gas Exchange, Osmoregulation, Acid-Base Regulation, and Excretion of Nitrogenous Waste. *Physiol. Rev.* 85, 97-177.

**Fenwick, J., Wendelaar Bonga, S. and Flik, G.** (1999). In vivo bafilomycin-sensitive Na<sup>+</sup> uptake in young freshwater fish. *J. Exp. Biol.* 202, 3659-3666.

**Galvez, F., Reid, S. D., Hawkings, G. and Goss, G.G.** (2002). Isolation and characterization of mitochondria-rich cell types from the gill of freshwater rainbow trout. *Am. J. Physiol. Reg. Int. Comp. Physiol.* 282, R658-668.

**Garcia-Romeu, F. and Masoni, A.** (1970). Sur la mise en évidence des cellules a chlorure de la branchie des poissons. *Arch. Anat. Microscop. Morphol. Exptl.* 59, 289-294.

**Genovese, G., Ortiz, N., Urcola, M.R. and Luquet, C.M.** (2005). Possible role of carbonic anhydrase, V-H<sup>+</sup>-ATPase, and Cl<sup>-</sup>/HCO<sub>3</sub><sup>-</sup> exchanger in electrogenic ion transport across the gills of the euryhaline crab *Chasmagnathus granulatus*. *Comp. Biochem. Physiol. A* 142, 362-369.

**Georgalis, T., Perry, S.F. and Gilmour, K.M.** (2006). The role of branchial carbonic anhydrase in acid-base regulation in rainbow trout (*Oncorhynchus mykiss*). *J. Exp. Biol.* 209, 518-530.

**Goss, G.G., Adamia, S. and Galvez, F.** (2001). Peanut lectin binds to a subpopulation of mitochondria-rich cells in the rainbow trout gill epithelium. *Am. J. Physiol. Reg. Int. Comp. Physiol.* 281, R1718-1725.

**Goss, G.G., Laurent, P. and Perry, S.F.** (1992). Gill morphology and acid-base regulation during hypercapnic acidosis in brown bullhead *Ictalurus nebulosus*. *Cell Tissue Res.* 268, 539-552.

**Goss G.G. and Perry, S.F.** (1993). Physiological and morphological regulation of acid-base status during hypercapnia in rainbow trout (*Oncorhynchus mykiss*). *Can. J. Zool.* 71, 1673-1680.

**Goss, G.G., Perry, S.F., Fryer, J.N. and Laurent, P.** (1998). Gill morphology and acid-base regulation in freshwater fishes. *Comp. Biochem. Physiol. A* 119, 107-115.

**Goss, G.G., Perry, S. and Laurent, P.** (1995). Ultrastructural and morphometric studies on ion and acid-base transport processes in freshwater fish. In: *Cellular and molecular approaches to fish ionic regulation* (ed. C. M.

Wood and T. J. Shuttleworth), pp. 257-278. San Diego, CA, USA: Academic Press.

**Goss G. G. and Wood, C.M.** (1991). Two-substrate kinetic analysis: A novel approach linking ion and acid-base transport at the gills of freshwater trout, *Oncorhynchus mykiss*. *J. Comp. Physiol. B* 161, 635-646.

**Goss, G.G., Wood, C.M., Laurent, P. and Perry, S.F.** (1994). Morphological responses of the rainbow trout (*Oncorhynchus mykiss*) gill to hyperoxia, base ( $\text{NaHCO}_3$ ) and acid (HCl) infusions. *Fish Physiol. Biochem.* 12, 465-477.

**Greco, A.M., Gilmour, A., Fenwick, J., and Perry, S.** (1995). The effects of softwater acclimation on respiratory gas transfer in the rainbow trout *Oncorhynchus mykiss*. *J. Exp. Biol.* 198, 2557-2567.

**Grosell, M. and Wood, C.M.** (2002). Copper uptake across rainbow trout gills: mechanisms of apical entry. *J. Exp. Biol.* 205, 1179-1188.

**Hästbacka, J., de la Chapelle, A., Mahatani, M.M., Cline, S.G., Reeve-Daily, M.P., Hamilton, B.A., Kusumi, K., Trivedi, B., Weaver, A., Coloma, A., Lovett, M., Buckler, A., Kaitila, I., and Lander, E.S.** (1994). The diastrophic dysplasia gene encodes a novel sulphate transporter: positional cloning by fine-structure linkage disequilibrium mapping. *Cell* 78: 1073-1087.

**Hawkings, G.S., Galvez, F. and Goss, G.G.** (2004). Seawater acclimation causes independent alterations in  $\text{Na}^+/\text{K}^+$ - and  $\text{H}^+$ -ATPase activity

in isolated mitochondria-rich cell subtypes of the rainbow trout gill. *J. Exp. Biol.* 207, 905-912.

**Hootman, S.R. and Philpott, C.W.** (1979). Ultracytochemical localization of  $\text{Na}^+$ ,  $\text{K}^+$ -activated ATPase in chloride cells from the gills of a euryhaline teleost. *Anat. Rec.* 193: 99-130.

**Jensen, L.J., Willumsen, N.J., Amstrup, J. and Larsen, E.H.** (2003). Proton pump-driven cutaneous chloride uptake in anuran amphibia. *Biochim. Biophys. Acta* 1618, 120-132.

**Karnaky, K.J., Kinter, L.B., Kinter, W.B. and Stirling, C.E.** (1976). Teleost chloride cell. II. Autoradiographic localization of gill  $\text{Na}^+/\text{K}^+$ -ATPase in killifish *Fundulus heteroclitus* adapted to low and high salinity environments. *J. Cell Biol.* 70, 157-177.

**Kato, F., Hyodo, S. and Kaneko, T.** (2003). Vacuolar-type proton pump in the basolateral plasma membrane energizes ion uptake in branchial mitochondria-rich cells of killifish *Fundulus heteroclitus*, adapted to a low ion environment. *J. Exp. Biol.* 206, 793-803.

**Kerstetter, T.H. and Kirschner, L.B.** (1972). Active chloride transport by the gills of rainbow trout (*Salmo gairdneri*). *J. Exp. Biol.* 56, 263-272.

**Kerstetter, T.H., Kirschner, L.B. and Rafuse, D.D.** (1970). On the mechanism of sodium ion transport by the irrigated gills of rainbow trout (*Salmo gairdneri*). *J. Gen. Physiol.* 56, 342-359.



**Keys A., and Wilmer, E.N.** (1932). "Chloride secreting cells" in the gills of fishes, with special reference to the common eel. *J. Physiol.* 76, 368-378.

**Kirschner, L. B.** (2004). The mechanism of sodium chloride uptake in hyperregulating aquatic animals. *J. Exp. Biol.* 207, 1439-1452.

**Ko, S.B., Zeng, W., Dorwart, M.R., Luo, X., Kim, K.H., Millen, L., Goto, H., Naruse, S., Soyombo, A., Thomas, P.J. and Muallem, S.** (2004). Gating of CFTR by the STAS domain of SLC26 transporters. *Nature Cell Biol.* 6, 343-50

**Kopito, R.R. and Lodish, H.F.** (1985). Primary structure and transmembrane orientation of the murine anion exchanger protein. *Nature* 316, 234-238.

**Krogh, A.** (1939). Teleostomi. In: *Osmotic regulation in aquatic animals*, pp. 130-153. Cambridge, UK: Cambridge University Press.

**Larsen, E.H.** (1991). Chloride transport by high-resistance heterocellular epithelia. *Physiol. Rev.* 71, 235-283.

**Laurent, P.** (1984). Gill internal morphology. In: *Fish Physiology*, vol. 10A (ed. H. S. Hoar and D. W. Randall), pp. 73-183. New York, NY, USA: Academic Press.

**Laurent P. and Dunel, S.** (1980). Morphology of gill epithelia in fish. *Am. J. Physiol. Reg. Int. Comp. Physiol.* 238, R147-159.

**Lidke, D.S. and Arndt-Jovin, D.J.** (2004). Imaging takes a quantum leap. *Physiol.* 19: 322-325.

**Lin, H., Pfeiffer, D., Vogl, A., Pan, J. and Randall, D.** (1994). Immunolocalization of H<sup>+</sup>-ATPase in the gill epithelium of rainbow trout. *J. Exp. Biol.* 195, 169-183.

**Lohi, H., Kujala, M., Kerkela, E., Saarialho-Kere, U., Kestila, M. and Krere, J.** (2000). Mapping of five new putative anion transporter genes in human and characterization of SLC26A6, a candidate gene for pancreatic anion exchanger. *Genomics* 70: 102-112.

**Lohi, H., Kujala, M., Makela, S., Lehtonen, E., Kestila, M., Saarialho-Kere, U., Markovich, D. and Krere, J.** (2002). Functional characterization of three novel tissue-specific anion exchangers SLC26A7, -A8, and -9. *J. Biol. Chem.* 277, 14246-14254.

**Lohi, H., Lamprecht, G., Markovich, D., Heil, A., Kujala, M., Seidler, U. and Kere, J.** (2003). Isoforms of SLC26A6 mediate anion transport and have functional PDZ interaction domains. *Am. J. Physiol. Cell Physiol.* 284, C769-779.

**Maetz, J. and Garcia-Romeu, F.** (1964). The mechanism of sodium and chloride uptake by the gills of a fresh-water fish, *Carassius auratus*. II. Evidence for NH<sub>4</sub><sup>+</sup>/Na<sup>+</sup> and HCO<sub>3</sub><sup>-</sup>/Cl<sup>-</sup> exchanges. *J. Gen. Physiol.* 47, 1209-1227.

**Maren, T.H.** (1967). Carbonic anhydrase: chemistry, physiology and inhibition. *Physiol. Rev.* 47, 595-781.

**Marshall, W.S.** (2002). Na<sup>+</sup>, Cl<sup>-</sup>, Ca<sup>2+</sup> and Zn<sup>2+</sup> transport by fish gills: retrospective review and prospective synthesis. *J. Exp. Zool.* 293, 264-283.

**Miles, E. W., Rhee, S. and Davies, D.R.** (1999). The Molecular Basis of Substrate Channeling. *J. Biol. Chem.* 274, 12193-12196.

**McCormick, S.D.** (1995). Hormonal control of gill Na<sup>+</sup>, K<sup>+</sup>-ATPase and chloride cell function. In: *Cellular and molecular approaches to fish ionic regulation*, (ed. C. M. Wood and T. J. Shuttleworth), pp. 285-315. San Diego, CA, USA: Academic Press.

**McDonald, D.G. and Wood, C.M.** (1981). Branchial and renal acid and ion fluxes in the rainbow trout, *Salmo gairdneri*, at low environmental pH. *J. Exp. Biol.* 93, 101-118.

**Morgan, I. and Potts, W.** (1995). The effects of thiocyanate on the intracellular ion concentrations of branchial epithelial cells of brown trout. *J. Exp. Biol.* 198, 1229-1232.

**Morgan I., Potts, W. and Oates, K.** (1994). Intracellular ion concentrations in branchial epithelial cells of brown trout (*Salmo trutta* L.) determined by X-ray microanalysis. *J. Exp. Biol.* 194, 139-151.

**Moseley, R.H., Hoglund, P., Wu, G.D., Siberg, D.G., Haila, D., de la Chapelle, A., Holmberg, C. and Krere, J.** (1999). Downregulated in adenoma gene encodes a chloride transporter defective in congenital chloride diarrhea. *Am. J. Physiol. Gastr. Liver Physiol.* 276, G185-192.

**Motais, R. And Garcia-Romeu,F.** (1972). Transport mechanisms in the teleostean gill and amphibian skin. *Ann. Rev. Physiol.* 34, 141-176.

**Mount, D.B. and Romero, M.F.** (2004). The SLC26 gene family of multifunctional anion exchangers. *Europ. J. Physiol.* 447: 710-721.

**Onken, H. and Putzenlechner, M.** (1991). A V-ATPase drives active, electrogenic and Na<sup>+</sup> independent Cl<sup>-</sup> absorption across the gills of *Eriocheir sinensis*. *J. Exp. Biol.* 198, 767-774.

**Parks, S. K., Tresguerres, M. and Goss, G. G.** (2007). Interactions between Na<sup>+</sup> channels and Na<sup>+</sup>-HCO<sub>3</sub><sup>-</sup> cotransporters in the freshwater fish gill MR cell: a model for transepithelial Na<sup>+</sup> uptake. *Am. J. Physiol. Cell Physiol.* **292**, C935-C944.

**Perry, S. F.** (1997). The chloride cell: structure and function in the gills of freshwater fishes. *Ann. Rev. Physiol.* 59, 325-347.

**Perry, S.F., Goss, G.G. and Laurent, P.** (1992). The interrelationships between gill chloride cell morphology and ionic uptake in four freshwater teleosts. *Can. J. Zool.* 70, 1775-1786.

**Perry, S.F. and Laurent, P.** (1989). Adaptational responses of rainbow trout to lowered external NaCl concentration: contribution of the branchial chloride cell. *J. Exp. Biol.* 147, 147-168.

**Perry, S.F. and Laurent, P.** (1990). The role of carbonic anhydrase in carbon dioxide excretion, acid-base balance and ionic regulation in aquatic gill breathers. In: *Animal nutrition and transport processes. 2. Transport, respiration and excretion: comparative and environmental aspects*, (ed. J.-P. Truchot and B. Lahlou), pp. 39-57. Basel, Switzerland: Karger.

**Perry, S.F. and Randall, D.J.** (1981). Effects of amiloride and SITS on branchial ion fluxes in rainbow trout, *Salmo gairdneri*. *J. Exp. Biol.* 215, 225-228.

**Perry, S.F., Shahsavaranti, A., Georgalis, T., Bayaa, M., Furmisky, M. and Thomas, S.L.Y.** (2003). Channels, pumps, and exchangers in the gill and kidney of freshwater fishes: their role in ionic and acid-base regulation. *J. Exp. Zool.* 300A, 53-62.

**Philpott, C.W.** (1966). The use of horseradish peroxidase to demonstrate functional continuity between the plasmalemma and the unique tubular system of the chloride cell. *J. Cell Biol.* 31, 86A.

**Philpott, C.W.** (1980). Tubular system membranes of teleost chloride cells: osmotic response and transport sites. *Am. J. Physiol. Reg. Int. Comp. Physiol.* 238, R171-184.

**Piermarini, P.M., Verlander, J.W., Royaux, I.E. and Evans, D.H.** (2002). Pendrin immunoreactivity in the gill epithelium of a euryhaline elasmobranch. *Am. J. Physiol. Reg. Int. Comp. Physiol.* 283, R983-992.

**Pisam, M.** (1981). Membranous systems in the “chloride cell” of teleostean fish gill: their modifications in response to the salinity of the environment. *Anat. Rec.* 200, 401-414.

**Pisam, M., Boeuf, G., Prunet, P. And Rambourg, A.** (1990). Ultrastructural features of mitochondria-rich cells in stenohaline freshwater and seawater fishes. *Am. J. Anat.* 187, 21-31.

**Pisam, M., Caroff, A. and Rambourg, A.** (1987). Two types of chloride cells in the gill epithelium of a freshwater-adapted euryhaline fish: *Lebistes reticulatus*, their modifications during adaptations to saltwater. *Am. J. Anat.* 179, 40-50.

**Pisam, M., Le, M.C., Auperin, B., Prunet, P. and Raumberg, A.** (1995). Apical structures of “mitochondria-rich” alpha and beta cells in euryhaline fish gill: their behaviour in various living conditions. *Anat. Rec.* 241, 13-24.

**Pisam, M. and Rambourg, A.** (1991). Mitochondria-rich cells in the gill epithelium of teleost fishes: an ultrastructural approach. *Int. Rev. Cytol.* 130, 191-232.

**Quentin, F., Chamberey, R., Trinh-Trang-Tan, M.M., Fysekidis, M., Cambillau, M., Paillard, M., Aronson, P.S. and Eladari, D.** (2004). The  $\text{Cl}^-/\text{HCO}_3^-$  exchanger pendrin in the rat kidney is regulated in response to chronic alterations in chloride balance. *Am. J. Physiol. Renal Physiol.* 287, F1179-1188.

**Rahim, S.M., Delaunoy, J.-P. and Laurent, P.** (1988). Identification and immunocytochemical localization of two different carbonic anhydrase isoenzymes in teleostean erythrocytes and gill epithelia. *Histochem.* 89, 451-459.

**Reid, S.D., Hawkings, G.S., Galvez, F. and Goss, G.G.** (2003). Localization and characterization of phenamil-sensitive  $\text{Na}^+$  influx in isolated rainbow trout gill epithelial cells. *J. Exp. Biol.* 206, 551-559.

**Rizzuto, R. and Pozzan, T.** (2006). Microdomains of intracellular  $\text{Ca}^{2+}$ : molecular determinants and functional consequences. *Physiol. Rev.* 86, 369-408.

**Royaux, I.E., Wall, S.M., Karniski, L.P., Everett, L.A., Suzuki, K., Knepper, M.A. and Green, E.D.** (2001). Pendrin, encoded by the Pendred syndrome gene, resides in the apical region of renal intercalated cells and mediates bicarbonate secretion. *PNAS* 98: 4221-4226.

**Sardet, C.** (1980). Freeze fracture of the gill epithelium of euryhaline teleost fish. *Am. J. Physiol. Reg. Int. Comp. Physiol.* 238, R207-212.

**Sardet, C., Pisam, M. and Maetz, J.** (1979). The surface epithelium of teleostean fish gills. Cellular and junctional adaptations of the chloride cell in relation to salt adaptation. *J. Cell Biol.* 80, 96-117.

**Satlin, L.M., Matsumoto, T. and Schwartz, G.J.** (1992). Postnatal maturation of rabbit renal collecting duct III. Peanut lectin-binding intercalated cells. *Am. J. Physiol. Cell Physiol.* 251, C347-355.

**Scott, D.A., Wang, R., Kreman, T.M., Sheffield, V.C. and Karniski, L.P.** (1999). The Pendred syndrome gene encodes a chloride-iodide transport protein. *Nature gen.* 21, 440-443.

**Silberg, D.G., Wang, W., Moseley, R.H. and Traber, P.J.** (1995). The Down regulated in Adenoma (dra) gene encodes an intestine-specific membrane sulphate transporter protein. *J. Biol. Chem.* 270, 11897-11902.

**Srere, P.** (1987). Complexes of sequential metabolic enzymes. *Ann. Rev. Biochem.* 56, 89-124.

**Srere, P.** (1993). Wanderings (Wonderings) in Metabolism. *Biol. Chem.* 374, 833-842.

**Sterling, D. and Casey, J.R.** (2002). Bicarbonate transport proteins. *Biochem. Cell Biol.* 80, 483-497.

**Sterling, D., Reithmeier, R. A. F. and Casey, J.R.** (2001). A Transport Metabolon. Functional interaction of carbonic anhydrase II and chloride/bicarbonate exchangers. *J. Biol. Chem.* 276, 47886-47894.

**Sullivan, G.V., Fryer, J.N. and Perry, S.F.** (1995). Immunolocalization of proton pumps ( $H^+$ -ATPase) in pavement cells of rainbow trout gill. *J. Exp. Biol.* 198, 2619-2629.

**Tresguerres, M., Katoh, F., Fenton, H., Jasinska, E. and Goss, G.G.** (2005). Regulation of branchial V- $H^+$ -ATPase,  $Na^+/K^+$ -ATPase and NHE2 in response to acid and base infusions in the Pacific spiny dogfish (*Squalus acanthias*). *J. Exp. Biol.* 208, 345-354.

**Tresguerres, M., Parks, S.K., Katoh, F. and Goss, G.G.** (2006). Microtubule-dependent relocation of branchial V- $H^+$ -ATPase to the basolateral membrane in the Pacific spiny dogfish (*Squalus acanthias*): a role in base secretion. *J. Exp. Biol.* 209, 599-609.

**Vince, J.W., Carlsson, U. and Reithmeier, R.A.** (2000). Localization of the  $Cl^-/HCO_3^-$  anion exchanger binding site to the amino-terminal region of carbonic anhydrase II. *Biochem.* 39, 13344-13349.

**Vincourt, J.B., Jullien, D., Amalric, F. and Girard, J.P.** (2003). Molecular and functional characterization of SLC26A11, a sodium-independent sulfate transporter from high endothelial venules. *FASEB* 17, 890-892.



**Voet, D. and Voet, J.G.** (1995). Rates of enzymatic reactions. In *Biochemistry* (2<sup>nd</sup> edition), (ed. L. Ardwin), pp. 345-370. USA: John Wiley & Sons Inc.

**Wagner, C.A., Finberg, K.E., Breton, S., Marshansky, V., Brown, D. and Geibel, J.P.** (2004). Renal vacuolar H<sup>+</sup>-ATPase. *Physiol. Rev.* 84, 1263-1314.

**Wagner, C.A., Finberg, K.E., Stehberger, P.A., Lifton, R.P., Giebisch, G.H., Aronson, P.S. and Geibel, J.P.** (2002). Regulation of the expression of the Cl<sup>-</sup>/anion exchanger pendrin in mouse kidney by acid-base status. *Kidney Int.* 62, 2109-2117.

**Wang, D.N., Sarabia, V.E., Reithmeier, R.A.F. and Kühlbrandt, W.** (1994). Three-dimensional map of the dimeric membrane domain of the human erythrocyte anion exchanger, Band 3. *EMBO* 13, 3230-3235.

**Wilson, J., Laurent, P., Tufts, B., Benos, D., Donowitz, M., Vogl A. and Randall, D.** (2000). NaCl uptake by the branchial epithelium in freshwater teleost fish: an immunological approach to ion-transport protein localization. *J. Exp. Biol.* 203, 2279-2296.

**Wilson, J. M., Morgan, J. D., Vogl, A. W. and Randall, D. J.** (2002a). Branchial mitochondria-rich cells in the dogfish *Squalus acanthias*. *Comp. Biochem. Physiol. A* 132, 365-374.

**Wilson, J.M., Whiteley, N.M. and Randall, D.J.** (2002b). Ionoregulatory changes in the gill epithelia of Coho salmon during seawater acclimation. *Physiol. Biochem. Zool.* 75, 237-249.

**Wilson, R. W., Wright, P. M., Munger, S. and Wood, C.M.** (1994). Ammonia excretion in freshwater rainbow trout (*Oncorhynchus mykiss*) and the importance of gill boundary layer acidification: lack of evidence for  $\text{Na}^+/\text{NH}_4^+$  exchange. *J. Exp. Biol.* 191, 37–58.

**Wood, C. M. and LeMoigne, J.** (1991). Intracellular acid-base responses to environmental hyperoxia and normoxic recovery in rainbow trout. *Resp. Physiol.* 86, 91-113.

**Xie, Q., Welch, R., Mercado, A., Romero, M.F. and Mount, D.B.** (2002). Molecular characterization of the murine Slc26a6 anion exchanger: functional comparison with Slc26a1. *Am. J. Physiol. Renal Physiol.* 283: F826-38.

**South American rainbow crab *Chasmagnathus granulatus***

## Chapter IX

**High  $[\text{HCO}_3^-]$  stimulates ion transport across isolated gills of the crab**

***Chasmagnathus granulatus*: involvement of apical anion exchangers,  
carbonic anhydrase and basolateral  $\text{Na}^+/\text{H}^+$  exchangers<sup>1</sup>**

<sup>1</sup>A version of this chapter has been submitted for publication. **Tresguerres, M.**, Parks, S.K. and Goss, G.G. *The Journal of Experimental Biology* (JEXBIO/2007/006148). Reproduced with permission of The Company of Biologists and the co-authors of the manuscript. Data from this manuscript that is not included in this chapter can be found in appendix II.

## Introduction

The posterior gills of crustaceans are involved in several physiological functions that rely on the transepithelial transport of ions. A major advantage of the gills of certain crustaceans is that they can be isolated and perfused with haemolymph-like saline using a peristaltic pump, while the transepithelial potential difference ( $V_{te}$ ) is measured with voltage electrodes (Siebers *et al.*, 1985). Although with some limitations (see Tresguerres *et al.*, 2003),  $V_{te}$  has been demonstrated to be a reliable measure of transepithelial ion transport and this technique is very useful for the study of branchial ion-transporting mechanisms in real-time. Inhibitors specific for ion-transporting proteins can be added to either the apical or basolateral side of the gill epithelium. Based on their effect on  $V_{te}$ , one can infer the participation of such proteins in ion-transport and, to a certain extent, their localization at the apical or basolateral membrane. Using this technique, several ion-transporting processes in different crustacean species have been extensively investigated. These studies include ion uptake (Bianchini and Gilles, 1990; Lucu and Siebers, 1986; 1987; Pequeux and Gilles, 1988; Siebers *et al.*, 1985; Spannings-Pierrot *et al.*, 2000), ion secretion (Martinez *et al.*, 1988; Luquet *et al.*, 2002), ammonia excretion (Weibrauch *et al.*, 2004) and pH regulation (Siebers *et al.*, 1994).

The ion uptake mechanisms across the posterior gills of *C. granulatus* are one of the better studied among crustaceans. The cellular model for ion uptake in brackish water includes basolateral  $\text{Na}^+/\text{K}^+$ -ATPase, and  $\text{Cl}^-$  and  $\text{K}^+$

channels (Luquet *et al.*, 2002; 2005; Onken *et al.*, 2003). In brackish water, and also in non-stimulated gills of low-salinity (2 ppt) crabs, the apical route of entry for  $\text{Cl}^-$  and  $\text{Na}^+$  are apical  $\text{Na}^+/\text{K}^+/\text{2Cl}^-$  (NKCC) cotransporters in parallel with  $\text{K}^+$  channels (Onken *et al.*, 2003; Luquet *et al.*, 2005). Dopamine stimulates ion uptake in these conditions *via* a D1-like receptor- $\text{G}_s$  protein-cAMP-PKA- $\text{Na}^+/\text{K}^+$ -ATPase pathway (Halperin *et al.*, 2004; Genovese *et al.*, 2006). A reduction in the osmolarity of the haemolymph-side of the isolated gill also stimulates ion uptake (Luquet *et al.*, 2002; Tresguerres *et al.*, 2003), which is at least partially mediated by cAMP and  $\text{Na}^+/\text{K}^+$ -ATPase (Tresguerres *et al.*, 2003). In crabs acclimated to low salinity, apical  $\text{V-H}^+$ -ATPases and  $\text{Cl}^-/\text{HCO}_3^-$  exchangers and carbonic anhydrase (CA) seem to be involved in  $\text{Cl}^-$  uptake under these stimulated conditions (Genovese *et al.*, 2005). Finally, dopamine partially inhibits hypo-osmotic-stimulated ion uptake through D2-like receptors probably linked to a  $\text{G}_{i/o}$  protein, which results in inhibition of adenylyl cyclase (Genovese *et al.*, 2006).

In this chapter, I have investigated the involvement of the gills of *Chasmagnathus granulatus* in acid/base relevant ion transport. With this in mind, I increased the  $[\text{HCO}_3^-]$  of the perfusion saline and monitored  $V_{te}$  across isolated and perfused gills. The results indicate that ion transport is stimulated by an increase in  $[\text{HCO}_3^-]$ , and that the cellular mechanism involves apical anion exchangers, carbonic anhydrase and basolateral  $\text{Na}^+/\text{H}^+$  exchangers.

## Materials and methods

### *Animals*

*Chasmagnathus granulatus* (Dana 1851) were collected by hand from a muddy beach at San Antonio Oeste (Rio Negro, Argentina) during the Austral summer of 2006. The animals were transported to the Laboratory of Aquatic Ecotoxicology CIEDE (San Martin de los Andes, Neuquén, Argentina), where the gill perfusion experiments were performed. Crabs were acclimated in plastic containers with aerated seawater of 2 ppt salinity for at least 5 days. Water temperature was kept at  $18 \pm 2^{\circ}\text{C}$ . The animals were fed twice a week with commercially available pellets of rabbit food. Stage C intermolt adult male crabs (Drach and Tchernigovtzeff, 1967) were selected for the study.

### *Transepithelial Potential Difference ( $V_{te}$ ) across isolated gills*

Crabs were sacrificed by destroying the ventral ganglia using a pair of scissors. The carapace was then removed, and the posterior gills 6 and 7 were dissected and placed in a Petri dish containing saline. Preliminary experiments had demonstrated that gill 6 and 7 responded in identical manner to the manipulations described in this paper (also see Luquet *et al.*, 2002). The afferent and efferent vessels were connected by polyethylene tubing (0.40 mm in diameter) to a peristaltic pump (afferent) and to a collecting tube (efferent). Tubing was held in place by a sponge-coated acrylic clamp. The preparation was placed into a glass beaker with the appropriate solution, which was constantly aerated. The perfusion rate was kept at 0.1 ml

min<sup>-1</sup>. All perfusions were performed under symmetrical conditions at all times (perfusate identical to bath), to avoid the passive movement of ions by diffusion.

Transepithelial potential difference ( $V_{te}$ ) was measured *via* Ag<sup>+</sup>/AgCl electrodes connected by agar bridges (3 % agar in 3 mol l<sup>-1</sup> KCl) to the bath (external side) and to the collecting tube (internal side).  $V_{te}$  was measured with two chart recorders equipped with mV-meters (Cole Palmer 8373-20, Chicago, IL, USA; and Kipp & Zonen BD 40, Holland).  $V_{te}$  is given as the difference in electrical potential between the external and internal medium. For the statistical analyses, I considered the  $V_{te}$  values after stabilization for at least 20 min in each treatment and controls.

#### *Solutions and reagents*

The control saline was similar to the haemolymph of crabs acclimated to 30 ppt. Gills from crabs acclimated to lower salinities maintain a basal, non-stimulated  $V_{te}$  when perfused with this saline (Luquet *et al.*, 2002; Onken *et al.*, 2003, Tresguerres *et al.*, 2003). The composition of the control saline was (in mmol l<sup>-1</sup>): 465.00 NaCl, 9.40 KCl, 7.50 MgCl<sub>2</sub>, 12.40 CaCl<sub>2</sub>, 2.50 NaHCO<sub>3</sub> and 5.00 Hepes; pH to 7.75 with Tris. In addition, the perfusates also contained 2.00 mmol l<sup>-1</sup> glucose. The “high HCO<sub>3</sub><sup>-</sup>”saline had 10 mmol l<sup>-1</sup> NaCl substituted with NaHCO<sub>3</sub><sup>-</sup>, which resulted in a final nominal [HCO<sub>3</sub><sup>-</sup>] of 12.50 mmol l<sup>-1</sup>, but with osmolarity similar to the control. The pH of this last saline was adjusted to 7.75 with Hepes. The Cl<sup>-</sup>-free saline was prepared with salts of NO<sub>3</sub><sup>-</sup> instead of Cl<sup>-</sup>.



Acetazolamide, amiloride, bafilomycin and SITS were purchased from Sigma (St. Louis, MO, USA). Stock solutions of all of these inhibitors were prepared in DMSO and were added at a final dilution of 0.1% to the bath (SITS) or perfusate (the rest). Addition of 0.1% DMSO alone to the control saline did not result in any significant effect on  $V_{te}$ .

### *Statistics*

All data are given as means  $\pm$  s.e.m. Differences between groups were tested using one way repeated measures analysis of variance (1-way ANOVA), followed by Dunnet's post test or Tukey's multiple comparisons test. Statistical significance was set at  $P < 0.05$ . All statistical analyses were performed on GraphPad Prism v.3.0 (GraphPad Software, San Diego California USA).

## Results

Raising  $[\text{HCO}_3^-]$  by  $10 \text{ mmol l}^{-1}$  produced an immediate and significant increase of  $V_{\text{te}}$  from  $4.76 \pm 0.59$  to  $7.25 \pm 0.92 \text{ mV}$  ( $N = 18$ ). Similarly to the low pH stimulation (see appendix II), the effect was fully reversible and repeatable. Based on the inhibitory effect of acetazolamide ( $200 \text{ } \mu\text{mol l}^{-1}$ ), carbonic anhydrase is involved in the  $\text{HCO}_3^-$ -stimulation of  $V_{\text{te}}$  (Fig. 9.1). However, and in contrast with the low pH stimulation (see appendix II), basolateral application of bafilomycin ( $100 \text{ nmol l}^{-1}$ ) did not exert any significant effect on the  $\text{HCO}_3^-$ -stimulated  $V_{\text{te}}$ , indicating that  $\text{V-H}^+$ -ATPase is not important in this process (Fig. 9.1).

In order to identify the basolateral route of exit of  $\text{H}^+$  from the cells into the haemolymph space, I tested the effect of basolateral amiloride ( $1 \text{ mmol l}^{-1}$ ). This treatment completely and reversibly blocked the  $\text{HCO}_3^-$ -stimulated  $V_{\text{te}}$ , suggesting that basolateral  $\text{Na}^+/\text{H}^+$  exchangers (probably electrogenic) are critical for the overall transepithelial transport mechanism (Fig. 9.2).

The last two experimental series were designed to test for the involvement of apical  $\text{Cl}^-/\text{HCO}_3^-$  exchangers. Introduction of  $\text{Cl}^-$ -free conditions produced a significant decrease in  $V_{\text{te}}$ . An increase of  $[\text{HCO}_3^-]$  under  $\text{Cl}^-$ -free conditions did not result in the typical stimulation of  $V_{\text{te}}$ , indicating that, unlike in the low pH response,  $\text{Cl}^-$  ions must be present for the stimulation to occur (Fig. 9.3). Returning to normal  $\text{Cl}^-$ -containing conditions did not restore the original  $V_{\text{te}}$ , probably because the unnatural  $\text{Cl}^-$ -free saline induced a new basal steady state of ion transport. However, the gill epithelium was able to

respond with the typical increase in  $V_{te}$  to a raise in  $[HCO_3^-]$ , indicating that it was still healthy and fully functional (Fig. 9.3). Trying to maximize the utility of the gill preparations, I next tested the effect of apical SITS ( $2 \text{ mmol l}^{-1}$ ) on the  $V_{te}$  stimulated by  $HCO_3^-$ , but this treatment did not result in any significant changes in  $V_{te}$  (not shown).

## Discussion

These results demonstrate that ion transport across posterior gills of *Chasmagnathus granulatus* is stimulated under acid/base disturbances (i.e. an increase in  $[\text{HCO}_3^-]$  and the decrease in pH shown in appendix II). This suggests that the posterior gills might be important in correcting acid/base disturbances in the haemolymph of crabs in the wild.

Although  $V_{te}$  measurements are a very good estimation of ion transport, they are not without certain limitations. In particular,  $V_{te}$  is a reflection of both current ( $I$ ) and transcellular and paracellular resistance ( $R$ ). In order to definitely separate between these two variables, the use of hemi-lamella mounted in an Ussing-like chamber provided with a two electrode voltage clamp is necessary. Although I have done these type of experiments in the past in *C. granulatus* (Onken *et al.*, 2003; Tresguerres *et al.*, 2003), I currently do not possess the necessary technology and thus am unable to repeat them. However, saline manipulations in the current chapter were always performed at constant osmotic pressure and thus it is unlikely that paracellular  $R$  changes in the dramatic fashion that could explain the changes in  $V_{te}$  that took place. Similarly, transcellular  $R$  would have to increase substantially, which could only happen by a reduction in the conductance of the ion-transporting proteins involved (most likely at the apical membrane). However, this hypothesis would make it difficult to explain the pharmacological inhibition of the stimulated  $V_{te}$  by low pH and  $\text{HCO}_3^-$ , and therefore I am confident that the  $V_{te}$  measurements are indeed a reasonable

estimation of net transepithelial ion transport (*I*) under our experimental conditions.

### *Carbonic anhydrase*

My results indicate that carbonic anhydrase (CA) is important in the response to both low pH and high  $[\text{HCO}_3^-]$ . The drug used in these studies does not allow me to differentiate between extracellular and intracellular CA, both of which are present in the posterior gills of *C. granulatus* (Genovese *et al.*, 2005). However, I propose that both iso-enzymes are important in the mechanisms. Extracellular CA would dehydrate  $\text{H}^+$  and  $\text{HCO}_3^-$  into  $\text{CO}_2$ , which can diffuse inside the ion-transporting cells. Once inside,  $\text{CO}_2$  can then be re-hydrated back into  $\text{H}^+$  and  $\text{HCO}_3^-$  (Fig. 9.4), the main intracellular substrates in the mechanisms stimulated by low pH and  $[\text{HCO}_3^-]$ .

### *High $[\text{HCO}_3^-]$ -stimulating mechanism*

*A priori*, I was expecting that a basolateral V- $\text{H}^+$ -ATPase energized the putative secretion of  $\text{HCO}_3^-$  as suggested for myxinooids (Tresguerres *et al.*, 2006b; 2007a; chapters VI and VII), elasmobranchs (Tresguerres *et al.*, 2005, 2006c, 2007b; chapters II-V) and teleost fish (Tresguerres *et al.*, 2006a; chapter VIII). However, and in contrast to the low-pH stimulating mechanism (see appendix II), the  $\text{HCO}_3^-$ -stimulated  $V_{\text{te}}$  was totally insensitive to bafilomycin. In search of an alternative basolateral route of exit for  $\text{H}^+$ , I found that amiloride did inhibit the stimulated  $V_{\text{te}}$  in a complete and reversible manner. Candidate targets for the amiloride sensitivity are a putative NHE1-like housekeeping protein and the electrogenic  $2\text{Na}^+/\text{H}^+$  NHE described in a

variety of crustacean (lobster) tissues, including the gills (Kimura *et al.*, 1994) (Fig. 9.4).

Finally, the lack of  $\text{HCO}_3^-$ -stimulation in  $\text{Cl}^-$ -free conditions indicate the involvement of apical  $\text{Cl}^-/\text{HCO}_3^-$  exchangers of some sort (Fig. 9.4). However, apical application of SITS did not have any significant effect in the stimulated  $V_{te}$ . It is interesting to note that apical SITS produced a small but significant inhibition of 16 % under hypo-osmotic stimulating conditions, and of 45 % in similar, but  $\text{Na}^+$ -free, perfusing saline (Genovese *et al.*, 2006). This was interpreted as indicative of the involvement of a  $\text{Cl}^-/\text{HCO}_3^-$  exchanger in  $\text{Cl}^-$  uptake. Lack of SITS inhibition in our experimental conditions indicate that either a different, SITS-insensitive,  $\text{Cl}^-/\text{HCO}_3^-$  exchanger participates in the  $\text{HCO}_3^-$ -induced  $V_{te}$  or that SITS did not cross the cuticle in my experiments.

I have only found one similar study in the literature, performed in isolated and perfused gills of the shore crab *Carcinus maenas* (Siebers *et al.*, 1994). This study reported that the gill could detect an unphysiologically high pH of 8.1 in the perfusate (haemolymph space) and reabsorb  $\text{H}^+$  in order to restore a normal pH of  $\sim 7.70$ . The stimuli seemed to be the combination of high pH and  $[\text{HCO}_3^-]$ , since a saline buffered to pH 8.10 with Tris did not affect  $\text{H}^+$  reabsorption significantly. Even though the authors tested the effect of basolateral application of a variety of ion-transporting protein inhibitors, none of them affected simultaneously  $V_{te}$  and  $\text{H}^+$  reabsorption, with the sole exception of ouabain. Therefore, either their experimental conditions caused

different effects compared to our study, or *C. maenas*, unlike *C. granulatus*, relies on electroneutral ion transport for acid/base balance purposes.

#### *Final remarks*

The low pH- and  $\text{HCO}_3^-$  stimulation of  $V_{te}$  reported in this study raise the following interesting questions: (1) Do these two mechanisms take place in the same gill cell type, or are there are specific cell subtypes for each of them? (2) Is ion uptake linked to acid/base regulation in the gills of crustaceans? (3) Given that both stimulating mechanisms depend on intra- and extra-cellular CA and  $\text{CO}_2$ , but they exert opposite overall effects in acid/base terms: what regulates the activation of one mechanism over the other? Is there any sort of extracellular pH sensor involved? These questions will represent the basis of future research goals.

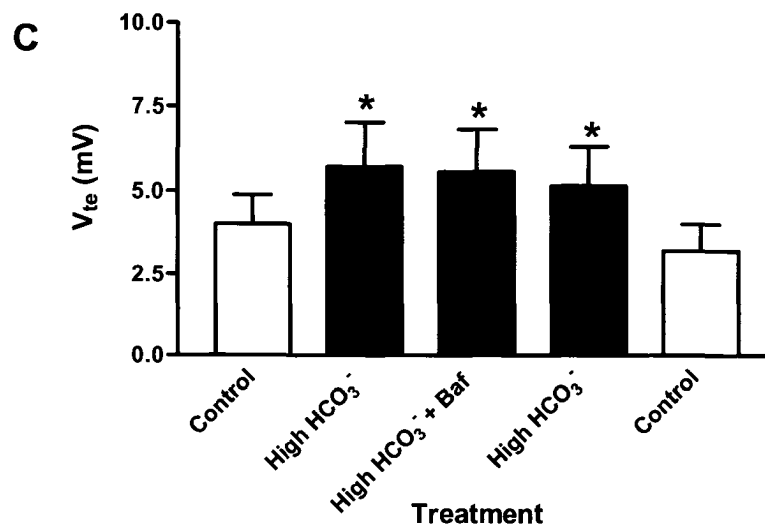
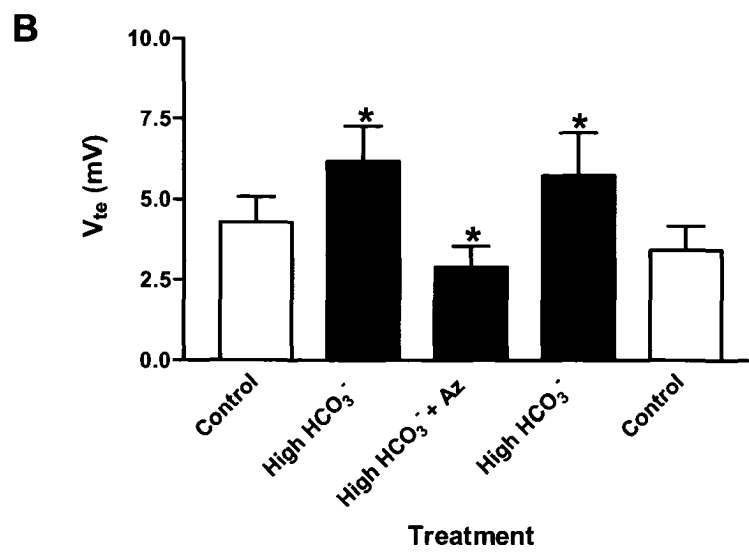
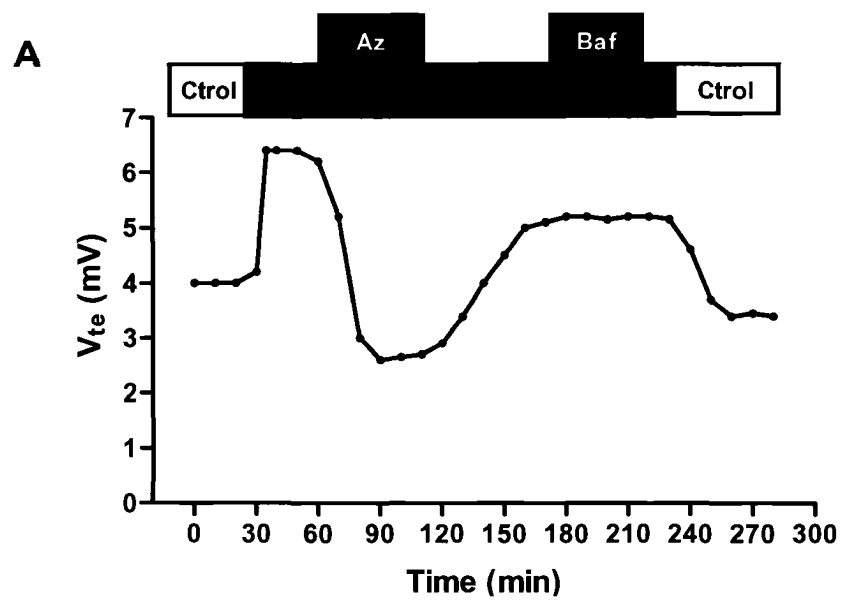




**Figure 9.1.**  $\text{HCO}_3^-$ -induced  $V_{te}$  stimulation, inhibition by basolateral acetazolamide and lack of inhibition by basolateral bafilomycin. (A) Representative trace of trial experiments where both drugs were applied to the same preparation in a consecutive manner. However, the data shown in *B* and *C* are from independent experiments. (B) Acetazolamide summary statistics (N=7). (C) Bafilomycin summary statistics (N=6). Ctlol: control saline, 2.50 mmol l<sup>-1</sup>  $\text{HCO}_3^-$ , pH 7.75. High  $\text{HCO}_3^-$ : 12.50 mmol l<sup>-1</sup>  $\text{HCO}_3^-$ , pH 7.75 saline. The asterisks indicate statistical differences with the control ( $p < 0.05$ ; N=7; 1-way ANOVA, Dunnett's multiple comparisons post-test).

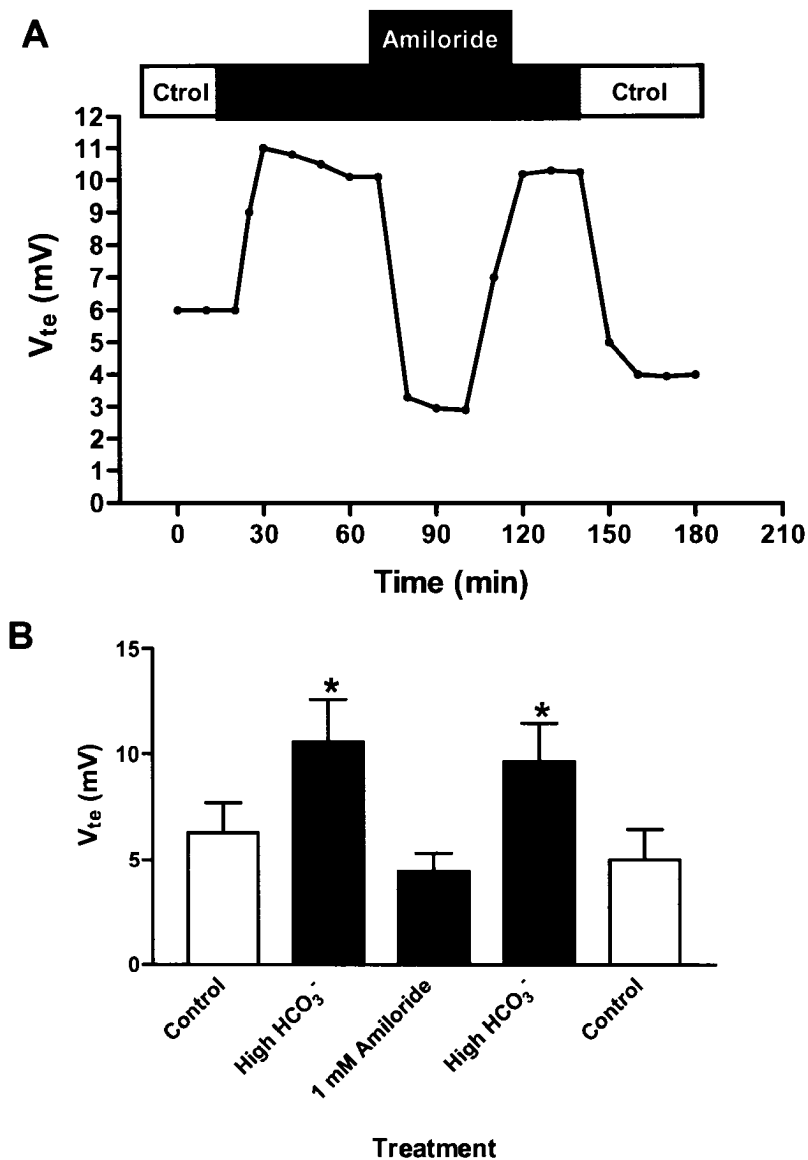


**Figure 9.2.** Inhibition of  $HCO_3^-$ -induced  $V_{te}$  stimulation by basolateral amiloride. (A) Representative trace. (B) Summary statistics.  $V_{te}$ : transepithelial potential difference. Ctrl: control saline,  $2.50 \text{ mmol l}^{-1} HCO_3^-$ , pH 7.75. High  $HCO_3^-$ :  $12.50 \text{ mmol l}^{-1} HCO_3^-$ , pH 7.75 saline. Amiloride ( $1.00 \text{ mmol l}^{-1}$ ) was added in the basolateral perfusate. The asterisks indicate statistical differences with the control ( $p < 0.05$ ; N=5; 1-way ANOVA, Dunnett's multiple comparisons post-test).

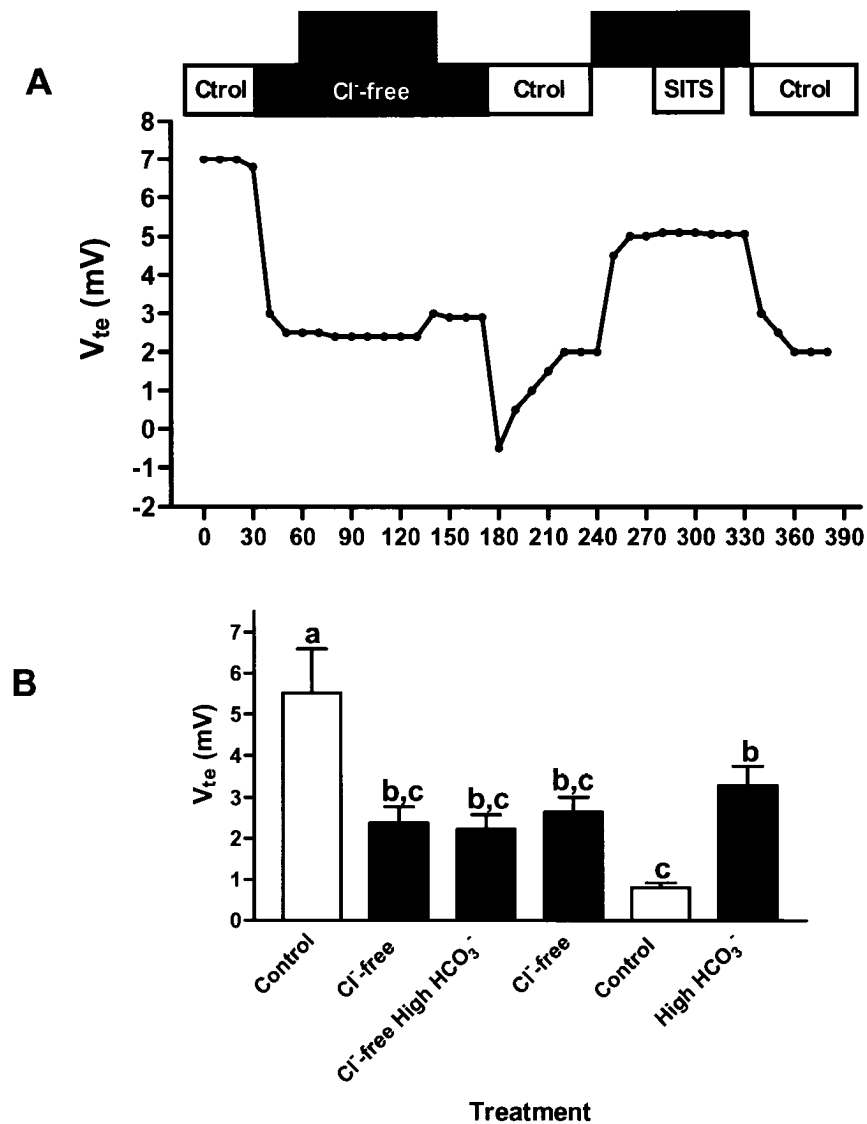


**Figure 9.3.** Lack of  $\text{HCO}_3^-$ -induced  $V_{te}$  stimulation in  $\text{Cl}^-$ -free conditions. (A) Representative trace. (B) Summary statistics (only the  $\text{Cl}^-$ -free part of the experiment was analyzed). Ctrol: control saline,  $2.50 \text{ mmol l}^{-1} \text{HCO}_3^-$ , pH 7.75.  $\text{Cl}^-$ -free: control saline with all the  $\text{Cl}^-$  substituted by  $\text{NO}_3^-$ ,  $2.50 \text{ mmol l}^{-1} \text{HCO}_3^-$ , pH 7.75.  $\text{Cl}^-$ -free saline, high bicarb:  $12.50 \text{ mmol l}^{-1} \text{HCO}_3^-$ . SITS:  $2.00 \text{ mmol l}^{-1}$  SITS added into the apical bath. The letters indicate different levels of statistical significance ( $p < 0.05$ ;  $N=5$ ; 1-way ANOVA, Tukey's multiple comparisons post-test).

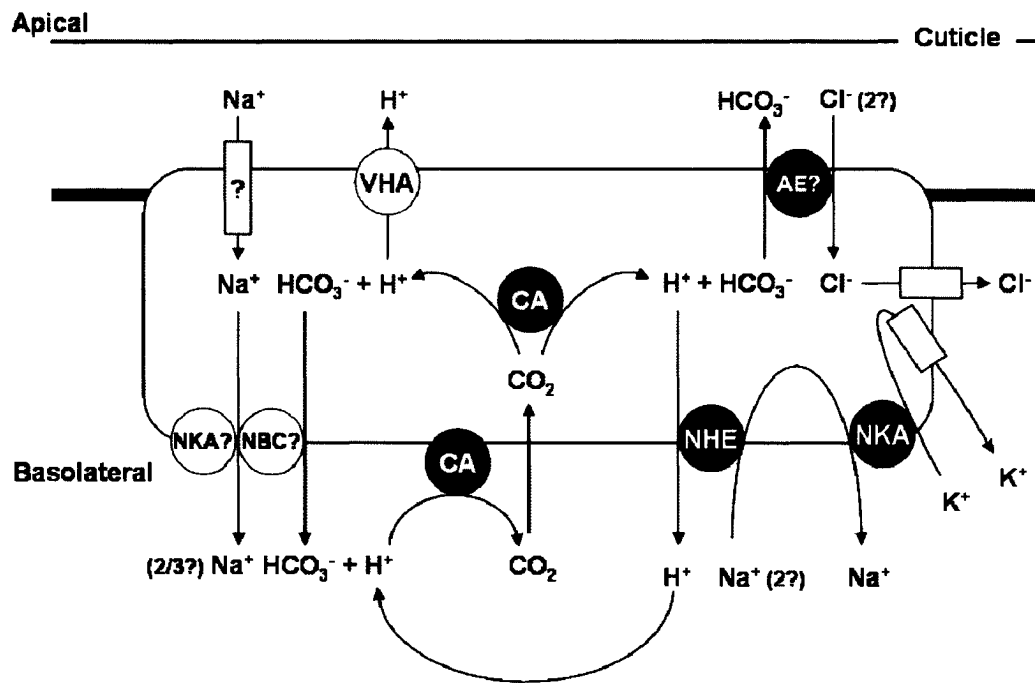


**Figure 9.4.** Model for acid/base regulation in the gill epithelium of *Chasmagnathus granulatus*. AE: anion exchanger; CA: carbonic anhydrase; NBC: Na<sup>+</sup>/HCO<sub>3</sub><sup>-</sup> cotransporter; NHE: Na<sup>+</sup>/H<sup>+</sup> exchanger; NKA: Na<sup>+</sup>/K<sup>+</sup>-ATPase; VHA: V-type H<sup>+</sup>-ATPase. This figure combines the results from this chapter and appendix II.

## References

- Bianchini, A. and Gilles, R.** (1990). Cyclic AMP as a modulator of NaCl transport in gills of the euryhaline Chinese crab *Eriocheir sinensis*. *Mar. Biol.* 104, 191-195.
- Drach, P. and Tchernig.C.** (1967). Method for Determining Intermoulting Stages and Its General Application to Crustacea. *Vie Et Milieu Serie a-Biologie Marine* 18, 597-607.
- Genovese, G., Ortiz, N., Urcola, M. R. and Luquet, C. M.** (2005). Possible role of carbonic anhydrase, V-H<sup>+</sup>-ATPase, and Cl<sup>-</sup>/HCO<sub>3</sub><sup>-</sup> exchanger in electrogenic ion transport across the gills of the euryhaline crab *Chasmagnathus granulatus*. *Comp. Biochem. Physiol. A* 142, 362-369.
- Genovese, G., Senek, M., Ortiz, N., Regueira, M., Towle, D. W., Tresguerres, M. and Luquet, C. M.** (2006). Dopaminergic regulation of ion transport in gills of the euryhaline semiterrestrial crab *Chasmagnathus granulatus*: interaction between D1- and D2-like receptors. *J. Exp. Biol.* 209, 2785-2793.
- Halperin, J., Genovese, G., Tresguerres, M. and Luquet, C. M.** (2004). Modulation of ion uptake across posterior gills of the crab *Chasmagnathus granulatus* by dopamine and cAMP. *Comp. Biochem. Physiol. A* 139, 103-109.
- Kimura, C., Ahearn, G., Busquets-Turner, L., Haley, S., Nagao, C. and Couet, H.** (1994). Immunolocalization of an antigen associated with the invertebrate electrogenic 2Na<sup>+</sup>/1H<sup>+</sup> antiporter. *J. Exp. Biol.* 189, 85-104.

**Kirschner, L. B.** (2004). The mechanism of sodium chloride uptake in hyperregulating aquatic animals. *J. Exp. Biol.* 207, 1439-1452.

**Lucu, C. and Siebers, D.** (1986). Amiloride-sensitive sodium flux and potentials in perfused *Carcinus* gill preparations. *J. Exp. Biol.* 122, 25-35.

**Lucu, C. and Siebers, D.** (1987). Linkage of  $\text{Cl}^-$  fluxes with ouabain sensitive  $\text{Na}^+/\text{K}^+$  exchange through *Carcinus* gill epithelia. *Comp. Biochem. Physiol. A* 87, 807-811.

**Luquet, C. M., Postel, U., Halperin, J., Urcola, M. R., Marques, R. and Siebers, D.** (2002). Transepithelial potential differences and  $\text{Na}^+$  flux in isolated perfused gills of the crab *Chasmagnathus granulatus* (Grapsidae) acclimated to hyper- and hypo-salinity. *J. Exp. Biol.* 205, 71-77.

**Luquet, C. M., Weihrauch, D., Senek, M. and Towle, D. W.** (2005). Induction of branchial ion transporter mRNA expression during acclimation to salinity change in the euryhaline crab *Chasmagnathus granulatus*. *J. Exp. Biol.* 208, 3627-3636.

**Martinez, C. B. R., Harris, R. R. and Santos, M. C. F.** (1998). Transepithelial potential differences and sodium fluxes in isolated perfused gills of the mangrove crab *Ucides cordatus*. *Comp. Biochem. Physiol. A* 120, 227-236.

**Onken, H., Tresguerres, M. and Luquet, C. M.** (2003). Active NaCl absorption across posterior gills of hyperosmoregulating *Chasmagnathus granulatus*. *J. Exp. Biol.* 206, 1017-1023.

**Pequeux, A. and Gilles, R.** (1988). The trans-epithelial potential

difference of isolated perfused gills of the Chinese crab *Eriocheir sinensis* acclimated to fresh-water. *Comp. Biochem. Physiol. A* 89, 163-172.

**Siebers, D., Lucu, C., Bottcher, K. and Jurss, K.** (1994). Regulation of pH in the isolated-perfused gills of the shore crab *Carcinus maenas*. *J. Comp. Physiol. B* 164, 16-22.

**Siebers, D., Winkler, A., Lucu, C., Thedens, G. and Weichart, D.** (1985).  $\text{Na}^+$ - $\text{K}^+$ -ATPase generates an active-transport potential in the gills of the hyperregulating shore crab *Carcinus maenas*. *Mar. Biol.* 87, 185-192.

**Spanings-Pierrot, C., Soye, D., Van Herp, F., Gompel, M., Skaret, G., Grousset, E. and Charmantier, G.** (2000). Involvement of crustacean hyperglycemic hormone in the control of gill ion transport in the crab *Pachygrapsus marmoratus*. *Gen. Comp. Endocrinol.* 119, 340-350.

**Tresguerres, M., Katoh, F., Fenton, H., Jasinska, E. and Goss, G. G.** (2005). Regulation of branchial V-H<sup>+</sup>-ATPase,  $\text{Na}^+/\text{K}^+$ -ATPase and NHE2 in response to acid and base infusions in the Pacific spiny dogfish (*Squalus acanthias*). *J. Exp. Biol.* 208, 345-354.

**Tresguerres, M., Katoh, F., Orr, E., Parks, S. K. and Goss, G. G.** (2006a). Chloride uptake and base secretion in freshwater fish: A transepithelial ion-transport metabolon? *Physiol. Biochem. Zool.* 79, 981-996.

**Tresguerres, M., Onken, H., Perez, A. F. and Luquet, C. M.** (2003). Electrophysiology of posterior, NaCl-absorbing gills of *Chasmagnathus granulatus*: rapid responses to osmotic variations. *J. Exp. Biol.* 206, 619-626.

**Tresguerres, M., Parks, S. K. and Goss, G. G.** (2006b). V-H<sup>+</sup>-

ATPase, Na<sup>+</sup>/K<sup>+</sup>-ATPase and NHE2 immunoreactivity in the gill epithelium of the Pacific hagfish (*Eptatretus stoutii*). *Comp. Biochem. Physiol. A* 145, 312-321.

**Tresguerres, M., Parks, S. K. and Goss, G. G. (2007a).** Recovery from blood alkalosis in the Pacific hagfish (*Eptatretus stoutii*): involvement of gill V-H<sup>+</sup>-ATPase and Na<sup>+</sup>/K<sup>+</sup>-ATPase. *Comp. Biochem. Physiol. A* (DOI j.cbpa.2007.03.032).

**Tresguerres, M., Parks, S. K., Wood, C.M. and Goss, G. G. (2007b).** V-H<sup>+</sup>-ATPase translocation during blood alkalosis in dogfish gills: interaction with carbonic anhydrase and involvement in the post-feeding alkaline tide. *Am. J. Physiol. Int. Reg. Comp. Physiol.* 292, 2012-2019.

**Tresguerres, M., Parks, S. K., Katoh, F. and Goss, G. G. (2006c).** Microtubule-dependent relocation of branchial V-H<sup>+</sup>-ATPase to the basolateral membrane in the Pacific spiny dogfish (*Squalus acanthias*): a role in base secretion. *J. Exp. Biol.* 209, 599-609.

**Weihrach, D., Morris, S. and Towle, D. W. (2004).** Ammonia excretion in aquatic and terrestrial crabs. *J. Exp. Biol.* 207, 4491-4504.



## **Chapter X**

### **General discussion**

## Dogfish

### *Synopsis*

The results from chapters II-V provide with a relatively complete picture about the cellular mechanisms for A/B regulation in dogfish gills. In chapter II, I have demonstrated the presence of different  $\text{Na}^+/\text{K}^+$ -ATPase- and  $\text{V-H}^+$ -ATPase-rich cells. This result has been recently confirmed elegantly by Choe *et al.* (2007), who performed immunolabeling on the same section using antibodies raised in mouse and rabbit. The results from chapter II also suggest that  $\text{Na}^+/\text{K}^+$ -ATPase and a NHE2-like protein (lp) are involved in acid secretion in dogfish gills. The novel finding that increased  $\text{V-H}^+$ -ATPase abundance and, especially, the  $\text{V-H}^+$ -ATPase translocation to the basolateral membrane under blood alkalosis was the foundation for the rest of my research on dogfish.

Chapter III shows that  $\text{V-H}^+$ -ATPase translocation requires functional microtubules, and that its prevention results in impaired blood pH recovery and  $\text{TCO}_2$  clearance during  $\text{NaHCO}_3$  infusions. Therefore, a relationship between  $\text{V-H}^+$ -ATPase translocation and  $\text{H}^+$  reabsorption and  $\text{HCO}_3^-$  secretion was established. In addition, a relatively simple differential centrifugation protocol allowed me to assess  $\text{V-H}^+$ -ATPase abundance by western blotting in whole gill homogenates and in a fraction enriched in cell membranes. In this way, I found that the short-term (6 h) branchial defense to blood alkalosis relies on  $\text{V-H}^+$ -ATPase translocation of pre-existing units, but the longer term (24 h) response probably also includes increased  $\text{V-H}^+$ -

ATPase synthesis *de novo*, although other processes such as a reduction in V-H<sup>+</sup>-ATPase degradation are also possible.

Chapter IV provides two important insights about V-H<sup>+</sup>-ATPase, H<sup>+</sup> reabsorption and HCO<sub>3</sub><sup>-</sup> secretion in dogfish gills. The first insight is that a functional carbonic anhydrase (CA) may be necessary for V-H<sup>+</sup>-ATPase translocation in response to blood alkalosis to occur. Blood pH and plasma *PCO*<sub>2</sub> and [HCO<sub>3</sub><sup>-</sup>] were at least as high as in the control (functional CA) treatment. This suggested to me that the stimulus that triggers V-H<sup>+</sup>-ATPase translocation could be changes in pH and/or [HCO<sub>3</sub><sup>-</sup>]<sub>i</sub> inside the V-H<sup>+</sup>-ATPase-rich cells. The second insight derived from chapter IV was that V-H<sup>+</sup>-ATPase translocation is demonstrated in a more natural regime, the post-feeding alkaline tide. This result puts the V-H<sup>+</sup>-ATPase translocation into physiological context and suggests that this is the general mechanism for increasing net HCO<sub>3</sub><sup>-</sup> secretion at the dogfish gill.

Finally, chapter V shows that V-H<sup>+</sup>-ATPase translocation takes place in isolated gill filaments incubated in a solution with high [HCO<sub>3</sub><sup>-</sup>] and *PCO*<sub>2</sub>. Although preliminary, these results are important because they demonstrate that all the components of the V-H<sup>+</sup>-ATPase translocation mechanism are present and functional at the gill level. In addition, these results suggest that no extrinsic hormonal or nervous inputs are required. Unfortunately, my attempt to use incubated isolated gill filaments to detect the intracellular components involved in sensing and triggering V-H<sup>+</sup>-ATPase translocation were unsuccessful. These experiments can set the basis and protocols for

future research. Finally, chapter V shows that cAMP production is activated by  $\text{HCO}_3^-$  in gill homogenates, a finding that strongly advocates for the involvement of soluble adenylyl cyclase in the response to blood alkalosis.

#### *Branchial cellular ion-transporting mechanisms for blood A/B regulation*

##### *i- Acid secretion*

The cells responsible for acid secretion are likely the  $\text{Na}^+/\text{K}^+$ -ATPase-rich cells. A proposed cellular mechanism is depicted in figure 10.1, and it includes basolateral  $\text{Na}^+/\text{K}^+$ -ATPase, CA and apical NHEs. The identity of the apical NHE is probably the most controversial component. The antibody I used in chapter II was designed against the mammalian NHE2. However, it is possible that this heterologous antibody recognizes a different NHE isoform in dogfish gills.

Recently, (Choe *et al.*, 2005) detected NHE3 immunoreactivity in the gills of the Atlantic stingray *Dasyatis sabina* using a specific stingray antibody. NHE3 immunoreactivity was located in the apical region of  $\text{Na}^+/\text{K}^+$ -ATPase-rich cells. NHE3 mRNA abundance increased upon acclimation from seawater to freshwater, suggesting a role in  $\text{Na}^+$  uptake. However, no changes in mRNA abundance were found after 4 h of environmental hypercapnia, which induces a respiratory acidosis in the blood (Choe *et al.*, 2006). Although this might argue against a role of NHE3 in  $\text{H}^+$  secretion, it is possible that NHE3-mediated  $\text{H}^+$  secretion during hypercapnia was activated by post-translational modification such as insertion in the membrane and/or phosphorylation. More recently, Choe *et al.* (2007) used the same  $\alpha$ -NHE3

antibody and found a similar immunolabeling pattern in dogfish gills. Induction of acidosis followed by assessment of NHE3 abundance has not been attempted in dogfish, but it is possible that the increased NHE2-like abundance that I have found in response to HCl infusion is in reality related to NHE3. The simplest way to test this hypothesis would be to use the NHE3 antibody designed by Choe *et al.* in the gill samples from my HCl infusions that I have kept frozen at -80°C. If the role of NHE3 in H<sup>+</sup> secretion in dogfish and stingray gills is confirmed, it would be very interesting from an evolutionary point of view. Briefly, it would be direct evidence for a transporter that originally worked in H<sup>+</sup> secretion in ancestral marine elasmobranchs that was co-opted for Na<sup>+</sup> uptake in euryhaline elasmobranchs, as suggested in the papers by Choe *et al.*

The basolateral routes of exit for HCO<sub>3</sub><sup>-</sup> and Na<sup>+</sup> in dogfish gills have not been investigated. Traditionally, Na<sup>+</sup> has been thought to leave the cell into the blood *via* Na<sup>+</sup>/K<sup>+</sup>-ATPases (reviewed in Evans *et al.*, 2005; McCormick, 1995; Perry *et al.*, 2003). However, novel results in our lab demonstrate that at least part of the Na<sup>+</sup>/K<sup>+</sup>-ATPase Na<sup>+</sup> movement can be through an electrogenic basolateral Na<sup>+</sup>/HCO<sub>3</sub><sup>-</sup> cotransporter (NBC). NBC would have the advantage of reabsorbing HCO<sub>3</sub><sup>-</sup> in concert with Na<sup>+</sup>. The presence of basolateral NBCs at the dogfish gill must be investigated.

#### *ii- Base secretion and H<sup>+</sup> reabsorption*

Almost certainly, HCO<sub>3</sub><sup>-</sup> secretion and H<sup>+</sup> reabsorption take place in the V-H<sup>+</sup>-ATPase-rich cells. This assumption is derived from the current thesis, in

combination with reports of apical Pendrin (an anion exchanger) immunoreactivity in V-H<sup>+</sup>-ATPase-rich cells of stingray (Piermarini *et al.*, 2002) and dogfish (Evans *et al.*, 2004). Other components of the mechanism are CA and V-H<sup>+</sup>-ATPase. Importantly, the basolateral membranes of fish gill cells have very low permeability to HCO<sub>3</sub><sup>-</sup> (Perry *et al.*, 1982; 1984; Gilmour *et al.* 2001; Wilson *et al.*, 2000). This implies that CO<sub>2</sub> must diffuse inside the cells, where it is hydrated into H<sup>+</sup> and HCO<sub>3</sub><sup>-</sup> by CA. Increased plasma [HCO<sub>3</sub><sup>-</sup>] accelerates CO<sub>2</sub> diffusion, which will result in reduced pH<sub>i</sub> and [HCO<sub>3</sub>]<sub>i</sub>. These two factors are potential triggers for the V-H<sup>+</sup>-ATPase translocation. I will not elaborate further about the V-H<sup>+</sup>-ATPase translocation mechanism because a detailed description can be found in chapters II-V, and also in the next section of this Discussion. However, I would like to again emphasize that the V-H<sup>+</sup>-ATPase translocation can take place in isolated gills filaments. A model showing the cellular components and mechanisms of branchial H<sup>+</sup> secretion and HCO<sub>3</sub><sup>-</sup> reabsorption is presented in figure 10.2. Research about the potential regulation of apical Pendrin by insertion/removal from the membrane and/or phosphorylation/ dephosphorylation under acidosis and alkalosis definitely deserves some attention.

### *iii- Integration of branchial H<sup>+</sup> and HCO<sub>3</sub><sup>-</sup> secretion at the cellular level*

From examining the models presented in figures 10.1 and 10.2 it is evident that both the H<sup>+</sup> and the HCO<sub>3</sub><sup>-</sup> secretory mechanisms depend on CO<sub>2</sub> diffusing into the cells. In both cell types, intracellular CO<sub>2</sub> is then hydrated into H<sup>+</sup> and HCO<sub>3</sub><sup>-</sup> by CA. The fundamental difference between H<sup>+</sup>

and  $\text{HCO}_3^-$  secreting cells is determined by the polarity of the ion-transporting proteins:  $\text{Na}^+/\text{K}^+$ -ATPase-rich cells secrete  $\text{H}^+$  and reabsorb  $\text{HCO}_3^-$ , while V- $\text{H}^+$ -ATPase-rich cells do the opposite.

One important question is the nature of the stimuli for  $\text{H}^+$  and  $\text{HCO}_3^-$  secretion. A possibility that is addressed in the present thesis is that  $\text{H}^+$  and  $\text{HCO}_3^-$  secretion are activated directly at the secreting cells by the A/B status of the blood. This hypothesis is supported by my results in isolated gills from dogfish, and indirectly by my results from crabs. Regarding  $\text{HCO}_3^-$  secretion, I have proposed that intracellular pH or  $[\text{HCO}_3^-]_i$  stimulate an intracellular sensor (e.g. sAC), which then triggers the V- $\text{H}^+$ -ATPase translocation to the basolateral membrane.

The problem with this model, however, is how  $\text{H}^+$  secretion is differentially activated. Since the  $\text{H}^+$  secreting mechanism also depends on CA-generated intracellular  $\text{H}^+$  and  $\text{HCO}_3^-$ , what prevents  $\text{H}^+$  secretion from becoming stimulated during a blood alkalosis? A complete long-term research project is necessary in order to address this fundamental question. Here I will hypothesize about one probable scenario, based on the integration of results from several chapters of my thesis.

The V- $\text{H}^+$ -ATPase translocation mechanism seems to depend mostly on an increase in  $[\text{HCO}_3^-]_i$  generated by CA. In the CA-inhibition experiments from chapter IV, blood pH ( $\text{pH}_e$ ) was at the same elevated value as the control ( $\sim 8.05$  pH units). Plasma  $[\text{HCO}_3^-]$  was even higher than controls, while  $\text{PCO}_2$  was elevated. However, V- $\text{H}^+$ -ATPase translocation did not occur

under these conditions. These results rule out  $\text{pH}_e$  and plasma  $[\text{HCO}_3^-]$  as the sole trigger for  $\text{V-H}^+\text{-ATPase}$  translocation, and support the idea of an intracellular sensor. In addition, ion transport was stimulated by plasma  $[\text{HCO}_3^-]$  in the isolated crab gill preparations, even though pH was kept at the same value as the controls. This also eliminates  $\text{pH}_e$  as the stimulus in the crab gill system. In these experiments on crab gills, the increased saline  $[\text{HCO}_3^-]$  probably just sped up  $\text{CO}_2$  diffusion into the ion-transporting cells, as proposed for dogfish (see section *ii*).<sup>1</sup>

The increased  $\text{PCO}_2$  in the CA-inhibition experiments in dogfish can be interpreted in two different manners. On one hand, it indicates that  $\text{CO}_2$  diffusion into the cells was not a problem during CA inhibition. This is important because acetazolamide most likely inhibits rbc CA and CA IV in addition to gill CA, which could theoretically slow down  $\text{CO}_2$  diffusion into the  $\text{V-H}^+\text{-ATPase}$ -rich cells. The second interpretation is that elevated  $\text{PCO}_2$  itself could inhibit  $\text{V-H}^+\text{-ATPase}$  translocation. On a related point,  $\text{PCO}_2$  could also activate  $\text{H}^+$  secretion in the  $\text{Na}^+/\text{K}^+\text{-ATPase}$ -rich cells. Such a regulatory system would be adaptive during hypercapnia, because the combination of increased  $\text{H}^+$  secretion and reduced  $\text{HCO}_3^-$  secretion would counteract the respiratory acidosis. However, the experiments on isolated dogfish gill filaments demonstrate that  $\text{V-H}^+\text{-ATPase}$  translocation can take place at a very high  $\text{PCO}_2$ . In addition, the activation of  $\text{H}^+$  secretion during metabolic acidosis cannot be explained by elevated  $\text{PCO}_2$ . For example, blood pH of dogfish subjected to the HCl infusions (chapter II) was fully compensated

<sup>1</sup>It is important to note that some components of the cellular mechanism for  $\text{HCO}_3^-$  secretion differ between crabs and fish (specifically, the basolateral  $\text{V-H}^+\text{-ATPase}$ ). However, it is likely that the fundamental principle for the sensor is conserved throughout evolution (more about this topic to follow).



after 12 h despite having the same  $PCO_2$  values as in the NaCl and  $HCO_3^-$  infusions. Similarly, HCl infusions in hagfish resulted in insertion of the NHE2-1p into the apical membrane and activation of a  $H^+$  secretory mechanism, in spite of the very low plasma  $PCO_2$  (based on the very low  $TCO_2$ ) (appendix I). An examination of the results in crab gills reveals an identical picture. The low-pH stimulating saline had almost negligible amounts of  $TCO_2$ , and hence low  $PCO_2$  (appendix II). Even though  $PCO_2$  sensors might enhance  $H^+$  secretion *via* an alternative pathway, it seems unlikely that it is involved in the gill responses to metabolic acidosis and alkalosis. However, a convoluted possibility is that a  $PCO_2$  sensor in a place other than the gills acts to inhibit the V- $H^+$ -ATPase translocation during hypercapnia. This would explain why V- $H^+$ -ATPase translocation takes place in isolated gill filaments subjected to high  $PCO_2$  and  $[HCO_3^-]$ , but not in the whole animal experiments involving CA inhibition during  $HCO_3^-$  infusion.

Combining the evidence presented above, it seems logical that a drop in  $pH_e$  activates  $H^+$  secretion by stimulating a pH sensor. Moreover, the results from crabs were performed on isolated gills, supporting the concept that the sensor(s) is in the secreting cells themselves or at least in some gill cells. The pH sensor might be facing the blood (thus sensing  $pH_e$  directly) or it might be intracellular. In the latter case, the sensor could be stimulated either by CA-generated  $H^+$  or by indirect changes in  $pH_i$  in response to  $pH_e$ . If the pH sensor is intracellular, it should be either absent in the V- $H^+$ -ATPase-rich cells or have an inhibitory effect on  $HCO_3^-$  secretion.

The existence of pH sensors, both intracellular and extracellular, is well documented. For example, proteins such as cofilin, villin and talin are candidate  $\text{pH}_i$  sensors to regulate cell motility in response to changes in  $\text{pH}_i$  in mammals (reviewed by Srivastava *et al.*, 2007). Moreover, the regulation of cell motility involves remodeling of cytoskeletal components at the cell front, where A/B relevant proteins such as NHEs, NBCs and  $\text{V-H}^+$ -ATPases seem to play a role (Srivastava *et al.*, 2007). In yeast, the extracellular domain of the protein Wsc1 is responsive to increases in  $\text{pH}_e$ , and results in specific activation of the Slk2 mitogen-activated protein kinase K (MAPK) pathway (Serrano *et al.*, 2006). Incubation in a medium with low pH causes NHE3 to insert into the apical membrane of isolated mammalian kidney cells (Yang *et al.*, 2000). Although the pH sensor was not identified in this study, the authors proposed that “exocytosis may provide a common mechanism for regulation of apical membrane transporters in response to changes in intracellular pH” (Yang *et al.*, 2000). Another example of cytoskeleton-dependent cellular redistribution of transporters in response to acid incubation in isolated kidney cells involves  $\text{V-H}^+$ -ATPase and CBE (Schwartz *et al.*, 2001). Numerous additional examples can be found in the literature, and could serve as reference to identify the putative pH sensor(s) in dogfish gill cells.

In summary, I propose that  $\text{HCO}_3^-$  secretion is activated by an intracellular  $[\text{HCO}_3^-]$  sensor (probably sAC), and that a pH sensor (intra or extracellular) activates  $\text{H}^+$  secretion. Part of this model is based on results from hagfish and the South American crab, and they should be confirmed in

dogfish. Conversely, part of the dogfish model may apply to other aquatic animals.

*iv- V-H<sup>+</sup>-ATPase translocation: physiological role*

When placing the V-H<sup>+</sup>-ATPase translocation into the regular dogfish physiology, it is convenient to relate it to the post-feeding alkaline tide (Wood *et al.*, 2005, 2007a) and to the responses of the rectal gland to blood A/B status (Shuttleworth *et al.* 2006, Wood *et al.*, 2006). In the wild, dogfish are opportunistic feeders (Jones and Green, 1977). In the inter-feeding period, the predominant branchial A/B transport likely is H<sup>+</sup> secretion associated with regular metabolism and exercise. Therefore, blood pH and [HCO<sub>3</sub><sup>-</sup>] are relatively low and branchial V-H<sup>+</sup>-ATPase is in cytoplasmic vesicles. The rectal gland is probably dormant in the inter-feeding period, because NaCl secretion in the rectal gland is inhibited by low pH (Siegel *et al.*, 1975; Silva *et al.*, 1992). After feeding, a sequence of events changes the A/B and ionic status of the blood. This will eventually trigger the compensating mechanisms of HCO<sub>3</sub><sup>-</sup> secretion and H<sup>+</sup> reabsorption at the gills, and NaCl secretion at the rectal gland.

The very first event in the feeding process is the swallowing of the prey and its transfer into the stomach. Together with the prey, an amount of seawater is also swallowed (Wood *et al.*, 2007a). Since the concentration of NaCl in seawater is roughly double to that in dogfish blood, the swallowed seawater represents an important NaCl load. NaCl from the prey (usually invertebrates with high salt content) will be an additional source of NaCl load.

Once the prey is swallowed,  $H^+$  is secreted into the stomach to aid in digestion. The  $H^+$  come from  $CO_2$  hydration inside the cells in the gastric mucosa, which also yields an equimolar amount of  $HCO_3^-$  that is reabsorbed into the blood (Wood *et al.*, 2007a). Therefore,  $H^+$  secretion into the stomach is accompanied by increases in  $[HCO_3^-]$  and pH in the blood. The changes in blood A/B status are visible between 1 to 30 hours after feeding (Wood *et al.* 2005; 2007a). In mammals, amphibians and reptiles changes in blood A/B status are compensated by a decrease in the ventilation rate, which results in a respiratory acidosis, and by secretion of the original  $HCO_3^-$  load into the small intestine (Wang *et al.*, 2001). Dogfish do not increase  $PCO_2$  after feeding (Wood *et al.*, 2005), which is not surprising if we consider the limitations on ventilation imposed by the solubility of  $CO_2$  and  $O_2$  in water (see General Introduction). In addition, dogfish do not secrete the  $HCO_3^-$  load into the intestine (Wood *et al.*, 2007a). The large  $HCO_3^-$  load must be secreted out of the organism in order to restore blood homeostasis and prevent damage to the cells and tissues. According to the review by Heisler (1988), the gills account for most of the A/B relevant ion transport (>97%) in elasmobranchs. My results from chapter IV demonstrate that the gills indeed secrete net  $HCO_3^-$  into the water in the post-feeding period. This has been confirmed by a more detailed study on base fluxes associated with the alkaline tide (Wood C.M., Bucking C., Fitzpatrick J. and Nadella S., unpublished observations). The  $V-H^+$ -ATPase translocation described in this thesis seems to be a specific gill mechanism involved in  $HCO_3^-$  secretion and  $H^+$  reabsorption.

Although I cannot discount the involvement of a feeding related hormone, the combination of elevated blood  $[\text{HCO}_3^-]$  and  $\text{PCO}_2$  is sufficient to produce the V- $\text{H}^+$ -ATPase translocation at the gills (probably by inducing an increase in  $[\text{HCO}_3^-]_i$ , see previous section). Since branchial  $\text{H}^+$  reabsorption and  $\text{HCO}_3^-$  secretion counteract the original activating stimulus, the overall process is a beautiful example of feedback mechanisms driven by  $\text{HCO}_3^-/\text{CO}_2$ .

Branchial  $\text{HCO}_3^-$  secretion is likely linked to the uptake of  $\text{Cl}^-$ . Based on the results from chapter IV, the  $\text{HCO}_3^-$  secretion rate (and potentially  $\text{Cl}^-$  uptake) is  $\sim 0.3 \text{ mmol l}^{-1} \text{ kg}^{-1} \text{ h}^{-1}$  between 12 and 24 h after feeding. Assuming that blood volume is between 40 and 70  $\text{ml kg}^{-1}$  (Thorson, 1958; Tort *et al.*, 1991), blood  $[\text{Cl}^-]$  would increase from  $\sim 250 \text{ mmol l}^{-1}$  to 300-340  $\text{mmol l}^{-1}$  during the 12-24 h post feeding period. Moreover, the magnitude of the post feeding alkaline tide, and hence the  $\text{Cl}^-$  load, most likely depends on the meal size (Wood *et al.*, 2007a). My  $\text{NaHCO}_3$  infusion experiments demonstrate that  $\text{HCO}_3^-$  secretion can be as great as  $1 \text{ mmol l}^{-1} \text{ kg}^{-1} \text{ h}^{-1}$ . The accompanying  $\text{Cl}^-$  uptake would result in plasma  $[\text{Cl}^-]$  increasing to at least 420  $\text{mmol l}^{-1}$  during a 12 h period if not secreted. The branchial  $\text{Cl}^-$  load adds to the  $\text{Cl}^-$  gained by swallowing seawater and that from the diet.

In elasmobranchs, the excess  $\text{NaCl}$  is secreted by the rectal gland (Burger and Hess, 1960). The rectal gland is normally quiescent, but certain conditions stimulate it to produce a 500  $\text{mmol l}^{-1}$   $\text{NaCl}$  secretion, twice as concentrated as the blood. Based on *in vitro* studies,  $\text{NaCl}$  secretion in the rectal gland is activated by vasoactive intestinal peptide (VIP) (Stoff *et al.*,

1979) and by increased blood volume (Solomon *et al.*, 1985). Recently, it has been demonstrated that increases in blood pH and  $[\text{HCO}_3^-]$  also stimulate NaCl secretion in the rectal gland in intact animals (Shuttleworth *et al.*, 2006) and also in isolated rectal glands (Wood *et al.*, 2007b). Although the latter study concluded that the main activating factor was an increase in  $\text{pH}_e$ , the stimulation of NaCl secretion was greatest when  $\text{pH}_e$  and  $[\text{HCO}_3^-]_e$  were increased together (150% greater than  $\text{pH}_e$  alone). Moreover, Wood *et al.* (2007b) do not discount an increase in  $\text{pH}_i$  as the potential activating factor of NaCl secretion in the rectal gland. It is thus possible that a variation of the mechanism that activates  $\text{HCO}_3^-$  secretion and  $\text{H}^+$  reabsorption at the gills is functional at the rectal gland to stimulate NaCl secretion. Likely ion-transporting proteins that might become activated in the rectal gland are basolateral  $\text{Na}^+/\text{K}^+$ -ATPase and NKCCs and apical CFTR-Ip. Interestingly, sAC has been shown to activate  $\text{Cl}^-$  extrusion *via* CFTR in mammalian airway epithelium (Wang *et al.*, 2005).

The overall response to feeding is shown in figure 10.3. Notice how all the responses that follow  $\text{H}^+$  secretion into the stomach can potentially be triggered by the increased  $[\text{HCO}_3^-]$  in the blood. Moreover, they could be maintained and regulated by the interaction of processes taking place at organ distant from each other such as the stomach, the gills and the rectal gland. In addition, branchial cellular ion-transport is an example of negative feedback, since increased plasma  $[\text{HCO}_3^-]$  activates  $\text{H}^+$  reabsorption (*via* an elevation in  $[\text{HCO}_3^-]_i$ ), which counteracts the original alkaline stress. The

combined response of these three organs could potentially restore and maintain blood A/B and ionic balance. In addition, certain hormones could also be involved (see chapter IV), which could potentiate the pre-existing functional cellular mechanisms at the gills and rectal gland. One potential hormone involved in activating NaCl secretion at the rectal gland is VIP. However, and unlike in the rectal gland, VIP receptors are only present at background levels at the gills (Bewely *et al.*, 2006). This rules out VIP as a component of the activating  $\text{HCO}_3^-$ -secreting mechanism at the gills.

### **Hagfish**

As opposed to dogfish, hagfish seem to have only one cell type for A/B regulation. The results from chapters VI and VII and appendix I show that  $\text{Na}^+/\text{K}^+$ -ATPase, a NHE2-like protein (Ip) and  $\text{V-H}^+$ -ATPase are all localized in the same cells. Western blotting in gill samples subjected to differential centrifugation revealed that metabolic blood alkalosis increased  $\text{V-H}^+$ -ATPase abundance in whole gill homogenates, and also in a fraction enriched in cell membranes. The same membrane-enriched fraction had lower  $\text{Na}^+/\text{K}^+$ -ATPase abundance in gills from alkalotic fish compared to controls. The former finding suggests that under blood alkalosis  $\text{V-H}^+$ -ATPase inserts into the basolateral membrane to reabsorb  $\text{H}^+$  back into the blood, like in dogfish. The latter finding is indicative of  $\text{Na}^+/\text{K}^+$ -ATPase removal from the membrane, probably to reduce  $\text{H}^+$  secretion and further enhance  $\text{H}^+$  reabsorption.

The NHE2-Ip inserts into the apical membrane during blood metabolic acidosis (appendix I). These experiments illustrate how a protein located in

the apical region of the cells looks like in immunolabeled sections. A direct comparison of the apical NHE2 signal during blood acidosis to the V-H<sup>+</sup>-ATPase signal during alkalosis is further evidence that the increased V-H<sup>+</sup>-ATPase abundance in the latter case must be related to V-H<sup>+</sup>-ATPase that inserted into the basolateral membrane. A diagram showing how A/B regulation in hagfish gills can take place through differential insertion of H<sup>+</sup> extruding proteins (Na<sup>+</sup>/K<sup>+</sup>-ATPase and NHE2-lp) and H<sup>+</sup> reabsorbing and HCO<sub>3</sub><sup>-</sup> secreting proteins (V-H<sup>+</sup>-ATPase) is shown in figure 10.4.

### **Freshwater rainbow trout**

The putative branchial mechanisms for HCO<sub>3</sub><sup>-</sup> secretion and Cl<sup>-</sup> uptake in gills of freshwater trout are discussed in detail in chapter VIII and are not repeated here. The most important point for the purpose of this General Discussion is that there is enough evidence to propose basolateral V-H<sup>+</sup>-ATPases as the energizers for Cl<sup>-</sup> uptake from freshwater. The mechanism could be the result of relatively simple modifications in the HCO<sub>3</sub><sup>-</sup>-secreting mechanism of dogfish. Specifically, it would require the development of a basolateral tubular system (TS) in the secreting cells from the basolateral infoldings present in dogfish. This would result in the basolateral V-H<sup>+</sup>-ATPase being in the vicinity of the apical CBE and CA, which could create defined intracellular microdomains with higher [HCO<sub>3</sub>]<sub>i</sub>. The elevated [HCO<sub>3</sub>]<sub>i</sub> could then drive the apical CBE despite the unfavorable gradient and result in electroneutral Cl<sup>-</sup>/HCO<sub>3</sub><sup>-</sup> exchange. Development of a basolateral tubular system from basolateral infoldings does not seem unreasonable. For



example, hagfish MR cells have a TS similar to teleosts, despite not being involved in NaCl secretion or uptake. I could not find any references regarding the origin and possible functions of the hagfish TS, but it could have evolved independently to the TS from teleosts. Moreover, ion-transporting cells from other physiological systems and organisms also count with TSs (Luquet *et al.*, 2002; Reilly and Ellison, 2000), and they probably evolved independently from each other. This indicates that the development of a basolateral TS in ion-transporting cells is a very likely process in evolutionary terms.

### **Crab *C. granulatus***

The experiments in crabs acclimated to freshwater demonstrate that  $\text{HCO}_3^-$  and  $\text{H}^+$  can directly activate ion transport in an isolated gill epithelium. Speculations about putative pH and  $\text{HCO}_3^-$  sensors can be found in chapter IX, in the section on dogfish earlier in this chapter and also in the section on future directions (see below).

The model for the  $\text{HCO}_3^-$ -stimulating mechanism in isolated crab gills involves CA (which generates  $\text{H}^+$  and  $\text{HCO}_3^-$  from  $\text{CO}_2$ ), apical CBEs (which extrude  $\text{HCO}_3^-$  in exchange for  $\text{Cl}^-$ ) and basolateral NHEs (to reabsorb  $\text{H}^+$  into the blood). Interestingly, it has been proposed that  $\text{Cl}^-$  uptake for ion regulation also takes place *via* an apical CBE (Genovese *et al.*, 2005). However, the same authors demonstrated that CBE is energized by apical V- $\text{H}^+$ -ATPases, and that it is significantly inhibited by SITS. The study by Genovese *et al.* (2005) and also other studies in other crabs suggested that the apical CBE is electroneutral (Onken and Riestenpatt, 1998). In my study,

SITS did not exert any effect on the  $\text{HCO}_3^-$ -stimulated mechanism. In addition, there is a good chance that the CBE is electrogenic, which would make it easier to explain the outside positive  $V_{te}$ . Therefore, it is probable that the CBE involved in ion uptake is molecularly different to that involved in the  $\text{HCO}_3^-$ -stimulated mechanism.

Assuming that the  $\text{HCO}_3^-$ -stimulated mechanism in crab gills has a function in  $\text{HCO}_3^-$  secretion and  $\text{H}^+$  reabsorption, the main difference with dogfish and hagfish is that the basolateral route of  $\text{H}^+$  exit are NHEs instead of V- $\text{H}^+$ -ATPases. However, it is important to note that dogfish and hagfish are marine species. For example, V- $\text{H}^+$ -ATPase is not involved in  $\text{H}^+$  secretion to seawater in dogfish or hagfish, but apical V- $\text{H}^+$ -ATPase functions for  $\text{H}^+$  secretion both in freshwater rainbow trout (see chapter VIII) and *C. Granulatus* (appendix II). Moreover, the role of basolateral V- $\text{H}^+$ -ATPases in freshwater trout has not been conclusively demonstrated or tested experimentally. Finally, the  $[\text{NaCl}]$  in the haemolymph of crabs acclimated to freshwater is more than double than in the blood of freshwater rainbow trout. It is thus possible that basolateral V- $\text{H}^+$ -ATPases have a role in  $\text{H}^+$  reabsorption and  $\text{HCO}_3^-$  secretion only in seawater, or when a specific osmotic/ionic gradient between the blood and the water is encountered. Even if the specific basolateral  $\text{H}^+$ -transporting protein is different, it would be a minuscule variation on the overall model if we consider that crabs and fish are separated by ~1.2 billion years of evolution (see Fig. 1.3).

### **Future directions**

*i- V-H<sup>+</sup>-ATPase translocation in dogfish gill cells*

Additional experiments using isolated gill filaments need to be performed in order to confirm the results presented in chapter V. It seems apparent that the stimulus(i) that results in V-H<sup>+</sup>-ATPase translocation must be present at the basolateral side of the epithelium. Therefore, I would recommend perfusing the gills through the heart using dogfish salines with different [HCO<sub>3</sub><sup>-</sup>], pH and PCO<sub>2</sub> before dissecting the gills and incubating them in the same solution and also in seawater. Clearing the gills from blood requires a large volume (>1 l for a 2 kg dogfish) of saline. Unfortunately, this protocol will likely not allow for the pharmacological characterization of the signaling pathway because of the large amount of drugs that would be needed. One way to solve this problem would be the use of smaller dogfish.

In the longer term, it would be ideal to design a protocol for the isolation of Na<sup>+</sup>/K<sup>+</sup>-ATPase- and V-H<sup>+</sup>-ATPase-rich cells from dogfish gills. The protocol should be based on trypsin/collagenase gill digestion followed by centrifugation in a percol density gradient column, as it is used for teleosts (Goss *et al.*, 2001; Galvez *et al.*, 2002; Hawkings *et al.*, 2004; Reid *et al.*, 2003; Parks *et al.*, 2007; Wong and Chan, 1999a, b). Some modifications of these protocols are expected in order to make it functional to elasmobranchs. For example, [NaCl] and especially [urea] should be adjusted to match the different blood composition of elasmobranchs.

I expect Na<sup>+</sup>/K<sup>+</sup>-ATPase- and V-H<sup>+</sup>-ATPase-rich cells to migrate into a specific density layer. Cells can then be identified using anti-Na<sup>+</sup>/K<sup>+</sup>-ATPase

and anti-V-H<sup>+</sup>-ATPase in immunocytochemistry experiments. Further characterization should include the use of mitochondria-specific dyes such as DASPMI (Goss *et al.*, 2001) and Mitotracker green-FM (Galvez *et al.*, 2002; Hawkings *et al.*, 2004). This will confirm or refute that the Na<sup>+</sup>/K<sup>+</sup>-ATPase- and V-H<sup>+</sup>-ATPase-rich cells are indeed MR cells.

After a cell fraction enriched in V-H<sup>+</sup>-ATPase-rich cells can be routinely obtained, it can be plated in the form of primary cultures. This would open a complete new avenue of research because a myriad of techniques would be applicable. Since Na<sup>+</sup>/K<sup>+</sup>-ATPase- and V-H<sup>+</sup>-ATPase-rich cells can easily be recognized using specific antibodies, further separation of cell subtypes might not be necessary for the following experiments. Initial experiments should be focused on the effect of [HCO<sub>3</sub><sup>-</sup>], pH and *P*CO<sub>2</sub> on V-H<sup>+</sup>-ATPase translocation to the basolateral membrane. This could be examined using immunocytochemistry and confocal microscopy. It will also be possible to test the effects of inhibitors on signaling pathway components (sAC, PKA, PKC, CA, etc.). Assuming a primary culture enriched in V-H<sup>+</sup>-ATPase-rich cells is developed, pH<sub>i</sub> imaging experiments using BCECF-AM (see Parks *et al.*, 2007) will also be possible.

The molecular characterization of the ion-transporting proteins could be another related project. However, the development of a separation technique for Na<sup>+</sup>/K<sup>+</sup>-ATPase- and V-H<sup>+</sup>-ATPase-rich cells might be required previous to this task.

*ii- Acid/base regulation in hagfish*

The results presented in chapters VI and VII and appendix I can be used as the foundation for many years of research on hagfish A/B physiology. Immediate projects should be focused on the definitive elucidation of the cellular localization of V-H<sup>+</sup>-ATPase, NHE and Na<sup>+</sup>/K<sup>+</sup>-ATPase under normal, alkalotic and acidic blood conditions. Immunogold is probably the most adequate technique for this project. However, preliminary trials will be required in order to optimize it for hagfish and obtain a reasonable trade-off between antigen recognition by the antibodies and preservation of the structure of the lipid basolateral tubular system. In the longer term, the design of hagfish-specific antibodies is required and would constitute a significant advance.

The results presented in chapter VII suggest that V-H<sup>+</sup>-ATPase is involved in H<sup>+</sup> reabsorption to the blood during alkalosis. However, it is possible that basolateral NHEs are also responsible for H<sup>+</sup> reabsorption (alone or in conjunction with V-H<sup>+</sup>-ATPase) like I have shown in the crab *C. granulatus* in chapter IX. This hypothesis can be tested by injecting amiloride and bafilomycin into the blood stream of hagfish and monitoring blood pH and [HCO<sub>3</sub><sup>-</sup>] recovery after HCO<sub>3</sub><sup>-</sup> infusions. However, potential problems associated with this project are that the low solubility of amiloride in hagfish blood, and that the amount of bafilomycin required to achieve an effective concentration in hagfish blood might be rather expensive.

Finally, it would be useful to identify potential natural causes of blood alkalotic stress in hagfish. The primary candidate is a potential post-feeding

alkaline tide like it has been described in detail in dogfish (Walsh *et al.*, 2006; Wood *et al.*, 2005; 2007). Based on the scavenger and opportunistic feeding habits of hagfish (Fernholm, 1998), I predict that it experiences a pronounced post-feeding alkalosis that is counteracted by  $\text{HCO}_3^-$  secretion at the gills like I have shown in chapter V in dogfish.

At first sight, the experiments proposed above may look like a mere repetition of experiments already performed in dogfish. However, given the basal phylogenetic position of hagfish in the vertebrate lineage, these experiments will be important for evolutionary analyses.

### *iii- Acid/base regulation in teleost fish*

Some future directions related to research on A/B and ion uptake mechanisms in freshwater fish are listed at the end of chapter VIII. To those, I shall only add a few, which are based on the results from experiments on the posterior gill of the crab *C. granulatus*. Briefly, the potential role of gill basolateral and electrogenic NHEs in mediating  $\text{H}^+$  reabsorption and apical  $\text{Cl}^-/\text{HCO}_3^-$  exchange should be investigated. This potential NHE could be acting instead of, or in addition to, the basolateral  $\text{V-H}^+$ -ATPases I have proposed in chapter VIII.

Some avenues for new research in seawater teleosts may include the physiological characterization of branchial  $\text{V-H}^+$ -ATPase.  $\text{V-H}^+$ -ATPase has been shown to be present in the gills of the marine longhorn sculpin (Catches *et al.*, 2006) and of the seawater-adapted rainbow trout (Hawkings *et al.*, 2003) and killifish (Scott *et al.*, 2004). The better studied ion transporting

function in the gills of marine fish is NaCl secretion. This mechanism involves basolateral  $\text{Na}^+/\text{K}^+$ -ATPases and NKCCs and apical CFTR-like channels (reviewed by Marshall and Grosell, 2005), but not V- $\text{H}^+$ -ATPases. The role of V- $\text{H}^+$ -ATPase has been proposed to be  $\text{H}^+$  reabsorption and  $\text{HCO}_3^-$  secretion (Catches *et al.*, 2006, Hawkings *et al.*, 2003), like in dogfish gills. However, this hypothesis has not yet been directly tested. The first efforts in this regards should include simple western blotting experiments in gill samples from fish previously made alkalotic *via*  $\text{NaHCO}_3$  infusions.

#### *iv- Acid/base regulation in aquatic crabs*

An interesting question regarding A/B regulation in crab gills is whether different  $\text{H}^+$  and  $\text{HCO}_3^-$  secreting cells are present as has been demonstrated in many vertebrate species. The initial experiments should involve immunohistochemistry using anti- $\text{Na}^+/\text{K}^+$ -ATPase and V- $\text{H}^+$ -ATPase antibodies. The heterologous antibodies against fish ATPases used in this thesis might be acceptable for preliminary experiments. However, it will be necessary to design and produce crab specific antibodies in the longer term.

The isolated gill preparation is ideal for the study of signaling pathways related to A/B regulation. For example, addition of inhibitors specific for PKA, PKC and sAC can be added into the perfusates in order to see their effect on the low pH- and high  $[\text{HCO}_3^-]$ -stimulating mechanisms described on this thesis. Although I cannot predict which signaling pathway(s) is involved in each case, I expect that some inhibitors will have a differential effect on the

low pH- and the high  $[\text{HCO}_3^-]$ -stimulating mechanisms. This preparation should also be used to determine the presence of pH and  $\text{HCO}_3^-$  sensors.

Finally, it would also be important to analyze the branchial A/B regulatory mechanisms in crabs acclimated to seawater. In particular, I would be very interested to find out if a basolateral  $\text{V-H}^+$ -ATPase is functional for  $\text{HCO}_3^-$  secretion in marine crabs.

### **Corollary**

I firmly believe that this thesis illustrates the advantages and power of comparative physiology. Although some of the specific components of the branchial cellular mechanisms for A/B regulation differ between the experimental animals tested, the general principles behind those mechanisms are almost identical. In the most basic form, the model for A/B regulation in aquatic animals must include:

- 1) an organ with sufficient surface area and elevated irrigation rate (e.g. the gill),
- 2) diffusion of  $\text{CO}_2$  into specific ion-transporting cell(s),
- 3) generation of intracellular  $\text{H}^+$  and  $\text{HCO}_3^-$  by carbonic anhydrase,
- 4) a polarized epithelium that allows for the differential transport of  $\text{H}^+$  and  $\text{HCO}_3^-$  across the apical and basolateral membranes as dictated by the A/B status of the blood,
- 5) apical ion-transporting proteins to extrude  $\text{H}^+$  in response to acidosis ( $\text{Na}^+/\text{H}^+$  exchangers or  $\text{V-H}^+$ -ATPases),



6) basolateral ion-transporting proteins to reabsorb  $\text{HCO}_3^-$  into the blood during acidosis ( $\text{Cl}^-/\text{HCO}_3^-$  exchangers or  $\text{Na}^+/\text{HCO}_3^-$  cotransporters)

7) apical  $\text{HCO}_3^-$ -extruding proteins during alkalosis (some sort of  $\text{Cl}^-/\text{HCO}_3^-$  exchanger), and

8) a basolateral route of exit for  $\text{H}^+$  (NHEs or  $\text{V-H}^+$ -ATPases).

It is rewarding to compare the components described above with Fig. 1.1. Almost the entire model for systemic A/B regulation in aquatic animals can be obtained by placing the transporters involved in  $\text{pH}_i$  regulation in specific locations in a polarized epithelium. If we add a few mechanisms involved in cell volume regulation (see Hoffman and Simonsen, 1989), we can “design” almost any known ion-transporting epithelium and many regulatory pathways as well. For example, cell swelling and shrinking are known to regulate ion uptake across a couple of isolated crustacean gill epithelia (Onken, 1996; Tresguerres *et al.*, 2003) and also across isolated fish operculum (Marshall *et al.*, 2000; 2005). The mechanisms for  $\text{pH}_i$  and cell volume regulation are almost certainly very conserved and antique, since they were probably essential for the most primitive and original forms of life.

My results in dogfish gills suggest that a cellular response to alkalosis can potentially regulate the A/B status of the extracellular fluids of the entire organism. It is also possible that a great part of the systemic A/B regulatory mechanisms and signaling is based in the chemistry of  $\text{CO}_2$  and  $\text{HCO}_3^-$ . The simplicity of such system is astonishing, and illustrates how a complex

physiological function in a multicellular organism could have evolved from basic cellular functions and chemistry.

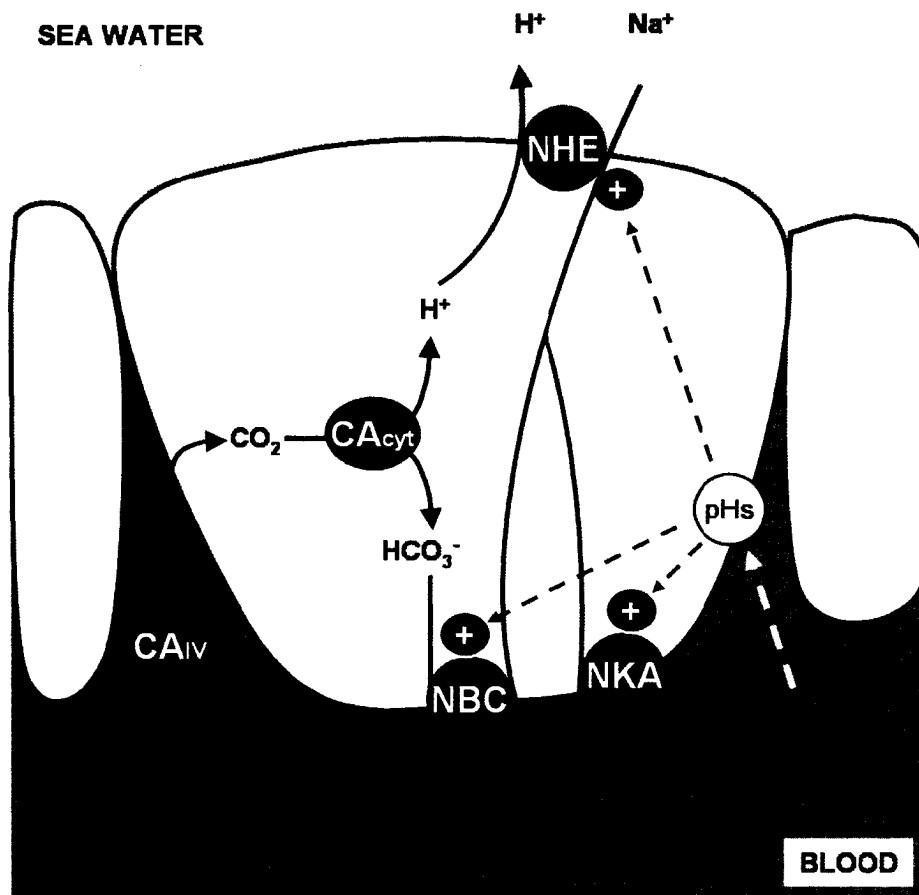


**Figure 10.1.** Cellular mechanism for  $H^+$  secretion and  $HCO_3^-$  reabsorption in dogfish gills. NHE:  $Na^+/H^+$  exchanger, probably NHE3 (Choe *et al.*, 2007); CA<sub>IV</sub>: extracellular carbonic anhydrase in the extracellular face of the basolateral membrane of pillar cells (Gilmour *et al.*, 2007). CA<sub>cyt</sub>: cytoplasmic carbonic anhydrase. NKA:  $Na^+/K^+$ -ATPase. NBC:  $Na^+/HCO_3^-$  cotransporter (after the results in trout by Parks *et al.*, 2007). CO<sub>2</sub> in plasma is also produced by CA in the red blood cells (not shown here, see fig. 10.3). pHs: pH sensor. The pHs senses a reduced pH<sub>e</sub> and/or pH<sub>i</sub> and activates NHE,  $Na^+/K^+$ -ATPase and/or NBC, probably by a pathway involving phosphorylation.

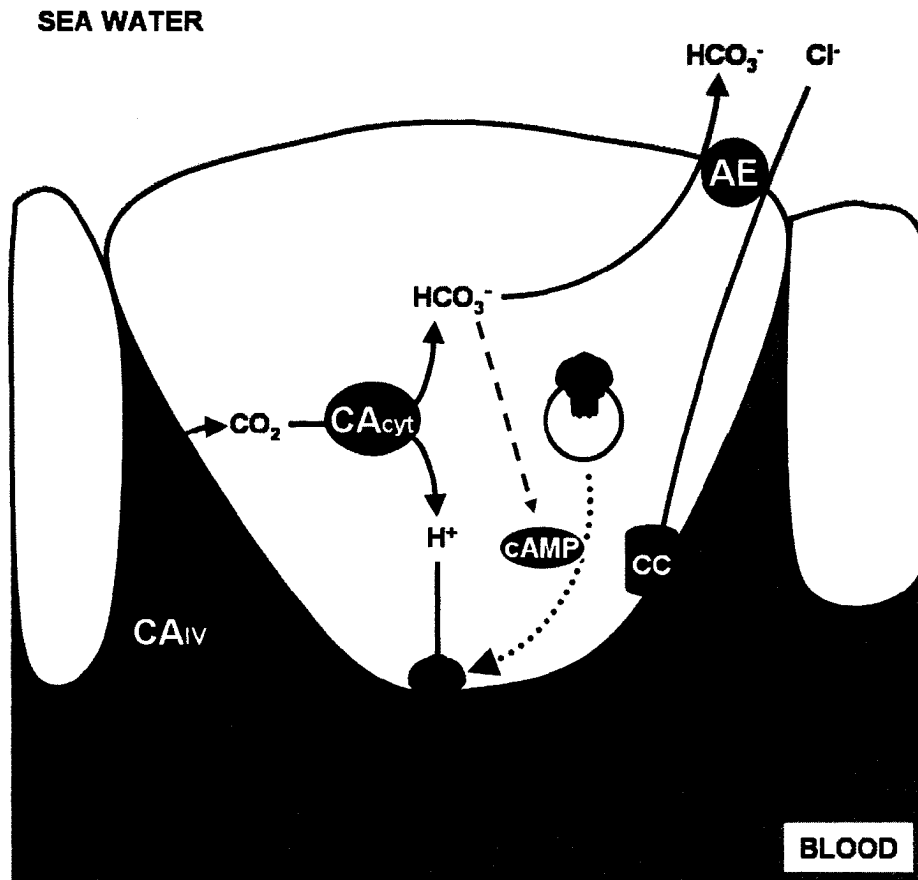


**Figure 10.2.** Cellular mechanism for  $\text{HCO}_3^-$  secretion and  $\text{H}^+$  reabsorption in dogfish gills. AE: anion exchanger, a Pendrin-like protein (Piermarini *et al.*, 2002; Evans *et al.*, 2004);  $\text{CA}_{\text{IV}}$ : extracellular carbonic anhydrase in the extracellular face of the basolateral membrane of pillar cells (Gilmour *et al.*, 2007).  $\text{CA}_{\text{cyt}}$ : cytoplasmic carbonic anhydrase. CC: chloride channel. Blue icon:  $\text{V-H}^+$ -ATPase.  $\text{CO}_2$  in plasma is also produced by CA in the red blood cells (not shown here, see fig. 10.3). Changes in intracellular pH or  $\text{HCO}_3^-$  triggers  $\text{V-H}^+$ -ATPase translocation from cytoplasmic vesicles to the basolateral membrane, where it mediates  $\text{H}^+$  reabsorption into the blood.

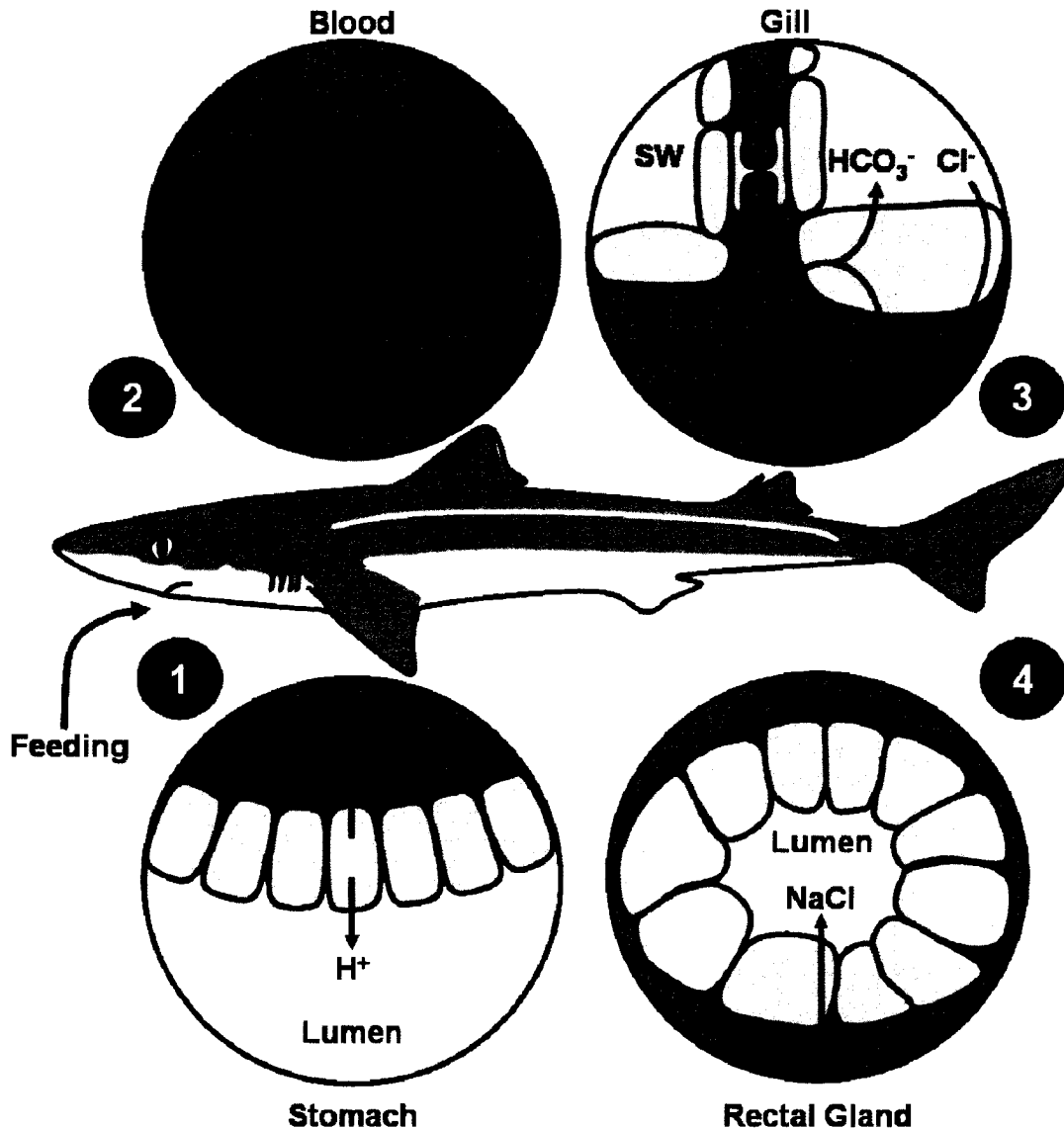


**Figure 10.3.** Integration of feeding, A/B at the gills and NaCl secretion at the rectal gland. 1)  $H^+$  secretion and  $HCO_3^-$  reabsorption into the blood related to food digestion. 2)  $CO_2$  generation in red blood cells (RBC). 3) Activation of  $HCO_3^-$  secretion and  $H^+$  reabsorption at the gills. See figure 10.2 for more details. 4) Activation of NaCl secretion at the rectal gland by an increase in  $pH_e$  (Shuttleworth *et al.*, 2006) and probably  $pH_i / [HCO_3^-]_i$ .

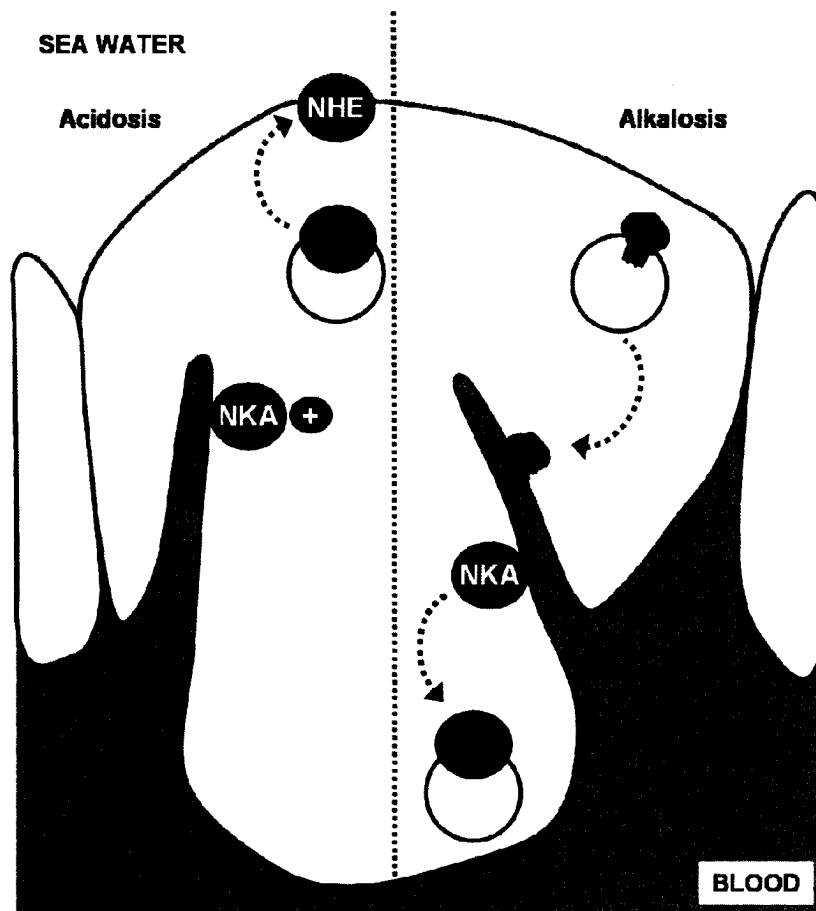


**Figure 10.4.** Insertion/removal of ion-transporting proteins involved in  $\text{HCO}_3^-$  and  $\text{H}^+$  secretion and reabsorption in hagfish gills. NHE:  $\text{Na}^+/\text{H}^+$  exchanger; NKA:  $\text{Na}^+/\text{K}^+$ -ATPase; blue icon:  $\text{V-H}^+$ -ATPase.

## References

- Bewely, M.S., Pena, J.T.G, Plesch, F.N., Decker, S.E. Weber G.J and Forrest, J.N.** (2006). Shark rectal gland vasoactive intestinal peptide receptor: cloning, functional expression, and regulation of CFTR chloride channels. *Am. J. Physiol. Reg. Integr. Comp. Physiol.* **291**,1157-1164.
- Burger, J.W. and Hess, W.N.** (1960). Function of the rectal gland in the spiny dogfish. *Science* **131**, 670-671.
- Catches, J.S., Burns, J.M., Edwards, S.L. and Claiborne, J.B.** (2006).  $\text{Na}^+/\text{H}^+$  antiporter,  $\text{V-H}^+$ -ATPase and  $\text{Na}^+/\text{K}^+$ -ATPase immunolocalization in a marine teleost (*Myoxocephalus octodecemspinosus*). *J. Exp. Biol.* **209**, 3440-3447.
- Choe, K.P., Edwards, S.L., Claiborne, J.B. and Evans, D.H.** (2007). The putative mechanism of  $\text{Na}^+$  absorption in euryhaline elasmobranchs exists in the gills of a stenohaline marine elasmobranch, *Squalus acanthias*. *Comp. Biochem. Physiol. A* **146**, 155-162.
- Choe, K.P., Kato, A., Hirose, S., Plata, C., Sindic, A., Romero, M. F., Claiborne, J.B. and Evans, D.H.** (2005). NHE3 in an ancestral vertebrate: primary sequence, distribution, localization, and function in gills. *Am. J. Physiol. Regul. Integr. Comp. Physiol.* **289**, R1520–R1534.
- Evans, D.H., Piermarini, P.M. and Choe, K.P.** (2004). Homeostasis: osmoregulation, pH regulation, and nitrogen excretion. In *Biology of Sharks and their relatives* (eds. J.C. Carrier, J.A. Musick and M.R. Heithaus), pp. 247-268. Boca Raton, FL, USA: CRC Press LLC.

**Evans, D.H., Piermarini, P.M. and Choe, K.P.** (2005). The multifunctional fish gill: dominant site of gas exchange, osmoregulation, acid-base regulation, and excretion of nitrogenous waste. *Physiol. Rev.* **85**: 97–177.

**Fernholm, B.** (1998). Hagfish systematics. In: *The Biology of Hagfishes* (eds. J. Jørgensen, J. Lomholt, R. Weber and H. Malte), pp 33-44. London: Chapman and Hall.

**Galvez, F., Reid, S.D., Hawkings, G. and Goss, G.G.** (2002). Isolation and characterization of mitochondria-rich cell types from the gill of freshwater rainbow trout. *Am. J. Physiol. Reg. Integr. Comp. Physiol.* **282**, R658-668.

**Genovese, G., Ortiz, N., Urcola, M. R. and Luquet, C. M.** (2005). Possible role of carbonic anhydrase, V-H<sup>+</sup>-ATPase, and Cl<sup>-</sup>/HCO<sub>3</sub><sup>-</sup> exchanger in electrogenic ion transport across the gills of the euryhaline crab *Chasmagnathus granulatus*. *Comp. Biochem. Physiol. A* **142**, 362-369.

**Gilmour, K., Bayaa, M., Kenney, L., McNeill, B. and Perry, S.** (2006). Type IV carbonic anhydrase is present in the gills of spiny dogfish (*Squalus acanthias*). *Am. J. Physiol. Reg. Integr. Comp. Physiol.* **292**: R556-567.

**Gilmour, K.M., Perry, S.F., Bernier, N.J., Henry, R.P. and Wood, C.M.** (2001). Extracellular carbonic anhydrase in the dogfish, *Squalus acanthias*: a role in CO<sub>2</sub> excretion. *Physiol. Biochem. Zool.* **74**, 477-492.



**Goss, G.G., Adamia, S. and Galvez, F.** (2001). Peanut lectin binds to a subpopulation of mitochondria rich cells in the rainbow trout gill epithelium. *Am. J. Physiol. Regul. Integr. Comp. Physiol.* **281**, R1718-R1725.

**Hawkings, G.S., Galvez, F. and Goss, G.G.** (2004). Seawater acclimation causes independent alterations in  $\text{Na}^+/\text{K}^+$ - and  $\text{H}^+$ -ATPase activity in isolated mitochondria-rich cell subtypes of the rainbow trout gill. *J. Exp. Biol.* **207**, 905–912.

**Heisler, N.** (1988). Acid-base regulation. In *Physiology of Elasmobranch Fishes* (ed. T. J. Shuttleworth), pp. 215-252. Berlin: Springer-Verlag.

**Hoffmann, E. K. and Simonsen, L. O.** (1989). Membrane mechanisms in volume and pH regulation in vertebrate cells. *Physiol. Rev.* **69**, 315-382.

**Jones, B. C. and Geen, G. H.** (1977). Food and feeding of spiny dogfish (*Squalus acanthias*) in British Columbia waters. *J. Fish. Res. Board Can.* **34**, 2067 -2078.

**Luquet, C.M., Genovese, G., Rosa, G.A. and Pellerano, G.N.** (2002). Ultrastructural changes in the gill epithelium of the crab *Chasmagnathus granulatus* (Decapoda: Grapsidae) in diluted and concentrated seawater. *Mar. Biol.* **141**, 753-760.

**Marshall, W.S., Bryson, S.E. and Luby, T.** (2000). Control of epithelial  $\text{Cl}^-$  secretion by basolateral osmolality in the euryhaline teleost *Fundulus heteroclitus*. *J. Exp. Biol.* **203**, 1897-1905.

**Marshall, W.S. and Grosell, M.** (2005). Ion transport, osmoregulation and acid-base balance. In *The Physiology of Fishes* (ed. D.H. Evans and J.B. Claiborne), pp. 177-230. Boca Raton, FL, USA: CRC Press.

**Marshall, W. S., Ossum, C. G. and Hoffmann, E. K.** (2005). Hypotonic shock mediation by p38 MAPK, JNK, PKC, FAK, OSR1 and SPAK in osmosensing chloride secreting cells of killifish opercular epithelium. *J. Exp. Biol.* **208**, 1063-1077.

**McCormick, S.D.** (1995). Hormonal control of gill  $\text{Na}^+$ ,  $\text{K}^+$ -ATPase and chloride cell function. In: *Cellular and Molecular Approaches to Fish Ionic Regulation* (eds. C.M. Wood and T.J. Shuttleworth). San Diego, CA, USA: Academic.

**Onken, H.** (1996). Active and electrogenic absorption of  $\text{Na}^+$  and  $\text{Cl}^-$  across posterior gills of *Eriocheir sinensis*: influence of short-term osmotic variations. *J. Exp. Biol.* **199**, 901-910.

**Onken, H. and Riestenpatt, S.** (1998). NaCl absorption across split gill lamellae of hyperregulating crabs: transport mechanisms and their regulation. *Comp. Biochem. Physiol. A* **119**, 883-893.

**Parks, S.K., Tresguerres, M. and Goss, G.G.** (2007). Interactions between  $\text{Na}^+$  channels and  $\text{Na}^+\text{-HCO}_3^-$  cotransporters in the freshwater fish gill MR cell: a model for transepithelial  $\text{Na}^+$  uptake. *Am. J. Physiol. Cell Physiol.* **292**, C935-C944.

**Perry S.F., Davie, P.S., Daxboeck, C. and Randall, D.J.** (1982). A comparison of  $\text{CO}_2$  excretion in a spontaneously ventilating blood-perfused

trout preparation and saline-perfused gill preparations: contribution of the branchial epithelium and red blood cell. *J. Exp. Biol.* **101**, 47–60.

**Perry, S.F., Payan, P. and Girard, J.P.** (1984). The effects of perfusate  $\text{HCO}_3^-$  and  $\text{PCO}_2$  on chloride uptake in perfused gills of rainbow trout (*Salmo gairdneri*). *Can. J. Fish Aquat. Sci.* **41**, 1768–1773.

**Perry, S.F., Shahsavarani, A., Georgalis, T., Bayaa, M., Furimsky, M. and Thomas, S.L.Y.** (2003). Channels, pumps, and exchangers in the gill and kidney of freshwater fishes: their role in ionic and acid-base regulation. *J. Exp. Zool.* **300**: 53–62.

**Piermarini, P.M., Verlander, J.W., Royaux, I.E. and Evans, D.H.** (2002). Pendrin immunoreactivity in the gill epithelium of a euryhaline elasmobranch. *Am. J. Physiol. Reg. Integr. Comp. Physiol.* **283**, R983-992.

**Reid, S.D., Hawkings, G.S., Galvez, F. and Goss, G.G.** (2003). Localization and characterization of phenamil-sensitive  $\text{Na}^+$  influx in isolated rainbow trout gill epithelial cells. *J. Exp. Biol.* **206**, 551–559.

**Reilly, R.F. and Ellison, D.H.** (2000). Mammalian distal tubule: physiology, pathophysiology, and molecular anatomy. *Physiol. Rev.* **80**, 277-313.

**Schwartz, G.J., Tsuruoka, S., Vijakumar, S., Petrovic, S., Mian, A., and Al-Awqati, Q.** (2001). Acid incubation reverses the polarity of intercalated cell transporters, an effect mediated by hensin. *J. Clin. Invest.* **109**, 89-99.

**Scott, G.R., Richards, J.G., Forbush, B., Isenring, P. and Schulte, P.M.** (2004). Changes in gene expression in gills of the euryhaline killifish *Fundulus heteroclitus* after abrupt salinity transfer. *Am. J. Physiol. Cell Physiol.* **287**, C300–C309.

**Serrano, R., Martin, H., Casamayor, A. and Ariño, J.** (2006). Signaling alkaline stress in the yeast *Saccharomyces cerevisiae* through the Wsc1 cell surface sensor and the Slr2 MAPK pathway. *J. Biol. Chem.* **281**, 39785-39795.

**Shuttleworth, T. J., Thompson, J., Munger, R. S. and Wood, C. M.** (2006). A critical analysis of carbonic anhydrase function, respiratory gas exchange, and the acid-base control of secretion in the rectal gland of *Squalus acanthias*. *J. Exp. Biol.* **209**, 4701-4716.

**Siegel, N.J., Silva, P., Epstein, F.H., Maren, T.H. and Hayslett, J.P.** (1975). Functional correlates of the dogfish rectal gland during *in vitro* perfusion. *Comp. Biochem. Physiol. A* **51**, 593-597.

**Silva, P., Epstein, F.H. and Solomon, R.J.** (1992). The effect of mercury on chloride secretion in the shark (*Squalus acanthias*) rectal gland. *Comp. Biochem. Physiol. C* **103**, 569-575.

**Solomon, R.J., Taylor, M., Sheth, S., Silva, P. and Epstein, F.H.** (1985). Primary role of volume expansion in stimulation of rectal gland function, *Am. J. Physiol. Reg. Int. Comp. Physiol.* **246**, R67–R71.

**Srivastava, J., Barber, D.L. and Jacobson, M.P.** (2007). Intracellular pH sensors: design principles and functional significance. *Physiol.* **22**, 30-39.

- Stoff, J.S., Sosa, R., Hallac, R., Solva, P. and Epstein, F.H. (1979).** Hormonal regulation of active chloride transport in the dogfish rectal gland. *Am. J. Physiol. Renal Physiol.* **237**, 138-144.
- Thorson, T.B. (1958).** Measurement of the fluid compartments of four species of marine Chondrichthyes. *Physiol. Zool.* **31**, 16-23.
- Tort, L. Gonzalez-Arch, F., Torres, P. and Hidalgo, J. (1991).** On the blood volume of the Mediterranean dogfish, *Scyliorhinus canicula*. *Fish. Physiol. Biochem.* **9**, 173-177.
- Tresguerres, M., Onken, H., Perez, A. F. and Luquet, C. M. (2003).** Electrophysiology of posterior, NaCl-absorbing gills of *Chasmagnathus granulatus*: rapid responses to osmotic variations. *J. Exp. Biol.* **206**, 619-626.
- Walsh, P.J., Kajimura, M. Mommsen, T.P. and Wood, C.M. (2006).** Metabolic organization and effects of feeding on enzyme activities of the dogfish shark (*Squalus acanthias*) rectal gland. *J. Exp. Biol.* **209**, 2929-2938.
- Wang, T., Busk, M. and Overgaard, J. (2001).** The respiratory consequences of feeding in amphibians and reptiles. *Comp. Biochem. Physiol. A* **128**, 533-547.
- Wilson, J.M., Randall, D.J., Vogl, A.W., Harris, J., Sly, W.S. and Iwama, G.K. (2000).** Branchial carbonic anhydrase is present in the dogfish, *Squalus acanthias*. *Fish Physiol. Biochem.* **22**, 329-336.
- Wang, Y., Lam, C.S., Wu, F., Wang, W., Duan, Y. and Huang, P. (2005).** Regulation of CFTR channels by HCO<sub>3</sub><sup>-</sup>-sensitive soluble adenylyl

cyclase in human airway epithelial cells. *Am. J. Physiol. Cell Physiol.* **289**, C1145-1151.

**Wong C.K. and Chan, D.K.** (1999a). Isolation of viable cell types from the gill epithelium of Japanese eel *Anguilla japonica*. *Am. J. Physiol. Reg. Int. Comp. Physiol.* **276**, R363-R372.

**Wong, C. K. and Chan, D. K.** (1999b). Chloride cell subtypes in the gill epithelium of Japanese eel *Anguilla japonica*. *Am. J. Physiol. Reg. Int. Comp. Physiol.* **277**, R517 -R522.

**Wood, C.M., Kajimura, M., Mommsen, T.P. and Walsh, P.J.** (2005). Alkaline tide and nitrogen conservation after feeding in an elasmobranch (*Squalus acanthias*). *J. Exp. Biol.* **208**, 2693-2705.

**Wood, C. M., Kajimura, M., Bucking, C. and Walsh, P. J.** (2007a). Osmoregulation, ionoregulation and acid-base regulation by the gastrointestinal tract after feeding in the elasmobranch (*Squalus acanthias*). *J. Exp. Biol.* **210**, 1335-1349.

**Wood, C. M., Munger, R. S., Thompson, J. and Shuttleworth, T. J.** (2007b). Control of rectal gland secretion by blood acid-base status in the intact dogfish shark (*Squalus acanthias*). *Resp. Physiol. Neurobiol.* **156**, 220-228.

**Yang, X., Amemiya, M., Peng, Y., Moe, O.W., Preisig, P.A. and Alpern, R.J.** (2000). Acid incubation causes exocytic insertion of NHE3 in OKP cells. *Am. J. Physiol. Cell Physiol.* **279**, 410-419.

## Appendix I

### Blood and gill responses to HCl infusions in the Pacific hagfish (*Eptatretus stoutii*)<sup>1</sup>

<sup>1</sup>A version of this appendix has been accepted for publication. Parks, S.K.\*, **Tresguerres, M.\*** and Goss, G.G. (2006). *The Canadian Journal of Zoology*.  
\*Both authors contributed equally to this work. Reproduced with permission of The National Research Council of Canada Press and the co-authors of the manuscript.

## Introduction

The hagfish is the only vertebrate with an internal ionic composition similar to that of the surrounding seawater (Alt *et al.*, 1980, Morris, 1965). Although hagfish do not osmoregulate their internal fluids to any appreciable extent, their gill epithelium possess great numbers of mitochondria-rich (MR) cells, which are similar to the typical “chloride” cells used for osmoregulation in other marine fishes (Mallatt *et al.*, 1987). In Atlantic and Pacific hagfish, MR cells on the trailing region of the gill express  $\text{Na}^+/\text{K}^+$ -ATPase,  $\text{Na}^+/\text{H}^+$  exchangers (NHE), carbonic anhydrase (CA), and  $\text{V-H}^+$ -ATPase (Choe *et al.*, 1999, Choe *et al.*, 2002, Edwards *et al.*, 2001, Mallatt *et al.*, 1987, Tresguerres *et al.*, 2006a; chapter VI). Since these transporters are implicated in both ionic and pH regulatory mechanisms in a variety of fishes (Evans *et al.*, 2005), it has been proposed that their role in the hagfish MR cells is primarily for acid-base regulation (Mallatt *et al.*, 1987).

All animals periodically face the challenge of adjusting blood pH due to respiratory or metabolic acidosis. Hagfish are under a continual challenge to maintain plasma pH at appropriate levels. They live in oxygen-poor conditions in the deep sea, which at least in the Atlantic hagfish is compensated by using anaerobic metabolism (Hansen and Sidell, 1983). Furthermore, they utilize sudden bursts of swimming in search of food that have been shown to cause a severe lactic acidosis in the blood of Pacific hagfish (Ruben and Bennet, 1980). Hagfish are also known to slightly hyper-regulate  $\text{Na}^+$  but not  $\text{Cl}^-$  in the plasma and Mallatt *et al.* (1987) proposed that this is likely due to a



net branchial excretion of  $H^+$  required for the acidosis produced by the animal in the conditions listed above.

Evans (1984) proposed that hagfish use the orthodox mechanism of acid-base regulation consisting of exchanging  $Na^+$  for  $H^+$  and  $Cl^-$  for  $HCO_3^-$  at the apical side of the gill. More recent studies have focused on the specific cellular mechanism for the pH compensating mechanism. Based on an increase in mRNA expression in response to metabolic acidosis (Edwards *et al.*, 2001), the primary candidate for apical  $Na^+/H^+$  exchange is a NHE-like protein. In addition, NHE2-like immunoreactivity (NHE2 L-IR) was shown in MR cells at the gill of Pacific hagfish (Tresguerres *et al.*, 2006a; chapter VI). Although the immunolabeling pattern was described as predominantly cytoplasmic, a minority of cells showed concentrated signal in apical regions and a role of NHE cycling from cytoplasmic vesicles to the apical plasma membrane was proposed to occur in response to acidosis. The goal of this study was to induce a metabolic acidosis *via* serial acid infusions ( $HCl$   $6000 \mu mol.kg^{-1}$ ) over a 24h period and investigate subsequent changes in abundance and cellular localization of an NHE-like protein found in Pacific hagfish. Our results confirm the role of an apical NHE in the mechanism for acid recovery at the hagfish gill.

## Materials and Methods

### *Animals*

Animals were captured and held in the same conditions as in chapter VII.

### *Antibodies and reagents*

Antibodies and reagents were the same as in chapters VI and VII.

### *HCl infusions*

Hagfish (mean body mass  $89.00 \pm 5.86$  g) were anaesthetized in seawater containing 1: 1000 tricaine methanesulfonate (TMS; AquaLife, Syndel Laboratories Ltd, Vancouver, BC, Canada) and suspended by the head, which causes blood to accumulate in the caudal subcutaneous sinus. After taking a 200  $\mu$ l blood sample ( $t=0$  h), acid ( $250 \text{ mmol l}^{-1}$  HCl,  $250 \text{ mmol l}^{-1}$  NaCl) was injected using a heparinized 21G syringe to achieve a HCl load of  $6000 \mu\text{mol. kg}^{-1}$ . A similar infusion protocol has been used successfully with sulphuric acid by McDonald *et al.* (1991) and Edwards *et al.* (2001). Hagfish were then inverted several times to facilitate mixing throughout the sinus and placed in individual seawater flow-through tanks (20 l) for the duration of the experiment. Subsequent blood samples were taken at  $t=3, 6, 9, 12, 18$ , and  $24$  h with acid infusions repeated at  $t=6, 12$ , and  $18$  h.

### *Blood sample analysis and terminal sampling*

These protocols were performed as explained in chapter VII.

### *Immunohistochemistry*

Gill fixation, sectioning and immunolabeling were done as in chapters VI and VII.

To detect potential changes in the cellular localization of NHE2-like proteins, we analyzed the staining pattern of NHE2-immunoreactive cells from 3 random fields of view (640x) of sections from 3 fish per treatment (9 fields of view per treatment). We analyzed a total of 178 cells from NaCl-infused fish, and 176 from HCl-infused fish.

#### *Western blotting*

Frozen gill samples were immersed in liquid nitrogen and pulverized in a porcelain grinder. The resultant powder was resuspended in 1:10 w/v of ice-cold homogenization buffer (250 mmol l<sup>-1</sup> sucrose, 1 mmol l<sup>-1</sup> EDTA, 30 mmol l<sup>-1</sup> Tris, 100 mg ml<sup>-1</sup> PMSF and 2 mg ml<sup>-1</sup> pepstatin, pH 7.40), and sonicated on ice (3 pulses of 5 sec each). Debris was removed by low speed centrifugation (3000 g, 10 min, 4°C). An aliquot of the supernatant was stored at -80°C (whole gill homogenate), and the remaining supernatant was centrifuged at high speed (100000 g, 60 min, 4°C) to obtain the whole membrane fraction of the gill. Aliquots of both the whole gill and gill membrane fractions were saved for protein determination (Pierce, IL, USA).

Processed gill samples were used for western blotting as explained in the previous chapters.

#### *Statistics*

All data are given as means ± s.e.m. Differences between groups were tested using one-way repeated measures analysis of variance (1-way

ANOVA), Student's t-test, Man Whitney one-tailed test, or two-way repeated measures analysis of variance (2-way-RM-ANOVA) followed by Bonferroni's post test when appropriate. Statistical significance was set at  $P < 0.05$ . All statistical analyses were performed on GraphPad Prism v.3.0 (GraphPad Software, San Diego California USA).

## Results

### *i- 24 HCl Infusions: Blood and plasma variables*

No notable changes in blood pH were found in NaCl infused controls, but a marked blood acidosis was induced upon injection of HCl. Blood pH was reduced from  $7.93 \pm 0.02$  at  $t=0$  h to  $6.21 \pm 0.07$  at  $t=3$  h (Fig. 11.1A). Remarkably, blood pH was restored to  $7.31 \pm 0.09$  by 6 h without any mortality. Secondary HCl infusions also resulted in blood acidification, but they were significantly less severe in comparison to the initial stress ( $6.21 \pm 0.07$  at  $t=3$  h vs.  $6.73 \pm 0.06$  at  $t=9$  h,  $p<0.05$ ,  $N=5$ ). The fact that the fish were infused at this point with an already depressed blood pH and did not experience an increased acidification compared to the original HCl infusion indicates that acid-recovery mechanisms had been initiated. Following this, blood pH was measured at 6 h time periods to prevent anemia. Blood pH remained stable at  $t=12$ , 18 and 24 h despite the repeated acid-infusions. Although this new steady state represented a significant recovery from the induced acidosis, it remained significantly lower than NaCl infused controls (Fig. 11.1A).

Total CO<sub>2</sub> levels followed a pattern similar to the pH changes induced by HCl infusion. Starting at a similar level to control, TCO<sub>2</sub> was essentially undetectable at  $t=3$  h ( $0.08 \pm 0.08$  mmol l<sup>-1</sup>), rebounded slightly at  $t=6$  h ( $1.82 \pm 1.38$  mmol l<sup>-1</sup>), returned close to 0 mmol l<sup>-1</sup> at  $t=9$  h ( $0.52 \pm 0.52$  mmol l<sup>-1</sup>) before returning to control levels at  $t=12$ , 18, and 24 h in HCl-infused fish (Fig. 11.1B). Although there were noticeable differences in TCO<sub>2</sub> between NaCl

and HCl infused fish, no statistical significance was recorded at any point likely due to the large variability in the samples.

Plasma  $[\text{Na}^+]$  in NaCl and HCl infused fish were similar at all time points except for  $t=3$  h where HCl infused fish had significantly reduced levels compared to control fish (Table 11.1). Both NaCl and HCl infused fish had an elevation of plasma  $[\text{Na}^+]$  from  $t=9-24$  h (Table 10.1). Analysis of plasma  $[\text{Cl}^-]$  showed no significant differences between treatments and sampling times.  $[\text{Cl}^-]$  values were quite variable ranging from mean lows of  $391.72 \pm 26.28$  to a mean high of  $511.86 \pm 24.29$   $\text{mmol l}^{-1}$ . We do not know the cause of this high variability, but some possible explanations are interference with  $\text{NO}_3^-$  or plasma proteins.

*ii-  $\text{Na}^+/\text{K}^+$ -ATPase,  $\text{V-H}^+$ -ATPase, and  $\text{Na}^+/\text{H}^+$ -exchanger 2 (NHE2) gill abundance*

There were no significant differences in  $\text{Na}^+/\text{K}^+$ -ATPase abundance in whole-gill ( $1.63 \pm 0.10$  vs.  $1.89 \pm 0.27$  a.f.u.,  $p>0.05$ ) and whole-membrane ( $0.75 \pm 0.11$  vs.  $0.74 \pm 0.16$  a.f.u.,  $p>0.05$ ) homogenates from NaCl and HCl infused fish.  $\text{V-H}^+$ -ATPase demonstrated no significant changes in abundance in both whole-gill ( $1.56 \pm 0.15$  vs.  $2.30 \pm 0.30$  a.f.u.,  $p>0.05$ ,  $N=5$ ) and whole-membrane ( $0.25 \pm 0.04$  vs.  $0.40 \pm 0.09$  a.f.u.,  $p>0.05$ ,  $N=5$ ) fractions from NaCl-infused fish compared to HCl-infused fish. HCl-infused fish exhibited a significant increase in NHE2-like abundance in whole gill compared to NaCl-infused fish ( $2.30 \pm 0.43$  vs.  $0.99 \pm 0.14$  a.f.u.,  $p<0.05$ ,  $N=5$ , Fig. 11.2A), indicating increased synthesis of a NHE-like protein in acidotic hagfish. The

whole-membrane fraction of HCl-infused fish also showed a significant increase in NHE2-like abundance compared to NaCl fish ( $2.10 \pm 0.23$  vs.  $1.14 \pm 0.29$  a.f.u.,  $p < 0.05$ ,  $N=5$ , Fig. 11.2B).

*iii- Na<sup>+</sup>/K<sup>+</sup>-ATPase, V-H<sup>+</sup>-ATPase, and NHE2 gill immunohistochemistry*

Serial sections revealed that control fish demonstrated that Na<sup>+</sup>/K<sup>+</sup>-ATPase, V-H<sup>+</sup>-ATPase, and NHE2 like-immunoreactivity (L-IR) was generally located in the same gill cells, as we noted previously (Tresguerres *et al.*, 2006a; chapter VI) (Fig. 11.3A, C, E). Na<sup>+</sup>/K<sup>+</sup>-ATPase, V-H<sup>+</sup>-ATPase, and NHE2 L-IR displayed an almost exclusive cytoplasmic distribution, but a minority of cells labeled slightly apically for NHE2 L-IR (Fig. 11.3E). In HCl-infused fish, Na<sup>+</sup>/K<sup>+</sup>-ATPase and V-H<sup>+</sup>-ATPase staining remained unchanged compared to controls (Fig. 11.3B, D). However, NHE2 L-IR was unique in that there was a clear increase in the intensity of labeling at the apical region in a large number of cells (Fig. 11.3F). This intensity of apical labeling was rarely observed in NaCl infused fish.

*iv- Quantification of cytoplasmic, intermediate, and apical NHE2 L-IR localization*

High magnification (1600x) images representing the three distinct cellular immunolabeling patterns for NHE2 L-IR are shown in figure 6. Many cells labeled strictly in the cytoplasm (Fig. 11.4A). Other cells had a more concentrated labeling in the apical region but were not as distinctly apical so as such were categorized as intermediate (Fig. 11.4B) while the remaining cells had a distinctly apical labeling pattern as noted in figure 11.4C.

Quantification of cells revealed that in control fish, ~73 % exhibited NHE2 L-IR in a cytoplasmic manner, 20 % labeled intermediate, and only 7 % labeled apically (Table 11.2). In contrast, HCl-infused fish cells had 54 % that labeled cytoplasmically, 19 % labeled intermediate, and 27 % labeled apically (Table 11.2). Apical localization in HCl infused fish was significantly higher than controls while cytoplasmic staining was significantly higher in control fish ( $p < 0.05$ , Table 11.2). Intermediate staining did not vary between treatments.



## Discussion

We have demonstrated that the Pacific hagfish can readily recover from metabolic blood acidosis. To our knowledge this is the greatest acidification of blood pH ever reported in the fish literature. As a comparison, when a similar HCl load was attempted in experiments on the Pacific spiny dogfish, mortality was 100% within a few hours (Tresguerres *et al.*, 2005; chapter II). This degree of acidosis, while large, is not unreasonable for the Pacific hagfish. Ruben and Bennet (1980) demonstrated that only 5 minutes of exercise resulted in a drop in blood pH by 0.70 units (1.5 hours following exercise) due to lactic acid build-up. Additionally, hagfish are known to live in extremely hypoxic, even anoxic conditions and utilize anaerobic metabolism which necessitates a strong  $H^+$  excretion mechanism.

Our results suggest that activation of a branchial  $H^+$  secretory mechanism is at least partially responsible for the strong pH recovery in hagfish. After the pronounced blood acidosis induced by the initial HCl load, subsequent acidification events are less pronounced. This suggests that activation of  $H^+$  secretion was initiated within 6 hours of the initial HCl load. Specific aspects of the branchial mechanism include increased synthesis of an NHE-like protein of currently unknown molecular identity. In addition, the density of this transporter increases at the apical region of the gill MR cells.

We must point out that our HCl infusion method is not without certain flaws, most of which are explained in detail by McDonald *et al.*, 1991. The greatest limitation is that the blood from the caudal sinus and that of systemic

vessels might be slow to equilibrate with each other (Forster *et al.*, 1989). However, equilibration required ~8 h (Forster *et al.*, 1989), which would give plenty of time for the diffusion of  $H^+$  from the subcutaneous sinus into the systemic blood in our 24 h infusion experiments. Supporting this assumption, the observed changes at the gill demonstrate that the systemic blood was indeed affected by the HCl infusions into the subcutaneous sinus, albeit the pH disturbance might have been of a smaller magnitude compared to the sinus blood. Similarly, injections of HCl,  $NH_4Cl$  and even urea into the peritoneal space (another compartment with presumably slow equilibration with the systemic blood) have been traditionally used in fish in order to induce acid/base disturbances of the systemic blood and look for branchial ion fluxes and/or changes in the abundance/expression of ion-transporting proteins (for recent works see Catches *et al.*, 2006; Claiborne *et al.*, 1997; 1999; Ip *et al.*, 2005; Lim *et al.*, 2004). Therefore, we consider that our infusion protocol was suitable for our goal of inducing blood acidosis.

Secretion of  $H^+$  using NHEs would result in a  $Na^+$  load in the blood. Although there were changes in plasma  $[Na^+]$  during the experiments, they occurred in both NaCl and HCl infused fish. Therefore, we can not relate them to activation of a NHE system in HCl-infused fish. Given the high  $[Na^+]$  of hagfish plasma, detection of the putative  $Na^+$  fluxes require the use radiotracer techniques.

Our results suggest a relocation of NHE within hagfish gill MR cells in response to acidosis, which is an event previously unreported in the fish

literature. The role of membrane transporter translocation from cytoplasmic vesicles to the plasma membrane with respect to ion transport and acid-base regulation has been well illustrated in a number of systems (Breton and Brown, 2007, Dames *et al.*, 2006, Pastor-Soler *et al.*, 2003, Tresguerres *et al.*, 2005, 2006*b*; chapters II and III). It is now evident from this study that membrane transporter translocation from cytoplasmic vesicles to the apical plasma membrane may be important also in the hagfish.

NHE involvement in acid-base regulation has been traditionally proposed for seawater animals (Claiborne *et al.*, 2002, Claiborne *et al.*, 1997, Edwards *et al.*, 2001, Edwards *et al.*, 2002, Evans *et al.*, 2005). However, determining the sub-cellular localization of both NHE2 and NHE3 like immunoreactivity has been difficult due to granular cytoplasmic staining in several marine elasmobranchs and teleosts (Catches *et al.*, 2004; Edwards *et al.*, 2002) thereby hindering conclusions about its specific function. More recently, Catches *et al.* (2006) used species-specific antibodies and demonstrated NHE2 localization in the apical region of certain gill cells of the longhorn sculpin. However, confocal microscopy showed that NHE was not located directly on the membrane and that the NHE signal was punctuated and in the cytoplasm in most immunoreactive cells. In addition, the abundance of this NHE did not change in response to four sequential intraperitoneal HCl infusions over an 8 h period. Nonetheless, the authors proposed that NHE2-containing vesicles move to the apical membrane during blood acidosis in order to secrete the excess  $H^+$ . Finally, apical, cytoplasmic

and/or basolateral NHE localization have been found in the spiny dogfish gill (Weakly *et al.*, 2003) as well as in a variety of mammalian tissues (Wakabayashi *et al.*, 1997). Our observation of an increased NHE2-like immunoreactivity (NHE2 L-IR) at the apical plasma membrane region under acid-stressed conditions and increased abundance in gill membranes suggests a role for NHE relocation and involvement in acid secretion for the hagfish.

We should note that we have used an antibody raised against mammalian NHE2 and there is the potential for cross-reactivity with other NHE isoforms. To date, only a partial NHE clone has been obtained from the Atlantic hagfish (Edwards *et al.*, 2001). The hagfish NHE was not closely related to any other vertebrate isoforms but was found to group closest to the mammalian NHE3 and the invertebrate NHE (Edwards *et al.*, 2001). This putative NHE was implicated in acid recovery though as there was a significant increase in NHE mRNA expression at 2 h post acid infusion. Conversely, NHE2 (Tresguerres *et al.*, 2006a; chapter VI) and NHE1 and 3 (Choe *et al.*, 2002) immunoreactivity have been shown in hagfish using mammalian antibodies. This coupled with the apical localization of NHE3 shown in Atlantic stingray (Choe *et al.*, 2005) make it possible that our results represent an increase and translocation of an NHE similar to NHE3. However, it is also conceivable that the observed changes in expression are due to multiple NHE isoforms of an identical molecular weight being detected and

differentially regulated during the acidosis. Unfortunately, using our techniques we cannot determine if this has occurred.

Recent research into acid- base regulatory mechanisms in both elasmobranchs (Choe *et al.*, 2005, Piermarini and Evans, 2001, Tresguerres *et al.*, 2005; chapter II) and teleosts (Catches *et al.*, 2006; Goss *et al.*, 2001, Galvez *et al.*, 2002, Parks *et al.*, 2007; Reid *et al.*, 2003) suggest that independent cell types exist for net acid and net base secretion. However, based on the data presented in this paper and previous research from our lab (Tresguerres *et al.*, 2006a; chapter VI), it appears that hagfish possess only a single MR cell type. This cell must perform either net  $H^+$  or net  $HCO_3^-$  secretion as required creating unique demands for subcellular control over surface expression of transporters. We hypothesize that the  $H^+$  transporting NHEs are normally sequestered into vesicles. During acidosis, the response of increasing synthesis of NHE (genomic response) must be coupled with insertion of new and existing NHEs into the apical membrane (post-translational response) and together this would ensure that acid secretion dominates over base secretion under these conditions.

In summary, we have demonstrated that Pacific hagfish can restore blood pH following an induced metabolic acidosis. This ability is likely enabled *via* the increased synthesis of a NHE-like protein in the gill coupled with an apparent translocation of this transporter to the apical region of the gill cells.

**Table 11.1.** Plasma  $[\text{Na}^+]$  ( $\text{mmol l}^{-1}$ ) of the experimental hagfish at the sampling times.

Time (h)	(NaCl Infused)	(HCl Infused)
0	473.67 $\pm$ 11.59	468.03 $\pm$ 5.42
3	473.78 $\pm$ 8.63	436.19 $\pm$ 16.61 <sup>#</sup>
6	470.88 $\pm$ 7.81	458.05 $\pm$ 10.67
9	517.89 $\pm$ 9.34*	505.90 $\pm$ 9.43*
12	529.64 $\pm$ 5.62*	520.73 $\pm$ 4.05*
18	522.35 $\pm$ 9.29*	506.14 $\pm$ 3.38*
24	531.02 $\pm$ 8.89*	534.29 $\pm$ 9.18*

Values are means  $\pm$  s.e.m (N=5) from both NaCl and HCl infused treatments.

<sup>#</sup> indicates significant differences between treatments for the given time point (2-way-RM-ANOVA, Boneferroni post test,  $p < 0.05$ ). \* indicate significant differences from  $t=0$  h within each treatment (1-way-RM-ANOVA, Dunnett's post test,  $p < 0.05$ ).

**Table 11.2.** NHE2 staining patterns from control infused (NaCl) and acid-infused (HCl) fish following 24 h experiments.

	<b>Cytoplasmic</b>	<b>Intermediate</b>	<b>Apical</b>
	<b>(%)</b>	<b>(%)</b>	<b>(%)</b>
NaCl	73 ± 2*	20 ± 2	7 ± 3
HCl	54 ± 5	19 ± 2	27 ± 5*

Descriptions of the staining patterns are found in results and figure 6. \* indicate values that are significantly higher between treatment groups ( $p < 0.05$ , Man Whitney one-tailed test) (N=3).

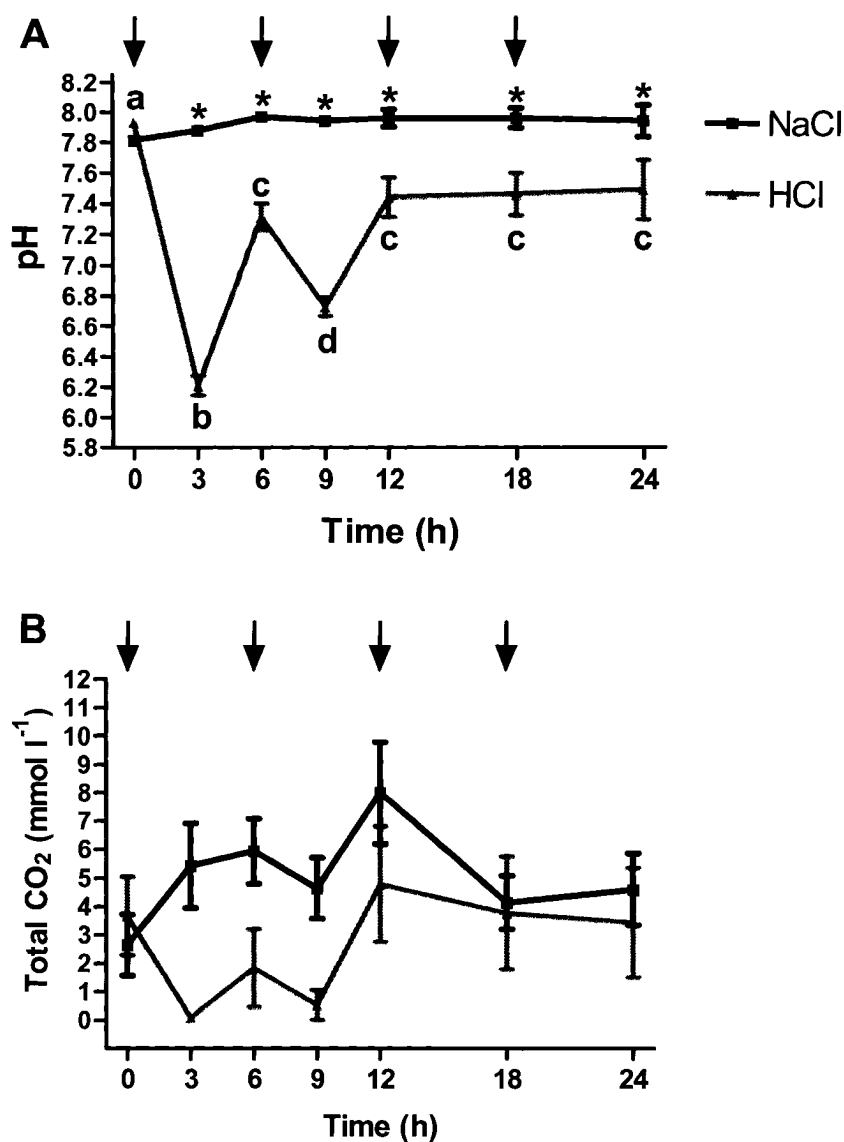


**Figure 11.1.** Blood parameters of hagfish injected with either 250 mmol l<sup>-1</sup> HCl (6000 mmol kg<sup>-1</sup>) or an equivalent volume of 500 mmol l<sup>-1</sup> NaCl (Mean  $\pm$  s.e.m., N=5). (A) Blood pH. (B) Plasma total [CO<sub>2</sub>]. Asterisks (\*) indicate significant differences between the experimental values (HCl infused) and control values (NaCl infused) for the respective time period ( $p < 0.05$ , 2-way-RM-ANOVA, Bonferroni's *post test*, N=5). Letters indicate significant differences within the HCl infused group only to analyze the kinetics of the acid-recovery period (One-way-RM-Anova, Bonferroni *post test*,  $p < 0.05$  N=5).



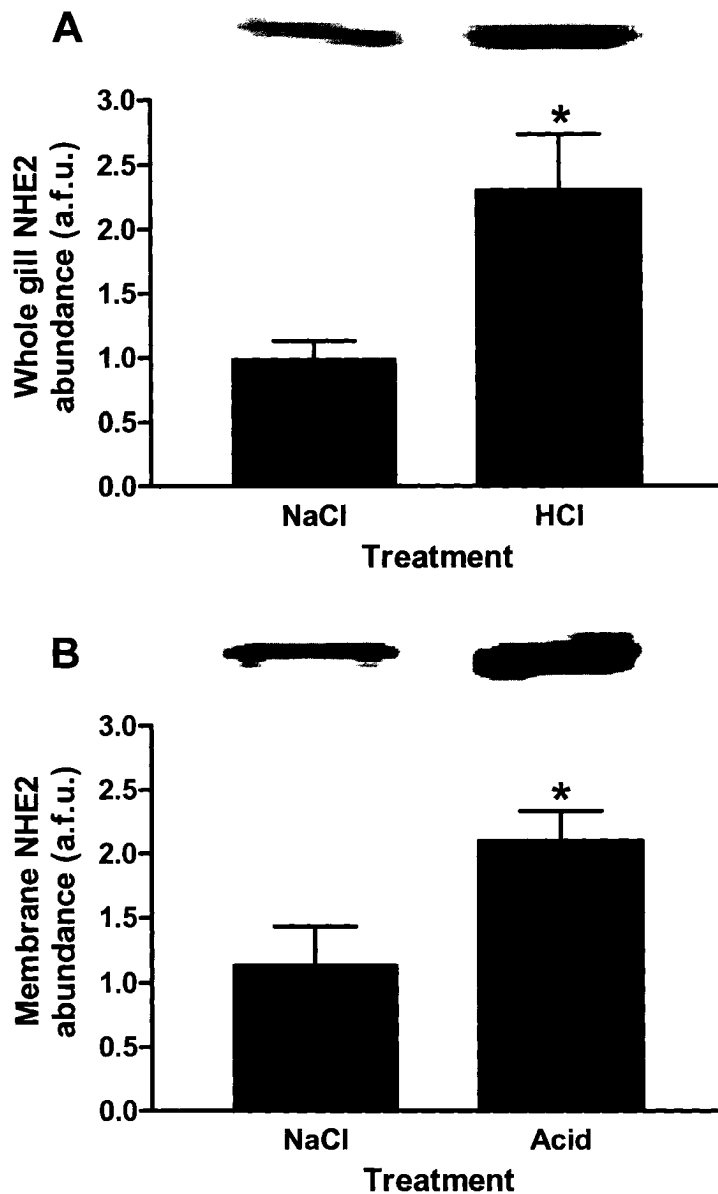


**Figure 11.2.**  $\text{Na}^+/\text{H}^+$  exchanger 2 (NHE2)-like abundance and representative western blots of whole gill (A) and membrane (B) fractions from NaCl and HCl infused hagfish. \* represent significant differences from control (NaCl) values ( $p < 0.05$ , Student's t-test,  $N=5$ ).

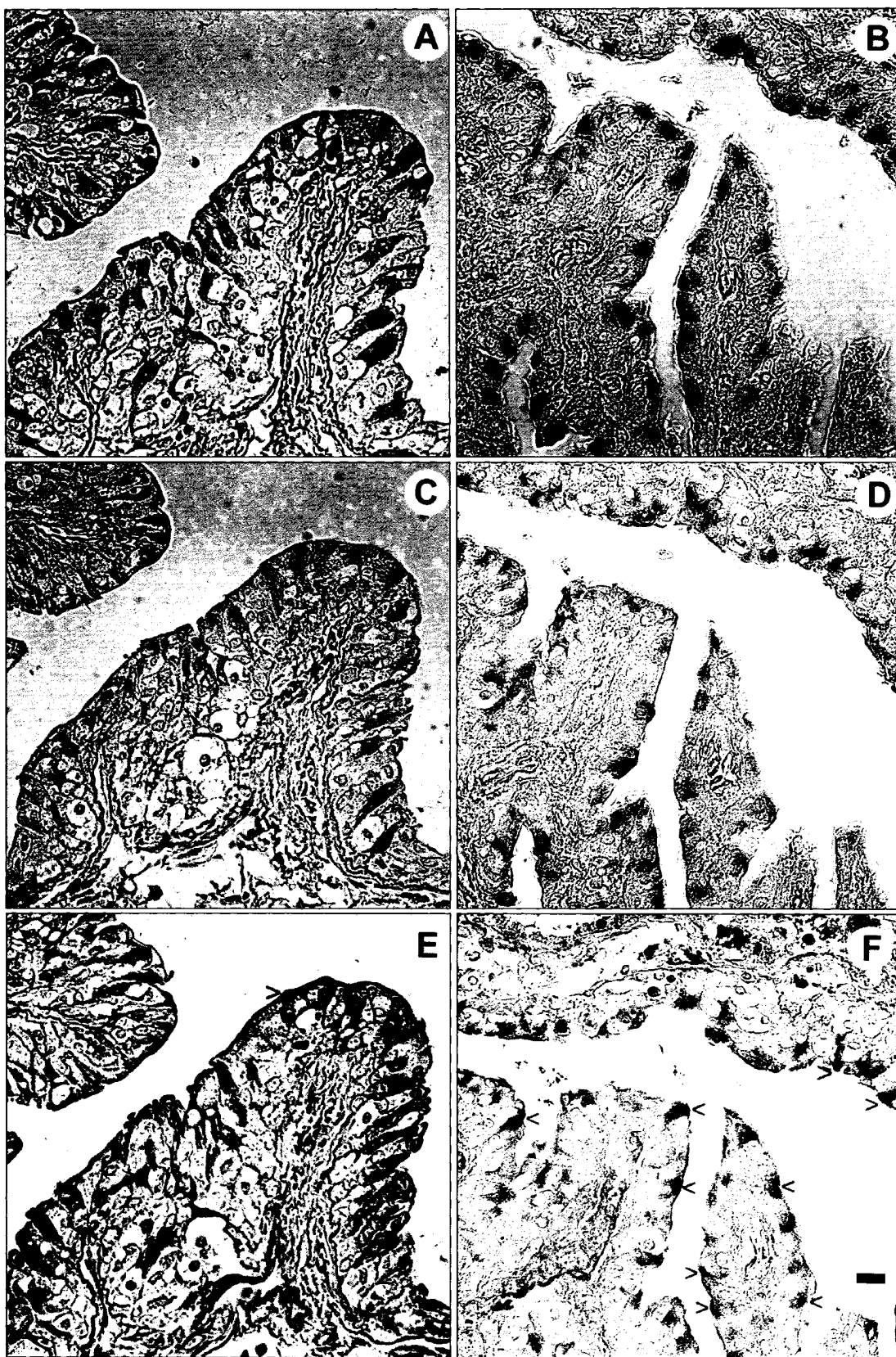


**Figure 11.3.**

**Figure 11.3.**  $\text{Na}^+/\text{K}^+$ -ATPase (*A, B*),  $\text{V-H}^+$ -ATPase (*C, D*), and NHE2 (*E, F*) like-immunoreactivity in consecutive sections from NaCl (*A, C, E*) and HCl (*B, D, F*) infused hagfish. Labelling patterns remain unaltered for  $\text{Na}^+/\text{K}^+$ -ATPase and  $\text{V-H}^+$ -ATPase in response to HCl infusions while NHE2 demonstrates a marked redistribution to the apical membrane as indicated by arrows in part *F*. Scale bar: 10  $\mu\text{m}$  .

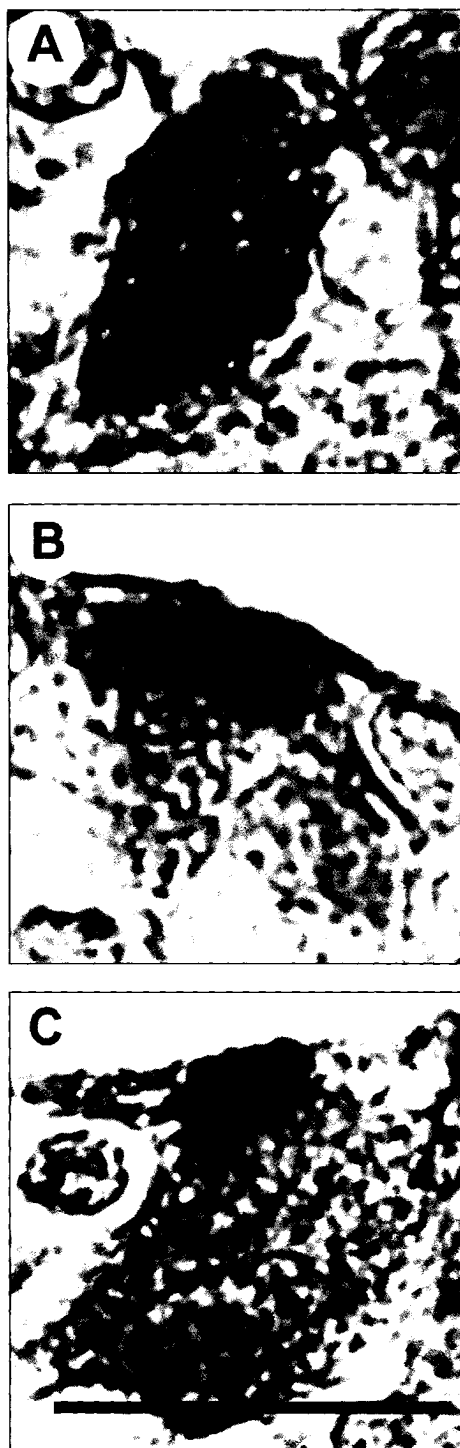


**Figure 11.4.** High magnification (1600x) pictures showing the stereotypical NHE2 like-immunoreactivity pattern for cytoplasmic (A), intermediate (B), and apical (C) localization as quantified in table 2. Scale bar: 10  $\mu$ m.

## References

- Alt, J.M., Stolte, H., Eisenbach, G.M. and Walvig, F.** (1981). Renal electrolyte and fluid excretion in the Atlantic hagfish *Myxine glutinosa*. *J. Exp. Biol.* **91**, 323-330.
- Bartels, H.** (1992). The gills of hagfishes. In: *The Biology of Hagfishes* (eds. J. Jørgensen, J. Lomholt, R. Weber and H. Malte), pp 205-222. London: Chapman and Hall.
- Breton, S. and Brown, D.** (2007) New insights into the regulation of V-ATPase-dependent proton secretion. *Am. J. Physiol. Renal Physiol.* **292**, 1-10.
- Catches, J.S., Burns, J.M., Edwards, S.L. and Claiborne, J.B.** (2006).  $\text{Na}^+/\text{H}^+$  antiporter,  $\text{V-H}^+$ -ATPase and  $\text{Na}^+/\text{K}^+$ -ATPase immunolocalization in a marine teleost (*Myoxocephalus octodecemspinosus*). *J. Exp. Biol.* **209**, 3440-3447.
- Catches, J.S. and Claiborne, J.B.** (2004). NHE2 and  $\text{Na}^+/\text{K}^+$ -ATPase immunoreactivity in *Myoxocephalus octodecimspinosus*. *Bull. Mt. Desert Isl. Biol. Lab.* **43**, 22–23.
- Choe, K.P., Edwards, S., Morrison-Shetlar A.I., Toop, T. and Claiborne, J.B.** (1999). Immunolocalization of  $\text{Na}^+/\text{K}^+$ -ATPase in mitochondrion-rich cells of the Atlantic hagfish (*Myxine glutinosa*) gill. *Comp. Biochem. Physiol. A.* **124**, 161-168.
- Choe, K.P., Kato, A., Hirose, S., Plata, C., Sindic, A., Romero, M. F., Claiborne, J.B. and Evans, D.H.** (2005). NHE3 in an ancestral

vertebrate: primary sequence, distribution, localization, and function in gills. *Am. J. Physiol. Regul. Integr. Comp. Physiol.* **289**, R1520–R1534.

**Choe, K.P., Morrison-Shetlar, A.I., Wall, B.P. and Claiborne, J.B.** (2002). Immunological detection of  $\text{Na}^+/\text{H}^+$  exchangers in the gills of a hagfish, *Myxine glutinosa*, an elasmobranch, *Raja erinacea*, and a teleost, *Fundulus heteroclitus*. *Comp. Biochem. Physiol. A* **131**, 375-385.

**Claiborne, J., Blackston, C., Choe, K., Dawson, D., Harris, S., Mackenzie, L. and Morrison-Shetlar, A.** (1999). A mechanism for branchial acid excretion in marine fish: identification of multiple  $\text{Na}^+/\text{H}^+$  antiporter (NHE) isoforms in gills of two seawater teleosts. *J Exp Biol* **202**, 315-324.

**Claiborne, J.B., Edwards, S.L. and Morrison-Shetlar, A.I.** (2002). Acid-base regulation in fishes: cellular and molecular mechanisms. *J. Exp. Zool.* **293**, 302–319.

**Claiborne, J.B., Perry, E., Bellows, S. and Campbell, J.** (1997). Mechanisms of acid-base excretion across the gills of a marine fish. *J. Exp. Zool.* **279**, 509–520.

**Dames, P., Zimmermann, B., Schmidt, R., Rein, J., Voss, M., Schewe, B., Walz, B. and Baumann, O.** (2006). cAMP regulates plasma membrane vacuolar-type  $\text{H}^+$ -ATPase assembly and activity in blowfly salivary glands. *Proc. Natl. Acad. Sci. USA* **103**, 3926-3931.

**Edwards, S.L., Claiborne, J.B., Morrison-Shetlar A.I. and Toop, T.** (2001). Expression of  $\text{Na}^+/\text{H}^+$  exchanger mRNA in the gills of the Atlantic

hagfish (*Myxine glutinosa*) in response to metabolic acidosis. *Comp. Biochem. Physiol. A* **130**, 81-91.

**Edwards, S.L., Donald, J.A., Toop, T., Donowitz, M. and Tse, C.-M.** (2002). Immunolocalisation of sodium/proton exchanger-like proteins in the gills of elasmobranchs. *Comp. Biochem. Physiol. A* **131**, 257-65.

**Evans, D. H.** (1984). Gill  $\text{Na}^+/\text{H}^+$  and  $\text{Cl}^-/\text{HCO}_3^-$  exchange systems evolved before the vertebrates entered freshwater. *J. Exp. Biol.* **113**, 465-469.

**Evans, D.H., Piermarini, P.M. and Choe, K.P.** (2005). The multifunctional fish gill: dominant site of gas exchange, osmoregulation, acid-base regulation, and excretion of nitrogenous waste. *Physiol. Rev.* **85**, 97-177.

**Forster, M.E., Davison, W., Satchell, G.H. and Taylor, H.H.** (1989). The subcutaneous sinus of the hagfish, *Eptatretus cirrhatus* and its relation to the central circulating blood volume. *Comparative Biochemistry and Physiology Part A: Physiology* **93**, 607-612.

**Galvez, F., Reid, S.D., Hawkings, G. and Goss, G.G.** (2002). Isolation and characterization of mitochondria-rich cell types from the gill of freshwater rainbow trout. *Am. J. Physiol. Regul. Integr. Comp. Physiol.* **282**, R658-R668.

**Goss, G.G., Adamia, S. and Galvez, F.** (2001). Peanut lectin binds to a subpopulation of mitochondria rich cells in the rainbow trout gill epithelium. *Am. J. Physiol. Regul. Integr. Comp. Physiol.* **281**, R1718-R1725.

**Hansen, C.A. and Sidell, B.D.** (1983). Atlantic hagfish cardiac muscle: metabolic basis of tolerance to anoxia. *Am. J. Physiol.* **244**, R356-R362.

**Ip, Y.K., Peh, K.B., Tam, W.L., Wong, W.P. and Chew, S.F.** (2005). Effects of intra-peritoneal injection with  $\text{NH}_4\text{Cl}$ , urea, or  $\text{NH}_4\text{Cl}$ +urea on nitrogen excretion and metabolism in the African lungfish *Protopterus dolloi*. *J. Exp. Zool.* **303A**, 272-282.

**Katoh, F. and Kaneko, T.** (2003). Short-term transformation and long-term replacement of branchial chloride cells in killifish transferred from seawater to freshwater, revealed by morphofunctional observations and a newly established 'time-differential double fluorescent staining' technique. *J. Exp. Biol.* **206**, 4113-4123.

**Katoh, F., Hyodo, S. and Kaneko, T.** (2003). Vacuolar-type proton pump in the basolateral plasma membrane energizes ion uptake in branchial mitochondria-rich cells of killifish *Fundulus heteroclitus*, adapted to a low ion environment. *J. Exp. Biol.* **206**, 793-803.

**Katoh, F., Shimizu, A., Uchida, K. and Kaneko, T.** (2000). Shift of chloride cell distribution during early life stages in seawater-adapted killifish, *Fundulus heteroclitus*. *Zool. Sci.* **17**, 11-18.

**Laemmli, U.K.** (1970). Cleavage of structural proteins during the assembly of the head of the bacteriophage T4. *Nature* **227**, 680-685.

**Lim, C.K., Chew, S.F., Ling Tay, E.S. and Ip, Y.K.** (2004). Effects of peritoneal injection of  $\text{NH}_4\text{HCO}_3$  on nitrogen excretion and metabolism in the



swamp eel *Monopterus albus* increased ammonia excretion with an induction of glutamine synthetase activity. *J. Exp. Zool.* **301A**, 324-333.

**Mallat, J., Conley, D.M. and Ridgway, R.L.** (1987). Why do hagfish have gill “chloride cells” when they need not regulate plasma NaCl concentration? *Can. J. Zool.* **65**, 1956-1965.

**McDonald, D.G., Cavdek, V., Calvert, L. and Milligan, C.L.** (1991). Acid-base regulation in the Atlantic hagfish *Myxine glutinosa*. *J. Exp. Biol.* **161**, 201-215.

**Morris, R.** (1965). Studies on salt and water balance in *Myxine glutinosa* (L.). *J. Exp. Biol.* **42**, 359-371.

**Parks, S.K., Tresguerres, M. and Goss, G.G.** (2007). Interactions between Na<sup>+</sup> channels and Na<sup>+</sup>-HCO<sub>3</sub><sup>-</sup> cotransporters in the freshwater fish gill MR cell: a model for transepithelial Na<sup>+</sup> uptake. *Am. J. Physiol. Cell Physiol.* **292**, C935-C944.

**Pastor-Soler N., Beaulieu V., Litvin T.N., Da Silva N., Chen Y., Brown D., Buck J., Levin L.R. and Breton S.** (2003). Bicarbonate regulated adenylyl cyclase (sAC) is a sensor that regulates pH-dependent V-ATPase recycling. *J. Biol. Chem.* **278**, 49523-49529.

**Piermarini, P.M. and Evans, D.H.** (2001). Immunochemical analysis of the vacuolar proton-ATPase B-subunit in the gills of a euryhaline stingray (*Dasyatis sabina*): effects of salinity and relation to Na<sup>+</sup>/K<sup>+</sup>-ATPase. *J. Exp. Biol.* **204**, 3251 -3259.

**Reid, S.D., Hawkings, G.S., Galvez, F. and Goss, G.G.** (2003). Localization and characterization of phenamil-sensitive Na<sup>+</sup> influx in isolated rainbow trout gill epithelial cells. *J. Exp. Biol.* **206**, 551–559.

**Ruben, J.A. and Bennett, A.F.** (1980). Antiquity of the vertebrate pattern of activity metabolism and its possible relation to vertebrate origins. *Nature* **286**, 886-888.

**Tresguerres, M., Katoh, F., Fenton, H., Jasinska, E. and Goss, G.G.** (2005). Regulation of branchial V-H<sup>+</sup>-ATPase, Na<sup>+</sup>/K<sup>+</sup>-ATPase and NHE2 in response to acid and base infusions in the Pacific spiny dogfish (*Squalus acanthias*). *J. Exp. Biol.* **208**, 345-354.

**Tresguerres, M., Parks, S.K. and Goss, G.G.** (2006a) V-H<sup>+</sup>-ATPase, Na<sup>+</sup>/K<sup>+</sup>-ATPase and NHE2 immunoreactivity in the gill epithelium of the Pacific hagfish (*Eptatretus stoutii*). *Comp. Biochem. Physiol. A.* **145**, 312-321.

**Tresguerres, M., Parks, S.K., Katoh, F. and Goss, G.G.** (2006b). Microtubule-dependent relocation of branchial V-H<sup>+</sup>-ATPase to the basolateral membrane in the Pacific spiny dogfish (*Squalus acanthias*): a role in base secretion. *J. Exp. Biol.* **209**, 599-609.

**Wakabayashi, S., Shigekawa, M. and Pouyssegur, J.** (1997). Molecular physiology of vertebrate Na<sup>+</sup>/H<sup>+</sup> exchangers. *Physiol. Rev.* **77**, 51-74.

**Weakley, J., Choe, K. P. and Claiborne, J.B.** (2003). Immunological detection of gill NHE2 in the dogfish (*Squalus acanthias*). *Bull. Mt. Desert Isl. Biol. Lab.* **42**, 81–82.

**Wood, C.M., Kajimura, M., Mommsen, T.P. and Walsh, P.J. (2005).**

Alkaline tide and nitrogen conservation after feeding in an elasmobranch

(*Squalus acanthias*). *J. Exp. Biol.* **208**, 2693-2705.

**Zall, D.M., Fischer, M.D. and Garner, Q.M. (1956).** Photometric

determination of chloride in water. *Anal. Chem.* **28**, 1665-1678.

## Appendix II

### **Low pH stimulates ion transport across isolated gills of the crab *Chasmagnathus granulatus*: involvement of apical anion V-H<sup>+</sup>-ATPase and carbonic anhydrase<sup>1</sup>**

<sup>1</sup>A version of this chapter has been submitted for publication. **Tresguerres, M., Parks, S.K. and Goss, G.G.** *The Journal of Experimental Biology* (JEXBIO/2007/006148). Reproduced with permission of The Company of Biologists and the co-authors of the manuscript. Data from this manuscript that is not included in this appendix can be found in chapter IX.

## Introduction and Materials and Methods

The introduction and materials and methods from chapter IX also apply to this appendix. Total CO<sub>2</sub> (TCO<sub>2</sub>) of the low-pH saline was measured using the method of Cameron (1971) in a thermostatted chamber (37°C) equipped with a CO<sub>2</sub> electrode (Radiometer, Copenhagen, Denmark). TCO<sub>2</sub> of the low-pH saline, and hence also [HCO<sub>3</sub><sup>-</sup>] and *P*CO<sub>2</sub>, was very low and almost negligible.

## Results

A reduction in the pH from 7.75 to 7.45 pH units in the perfusion conditions produced an immediate and significant stimulation of  $V_{te}$  from  $3.68 \pm 0.58$  to  $6.32 \pm 0.72$  mV ( $N=13$ ). The original  $V_{te}$  was restored upon application of the original pH of 7.75. The low pH-stimulated  $V_{te}$  and subsequent wash-out was a repeatable event (Fig. 12.1).

To test if carbonic anhydrase is involved in the low pH-stimulating mechanism we added  $200 \mu\text{mol l}^{-1}$  acetazolamide into the 7.45 pH perfusate of isolated gills that had already been stimulated by low pH. Acetazolamide completely and reversibly abolished the stimulated  $V_{te}$  (Fig. 12.2).

The involvement of  $\text{V-H}^+$ -ATPase was next investigated. Basolateral bafilomycin ( $100 \text{ nmol l}^{-1}$ ) also inhibited the low pH-stimulated  $V_{te}$ , but, unlike acetazolamide, its effect was not completely reversible (Fig. 12.3). However, the original resting  $V_{te}$  was restored upon re-introduction of the control pH 7.75 saline, indicating that the inhibitory effect of bafilomycin specifically acts on the mechanism stimulated by low pH.

In order to determine if the low-pH stimulated  $V_{te}$  depends on the transepithelial movement of  $\text{Cl}^-$ , we performed a series of experiments using  $\text{Cl}^-$ -free solutions. As shown in fig. 12.4, the  $\text{Cl}^-$ -free condition abolished and even reversed  $V_{te}$ . Nonetheless, the subsequent introduction of  $\text{Cl}^-$ -free pH 7.45 saline induced a significant increase of  $V_{te}$  of a magnitude comparable to that in normal,  $\text{Cl}^-$ -containing, saline. The effect of low pH under  $\text{Cl}^-$ -free conditions was partially reversible (fig.12. 4).

Lastly, we tested the involvement of apical  $\text{Na}^+$  channels and basolateral  $\text{Na}^+/\text{HCO}_3^-$  co-transporters by adding apical phenamil ( $50 \mu\text{mol l}^{-1}$ ) and basolateral DIDS ( $1 \text{ mmol l}^{-1}$ ), respectively, under low-pH stimulating conditions. The effect of phenamil only took place in certain preparations, and its magnitude was highly variable and thus it is not shown or analyzed. On the other hand, DIDS totally reduced the stimulated  $V_{\text{te}}$ , although it first produced an important ( $\sim 10 \text{ mV}$ ) hyperpolarization of  $V_{\text{te}}$  in most of the preparations (Fig. 12.5). The inhibitory effect of DIDS was not reversible. DIDS did not cause any significant changes when applied under control pH conditions (Fig. 12.5), indicating that the both the initial hyperpolarization and the inhibitory effect observed are related to the low pH-stimulating mechanism.

## Discussion

Chapter IX contains a more general discussion including the results from this appendix. Below is presented a discussion specific to the results of appendix II.

### *Low pH-stimulating mechanism*

The inhibition of the low pH-stimulated  $V_{te}$  by bafilomycin is a good indicator of the importance of V-H<sup>+</sup>-ATPase in this response. Based on the outside positive  $V_{te}$ , we propose that V-H<sup>+</sup>-ATPase is located in the apical membrane and acts to secrete the excess H<sup>+</sup> into the water covering the gills. Although bafilomycin was applied to the basolateral space, it is a membrane-permeable compound (Dröse and Altendorf, 1997) and thus it can inhibit V-H<sup>+</sup>-ATPase located at the apical membrane even if applied at the basolateral space.

Apical V-H<sup>+</sup>-ATPase has been proposed to energize apical Cl<sup>-</sup> absorption in some strong hyper-regulating freshwater crabs (Onken *et al.*, 1991; Onken and Putzenlechner, 1995; Riestenpatt *et al.*, 1995; Onken and McNamara, 2002; Weihrauch *et al.*, 2004), and also in *C. granulatus* (Luquet *et al.*, 2005; Genovese *et al.*, 2005). However, the Cl<sup>-</sup>-independence demonstrated in our study suggests that the low-pH stimulating mechanism is different from the Cl<sup>-</sup>-uptake mechanism. Based on Na<sup>+</sup>-uptake models from certain aquatic organisms (for a review see Kirschner, 2004), we tested for the putative involvement of apical Na<sup>+</sup> channels by applying apical phenamil on gills with stimulated  $V_{te}$ . Although phenamil did inhibit the stimulated  $V_{te}$  in



certain preparations, the effect was not consistent, probably due to permeability issues at the apical cuticle. Our preliminary model presented here includes apical  $\text{Na}^+$  channels (Fig. 5 in chapter 9), although further investigation is required to confirm this component.

Based on a recent study in isolated fish gill cells (Parks *et al.*, 2007), we had hypothesized that basolateral electrogenic  $\text{Na}^+/\text{HCO}_3^-$  cotransporters (NBCs) could be the way of exit of  $\text{HCO}_3^-$  and  $\text{Na}^+$ . Basolateral DIDS produced an initial further stimulation of the  $V_{te}$  already stimulated by low pH, followed by a rapid, complete and irreversible inhibition. We tentatively propose that DIDS indeed inhibits basolateral NBCs and that the initial  $V_{te}$  stimulation is due to the pumping of protons by apical  $\text{V-H}^+$ -ATPases, which is not totally compensated due to the reduction in the apical uptake of  $\text{Na}^+$  as a result of the inhibition of the basolateral transport of  $\text{Na}^+$ . In the longer term, the apical  $\text{V-H}^+$ -ATPase probably simply shuts down, thus inhibiting  $V_{te}$ . In addition, the stimulation of  $V_{te}$  in the absence of  $\text{Cl}^-$  suggests that the low pH-induced change in  $V_{te}$  is due to a current carried by  $\text{Na}^+$ . This leaves only the possibility of an NBC or  $\text{Na}^+/\text{K}^+$ -ATPase on the basolateral side. The NBC would be more likely as the  $\text{HCO}_3^-$  produced via CA hydration of  $\text{CO}_2$  would need to be transported across the basolateral surface to maintain the charge distribution as the  $\text{H}^+$  is pumped out apically. Furthermore, testing for the presence of  $\text{Na}^+/\text{K}^+$ -ATPase is not feasible due to the effect of ouabain in shutting down the gill function (Luquet *et al.*, 2002; Onken *et al.*, 2003).

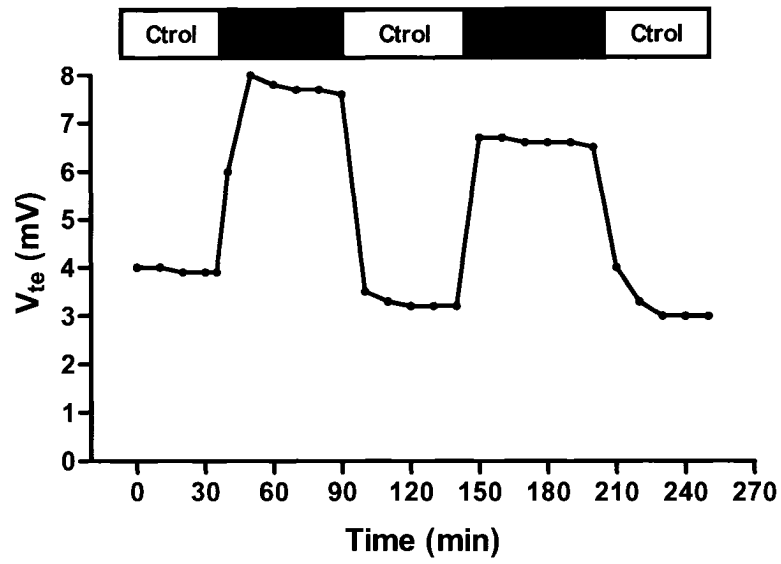


**Figure 12.1.** Repeatability of the acid-induced  $V_{te}$  stimulation.  
Representative trace. Ctrol: control saline, pH 7.75. Low pH: pH 7.45 saline.

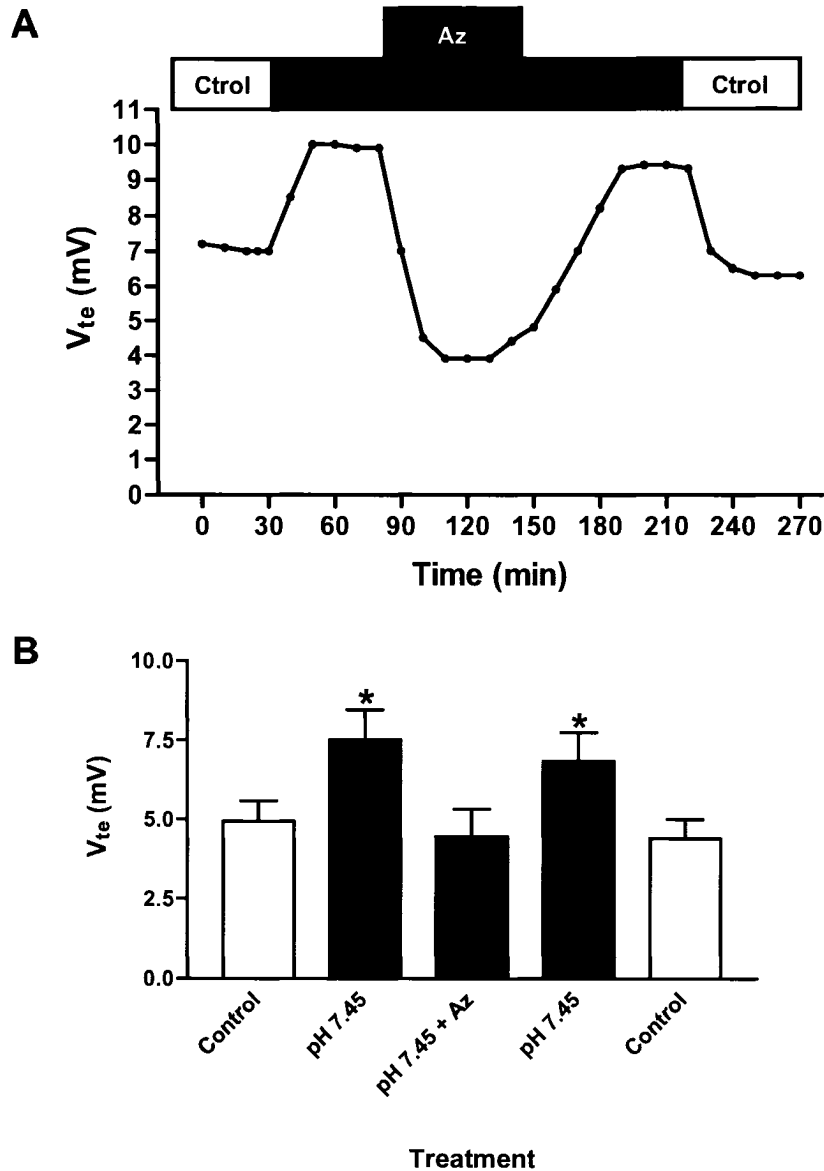


**Figure 12.2.** Inhibition of the acid-induced  $V_{te}$  stimulation by basolateral acetazolamide. (A) Representative trace. (B) Summary statistics.  $V_{te}$ : transepithelial potential difference. Ctrol: control saline, pH 7.75. Low pH: pH 7.45 saline. Az: 200  $\mu\text{mol l}^{-1}$  acetazolamide added in the basolateral perfusate. The asterisks indicate statistical differences with the control ( $P < 0.05$ ;  $N = 7$ ; 1-way ANOVA, Dunnett's multiple comparisons post-test).

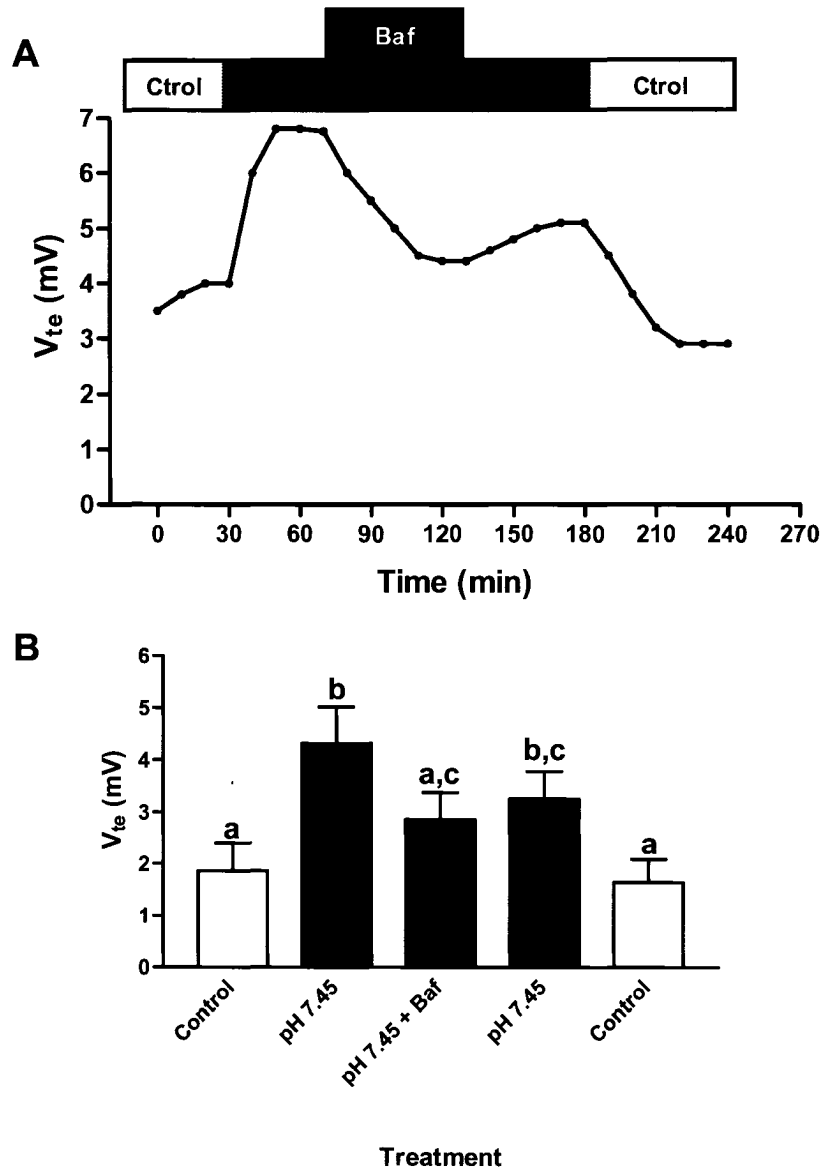


**Figure 12.3.** Inhibition of the acid-induced  $V_{te}$  stimulation by basolateral bafilomycin. (A) Representative trace. (B) Summary statistics.  $V_{te}$ : transepithelial potential difference. Ctlol: control saline, pH 7.75. Low pH: pH 7.45 saline. Baf: 100 nmol l<sup>-1</sup> bafilomycin added in the basolateral perfusate. The letters indicate different levels of statistical significance ( $P < 0.05$ ;  $N = 5$ ; 1-way ANOVA, Tukey's multiple comparisons post-test).

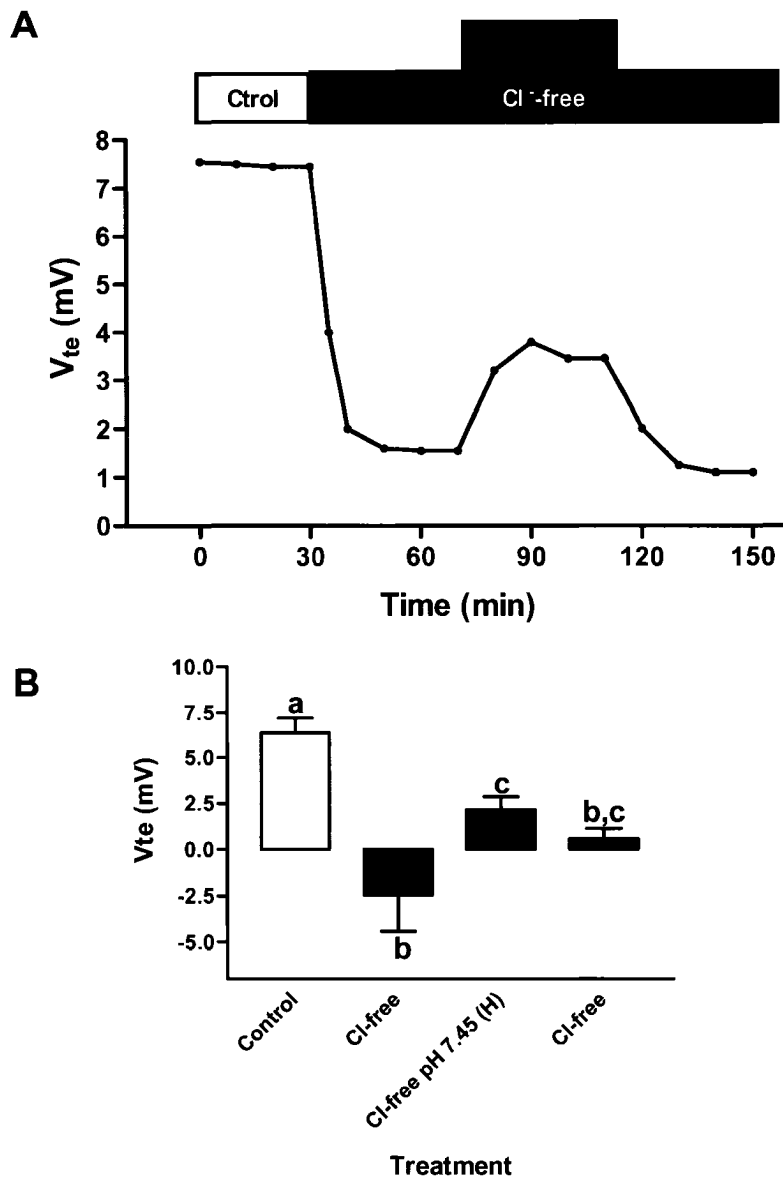


**Figure 12.4.** Acid-induced  $V_{te}$  stimulation in  $Cl^-$ -free conditions. (A) Representative trace. (B) Summary statistics.  $V_{te}$ : transepithelial potential difference. Ctrol: control saline, pH 7.75.  $Cl^-$ -free: control saline with all the  $Cl^-$  substituted by  $NO_3^-$ , pH 7.75. Low pH: pH 7.45,  $Cl^-$ -free saline. The letters indicate different levels of statistical significance ( $P < 0.05$ ;  $N = 5$ ; 1-way ANOVA, Tukey's multiple comparisons post-test).

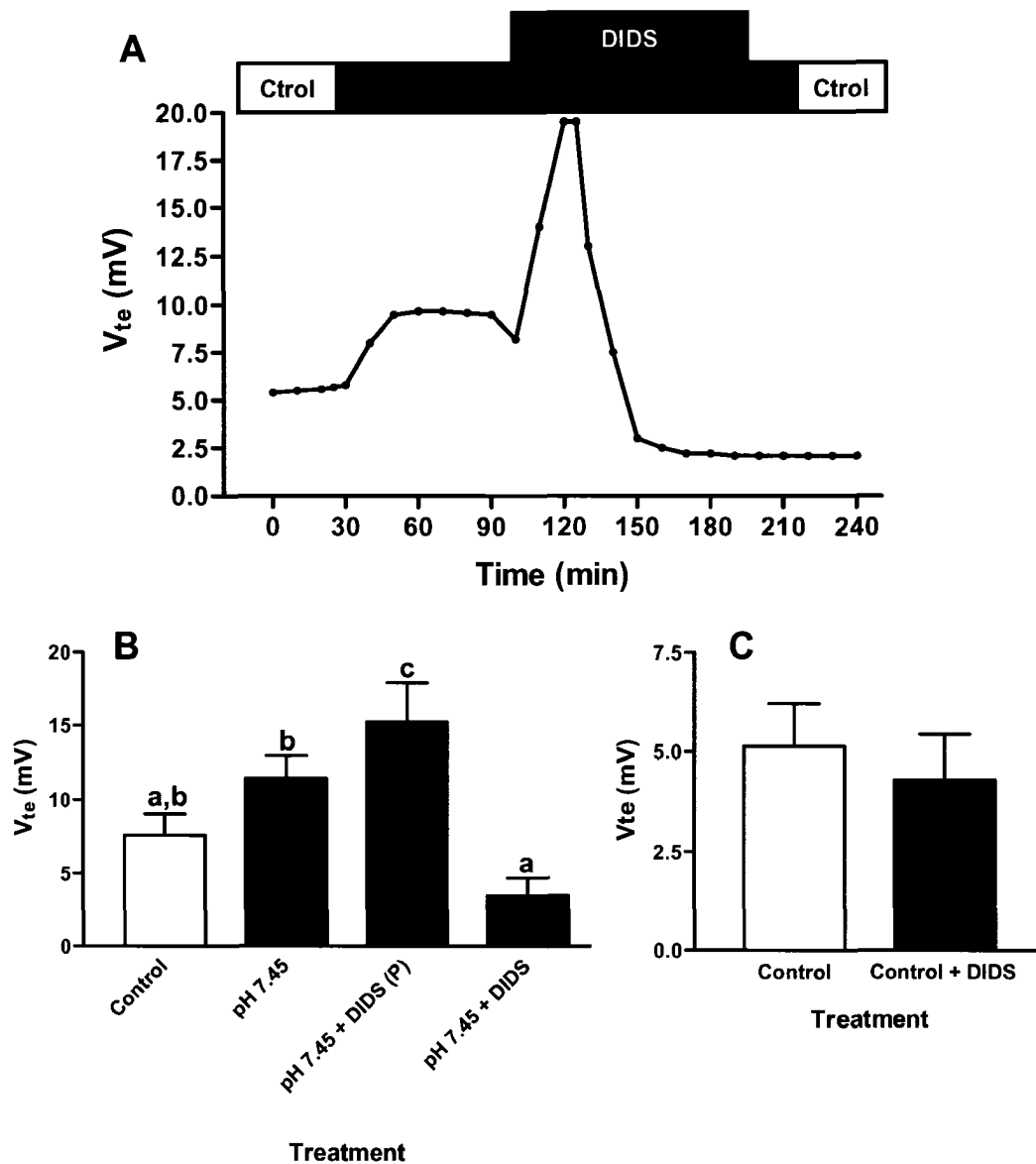


**Figure 12.5.** Inhibition of the Acid-induced  $V_{te}$  stimulation by basolateral DIDS. (A) Representative trace. (B) Summary statistics in pH 7.45 saline (N=5). (C) Summary statistics in control pH 7.75 saline (N=3).  $V_{te}$ : transepithelial potential difference. Ctrol: control saline, pH 7.75. Low pH: pH 7.45 saline. DIDS: 1 mmol l<sup>-1</sup> DIDS added in the basolateral perfusate. The letters indicate different levels of statistical significance ( $P < 0.05$ ; 1-way ANOVA, Tukey's multiple comparisons post-test).

## References

- Cameron, J.N.** (1971). Rapid method for determination of total carbon dioxide in small blood samples. *J. Appl. Physiol.* 31, 632-634.
- Drose, S. and Altendorf, K.** (1997). Bafilomycins and concanamycins as inhibitors of V-ATPases and P-ATPases. *J. Exp. Biol.* 200, 1-8.
- Genovese, G., Ortiz, N., Urcola, M. R. and Luquet, C. M.** (2005). Possible role of carbonic anhydrase, V-H<sup>+</sup>-ATPase, and Cl<sup>-</sup>/HCO<sub>3</sub><sup>-</sup> exchanger in electrogenic ion transport across the gills of the euryhaline crab *Chasmagnathus granulatus*. *Comp. Biochem. Physiol. A* 142, 362-369.
- Kirschner, L. B.** (2004). The mechanism of sodium chloride uptake in hyperregulating aquatic animals. *J. Exp. Biol.* 207, 1439-1452.
- Luquet, C. M., Postel, U., Halperin, J., Urcola, M. R., Marques, R. and Siebers, D.** (2002). Transepithelial potential differences and Na<sup>+</sup> flux in isolated perfused gills of the crab *Chasmagnathus granulatus* (Grapsidae) acclimated to hyper- and hypo-salinity. *J. Exp. Biol.* 205, 71-77.
- Luquet, C. M., Weihrauch, D., Senek, M. and Towle, D. W.** (2005). Induction of branchial ion transporter mRNA expression during acclimation to salinity change in the euryhaline crab *Chasmagnathus granulatus*. *J. Exp. Biol.* 208, 3627-3636.
- Onken, H., Graszynski, K. and Zeiske, W.** (1991). Na<sup>+</sup>-independent, electrogenic Cl<sup>-</sup> uptake across the posterior gills of the Chinese crab (*Eriocheir sinensis*) - Voltage-clamp and microelectrode studies. *J. Comp. Physiol. B* 161, 293-301.

**Onken, H. and McNamara, J. C.** (2002). Hyperosmoregulation in the red freshwater crab *Dilocarcinus pagei* (Brachyura, Trichodactylidae): structural and functional asymmetries of the posterior gills. *J. Exp. Biol.* **205**, 167-175.

**Onken, H. and Putzenlechner, M.** (1995). A V-Atpase drives active, electrogenic and  $\text{Na}^+$ -independent  $\text{Cl}^-$  absorption across the gills of *Eriocheir sinensis*. *J. Exp. Biol.* **198**, 767-774.

**Parks, S. K., Tresguerres, M. and Goss, G. G.** (2007). Interactions between  $\text{Na}^+$  channels and  $\text{Na}^+\text{-HCO}_3^-$  cotransporters in the freshwater fish gill MR cell: a model for transepithelial  $\text{Na}^+$  uptake. *Am. J. Physiol. Cell Physiol.* **292**, C935-C944.

**Riessenpatt, S., Petrausch, G. and Siebers, D.** (1995).  $\text{Cl}^-$  influx across posterior gills of the Chinese crab (*Eriocheir sinensis*) - potential energization by a V-Type  $\text{H}^+$ -Atpase. *Comp. Biochem. Physiol. A* **110**, 235-241.

**Weihrauch, D., McNamara, J. C., Towle, D. W. and Onken, H.** (2004). Ion-motive ATPases and active, transbranchial NaCl uptake in the red freshwater crab, *Dilocarcinus pagei* (Decapoda, Trichodactylidae). *J. Exp. Biol.* **207**, 4623-4631.